GEOLOGY AND METAMORPHIC PETROLOGY OF PART OF THE DAMARA OROGEN ALONG THE LOWER SWAKOP RIVER, SOUTH WEST AFRICA

by

ROGER E. JACOB

Thesis submitted in fulfilment of the
requirements for the degree of
Doctor of Philosophy in the
Faculty of Science

University of Cape Town

1974

The copyright of this thesis is held by the University of Cape Town.
Reproduction of the whole or any part may be made for study purposes only, and not for publication.

The copyright of this thesis vests in the author. No quotation from it or information derived from it is to be published without full acknowledgement of the source. The thesis is to be used for private study or non-commercial research purposes only.

Published by the University of Cape Town (UCT) in terms of the non-exclusive license granted to UCT by the author.

University of Cape Town

GEOLOGY AND METAMORPHIC PETROLOGY OF PART OF THE DAMARA OROGEN ALONG THE LOWER SWAKOP RIVER, SOUTH WEST AFRICA

ABSTRACT

The stratigraphic nomenclature of the *Damara* and *Nosib Groups* has been revised and a purely lithostratigraphic terminology is here adopted. Clastic sediments of the *Etusis* and *Khan Formations* of the Nosib Group were deposited in shallow water above, and on the flanks of, the Abbabis swell and were followed by clastic-carbonate shoreline sediments of the *Rössing Formation* of the Damara Group. Deposition of glacial-marine sediments of the *Chuos Formation*, which forms the base of the *Khomas Subgroup*, followed a period of erosion. Further subsidence led to the accumulation in the west of carbonate and pelitic sediments of the *Husab* and *Witpoort Formations*, respectively, and mixed pelitic and siliceous carbonate sediments of the *Tinkas Formation* in the east.

Two major phases of deformation (F_1 and F_2) generated northeast-trending isoclinal folds and associated foliations and were followed by local minor folding in the southeast during F_3. The F_4 deformation produced north-northeast- to northwest-trending folds and accentuated dome structures initiated during F_2.

High T/P regional metamorphism accompanied F_1 and F_2 and outlasted the latter. Mineral assemblages throughout the area are those of the amphibolite facies, but there is an increase in metamorphic grade from medium stage in the southeast to high stage in the northwest. In calc-granofelses in the south-eastern part of the area epidote has reacted with quartz to form grossularite/andradite. The stability of these minerals was largely controlled by the composition of the fluid phase (X_{CO_2}) and oxygen fugacity. The origin of narrow para-amphibolite bands in the Tinkas Formation is ascribed to the reaction of incompatible biotite, calcite and quartz along the contacts of calcareous and pelitic layers. Forsterite appears to have formed after diopside in siliceous dolomitic marbles. The An-content of plagioclase in amphibolites increases with increasing metamorphic grade from An_{30-60} in the southeast to $An_{>80}$ in the northwest.

Andalusite, sillimanite, cordierite, staurolite and almandine are present in medium-stage metapelites and cordierite, sillimanite, K-feldspar and almandine in high-stage metamorphites. Isograds have been mapped in the field and interpreted in terms of mineral reactions. With increasing grade of metamorphism staurolite and andalusite disappeared from pelitic assemblages, partial anatexis and migmatisation became widespread, muscovite and quartz reacted to form sillimanite and K-feldspar, and biotite, sillimanite and quartz reacted to form cordierite and K-feldspar (± almandine).

Metamorphic temperatures in the southeast and northwest are estimated to have attained 650° C and 750° C respectively. Evidence provided by the co-existence of andalusite-sillimanite, cordierite-staurolite and cordierite-garnet, and the final disappearance of staurolite just short of the anatexis boundary as well as the breakdown of muscovite + quartz beyond the same boundary, indicates that prevailing pressures were between 4 and 5 kb. This

corresponds to a depth of burial of 14-17 km and a geothermal gradient of 40-50° C per km.

The autochthonous and parautochthonous syntectonic rocks of the Red Granite-Gneiss and Salem Granite suites are located on the northwestern side of the anatexis boundary. The former granite-gneisses are in part products of anatexis of Nosib metamorphites and in part reactivated mantled gneiss domes. The Salem Granite Suite comprises three members occurring in synclinal structures above the level of the Chuos Formation and originated by anatexis of Khomas Subgroup rocks. Late- to post-tectonic intrusive granites are common.

Homogeneous pegmatites of metamorphic origin formed syntectonically and are older than the zoned and layered pegmatites derived by fractionation from the intrusive granites.

CONTENTS

ABBREVIATIONS

A number of abbreviations have been used in the text. A list of these is presented below.

mm - millimetre(s)
cm - centimetre(s)
m - metre(s)
km - kilometre(s)
n - refractive index
kb - kilobar(s)
Ma - million years
T - temperature
fO_2 - oxygen fugacity
X_{CO_2} - mole fraction CO_2
P_{H_2O} - partial pressure H_2O
P_{CO_2} - partial pressure CO_2
P_f - fluid (gas) pressure
P_T - total pressure
K_D - distribution coefficient
all - allanite
amph - amphibole
An - anorthite
andal - andalusite
ap - apatite
bi - biotite
cc - calcite
chond - chondrodite
clz - clinozoisite
cord - cordierite
di - diopside
dol - dolomite
epid - epidote
for - forsterite
gar - garnet
gr - grossularite
graph - graphite
hb - hornblende
Kf - K-feldspar
ky - kyanite
mcl - microcline
musc - muscovite
phl - phlogopite
piem - piemontite
plag - plagioclase
qtz - quartz
sauss - saussurite
scap - scapolite
serp - serpentine
sill - sillimanite
sph - sphene
staur - staurolite
ta - talc
tourm - tourmaline
tr - tremolite
vesuv - vesuvianite
woll - wollastonite
zrn - zircon

1. INTRODUCTION

1.1. General

The area investigated during this survey (Map 1) is situated 75 km east of Swakopmund and 190 km west of Windhoek, in the Namib Desert of South West Africa. It covers approximately 2600 km^2 and is bounded by the Tinkas Flats in the southeast, the Tubas and Gawib Flats in the southwest and the Rio Tinto Concession in the northwest. It lies between latitudes 22°25' and 22°56'S and longitudes 14°52' and 15°41'E.

The morphology, climate, vegetation and drainage in this general region have been adequately described by Smith (1965) and little further need be added. The area is drained by two major rivers, the deeply incised Khan and Swakop Rivers. In the northwest and south, the Welwitschia and Gawib Flats form part of the Namib Plain. The eastern part of the area consists of rugged, hilly terrain, and is readily accessible only on foot. The major portion of the area is occupied by the Namib Desert Park, a game reserve, and the remainder is virtually unpopulated.

1.2. Previous work

Early investigations by German workers have been summarised by Smith (1965) and none of these dealt specifically with the area mapped by the author. The first comprehensive studies were carried out by Gevers (1931a, 1934a, 1934b, 1935), who mapped a very large area in western South West Africa including the region dealt with in this report at a scale of 1 : 100 000. These maps were compiled without topographic control or aerial photographs and neither the geographical nor geological features match completely with the present findings. However, the maps proved useful as a basis for more detailed investigations.

Smith (1965) described the geology to the north. There is a small overlap of mapping on Bloemhof 109 and Vlakteplaas 110. More recently, Nash (1971) studied the metamorphism in a small area northwest of the region mapped by the writer.

1.3. Present investigation

The main purpose of this investigation was to study the metamorphism of this part of the Damara Orogen and to relate it to the genesis of pegmatites and radioactive mineralisation. To this end it was necessary to compile a geological map and to undertake studies of the stratigraphy, structure and granites. The work was performed at the instigation of, and with the generous financial support of, the Atomic Energy Board, while the author was attached to the Precambrian Research Unit of the University of Cape Town and later to the Department of Geology at Rhodes University.

Fifteen months were spent on fieldwork during 1969 and 1970. Mapping was carried out on aerial photographs (scale 1 : 36 000), from which data

were transferred, by means of an optical pantograph and radial-line plotter, onto 1 : 50 000 topographic maps. Laboratory investigations were carried out at the University of Cape Town until April, 1971, and thereafter at Rhodes University.

1.4. Acknowledgements

The writer wishes to express his gratitude to several persons and organisations for assistance given during the course of this project. Firstly, to the late Professor John de Villiers, under whose supervision most of the investigation was made, for arranging the project, for his continued interest and for many valuable discussions. Dr. A. Kröner took over the supervision in the final stages and edited various drafts. Sincere thanks are due to him for this onerous task and for constructive comments and criticism.

It is a pleasure to acknowledge the financial support of the Atomic Energy Board for the project and to thank Dr. J.W. von Backström for his personal interest and help in the procurement of chemical analyses and radioactive-mineral identifications. Thanks are due to Mr. J. Berning and Mr. R. Cooke of Rio Tinto Exploration Ltd., Swakopmund, for their hospitality and facilities extended to the writer while in the field.

Professor L.H. Ahrens of the Department of Geochemistry, University of Cape Town, permitted the author to make use of electron microprobe facilities under the guidance of Mr. J.P. Willis, whose help and patience is gratefully acknowledged. Mr. Willis kindly processed the raw data. The cost of the analyses was defrayed from a Rhodes University Council Research Grant. The National Institute for Metallurgy is thanked for the chemical analyses. The support received from the Deputy Director, Mr. L.N.J. Engelbrecht, and the staff of the Geological Survey office in Windhoek is very much appreciated.

A special vote of thanks is due to Professor H.V. Eales for making available the facilities of the Department of Geology at Rhodes University, for critical reading of the manuscript and for taking considerable trouble in arranging departmental duties so as to expedite the research. Thanks are due, too, to Mr. D.S. Cawood, technician in the Department of Geology for considerable co-operation, and to Mrs. A. Wicks for typing the manuscript.

Finally, I wish to express my appreciation to my wife Anamié for her help during the course of the research.

2. FIELD RELATIONSHIPS, STRATIGRAPHY AND LITHOLOGY

2.1. Classification and nomenclature

The Geological Survey of South Africa has, until recently, employed a chronostratigraphic terminology in stratigraphic studies in the Damara Orogen (Smith, 1965). Hälbich (1970) used chronostratigraphic subdivisions for what he termed the Damara System and regarded the Chuos glacial horizon as a suitable time marker. This formation, however, is not present everywhere in the orogen and, furthermore, lithological boundaries between other rock units, stratigraphically removed from the Chuos, may not represent time boundaries. As there are no other suitable time markers that can be used with confidence for purposes of subdivision, a lithostratigraphic classification has been adopted for the stratigraphic units east of the confluence of the Khan and Swakop Rivers, following the recommendations of Hedberg (1961, 1970), van Eysinga (1970), and the South African Committee for Stratigraphy (1971).

During final preparation of this thesis and after printing of the accompanying map (Map 1, in pocket) the S.A.C.S. Working Group post-Waterberg/pre-Cape (Kröner et al., 1974) put forward proposals for the stratigraphic classification and nomenclature of rocks of the Damara Orogen. The suggested terminology (Kröner et al., 1974) is compared with that adopted in this work and those used by Smith (1965), Hälbich (1970), Nash (1971) and Miller (1972) in Table 1.

Martin (1965), following Geological Survey practice, used a chronostratigraphic classification for the Nosib and Damara metasediments and he proposed the term Outjo Facies and Swakop Facies for two probably coeval successions that had previously been called Otavi System and Damara System respectively. The two facies were included in the Damara System by Martin, but the lithostratigraphic terminology makes no provision for formal use of the term "facies". The term Damara Group is used in this work for those rocks which Smith (1965) included in the Damara System, and which are part of the Swakop Facies as suggested by Martin (1965).

Martin (op. cit.) included the Nosib Formation in the Damara System as the basal psammitic portion of this System. Several authors have not followed Martin (op. cit.) in grouping the Nosib Formation with the Damara System and these include Smith (1965), Guj (1970), Hälbich (1970), Nash (1971), Kröner (1971), Miller (1972), Schalk (1973) and the writer.

The term *Nosib Group* is used here, instead of Nosib Formation (Smith, 1965) for a sequence of largely psammitic rocks, lithologically distinct from those of the Damara Group. It has been separated from the Damara because the latter group overlaps the Nosib and because unconformities have been found between rocks of the two Groups. Unlike Guj (1970) however, the author has not found evidence for a metamorphic and tectonic event separating the Nosib and Damara rocks in time. Martin (1965) has also pointed out that the unconformity between Nosib and Damara rocks does not appear to be the result of a major orogeny. In a lithostratigraphic classification a Group is "... an assemblage of two or more contiguously associated formations

Table 1. Stratigraphic terminology for the Nosib and Damara rocks of the Damara Orogen.

Smith (1965)			Hälbich (1970)			Miller (1972)			Nash (1971)		Present Investigation			Kröner et al. (1974)		
Khan/Swakop area			Windhoek			Omaruru			Khan River		Khan/Swakop area			Khan/Swakop area		
	Series	Stage		Series	Stage		Subgroup	Formation	Group	Formation		Subgroup	Formation		Subgroup	Formation
Damara System	Khomas		Damara System	Khomas	Windhoek	Damara Group	Swakop	Khomas			Damara Group	Khomas	Witpoort in west Tinkas in east	Swakop Group	Khomas	Witpoort and Tinkas
	Hakos	Upper			Auas				Hakos				Tinkas in east Husab in west			Karibib
		Chuos			Onnaams			Chuos		Chuos			Chuos			Chuos
		Transgressive overlap		Discordance			Unconformity					Unconformity				
		Lower		Hakos	Berghof		Hakos	Orusewa		Rössing			Rössing		Hakos	Rössing
					Verloren			Okatjise								
Conformable transition			Unconformity			Unconformity			Paraconformity		Paraconformity, Unconformity					
	Nosib Formation	Upper		Rehoboth Formation		Nosib Group		Naauwpoort	Nosib	Khan	Nosib Group		Khan	Nosib Group		Khan
		Lower								Etusis			Etusis			Etusis
MAJOR UNCONFORMITY																

with significant unifying lithological features in common" (Von Eysinga, 1970, p. 271). For this reason also the pelitic/calcareous Damara Group is separated from the largely psammitic Nosib Group.

In the area here described the Nosib Group has been subdivided into a lower *Etusis Formation* and an upper *Khan Formation*. The author has followed Nash (1971) in assigning these formation names. The term Etusis Formation is derived from the farm Etusis 75 where a very considerable thickness of psammitic rocks builds the Otjipateraberge. The locality has been described by Gevers (1931a) and Smith (1965). According to Gevers (1963, p. 204) the Geological Survey made use of the term Etusis Quartzite Member, in the place of what had previously been called Chuos Quartzites by Gevers (1931a) and Smith (1961). The name "Chuos", for glaciogenic sedimentary rocks overlying the quartzites has become entrenched in the literature and is now reserved for these rocks. The Lower Stage of Smith's Nosib Formation (1965) is termed the Etusis Formation in this work.

The term *Khan Formation* is derived from the area of the Lower Khan River where this formation is best developed. Gevers (1931a) and Smith (1961) used the term Khan Quartzites for these rocks, which consist largely of quartzo-feldspathic pyroxene-amphibole gneisses. The Khan Formation, as defined in this work, is the equivalent of the Calc-Granulite Facies of the Upper Stage of the Nosib Formation as defined by Smith (1965).

The metasedimentary rocks overlying the Nosib Group belong to the *Damara Group*. The group consists of mixed lithologies at the base followed by essentially calcareous and then pelitic lithotypes. In the present area the group has been subdivided into five formations. In part, the author has followed the nomenclature of Nash (1971) who studied the lowest part of the Damara succession in considerable detail in the SJ Area, 50 km east-northeast of Swakopmund, where low-grade uranium mineralisation had been discovered. The term *Rössing Formation* is applied to what was previously called the Lower Stage of the Hakos Series. The formation is characterised by rapid lithological variation throughout the sequence.

The *Chuos Formation*, which is the equivalent of the Chuos "tillite" or Middle Stage of the Hakos Series (Smith, 1965), is normally thin and is patchily developed. It overlies older rocks with a transgressive overlap and, in places, it is also found lying unconformably on rocks of the Nosib Group. The name is derived from the Chuos Mountains, which build rugged country north of the mapped area, and along the eastern slopes of which the formation is thickest and best exposed (Gevers, 1931b).

The *Husab Formation* follows conformably on the Chuos Formation. The name is derived from the Husab Gorge which joins the Swakop River six kilometres west of the Witpoortberge-Husabberg range. The general area here is known as the Husab area. The formation is predominantly calcareous in character and is best developed along the Husabberg.

The *Witpoort Formation* conformably overlies the Husab Formation and comprises pelitic schists and gneisses. The name is derived from the Witpoort which is the point where the Swakop River cuts through the marble horizon that builds the Witpoortberge and Husabberg.

The Husab and Witpoort Formations undergo facies changes towards the

east and southeast, and these changes in lithology are taken into account by the introduction of the term *Tinkas Formation*. This formation, found in the southeastern part of the region, is probably the chronostratigraphic equivalent of the Husab and Witpoort Formations in the west and is composed of a mixed calcareous/pelitic sequence of rocks. The formation takes its name from the Tinkas River, which is situated east of the Langer Heinrich and Bloedkoppie, and from the Tinkas Flats, which are extensive sand- and calcrete-covered plains situated just southeast of the mapped region.

The sediments of the Chuos, Husab, Witpoort and Tinkas Formations accumulated under relatively quiet sedimentary conditions in comparison with underlying formations and they are more widespread. The gradational contacts between these four formations, and the transgressive overlap onto successively older rocks in an easterly direction, allows a grouping of them into a subgroup which distinguishes this prolonged unbroken cycle of sedimentation from the more localised, preceding cycles. It is proposed to include the above formations into the *Khomas Subgroup*. The term Khomas has become entrenched in the literature and the bulk of the subgroup (i.e. Witpoort and Tinkas Formations) is composed of rocks that would have been included in the Khomas Series (Martin, 1965; Smith, 1965) in the chronostratigraphic terminology.

The lithology of Damara and Nosib rocks is briefly summarised in Table 2.

Large parts of the area are underlain by a variety of igneous rocks of different ages. The ultrametamorphic equivalent of the rocks of the Nosib Group is the Red Granite-Gneiss while that of the Damara Group is the Salem Granite Suite. Most of the other granitic rocks are very late tectonic to post-tectonic in age and have been given a variety of names in order to facilitate description. The Bloedkoppie, Achas and Gawib Granites occur in the form of stocks, the Horebis Granite and Alaskitic Pegmatitic Granite as irregular small bodies and veins and the Donkerhoek Granite as large batholithic masses. This last granite occupies only a very small area on the map. Most of it is found outside of the mapped area to the southeast and east. Pegmatites are widespread in the area and they will be discussed in detail in chapter 6.

2.2. Nosib Group

Rocks which have been assigned to this group crop out fairly extensively in the area under consideration and also to the north and northeast (Smith, 1965; Gevers, 1931a; Gevers, 1963). In general the rocks are psammitic in character and, being resistant to erosion, build hilly country or conspicuous landmarks such as the Langer Heinrich.

2.2.1. Etusis Formation (Ns_1)

This formation is found in anticlinal and dome structures. Although it underlies the Khan Formation it does in part display a lateral change to Khan Formation lithotypes as is clearly shown on Smith's map to the north of this area. Lithologically, the Etusis Formation exhibits greater variation than previous authors have indicated. Quartzites and conglomerates are very

Table 2. Summary of lithology of the Nosib and Damara Groups.

		Formation	Lithology
DAMARA GROUP	Khomas Subgroup	Witpoort in west Tinkas in east	Witpoort: pelitic and semipelitic migmatitic biotite schist and gneiss containing cordierite, K-feldspar, sillimanite, almandine; migmatite; minor calc-granofels. Tinkas: biotite schist containing muscovite, cordierite, andalusite, sillimanite, almandine, staurolite, hornblende; calc-granofels; marble; para-amphibolite.
		Tinkas in east Husab in west	Tinkas: see above Husab: pelitic schist; calc-granofels; calc-silicate gneiss; dolomitic and calcitic marble.
		Chuos	Schistose diamictite containing inclusions of igneous and sedimentary origin.
		Rössing	Pelitic schist and gneiss containing cordierite, K-feldspar, sillimanite, almandine; marble; quartzite; conglomerate; calc-granofels.
Para- and unconformity			
NOSIB GROUP		Khan	Hornblende-biotite schist and gneiss; migmatitic banded and mottled quartz-K-feldspar-plagioclase-clinopyroxene-hornblende gneiss.
		Etusis	Quartzite; conglomerate; quartzofeldspathic gneisses containing sillimanite, cordierite, biotite; banded quartzofeldspathic clinopyroxene-hornblende gneiss; migmatite; pelitic schists; minor marble.

common and a variety of paragneisses and schists are also found. In many places granitic gneisses have formed from feldspathic quartzites, as for example in the Ida dome, west of the Ida Mine, where distinction becomes difficult.

A conspicuous anticline occurs on the northwestern side of the Swakop River on Vredelus 112 and east of Modderfontein 131. This is made up of a large variety of rock types belonging to the Etusis Formation and presents the most complete stratigraphic section to be found in the area. It is not possible, however, for accurate measurements of thickness to be made because of the very intense degree of deformation.

In the core of the anticline, red augen gneisses and red gneissic granites are found, which, in places, are distinguished from later intrusive granites only with difficulty.

Immediately overlying the augen gneisses, on the eastern side of the core, are red and grey quartzofeldspathic gneisses of the Etusis Formation. The contact is not everywhere sharp as interfingering of the augen gneisses and the other gneisses occurs. On the western side of the core the augen gneisses are overlain by conglomerate bands.

Upwards, grey to pale green quartzofeldspathic clinopyroxene-amphibole gneisses, similar to those of the Khan Formation are encountered, interbedded with quartzites and conglomerates. These rocks are followed by a thin, but laterally persistent zone of pelitic schists, migmatites, marbles, calc-granofelses (Goldsmith, 1959) and quartzites. These rocks are rather similar to those of the Rössing Formation.

The above sequence is overlain by a succession of grey and pink quartzites, interbedded with quartz-feldspar-clinopyroxene-amphibole gneisses, quartzofeldspathic biotite gneisses and thin amphibolite bands. They are followed by pebbly and pink quartzites. These pink quartzites form a prominent hill close to the Swakop River just east of the boundary between Vredelus 112 and Horebis Nord 61. They also form the Salemberge at the nose of the anticline.

On either side of the Vredelus 112/Horebis Nord 61 boundary the quartzites just mentioned are overlain by a succession of rocks which is not found further southwest towards the Salemberge. These rocks comprise interbedded red feldspathic and grey quartzites, and biotite schists with several thin para-amphibolite beds. Marble bands were not found in the succession. The rocks pinch out southwards close to the Swakop River. Smith's statement (1965, p. 17) that "southeast of the Swakop River ... (the quartzite) becomes subordinate to thinly bedded quartz-biotite schist ..." probably refers to this sequence.

The intercalated quartzite/biotite schist zone is overlain by a rather conspicuous gneissic rock which is found on Horebis Nord 61 and along a lengthy portion of the anticline on both the eastern and western sides. The rock is a highly deformed migmatitic gneiss containing abundant quartz-feldspar "augen" which, in places, resemble pebbles and boulders. On the eastern side of the anticline, 4 km southwest of the Zebraschlucht, the gneiss contains boulders of several rock types, including one of schist, 60 x 80 cm

in size. A superficial resemblance to the Chuos rocks is apparent. However, because of the intense deformation and migmatisation its correlation with the Chuos Formation is most uncertain and it has been included in the Etusis Formation. A similar gneiss has also been recognised in places southeast of the Swakop River.

Marbles of the Husab Formation overlie the Etusis Formation, in places unconformably, on both the eastern and western sides of the anticline.

On the southeastern side of the Swakop River the Etusis Formation builds hilly country and outcrops in the form of a southwesterly trending anticlinorium extending from Rooikuiseb 109 to the Tinkas River. The peaks of the highest hills rise more than 700 m above the Swakop River.

Pink resistant quartzites are more abundant here than on the northwestern side of the Swakop River and more extensive exposures of metasediments, reconstituted to Red Granite-Gneiss, are found.

The succession from the lowest exposed horizon upwards is as follows. In the core of the anticlinorium dark grey quartzites and remnants of amphibolite occur besides the Red Granite-Gneiss, which is normally an augen gneiss and in which lenticular remnants of quartzite (not shown on the map) are found. Feldspathic quartzites, migmatites, biotite and hornblende-biotite schists and quartzofeldspathic biotite-sillimanite and clinopyroxene-hornblende paragneisses overlie the Red Granite-Gneiss. These are followed by red augen gneisses and then by more quartzites, together with migmatitic schists and quartzofeldspathic biotite-sillimanite and clinopyroxene-hornblende gneisses. The biotite schist/quartzite alternation already described along the Vredelus 112/Horebis Nord 61 boundary occurs in places on the southeastern side of the Swakop River. Where this succession is developed, the contact between the Etusis Formation and the Tinkas Formation, particularly on Horebis Süd 108, is difficult to ascertain. This is because the marbles of the Husab Formation are no longer present and intrusion of Salem and Horebis granites has complicated the picture. A similar zone of rapidly alternating quartzites and schists occurs in a syncline northeast and southwest of the point where the farm boundary separating Rooikuiseb 109 from Wilsonfontein 110 crosses the Achas River. Here early pegmatitic mobilisates have been boudinaged and disrupted and the rocks are migmatitic in character. Extrapolation of this zone further to the northeast beyond the mapped area links up with a syncline mapped by Smith (1965) in which rocks of the Tinkas Formation crop out. The presence of pink and grey quartzites interbedded with the schists in the syncline at the Achas River has led the author to include all those rocks in the Etusis Formation. Similar quartzites do not occur in the Tinkas Formation on the southeastern side of the anticlinorium.

Along the southeastern margin of the anticlinorium, in the vicinity of the Aram Mountains and further to the northeast, the uppermost part of the succession consists of fine-grained, micaceous, quartzofeldspathic gneisses, rich in microcline. These rocks resemble porphyritic acid volcanics but in most places recrystallisation and deformation have destroyed original textures and structures.

Further to the northeast, on Rooikuiseb 109, in the area mapped by Smith (1965), similar rocks occur at about the same stratigraphic level.

Here recrystallisation has not obliterated original features to the same extent and the rocks show a strong resemblance to quartz-feldspar porphyries. Thin conglomerate bands are interbedded with some of these fine-grained gneisses. Similar rocks are not found at the top of the Etusis Formation along the northwestern margin of the anticlinorium on Horebis Süd 108.

Acid volcanic rocks have so far not been reported from the Etusis Formation in this part of Damara belt, but reports of volcanic horizons in the other areas exist. Frets (1969) in discussing volcanic rocks of the Naauwpoort Formation suggested a possible correlation with either the Khoabendus- or the Nosib Formation. Miller (1972) gave a detailed account of the Naauwpoort volcanics and he presented strong evidence for regarding them as part of the Nosib Group. The author has studied samples of the Naauwpoort volcanics, provided by Dr. Miller, and their mineral compositions and textures are nearly identical to those in samples from the Aram Mountains and Rooikuiseb 109.

The Langer Heinrich forms a conspicuous landmark south of the Swakop River where the psephitic and psammitic character of the Etusis Formation is well displayed. There is very minor development of Red Granite-Gneiss and the rocks are generally feldspathic and gritty quartzites, pink to reddish in colour, with thin interbeds of epidote-bearing quartzofeldspathic gneisses. Conglomerate bands occur in many places in the succession, and their thickness varies from a few centimetres to composite bands greater than 15 m. The conglomerates are normally oligomictic with quartz being by far the most common pebble type, but pebbles of quartzite, chert and amphibolite are also found. The pebbles are well-rounded and reasonably well sorted but have been considerably stretched out and deformed so as to resemble "augen". They are generally 2 to 3 cm in size with some conglomerates carrying cobbles up to 10 cm in diameter.

At the southern tip of the mapped area the Etusis rocks form the Rabenrücken. The rocks here are feldspathic cross-bedded quartzites with thin bands of quartzofeldspathic augen gneiss, quartz-feldspar-pyroxene-hornblende gneisses and conglomerates, which have been intensely deformed. The conglomerates are not as clean as at the Langer Heinrich and not as well sorted. The pebbles consist of quartz, biotite schist, amphibolite, granite and pale coloured amphibole-rich gneiss. Feldspar porphyroblasts have grown in the matrix, giving the conglomerates a rather attractive appearance.

A limited area of Etusis Formation outcrop has been mapped on Vlakteplaas 110 where relief is low and where much of the ground is sand-covered. Pink feldspathic quartzites and fine-grained red quartzites that are similar to aplites in appearance are the most common rock types next to minor amounts of quartzofeldspathic pyroxene-hornblende gneisses, containing epidote as a retrograde phase. The rocks assigned to the Etusis Formation at the Geisebberge on Bloemhof 109 are similar. Here, well stratified and occasionally cross-bedded quartzites are gritty in places and quartzofeldspathic pyroxene-hornblende gneisses are found in the succession. Sillimanite is commonly found in the more feldspathic varieties and retrograde epidote, where present, lends a pale greenish tint to the rocks.

Near the centre of the mapped area the Etusis beds form a complex dome

which has a general northeast-southwest trend and which extends from the western corner of Modderfontein 131 to south of the Swakop River. The most common rocks here are pink to red feldspathic quartzites which form the most prominent hills, the Rote Adlerkuppe, and surrounding smaller hills. Conglomerates are not developed to the same degree as at the Langer Heinrich but quartz-feldspar-pyroxene-amphibole gneisses, similar to those on Vredelus 112 and in the Khan Formation are again found although not in any great amount. Quartzofeldspathic paragneisses are commonly interbedded with the dominant quartzites, which display cross-bedding.

In the southwestern part of this anticlinal structure, on either side of the Swakop River, the distinction between Red Granite-Gneiss and metasediments is made only with difficulty in the field. Because of this difficulty and the widespread occurrence of the Red Granite-Gneiss the contacts cannot be fixed with precision and a fairly large area has been included as Red Granite-Gneiss. On Modderfontein 131 and Geluk 116, Red Granite-Gneiss appears directly below the Husab Formation marbles and may possibly represent a similar horizon to that described in the Aram Mountains (see p. 10).

On the southeastern side of the dome, north of the Swakop River, and east of Skeleton Gorge the Etusis quartzites are in unconformable contact with overlying metasediments, which are extensively intruded by the Salem Granite and preserved only as thin remnants.

West of the Husabberg the rocks of the Etusis Formation are not topographically prominent and underly a lesser area than in the east because it has mostly been reconstituted to the Red Granite-Gneiss. Here the Khan and Husab Formations build up the hilly country.

West of the Zebraberge and Soutberg only the uppermost part of the Etusis Formation is still preserved, where it consists mainly of quartzites with conglomerate bands. The more feldspathic layers of quartzitic rock are found to be recrystallised into gneisses and migmatites.

The dome structure just west of the Ida Mine reveals a variety of rocks belonging to the Etusis Formation and on the western side contact relationships with the Khan Formation are well displayed. From the top downwards the Etusis sequence consists of pink quartzites, which grade downwards into migmatitic quartz-feldspar-biotite gneisses, and which are underlain by red granitic gneisses, in places showing augen structures. Several zones of gneisses similar to those of the Khan Formation are also found.

Much of the dome has been mapped as Red Granite-Gneiss although quartzite remnants are not uncommon. In addition to the Red Granite-Gneiss much Alaskitic Pegmatitic Granite (G_4) is found here and because of the great difficulties in distinguishing between the two rock types in the field the outcrop areas of the Alaskitic Pegmatitic Granite are not shown on the map. Its presence is indicated by the designation G_4.

In the vicinity of the Husab Mine outcrops are generally covered by a thin veneer of sand and gravel. East of the mine, psammitic rocks of the Etusis Formation consist of quartzites, sillimanite gneisses, quartzofeldspathic gneisses and schists.

Pink quartzites, which continuously show gradations into Red Granite-

Gneiss, and which are intruded by Alaskitic Pegmatitic Granite occur on either side of the Husab Gorge. It is uncertain whether these rocks belong to the Etusis or Rössing Formations.

2.2.2. Khan Formation (Ns_2)

The rocks of this Formation consist of quartz-feldspar-clinopyroxene-amphibole gneisses, in places carrying garnet, and they are generally somewhat migmatitic in character.

The Khan Formation overlies the Etusis Formation with a gradational contact, which is clearly displayed in several places. At the Geisebberge, for example, the Etusis quartzites and Khan Formation gneisses alternate with each other over a width of about ten metres. North of the Swakop River at the Soutberg, just west of the Ida dome, pink quartzites and gneisses alternate with green pyroxene-hornblende gneisses and quartzofeldspathic-biotite gneisses of Khan type. Proceeding upwards the bands of Khan gneiss become thicker and the quartzites die out.

The Khan Formation was originally mapped by Gevers (1931a) as the Khan Quartzite. However, although quartz is present, it makes up less than 50 per cent of the rock; untwinned plagioclase is common and this resembles quartz on cursory inspection. Nash (1971) described the rocks as basic gneisses but the term is not quite appropriate as quartz is common and the silica content normally exceeds 60 per cent (Nash, 1971; Table 7). In hand specimen the rocks are banded with quartzofeldspathic and mafic layers (Pl. 1), or they have a mottled appearance. Migmatisation has occurred both parallel to the banding and as unoriented irregular pods in the form of granitoid, quartzofeldspathic mobilisates that contain small amounts of pyroxene and/or hornblende. More appropriate terms are banded gneiss, and mottled gneiss for the stictolithic varieties. From a distance the hills formed by these gneisses have a bluish-grey appearance, giving rise to names such as Blauer Heinrich (Smith, 1965). Thin layers of hornblende-biotite schist are present towards the top of the succession.

The Khan Formation has been recognised as such only west of the Husabberg-Pforteberg range. Smith (1965) did not encounter this horizon southeast of the Otjipateraberge-Chuos Mountains range but he found that the Upper Stage of the Nosib Formation (now Khan Formation) is widely and thickly developed towards the west. This also holds for the present area but it should be remembered that rocks similar to those of the Khan Formation occur interbedded with Etusis quartzites further east in the Vredelus anticline. Thus similar depositional environments existed during Etusis times in the east and later during Khan times in the west.

The greatest development of these rocks is in the Zebraberge and Soutberg. The former hills received their name from the intrusion of pale-coloured granite and pegmatite veins into dark Khan gneisses resulting in a streaky or striped appearance from a distance. Several hundred metres of banded gneisses are preserved in a syncline but accurate estimates of the thickness cannot be made because the full thickness is not exposed. Difficulties in estimating thickness also exist on the eastern side of the dome,

in the Ida mine area, where only remnants of the Khan gneisses are still preserved.

Just east of Arcadia 80 the gneisses are preserved in a tight syncline that crosses the Swakop River. These rocks were originally mapped by Gevers (1931a), during a reconnaissance survey, as intrusive diorite. However, although the banding here is not quite as conspicuous as in the Zebraberge, the gneisses are definitely part of the Khan Formation.

Along the western slopes of the Husabberg a well developed horizon of strongly foliated quartz-feldspar-biotite gneiss is exposed, and it was found difficult to place these beds into any of the mapped formations. This gneiss underlies the Chuos and Husab Formations, which here appear to be of lower metamorphic grade, judging from the appearance in hand specimen, and it underlies at least part of the Rössing Formation. On the flats at the foot of the Husabberg it appears to overlie the Etusis Formation, and it has consequently been included into the Khan Formation, but there remains some doubt about this classification because biotite is not very common in the Khan Formation. Furthermore, sillimanite occurs in these gneisses but has not been found in other exposures that are certainly correlated with the Khan Formation. On the other hand, however, Nash (1971) reported amphibole-biotite schists from the top of the Khan Formation in the SJ Area, to the northwest, beyond the Khan River, and on the northern slopes of the Husabberg exposures of biotite amphibolite occur in addition to the quartz-feldspar-biotite gneisses.

2.3.Damara Group

The Damara Group comprises, for the most part, pelitic and calcareous lithotypes and thus differs from the Nosib Group which is predominantly psammitic in character.

The Group has been subdivided as in Table 1 and Figure 1 and the various formations will be discussed in their lithostratigraphic order.

2.3.1. Rössing Formation (D_1)

This formation forms the base of the Damara Group in the western part of the area under consideration and is recognised only to the west of the Husabberg. The rocks must have been deposited under conditions of constantly changing environment since the succession includes a large variety of different lithotypes such as marbles, quartzites, conglomerates, migmatites, calc-granofelses, cordierite gneisses, biotite-cordierite-sillimanite-K-feldspar gneisses and, locally, clinopyroxene-hornblende gneisses, similar to those of the Khan Formation.

Nash (1971) presented a detailed subdivision of part of the Rössing Formation in the SJ Area of the Rössing Uranium Mine and Smith (1965), who mapped the formation over a much larger area, emphasised the variability of the stratigraphy in different places.

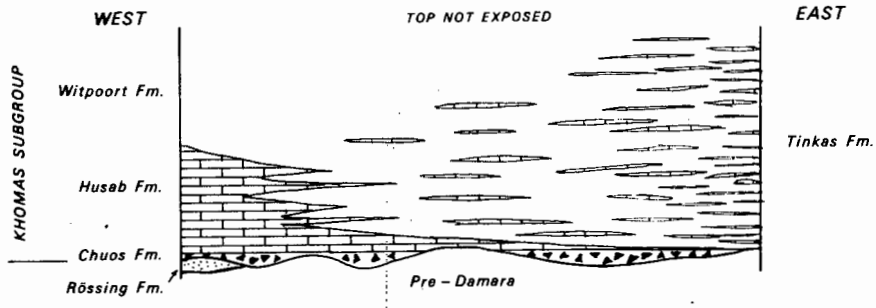

Figure 1. Schematic section showing the various formations of the Damara Group, and in particular the relationship between the Husab, Witpoort and Tinkas Formations.

In the mapped area, the upper part of the succession, consisting of pelitic and psammitic metasediments as illustrated by Nash (1971, Folder 1), appears to be well developed at the expense of the marble horizons, which are subordinate in amount.

A reasonably complete, albeit thin, succession is exposed along the western limb of a syncline in the shallow valley between the Soutberg and Gürtel Hills. Deformation has probably resulted in thinning of the formation at this locality. The contact between the Khan and Rössing Formations is partly obscured by sand but appears to be conformable and perhaps even gradational. Smith (1965) and Nash (1971) reported similar relationships.

The following true thicknesses were measured (from the top downwards):

37m Microcline-cordierite gneiss, strongly foliated and porphyroblastic

33m Pebbly quartz-biotite schist

80m Quartzite with bands of sillimanite gneiss

4m Marble and calc-granofels

3m Quartzite with lenses of cordierite gneiss and sillimanite gneiss

5m Marble and calc-granofels

6m Quartzite

34m Gritty quartzite with intercalations of quartzofeldspathic biotite gneiss and quartzofeldspathic hornblende gneiss.

Just north of the Ida dome outcrops are partly sand covered. The contact with the Khan Formation is again established only with some difficulty. It is quite apparent that the Rössing Formation metasediments pinch out and are cut off by a well-developed marble horizon. The exact stratigraphic position

of the marble is uncertain but it is assigned to the Husab Formation for the following reasons:

(a) marble bands are only weakly developed in the Rössing Formation just east of the Soutberg,

(b) the Husab Formation contains a considerable thickness of marble in the Gürtel Hills just to the west, and in the Welwitsch Hills 8 km to the northeast,

(c) east of this marble occurs the Salem granite, which represents reconstituted Witpoort Formation. The Witpoort Formation, which immediately overlies the Husab Formation at the Husabberg, is also found directly overlying the above-mentioned marble band in the Swakop River south-southeast of the Ida Mine.

A belt of very highly deformed and disrupted rocks of the Rössing Formation trends southwards from the Welwitsch Hills towards the Swakop River. This formation is here represented by the following rock types which are repeated by recurrent isoclinal folding. The rock types are marble, calc-granofels, K-feldspar-cordierite-sillimanite gneiss sometimes containing appreciable amounts of magnetite, conglomerate, then para-amphibolite, biotite-amphibolite, hornblende-biotite schist, migmatite, quartz-feldspar-biotite gneiss and schist and banded pink and grey quartzite (± sillimanite). Marble bands appear at different stratigraphic levels and have been disrupted by deformation so that they are now found as lenticular unconnected bodies.

Along the eastern slopes of the Welwitsch Hills sillimanite-bearing psammitic gneisses and quartzites are found together with thin conglomerate bands.

In the general area of the Husab Gorge, anatectic effects, granite and pegmatite intrusion and intense folding make correlation an extremely difficult exercise. It is difficult to distinguish between Husab and Rössing marbles or between Etusis and Rössing quartzites. The transformation of many psammitic and pelitic rocks into Red Granite-Gneiss is very advanced in most places, and only skialiths (Goodspeed, 1948) and, in places, more or less continuous lenses of marble, calc-granofels, grey, red and brown sugary quartzite, quartz-biotite schist, banded gneisses and biotite-hornblende schist remain of the original sequence. The Etusis, Khan and Rössing Formations are all represented here.

A narrow, discontinuous zone of red, sugary quartzites occurs along the western slopes of the Husabberg and can also be seen along the banks of the Swakop River. The rocks overlie the quartzofeldspathic biotite gneisses, which were discussed on page 13.

In summary, the Rössing Formation is characterised by rapid variations in lithology and substantial changes in thickness over relatively short distances. It has not been recognised as a mappable unit east of the Husabberg. Deposition probably took place in local depositories of limited extent. The variation in thickness is possibly due, to some extent, to erosion prior to deposition of the Chuos Formation (Smith, 1965) and/or the Husab Formation.

2.3.2. Chuos Formation (D_2G)

Martin (1965) considered this formation to be a substage of the Hakos Series whereas Smith (1965) gave it the status of a stage of that series. Schalk and Hälbich (1965) and de Waal (1966) proposed that the boundary between the Hakos and Khomas Series be taken at the base of the Chuos glacial horizon and this suggestion effectively placed the Chuos "tillite" in the Khomas Series. These authors referred to a minor but regionally extensive discordance at the base of the glacial bed. Hälbich (1970) included the glacial horizon as a member within the Khomas Series whereas Nash (1971) and Miller (1972) recognised a Chuos Formation which is equivalent to the Chuos Tillite (Gevers, 1931a, 1931b), Tillite Substage (Martin, 1965) and Chuos Stage (Smith, 1965). Because the term Chuos is so well entrenched in the literature the author has adopted the name Chuos Formation as the lithostratigraphic term for the pebble- and boulder-bearing schistose unit to be described in the following paragraphs and which is a correlate of the "Chuos Tillite" as described by Gevers (1931b).

In the mapped area the Chuos Formation is only locally present but has proved to be a very useful marker horizon. It follows paraconformably on a variety of older rocks, with the overlapping contacts well exposed at various localities. For example, at the Gürtel Hills the glacial horizon overlies the Rössing Formation, along the Husabberg it follows on the Khan Formation and at the Langer Heinrich it overlies the Etusis Formation.

The formation is most prominently developed on the northern slopes of the Langer Heinrich where the thickness varies from zero to 250 metres. The rock consists of angular and subrounded boulders and cobbles, mainly of granite and quartzite, scattered throughout a schistose matrix. Migmatisation has occurred and the clasts have been deformed so that in places tectonically stretched pebbles and quartz-rich secretion lenses resemble one another. Towards the top of the Chuos smaller clasts are common and the rock eventually grades into schist of the Tinkas Formation. On the western slopes of the Langer Heinrich metamorphism has caused the rock to take on a gneissic appearance. Where the Chuos Formation is cut by the Gawib River the succession bears but little resemblance to the more typical exposures described above. Here it is essentially a schist with lenticular pebbles and disrupted secretion quartz veins.

Along the western slopes of the Rabenrücken the Chuos rocks bear a strong resemblance to the Dwyka tillite. The formation here has a thickness of 100 to 150 m and the micaceous-quartzitic matrix surrounds an assortment of clasts of rather irregular to rounded shape which have been somewhat flattened by deformation. Generally the clasts are not larger than 0,3 m in diameter but sizes approaching 1 metre were measured in places. The clasts consist of Etusis quartzite, vein quartz, pink granite, sugary quartzite, leucogneiss, biotite gneiss and aplite. Upwards in the succession the inclusions decrease in size and eventually they disappear so that a gradational contact exists between the Chuos and Tinkas Formations.

The base of the Chuos Formation at the Rabenrücken rests with a conspicuous unconformity on the Etusis Formation quartzites and psammitic gneisses. The angle between bedding in the Etusis Formation and the Etusis-Chuos contact

reaches 63° but is normally less.

Elsewhere in the area the Chuos Formation is thin or missing altogether. Along the southeastern side of the Rooikuiseb anticlinorium, between the Tinkas and Onanis Rivers, it is generally less than six metres thick and along the northern and western slopes of the Husabberg the thickness varies between zero and 3 to 10 metres. It contains clasts generally less than 15 cm in size, overlies the Khan Formation biotite gneiss paraconformably and grades upward into the Husab Formation through a semipelitic zone of schists.

Outcrops of the Chuos Formation are very sporadic in the area and, although the rocks are unbedded and unsorted, there is no strong evidence for a glacial origin as primary textures and structures have been virtually obliterated during deformation and metamorphism. Nevertheless, the correlation of these metasediments with the Chuos Formation, along the Chuos Mountains, is not doubted. Several terms have been suggested in the literature for tillite-like rocks of uncertain or unknown origin, and appropriate terms for the rocks described above are diamictite (Flint et al., 1960), mixtite (Schmermerhorn, 1966; Kröner and Rankama, 1972) or tilloid in the sense recommended by Harland et al. (1966).

Martin (1965) has suggested that much of the Chuos Formation is glacial-marine in origin. The general decrease in clast size upwards and the lack of any glacial pavements support Martin's view that the Chuos is of glacial-marine origin rather than a moraine, if a glacial origin is accepted. Miller (1972) demonstrated a glacial origin for the Chuos Formation in the Omaruru area.

2.3.3. Husab Formation (D_3C)

The Husab Formation is the lithostratigraphic equivalent of the Upper Stage of the Hakos Series, in the vicinity of the lower Khan River, as mapped by Smith (1965). In the area under consideration the Husab Formation consists of a relatively thin sequence of mixed pelitic and calcareous rocks, overlain by massive marble. The formation is prominently developed in the western part of the area where it generally forms elevated country. In many places it forms lines of low hills or individual inselbergs that stand out above the sand and calcrete flats, e.g. in the Welwitschia and Gawib Flats and, in particular, south of the mapped area, in the Tubas Flats. The marbles form the range of hills that includes the Witpoortberge, Husabberg and Pforteberge which form such conspicuous landmarks and which show up so clearly on satellite photographs of this part of the Namib Desert (Haughton, 1969, Pl. 1).

At the Husabberg, the Husab Formation overlies the Chuos beds conformably and where the diamictite is not developed it rests paraconformably on the Khan Formation. A representative section is presented below, measured on the northern slopes of the Husabberg.

True thickness in metres	Rock type
300 (variable)	Main massive marble
2,2	Calc-silicate gneiss
2,2	White marble
1,6	Calc-silicate gneiss
2,5	White marble
9,7	Interbedded biotite schist and calc-silicate gneiss
3,3	Mottled calc-silicate gneiss with thin marble bands
11,3	White marble
12,8	Biotite schist with calc-granofels bands
2,4	White marble
5,1	Marble with intercalated schist and calc-granofels

9	Chuos Formation; sandy schist and biotite-hornblende schist, transitional zone grading downwards to diamictite

The sequence varies slightly in different parts of the area due to the lenticular nature of most stratigraphic units. The lower part of the massive marble at the Husabberg is white to creamy in colour. Towards the top it becomes dark grey to blue-grey but this feature is not consistently found throughout the area. The top of the formation consists of interbedded calc-granofels, siliceous marble and chert. The contact with the overlying rocks is conformable.

The main marble makes up most of the formation. Its thickness averages between 200 and 500 metres over long distances along the Witpoortberge -Husabberg-Pforteberge range, but at the Husabberg the thickness is considerably increased, due to flowage of these incompetent rocks into hinge zones of folds. This feature of tectonic thickening is common in the area, as in the Gürtel Hills and Welwitsch Hills, but not all of the variation in thickness is due to deformation. There is a general decrease in thickness of the formation in an easterly direction from the Husabberg.

At the Welwitsch Hills the base has been taken as the first marble band above which no psammitic rocks occur since, in the absence of the Chuos Formation, there is some doubt as to the exact position of the contact. The Husab Formation at the Gürtel Hills comprises biotite schists with thin marbles and calc-granofelses, overlain by a thick coarse-grained marble which grades into the overlying Witpoort Formation through a series of interbedded schists, marbles and calc-silicate rocks.

The Husab Formation directly overlies the Etusis quartzite and psammitic gneisses and frames the dome structure in the vicinity of the Rote Adlerkuppe. Marbles are the most prominent rocks here but minor calc-silicate rock and biotite schist are also present. Close to the Swakop River, at Skeleton Gorge, lenticular remnants of marble are preserved in an isoclinal syncline. The thickness of the formation is generally less than 100 metres and in places, less than 20 metres; locally it may be missing. Xenolithic fragments of

marble persist in the body of Salem Granite which has invaded the central portion of the dome, west of Skeleton Gorge.

Around the Vredelus anticline the Husab Formation is represented by a thin but persistent marble band (0-20 metres) which has proved to be a very useful marker here. It lies paraconformably or unconformably (Horebis Nord 61) on Etusis quartzites and quartzofeldspathic gneisses. On the northern slopes of the Langer Heinrich a thin lenticular marble band (0-3 metres), not shown on the geological map, overlies the Chuos Formation conformably.

In general, the Husab Formation is weakly developed east of the Rote Adlerkuppe dome and the prominent marbles and overlying schists of the Witpoort Formation undergo facies changes eastwards to a sequence consisting of rapid alternations of schist, calc-granofels and thin, generally impure marble bands. Examination of Smith's (1965) description and map shows that a similar situation occurs north of the present area. Smith has used a chronostratigraphic terminology* with the result that the prominent marbles and the mixed sequence of schists and calcareous rocks fall into the Upper Stage of the Hakos Series. This has led to considerable difficulty in interpreting the largely pelitic horizons in the southeastern part of Smith's area.

The lithostratigraphic subdivision adopted here overcomes this problem by recognition of a new formation, the Tinkas Formation, to take account of this facies change. Where the marbles form the base of the Khomas Subgroup in the east they have been placed in the Husab Formation, and where they occur as thin interbeds in a largely pelitic sequence, they become part of the Tinkas Formation. Along the flanks of the Rooikuiseb anticlinorium, southeast of the Swakop River, the Husab Formation is not found but marbles do occur in the metasediments overlying the Etusis Formation. Farther north, on Tsaobismund 85, Smith (1965) has reported 20 marble bands in a zone of biotite schist, 900 metres in thickness.

2.3.4. Tinkas Formation (D_4S)

The Tinkas Formation is found south and southeast of the Swakop River extending from the margins of the Gawib Flats to Horebis Süd 108, Rooikuiseb 109, and beyond the mapped area.

The best exposures of this formation are to be found in the Schieferberge, south of the Langer Heinrich. Here there are rapid alternations of fine-grained pelitic schists, both porphyroblastic and non-porphyroblastic, and thin calc-granofels bands. Marble beds, generally thin, are found in the succession but are subordinate in amount. In the field the rocks have a banded appearance due to the alternation of schist and calc-granofels layers of varying thickness (see Pls. 3 and 12). Figure 2 shows a

---

* At the time, the Geological Survey of South Africa used what is now a chronostratigraphic nomenclature for lithostratigraphic subdivisions. Truswell (1967) has reviewed the reasons for this policy.

representative sequence of these banded rocks as measured at the Schieferberge.

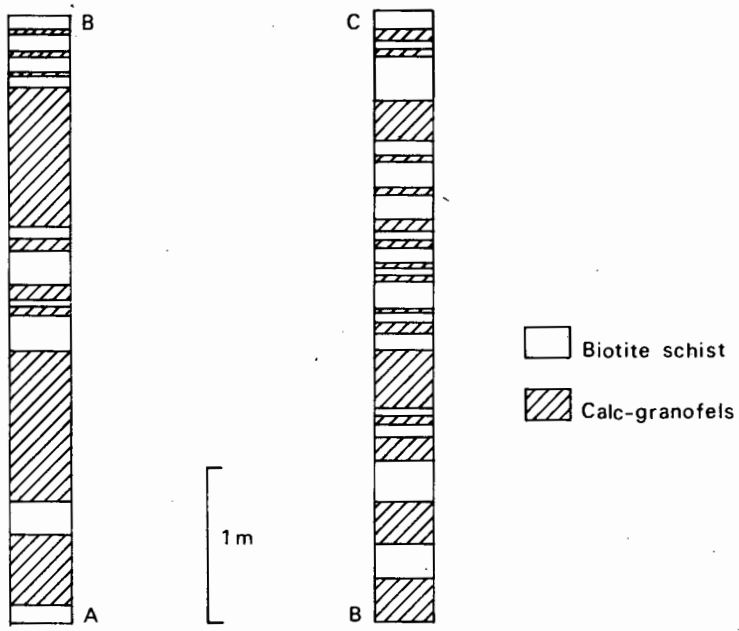

Figure 2. Section through part of the Tinkas Formation along the Gemsbok River, illustrating the lithological alternation.

Gevers (1931a; 1931b) has termed these alternating bands "ancient varves" and thought that they were deposited on his Chuos Tillite. The rocks, however, cannot be interpreted as varves because of the thickness of each layer and because of strongly contrasting mineralogy of the alternating bands.

In places the calc-granofels bands have behaved more competently during folding than the schists and have been boudinaged and also transposed into lenses in B_2 fold hinges (see Pl. 4).

On Horebis Süd 108 the Tinkas Formation consists mainly of schists, with interbeds of marble and calc-granofels, and does not display the prominent banding of the Schieferberge occurrences. The schists are migmatitic in character and are extensively veined by intrusive Salem Granite and pegmatite. Ptygmatic quartz veins are also frequently found. The calc-granofels and marble bands have resisted melting and migmatisation and are still preserved, although deformed. On Horebis Süd 108 there is some difficulty in placing the exact contact between the Etusis and Tinkas Formations because the top of

the Etusis consists of schists with interbedded quartzite while the base of the Tinkas also consists very largely of schists. In this case the contact has been taken at the first marble or calc-granofels band in the succession. On the southeastern side of the Rooikuiseb anticlinorium contact relationships are generally quite clear.

The belt of Tinkas Formation rocks extending from Wilsonfontein 110 southwestwards to the Schieferberge is remarkable for its uniformity and the persistence of individual lithological units. It is noteworthy, however, that near the southeastern boundary of the map, in the vicinity of the Hottentottenkirche and southwest of the Wilsonfontein 110/Namib Desert Park boundary, the rocks take on a rather different appearance with the amount of calc-granofels decreasing and the schists becoming coarser grained and crumpled. Calc-silicate rocks still occur in the schists but the conspicuous banding is lost. The change in appearance of the schists is due to intrusion of large bodies of Donkerhoek Granite just to the southeast accompanied by pegmatites, related to the intrusion of the granite.

Smith (1965) has placed the contact between the Hakos and Khomas Series more or less at the stratigraphic level where the amount of calc-granofels diminishes but an examination of aerial photographs and outcrops in the field shows that this has not been done consistently.

It is apparent that the Husab and at least the lower part of the Witpoort Formations have undergone a sedimentological facies change from thick calcareous and pelitic lithologies in the west to thinly interbedded mixed calc-silicate and pelitic rocks in the east and southeast. The Tinkas Formation thus occupies the position of the Husab and Witpoort Formations and is to be correlated with them.

Further to the east, in the Khomas Hochland, beyond the outcrop of the Donkerhoek Granite, Porada (1973) has described calc-silicate layers and lenses in the Khomas Series. These layers do not occur towards the top of the succession in an area west of Windhoek. The calc-silicate bodies described by Porada are neither as abundant nor as continous as those in the Tinkas Formation.

2.3.5. Witpoort Formation

The Witpoort Formation is the equivalent of Smith's (1965) Khomas Series and comprises pelitic schists and gneisses which are found west of Jakalswater 13. Because of its susceptibility to erosion it forms valleys and subdued topography. It is not as extensively developed as in the Khomas Hochland, and this is largely due to the fact that its place has been taken, through ultrametamorphism, by the equivalent Salem Granite (see p.151). Almost everywhere in the Damara Belt the Salem suite of granitic rocks is found at the stratigraphic level of the Khomas Series (Martin, 1965; Smith, 1965; Miller, 1973) and were it not for its presence, the central part of the mapped area would consist very largely of the Witpoort Formation.

The Witpoort Formation consists essentially of quartz-biotite schists, biotite schists and knotty, porphyroblastic cordierite-biotite schists,

In the Rote Adlerkuppe dome the Gn_1 is similar to that farther west, and metasedimentary remnants are common. Where the Klein Gawib River enters the Swakop River Red Granite-Gneiss and Salem Granite are virtually in contact with the boundary generally somewhat sheared and occupied by pegmatite but red granite veins from the Gn_1 cut the Salem granite. Thus at least some of the red granitic rocks are younger than part of the Salem Granite.

In the Vredelus anticline the Gn_1 is found both as augen gneiss and as gneissic granite. The rocks are overlain in places by conglomerates, but definite sedimentary contacts were not found. In the vicinity of the Zebraschlucht, however, gradations do exist between Gn_1 and the Etusis gneisses. The conclusion that these rocks do not represent pre-Nosib lithologies here is strengthened by the presence of similar augen gneisses further southwestwards near the nose of the anticline.

The bulk of the Gn_1 in the Rooikuiseb anticlinorium, on the southeastern side of the Swakop River, is composed of red augen gneisses, red granite-gneisses and gneissic granite, which is barely foliated in several places. Here again there is an intimate mixing of the different rock types. Along the Aram mountains the fine-grained quartzofeldspathic gneissic rocks at the top of the Etusis Formation (see p. 9) are underlain by deep-red Gn_1, which differs from other Gn_1 in the Rooikuiseb anticlinorium in its finer grain size, deeper colour, higher microcline- and lower biotite-content. Intrusive contacts were not found but the Gn_1 grades upwards into those rocks thought to be volcanic and may have been derived from the latter.

2.4.2. Salem Granite Suite (Gn_2)

The granitic rocks of the Salem suite occupy a large area in the central portion of the area mapped. The first description was by Gürich (1892) from the neighbourhood of the farm Salem 102 on the banks of the Swakop River and the name has since become firmly established in the South West African geological literature. Nearly everywhere the Salem granites occupy the stratigraphic position of the Witpoort and Tinkas Formations, i.e. they occur above the Husab Formation, or where this is not present, in the east, above the Etusis Formation. The rocks comprising the Salem suite to the north of this area have been described by Gevers (1931a), Smith (1965) and Miller (1973).

The Salem granites weather rather evenly and this has resulted in a somewhat subdued topography with sometimes sand-covered outcrop areas. Exposures in the vicinity of the Swakop River are excellent but deteriorate towards the north, as on Geluk 116.

A characteristic feature of the Salem granite is its confinement to originally synclinal structures of the Khomas Subgroup. Equally striking is the dearth of strongly discordant contacts with the country rocks on a regional scale. This led Smith (1965) to the conclusion that the Salem granite is autochthonous and originated through granitisation processes *in situ* during high-grade metamorphism. However, although the granitic rocks are concordant over long distances, discordant contacts do exist locally. At the Rote Adlerkuppe and along the Tinkas River, east of the Langer

Heinrich, cross-cutting contact relationships are quite clear.

The Salem granite suite comprises three members in this area. These are:

(i) non-porphyritic, gneissic granite
(ii) porphyritic biotite granite
and (iii) leucogranite.

2.4.2.1. Non-porphyritic gneissic granite

This medium-grained rock usually forms a partial envelope around areas of the main porphyritic granite phase and displays a marked gneissic structure. It is found along basal contacts of the large granite bodies and is very well developed around the Vredelus anticline, around the Rote Adlerkuppe dome and north and northwest of it.

Between 5 and 6 km southeast of the Husabberg trigonometrical beacon a very early phase of the gneissic granite is found as a hybrid granitoid, formed more or less *in situ*. At this locality the rock is a mobilised nebulitic migmatite in which the distinction between leuco- and melanosomes (Mehnert, 1968, p. 8) can no longer be drawn. The rock is characterised by biotite schlieren and diffuse xenoliths of schist, is pre-F_2 in age (see chapter 3), and is intermediate in appearance between the gneissic granite-proper and Witpoort metapelites.

More common and widespread than this, however, is the gneissic granite, which is a foliated rock of granitic to tonalitic composition. In the east the gneissic granite is generally in sharp contact with the country rocks (Tinkas and Husab Formations), but in the neighbourhood of the Rote Adlerkuppe dome gradational contacts with migmatitic Witpoort schists occur. This is clearly seen just north and northwest of the dome on Geluk 116 and southwest of the corner beacon although exposures are generally poor. The intimate mixing of schist, migmatite and gneissic granite is well displayed in railway cuttings on Geluk 116. Just west and north of the long narrow body of G_5 granite, about 5 km south of where the road crosses the Pforteberg, the well-exposed contact is sharp and concordant. South of the Swakop River, around the southwestern nose of the Rote Adlerkuppe dome, contacts between the gneissic granite, Witpoort migmatites and porphyritic biotite granite are rather nebulous and veining by a younger intrusive granite (G_5) commonly occurs.

2.4.2.2. Porphyritic biotite granite

The non-porphyritic envelope encloses the main granitic body which is a grey to dark-grey porphyritic, medium- to coarse-grained biotite-rich granite. This is the typical "Salem Granite" as described by Gürich (1892), Gevers (1931a) and Smith (1965). Over fairly wide areas, but normally closer to the outer contacts, the rock is foliated and the microcline phenocrysts are then aligned parallel to the foliation, which is commonly parallel to that of the

underlying metasediments. In many places, however, there is no detectable foliation in the granite. The potash feldspar phenocrysts vary in abundance and their size normally ranges from one to five centimetres.

The porphyritic granite is in sharp contact with the gneissic granite around the Vredelus anticline but around the Rote Adlerkuppe dome both sharp and gradational contacts are exposed. Wherever cross-cutting relationships were observed the porphyritic biotite granite is later in age than the non-porphyritic gneissic variety.

In the southern part, along the Tinkas River, the porphyritic granite has a very high biotite content and very clear intrusive contacts with Tinkas rocks are common. Xenoliths of calc-granofels have largely escaped assimilation and persist as lenticular bodies, in many places apparently undisturbed. The country rocks show evidence of contact metamorphic effects with the development of wollastonite in calc-granofelses and hypersthene in pelitic schists. Between the Tinkas River and the Langer Heinrich, local feldspathisation of schists has occurred within several metres of the granite contact. Feldspar porphyroblasts, similar to the feldspar in the granite have grown in the schists, resulting in *dent de cheval* structures. In places the exact contact cannot be accurately determined because the feldspar porphyroblasts increase in abundance while the schist becomes coarser-grained closer to the granite.

Northeast and southwest of the boundary between Horebis Süd 108 and the Namib Desert Park the porphyritic granite intrudes the Tinkas Formation and in places almost appears to be part of a layered succession. The granitic veins lie parallel to the foliation of the schists and have been folded during F_2, indicating that at least part of the Salem suite is early syntectonic in age. Gradational contacts are also found. Around the Achas River non-porphyritic adamellite intrudes the topmost beds of the Etusis Formation but has hardly disturbed them. On both Horebis Nord 61 and Horebis Süd 108 the porphyritic, gneissic granite is extensively invaded by a later intrusive granite, the Horebis Granite.

The Rote Adlerkuppe is one of the few localities where the porphyritic biotite granite is found intruding the Etusis Formation on more than a merely local scale. West of Skeleton Gorge, the southern margin of the granite is in contact with lenses of the Husab marbles indicating limited movement, but a little farther west the granite has assimilated Etusis psammites resulting in the formation of a hybrid reddish coloured granitic rock. The northern margin of this intrusive body is largely defined by a thrust fault. Veins of the granite along Skeleton Gorge are boudinaged and show pinch-and-swell structures.

The contact between the Salem granite and schists of the Witpoort Formation is very clearly exposed in the Swakop River some 1500 m east of the Witpoortberge. The contact is sharp, vertical and roughly parallel to the foliation in the schists but discordant in detail (see Pl. 6). Very close to the contact the schists have been disturbed. The granite at the contact has only a slightly gneissic appearance, is rather finer grained than further away, and phenocrysts are small and scattered.

A fairly small area of porphyritic granite with a somewhat discontin-

uous gneissic envelope is exposed between the Ida dome and the Welwitsch Hills west of the Husabberg. The main body is only slightly porphyritic and has a gneissic structure. Elongated xenoliths of biotite schist are very common and the rock is cut by many aplitic granite veins.

2.4.2.3. Leucogranite

The third member of the Salem suite has not been shown separately on Map 1 but occupies a fairly extensive area within the central part of the Salem occurrences. The leucogranite has a wide distribution on Modderfontein 131, Jakalswater 13 and Geluk 116, but is generally obscured under a thin sand cover. The approximate distribution of the granite is shown in Figure 3.

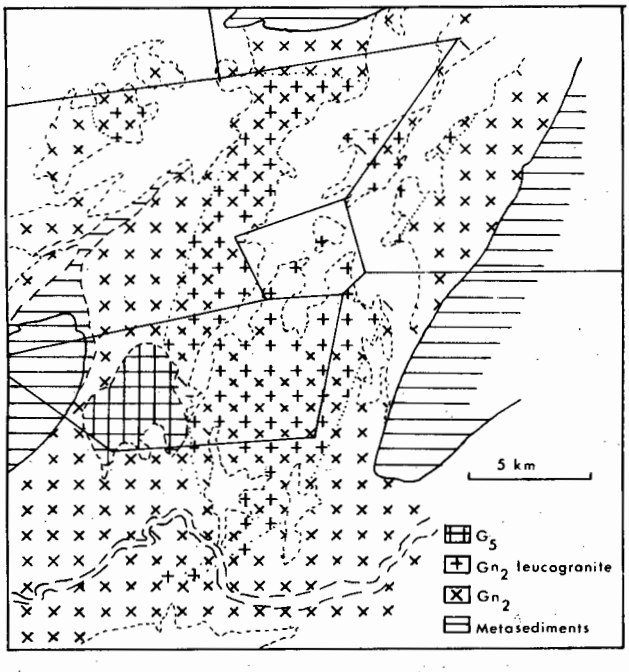

Figure 3. Map showing the distribution of Salem leucogranite. Superimposed ornamentation indicates the presence of both the porphyritic biotite granite and the leucogranite.

It is medium-grained and differs from the porphyritic biotite granite in that it contains a lower percentage of biotite and thus there is usually no difficulty in distinguishing the two rock types. The prefix leuco- has been added to facilitate the description. The leucogranite is also porphyritic but not as notably as the porphyritic variety described earlier. In

places the porphyritic texture is not developed at all, and even where present it is not conspicuous, largely because of the lack of dark minerals. The rock also differs from much of the porphyritic granite in that the leucogranite has only locally a gneissic structure. A feature of the outcrops in many places, especially around Jakalswater 13, is a brown speckling or spotting, scattered throughout the rock, but more common in coarser grained, pegmatitic zones. The spotting is caused by radioactive allanite.

The leucogranite is younger than the porphyritic biotite granite and generally intrudes it with sharp contact relationships. Southwest of the nose of the Vredelus anticline, in the vicinity of the Nabas River, on both sides of the Swakop River, the leucogranite forms wide, occasionally irregular, lenticular patches in the host porphyritic granite.

2.4.3. Basic Intrusives

Post-Nosib basic intrusives are generally found as amphibolites. These are normally dyke-like or sill-like in form and have been boudinaged and disrupted during folding (see Pl. 5). Because of their limited size, most have not been shown on the map. Amphibolites are also found as isolated resisters and xenoliths in the Red Granite-Gneiss near the Khan and Swakop Rivers and at the foot of the Husabberg where their trend is discordant to the foliation. Small dyke-like amphibolites are well exposed along Skeleton Gorge at the Rote Adlerkuppe and are also found in the Vredelus and Rooikuiseb anticlines. Ortho-amphibolites appear to be less common in the Damara rocks. However, the metasediments of the Khomas Subgroup, with the exception of the marble bands, are generally dark in colour and therefore intrusive amphibolites are not as easily recognised here as in the Etusis Formation.

Only two basic bodies have been shown on the map. One is a small intrusive of saussuritised biotite amphibolite occurring 2 km southwest of the Zebraschlucht in the Vredelus anticline and the other is a long, dyke-like body, not everywhere continuous, in the Rooikuiseb anticlinorium, south of the Achas River. This amphibolite is intrusive, it is cut by later pegmatites, and near the Achas River it is associated with a body of quartz hyperite, which is unmetamorphosed and probably of Karoo age.

2.4.4. Bloedkoppie Granite (G_1)

This granite forms the Bloedkoppie, which is a small but prominent exfoliated dome (Pl. 7). The rock is granitic in composition, is medium-grained, contains a small amount of biotite and is weakly foliated at many outcrops.

The granite displays cross-cutting relationships with Etusis and Tinkas rocks. Pre-existing folds and foliations are cut by the granite but the intrusion must have been subtle and quiet because the metamorphites have hardly been disturbed. Small xenoliths of schist are common in the granite. The granite shows no chilling effects at the contact although small feldspar phenocrysts are frequent here and fine-grained apophyses extend into the

metasediments. The country rock schists and calc-granofelses of the Tinkas Formation show virtually no effects of contact metamorphism.

The granite contains aplitic phases which merge into the medium-grained type. Small west-northwest-striking faults are common and thin pegmatite veins are frequently found along the same direction. The pegmatites are younger than the aplitic zones and cut them.

The Bloedkoppie granite strongly resembles the leucogranite of the Salem suite in its pattern of weathering and appearance in hand specimen. However, it is nowhere found in contact with rocks of the Salem suite although at the Tinkas River the two rock types occur in close proximity, separated by less than 500 m of Tinkas schists. It is also exposed close to the Donkerhoek granite 3 km southeast of the Bloedkoppie, just southeast of the map boundary, but here again the two are not found in contact. The appearance of the Bloedkoppie granite is different from that of the Donkerhoek granite in that the former contains biotite as the dominant phyllosilicate while muscovite is more common in the Donkerhoek granite.

2.4.5. Achas Granite (G_2)

This body of granodioritic to tonalitic composition is found in the eastern part of the map on Rooikuiseb 109 and Wilsonfontein 110, where it is intrusive into both the Etusis and Tinkas Formations. In hand specimen the grey medium-grained rock resembles the Salem Granite but it is barely porphyritic.

The granite is not noticeably chilled against the country rocks. Xenoliths of country rock are not uncommon in the granodiorite and are generally most abundant nearer the contact. A narrow contact metamorphic aureole is present around the stock and local metasomatic effects such as *dent de cheval* structure are found in the schists on Rooikuiseb 109.

The mechanism of intrusion also differs from that of the Gawib Granite (see p. 30) because the bedding and foliation of the country rocks have not been forced outwards so as to curve around the stock. For this reason the Achas Granite has not been grouped with the Gawib Granite although both intrusives may be of similar age.

A conspicuous feature west of the centre of the body is a broad curved zone of pale buff-coloured aplitic granite veins. Even more conspicuous, however, is the abundance of eastward trending pegmatites. Pegmatite rubble covers large portions of the outcrops so that, on first appearance, the Achas Granite appears to consist mainly of pegmatite. The pegmatites are a later feature which are related to the intrusion of the nearby Donkerhoek Granite. Intrusion of the Achas Granite has been more forceful than than of the Bloedkoppie granite for the Etusis psammites have been brecciated at the contact and Tinkas schists have been crumpled.

The Achas granite is younger than the Red Granite-Gneiss since xenoliths of the latter are common in the northern exposures. It is, however, older than the Donkerhoek granite as shown above and the weak foliation of the granodiorite suggests a late-tectonic age.

2.4.6. Gawib Granite (G_3)

The Gawib granite occurs as two separate stocks in the mapped area. The larger of these is found just south of the Gawib Flats as an oval-shaped intrusion measuring 8 km by more than 11 km in size and extending southwards beyond the mapped area. The other body occurs 30 km to the north, east of the Pforteberge, around the western boundary of Geluk 116 and measures approximately 6 x 3 km. Compositionally, the Gawib granite varies between granodiorite and granite.

A very characteristic feature is the style of weathering, which differs from that of the Red Granite-Gneiss and the Salem suite. The rocks weather to piles of rounded boulders, resembling tors, while the Salem granites weather to large, low exfoliation domes. The Gawib Granite has a sharp intrusive contact with the surrounding metasediments, whose bedding and foliation surround the bodies more or less concordantly.

The eastern and northern granodioritic margins of the southern stock are strongly gneissic and discordant contacts with Tinkas metamorphites are preserved on the northern side. The gneissic margin is older than the main body of granodiorite/granite and is not present on the western side. The younger granitic rock has a gradational contact with the gneissic granodiorite along the Bonfire River but clear intrusive contacts are found near the Schieferberge and just west of the Rabenrücken, where the later phase cuts across the gneiss and tongues of the main body cut discordantly across Etusis Formation psammites.

The granodiorite/granite in the southern stock is slightly gneissic in places. The texture is somewhat variable; medium-grained porphyritic, and fine-grained, almost aplitic, non-porphyritic phases crop out and contacts between the textural varieties are usually gradational.

The northern stock, near the Pforteberge, is a non-porphyritic slightly gneissic granodiorite which does not have a pronounced gneissic margin like the southern body. The intrusive contact is not well exposed, but where observed it is conformable. The foliation in the Witpoort schists is deflected around the margins of the body.

Contact relationships of the Gawib granite are typical of those found in mesozonal environments as described by Buddington (1959). The two stocks appear to be similar to the bodies of quartz diorite and diorite-gneiss described by Smith (1965), as far as their form and contact relationships with country rocks are concerned. Smith indicated that these rocks are generally older than the Salem granite and are intruded by it (Smith, 1965, p. 47). He was uncertain about the relative ages of the Salem gneiss and the quartz diorite-gneiss but concluded, "as far as can be judged these two gneisses are contemporaneous ...." (Smith, op. cit., p. 49).

The Gawib Granite and rocks of the Salem suite are not found in contact anywhere in the present area. The main differences between the two groups are the weathering pattern and mode of emplacement. The rocks of the Salem suite do not appear to have caused the wall rocks to yield by plastic flowage as the Gawib stocks have done. The Gawib intrusives appear to be late tectonic in age.

2.4.7. Alaskitic Pegmatitic Granite (G_4)

The best development of the Alaskitic Pegmatitic Granite is west of the Husabberg in the area largely underlain by Red Granite-Gneiss although, for reasons already discussed, it has not been separately shown in areas of Gn_1 outcrop.

The rocks are characterised by variable grain size ranging from fine to coarse and by a very low content of dark minerals. Colour varies from white, through pink, to reddish. The granites are of different ages because some are foliated while others are not; most of the G_4 is post-F_2 in age and thin dykes emplaced along B_2 axial planes are commonly encountered (see Pl. 1). Contact relationships with other rocks vary depending on the intruded country rock. In rocks of the Khan Formation clearcut sharp contacts are common, whereas in the Gn_1 contacts may be either sharp or diffuse.

Most of the G_4 is found stratigraphically below the Husab Formation and fairly large bodies are present southeast of the Ida Mine.

Proceeding eastwards the typical alaskite is less common but is still found in the Rote Adlerkuppe and the Vredelus anticline, where the largest bodies are concentrated more or less along the trace of the axial surface of this structure. Thin veins are very common along the Rosagberg and on Vredelus 112. Although the G_4 is found in the Rooikuiseb anticlinorium it is far less common here than in the west, and is present as thin dyke-like bodies only.

2.4.8. Horebis Granite (G_5)

Post-tectonic intrusive granitic rocks which do not fall in any of the previously-mentioned groups have been included in this group. Thus the Horebis Granite category includes a variety of rocks of rather different appearance with the exception of the Donkerhoek granite which is to be described hereafter. The granites are late in age and largely correlate with Smith's category of Red homogeneous granite (Smith, 1965).

On Horebis Nord 61 and Horebis Süd 108 the Salem granite is heavily veined and intruded by a younger pale buff-coloured G_5 granitic rock of variable grain size which anastomoses over a wide area but does not develop large bodies. Its presence is indicated on the map by horizontal widely-spaced dark green ornamentation. Near the boundary between Horebis Süd 108 and the Namib Desert Park, fine examples of agmatic structure are displayed where the granite fills fractures in the Salem granite (see Pl. 8).

Homogeneous reddish intrusive granite has been mapped in the Vredelus anticline. It is more abundant than actually shown on the map, but, due to small size and irregular shape, many of the bodies have not been shown. The Horebis Granite here, together with that along the western margin of the Vredelus anticline, which is intrusive into the Salem granite, is identical in appearance to the Red homogeneous granite around Abie trigonometrical beacon on Marmor 111, as mapped by Smith (1965).

In the Rooikuiseb anticlinorium east of the Tinkas River, the G_5 granite is homogeneous and because of lack of any gneissic structure, and its intrusive character, the rock has been included with the Horebis group, although its appearance is very similar to some of the Red Granite-Gneiss to the northwest. In places where transitional rock types occur the distinction between these two intrusives is almost arbitrary. The Horebis Granite here has a monzogranite composition and contains xenoliths of quartzite and Red Granite-Gneiss.

On the southern side of the Swakop River, near the Rote Adlerkuppe dome, the Salem suite has been invaded by anastomosing G_5 granite veins in the same manner as found on Horebis Nord 61 and Horebis Süd 108.

Northeast of this locality, on Modderfontein 131, a red, aplitic, weakly foliated granite occurs in the form of a small stock. In thin section the rock displays the allotriomorphic granular texture which is characteristic of aplites. This aplogranite is younger than both the porphyritic Salem granite and the leucogranite. A very similar aplitic granite occurs on the western side of the Rote Adlerkuppe dome in the form of a long tongue, intrusive into rocks of the Salem suite and Witpoort migmatites.

Most of the occurrences of the Horebis Granite occur close to, or within, areas of outcrop of Etusis Formation and Red Granite-Gneiss suggesting that much of the G_5 has been derived from these rocks. The reddish colour of many outcrops also lends support to this conclusion. Miller (1972) has described the Sorris-Sorris granite in the Omaruru/Welwitschia area which shows similar field relationships as the G_5 granites and which appears to have been derived from the Naauwpoort Formation, a possible equivalent of the Etusis succession. It is likely that the Horebis granite and the Sorris-Sorris granite can be correlated regarding their respective positions in the tectono-metamorphic history of the two areas. Both intrusives are post-tectonic in age.

2.4.9. Donkerhoek Granite (G_6)

The Donkerhoek Granite occurs almost entirely beyond the mapped area, to the east and southeast, so that only a brief description is given here. The granite has been described by Gevers (1963), who named it, and has also been the subject of a detailed study by Faupel (1973). It differs from most of the previously described granitic rocks in that the most abundant phyllosilicate is muscovite.

The granite has a light buff colour and was emplaced in the form of oval bosses, stocks and bodies of batholithic dimensions. Near the southeastern boundary of the area studied, the foliation and bedding of the largely schistose country rocks have been deflected and crumpled in such a way that they wrap conformably around the oval-shaped masses. Emplacement has thus been forceful in places. Some of the granite is weakly foliated.

A most striking feature of the granite is the tremendous amount of pegmatites which is found close to the contacts. They are far too numerous to be shown on the map and the designation "heavily intruded by pegmatite" has been inserted in such places. In the vicinity of the contacts pegmatites are concordantly emplaced in the schists and both the foliation and pegmatites are arranged concentrically around the dome-shaped G_6 intrusions. To the north-

west, farther from the contacts, the pegmatites change their orientation and trend roughly at right angles to the structural grain of the Tinkas metasediments.

In the present area the Donkerhoek granite is not in contact with any of the other granitic rocks described before. Aplitic veins and small bodies of buff-coloured granite, likely to be of Donkerhoek age, are, however, intrusive into the Achas granite and pegmatites of similar age also cut it. Thus the Donkerhoek granite appears to be younger in age than the Achas Granite. The mode of intrusion and the presence of a contact metamorphic aureole suggest a very late to post-tectonic origin (see Faupel, 1973, p. 333). The granite is certainly younger than the main F_2 deformation.

2.4.10. Pegmatites

Early syntectonic to post-tectonic pegmatites are very abundant in the area, and different types were recognised, e.g. homogeneous, zoned and layered. They are exceedingly abundant near the Donkerhoek granite and in the Witpoort Formation northeast and southeast of the Husabberg, but are present only in small amount in the Salem granites in the centre of the area and in the south, around the Gawib body.

The discussion on pegmatites is left for a later chapter (see p. 154 ff).

2.4.11. Dolerite

The area contains a number of thin dykes and sheets of resistant, hard and fresh dolerite which generally follow a northeasterly trend and cut all pre-existing structures.

The dykes are probably associated with Karoo volcanicity and K-Ar ages determined on whole rock samples collected north and west of the mapped area vary between 114 and 196 Ma (Siedner and Miller, 1968).

2.5. Superficial Deposits

The Welwitschia Flats and the Gawib Flats are underlain by gypsiferous sands and calcrete terrace deposits. The calcretes are gritty in character with small rounded and angular pebbles in a calcareous cement. Remnants of high-level calcrete terraces are also preserved on the southern side of the Langer Heinrich, along streams at Horebis Nord 51, Vredelus 112 and in the general area of the Rooikuiseb anticlinorium. Unconsolidated deposits consist of sand and scree. Scree is found around the Schieferberge and Geisebberge while sand is found along river and stream courses, over large areas underlain by rocks of the Salem suite (e.g., Geluk 116) and banked up against the Pforteberge, Welwitsch Hills, Gürtel Hills and Soutberg. Aeolian sand is most common in the west. Here and there on the Gawib Flats and exposed along banks of the streams, are thin (about one metre) layers of horizontal, unmetamorphosed flaggy sandstone and shale. These may represent uneroded remnants of Karoo rocks.

3. STRUCTURE

The Damara orogen is exposed over a large area in central South West Africa where it displays a prominent northeast trend. In the west, however, to the north and south, the trends are roughly parallel to the coast. The area studied is characterised by northeast-trending structures and its position is shown in Map 1 and Figure 21.

Detailed work has been carried out on the structure of several disconnected areas in this orogen and has been reported in university theses but surprisingly little has been published. Previous work will be reviewed later in this chapter (p. 55) but to date no detailed synthesis of all information on the tectonics of the orogen has been published, largely because of the lack of complete mapping and sporadic distribution of structural analyses.

3.1. Terminology and Methods

Detailed structural analysis in an area of this size and structural complexity demands large numbers of measurements on foliations, lineations, fold axes and axial planes. Because of the non-cylindrical nature (Turner and Weiss, 1963) of the folding, even over very limited areas, it is necessary for small subareas to be delineated and studied separately. During the period of fieldwork the stratigraphy, metamorphism, igneous rocks, pegmatites and uranium mineralisation were also studied and it was not possible for a complete and detailed structural analysis to be undertaken; this account should thus be regarded as introductory.

Much attention was paid to mesoscopic features in a number of small, scattered subareas. These areas are shown on Map 2 (in pocket), which also shows the major structural features. Four vertical sections illustrate the structure in Map 1. However, in areas that have suffered polyphase deformation accurate predictions cannot be made about subsurface extensions of structures (Turner and Weiss, 1963; Whitten, 1966) and, as the complexity of folding cannot be represented adequately in two dimensions, it has been necessary to simplify the structural sections.

At least four phases of folding have been recognised. They have been designated F_1, F_2, F_3 and F_4 from oldest to youngest. Determination of the succession of fold phases was based on the following criteria (cf. Tobisch, 1966):

(i) Refolding of earlier axial planes, axial-plane foliations and lineations
(ii) Orientation of axial planes of folds
(iii) Style of folds
(iv) Recrystallisation accompanying folding
(v) In the case of similar folding the superimposed lineations and fold axes lie essentially in the new axial plane.

Some of the criteria, e.g. (i) above, are more reliable than others,

e.g., style of folds. Conclusions have been based on a combination of criteria rather than on any single one. Park (1969) has discussed the use of these criteria in structural correlation in metamorphic belts and has criticised the use of style, fold orientation and fold symmetry for correlation purposes. Although Park's criticism certainly applies in the case of correlation over large areas these criteria have nevertheless proved useful. Joubert (1971), for instance, found style and fold orientation to be useful in deciphering the structural history of a large area, measuring about 12 000 km^2, in Namaqualand.

The term "foliation" is used here in the sense of Turner and Weiss (1963) and Whitten (1966), embracing "all types of mesoscopically recognisable s-surface of metamorphic origin". The term thus covers slaty cleavage, axial plane cleavage and schistosity. The s-surfaces, including axial planes of folds are designated s_0, s_1, s_2 ..... s_n, the symbol ss being applied to bedding where this can be recognised. s_0 is the earliest recognisable s-surface of tectonic origin and where the relative order of development of other s-surfaces can be determined the subscripts denote that order.

Linear structures that are penetrative in hand specimen or in small exposures are termed lineations here (Turner and Weiss, 1963) and include several varieties: intersections of s-surfaces, aggregates of minerals, deformed pebbles, linear preferred orientation of prismatic or tabular mineral grains and axes of minor crenulations of s-surfaces. Larger linear structures measured include fold axes of mesoscopic folds, mullions and rods. The designations l_1, l_2, l_3, etc. are applied to the above lineations and linear structures, particularly intersection lineations.

Fold axes are designated B. A subscript denotes the fold phase, e.g. B_1.

The following tabulation sets out the terminology used:

Fold phase	F_1	F_2	F_3	F_4
Bedding	ss	ss	ss	ss
Bedding foliation	s_0	s_0	s_0	s_0
Axial-plane foliation and axial planes	s_1	s_2	s_3	s_4
Fold axes	B_1	B_2	B_3	B_4
Associated *b*-lineation	l_1	l_2	l_3	l_4

In many places, as a result of isoclinal folding, it is not possible to distinguish between s_0 and s_1; in such cases the symbol s_{01} is used. A sketch illustrating the s-surface terminology is shown in Figure 4.

All structural data shown on stereographic projections have been plotted on the lower hemisphere of a Schmidt equal-area net. As there are certain limitations to the use of β-diagrams (Ramsay, 1964), π-diagrams have been used as far as possible. The point distributions were contoured by means of a counter recommended by Turner and Weiss (1963, p. 60).

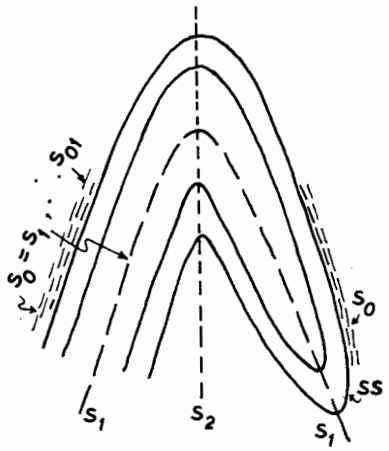

Figure 4. Diagrammatic sketch of B_2 fold superimposed on B_1 fold showing bedding (ss), bedding foliation (s_0), axial plane foliation, B_1 fold (s_1), axial plane foliation, B_2 fold (s_2). The symbol s_{01} is used where s_0 and s_1 cannot be distinguished.

3.2. Structural Data

Deformation during the first and second phases of folding was most intense and the dominant structural trend in the area is northeast-southwest, seen as the result of F_2 folding. Later structures are not penetrative on the same scale as those of F_1 and F_2.

3.2.1. F_1 structures

The earliest phase of deformation represented by penetrative structures, which modify bedding of the Damara Group rocks, has been termed F_1. Earlier tilting or movement must have occurred because unconformities are preserved in places; for example, at the Rabenrücken a 62° unconformity is locally indicative of movement prior to the deposition of the Chuos Formation. In contrast to the findings of Guj (1970), however, no major period of deformation and metamorphism has been found separating the Nosib and Damara Groups in this area.

The Red Granite-Gneiss that crops out west of the Husabberg has not been studied structurally mainly because of the difficulty in obtaining readings on minor structures other than foliation and therefore discussion of the Red Granite-Gneiss and its possible age is left for a later chapter (p.150). Detailed work in that area may reveal fold episodes earlier than F_1.

The F_1 phase was a period of intense deformation accompanied by high

grade metamorphism and migmatisation. During F_1, early flexural-slip folding produced a penetrative regional foliation (s_0), which is parallel to bedding, where the latter can still be recognised (bedding foliation). Further deformation resulted in the formation of an axial plane foliation (s_1) which is parallel to s_0 in the limbs of isoclinal B_1 folds. The gneissic foliation of most paragneisses, including that of the banded gneisses of the Khan Formation (see p. 91), formed during F_1. In places it is s_0 but in others it is s_1. Linear structures of F_1 age (l_1) are difficult to recognise because of the parallelism of ss or s_0 and s_1 and recrystallisation during subsequent metamorphism and deformation.

s_1 is axial planar to mesoscopic isoclinal folds of s_0 which are commonly observed on close inspection of outcrops (Pl. 9). Axial planes of B_1 folds display a variety of orientations as a result of later deformations. In the core of the Vredelus anticline and the Rooikuiseb anticlinorium, recumbent isoclinal folds of F_1 age are clearly exposed (Pl. 10) where s_1 and s_0 are parallel along the limbs of the fold but not in the hinge area.

Macroscopic B_1 folds are not easy to recognise because of the similarity in style of B_1 and B_2 folds and in places because of their similar orientation. The Arysap Hills syncline and the Rote Adlerkuppe dome possibly represent B_1/B_2 interference structures (see Map 2). F_1 structures are well developed west of the mapped region in the form of the Nose Structure anticline, Welwitsch syncline and Rössing Mountain structure (Smith, 1965).

Figure 5 (a) shows a contoured plot of poles to ss and s_0 from the Gürtel Hills syncline (5. in Map 2) and Figure 5 (b) a contoured plot of poles to s_1 measured in schists at the same locality. The great circles through the girdle-shaped contours are essentially identical in both figures thus illustrating the essential parallelism of ss, s_0 and s_1. The s_1 planes measured are axial planar to minor, tightly appressed, isoclinal B_1 folds. Both s_0 and s_1 have been folded during F_2.

The very prominent foliation in the gneisses on the northern and western slopes of the Husabberg (Fig. 9) represents s_1 and it is axial planar to isoclinal folds in pegmatitic and granitic veins. At this particular locality, later folding of s_1 was found to be non-cylindrical on a small scale even though measurements were confined to a restricted area.

At the Rote Adlerkuppe, poles to axial planes of tight, minor B_1 folds in Witpoort schists fall on a great circle (Fig. 10a). This great circle is identical to that which fits the contoured plot of poles to s_1 (Fig. 10b), thus demonstrating that s_1 is an axial plane foliation here. The distribution of poles along a great circle is due to later folding. The hinges of B_1 folds define fold axes which are co-axial with later, superimposed, B_2 folds. At the Vredelus anticline (Fig. 11a) poles to B_1 axial planes (s_1) and s_{01} have similar distributions, indicating that s_{01} is locally an axial plane foliation. At this particular locality later folding is non-cylindrical.

Folds of F_1 age have not been observed in rocks of the Tinkas Formation south of the Langer Heinrich. It is difficult in the field to recognise s_1 in the schists of this mixed pelitic-calcareous sequence, partly because of the fine grain size (0,05 - 0,1 mm) and partly because transposition of ss,

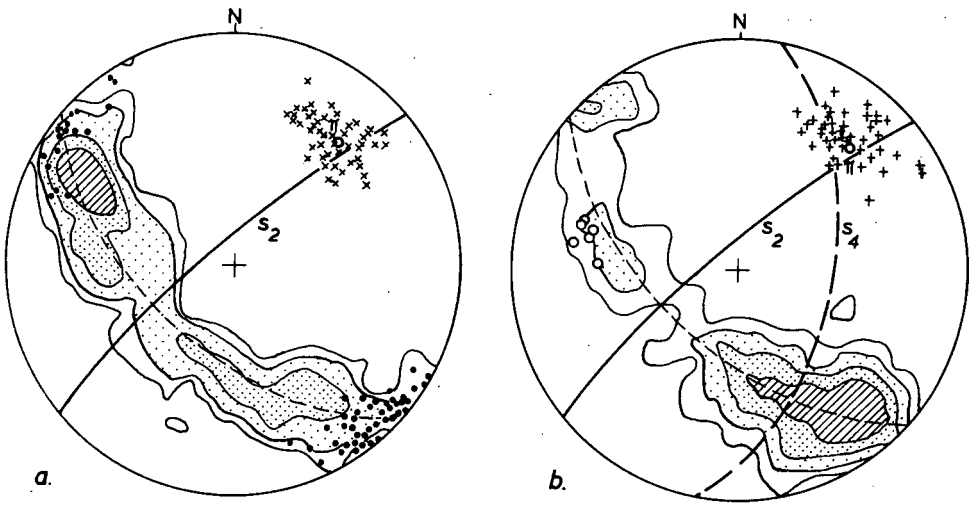

Figure 5. Structural data from the Gürtel Hills subarea.

(a) 108 poles to bedding (ss) and bedding foliation (s_0), contours 1-2-4-6 %.

(b) 142 poles to axial plane foliation (s_1), contours 1-2-4-6 %.

(•) poles to axial planes of minor B_2 folds and axial plane foliation (s_2)
(o) poles to non-penetrative post-F_2 cleavage (s_4)
(×) fold axes of minor B_2 folds and intersection s_0/s_2 (l_2)
(+) long axes of deformed pebbles

s_0 and s_1 into s_2 has occurred.

3.2.2. F_2 structures

The F_2 phase is responsible for the northeast structural grain of the mapped area. The major anticlinoria and synclinoria produced during this episode maintain a wavelength of approximately 10 km. Longitudinally the fold structures persist for long distances; for example, the Rooikuiseb anticlinorium can be traced for more than 40 km. The F_2 folding was also very intense with the result that isoclinal folds were produced. Several very tight macroscopic folds can be seen on the map: these include the Gürtel Hills syncline, the Welwitsch Hills syncline and the Rabenrücken anticline.

The style of folding, however, is dependent on the competency of the

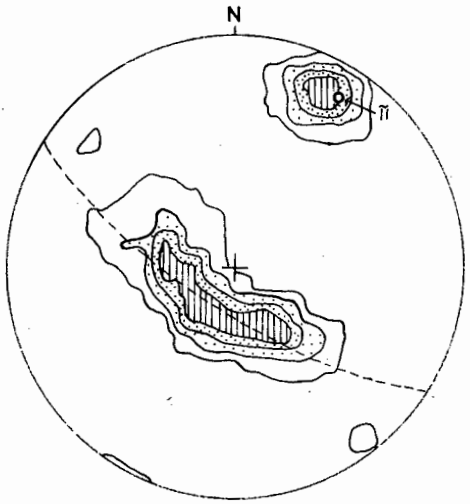

Figure 6. Structural data from the Zebraberge subarea.

104 poles to gneissic banding (s_0), contours 1-4-8-12 %
48 long axes of hornblende grains, contours 2-15-29-44 %

rocks. The competent quartzites of the Etusis Formation have been concentrically folded by flexural and flexural-slip processes (Pl. 11) and disharmonic folding is not uncommon where this mechanism has been operative. The less competent schists have suffered similar folding by slip on s_2 (Pl. 12) and in places by flow (Pl. 13). The marbles of the Rössing and Husab Formations have undergone flow folding in the west and have been tectonically squeezed and disrupted to a remarkable extent.

Following is a description of the geometry of B_2 folds in the various subareas (see Map 2).

The foliation s_0 of the banded gneisses of the Khan Formation is of pre-F_2 age and at the Zebraberge this foliation has been folded about northeast-plunging axes (see Pl. 1). Here the fold axes are parallel to l_2, defined by the orientation of long axes of hornblende crystals that lie in s_0 (Fig. 6). The hornblende crystallised during F_2, partly at the expense of clinopyroxene, to form the lineation. The situation is similar near Arcadia 80 (Fig. 7) where s_{01} in banded gneisses and overlying pelitic/psammitic rocks has been folded during F_2. The lineation l_2 is defined by s_{01}/s_2 intersections and the direction of elongation of hornblende crystals. The B_2 axial planes are nearly vertical at this locality.

At the Gürtel Hills syncline s_0 and s_1 have been folded about northeasterly plunging B_2 axes which have vertical axial planes and the accompanying lineation (l_2), defined by the intersection of s_0 and s_2, is shown in

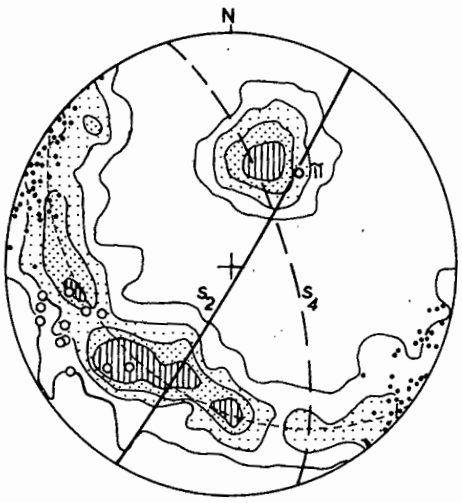

Figure 7. Structural data from subarea 2 km northeast of Arcadia 80.

124 poles to bedding-/axial plane-foliation (s_{01}), contours 1-2-4-6 %
50 lineations: long axes of hornblende crystals and intersection of s_{01}/s_2, contours 2-8-16-24 %
(•) poles to axial planes of minor B_2 folds and axial plane foliation (s_2)
(o) poles to axial planes of minor crenulation folds (s_4)

Figure 5 (a). At this locality the Chuos diamictite contains very highly deformed pebbles. These inclusions are flattened in s_0 and their long axes are parallel to B_2 (Fig. 5 b), their plotted positions being coincident with l_2. While no kinematic analysis is attempted here, Smith's findings (Smith, 1961, 1965) should be mentioned. He concluded that although the elongation of pebbles in the Khan Gorge region is parallel to B_2 fold axes, this was nevertheless the 'a' tectonic axis of the F_2 folding.

At the Welwitsch Hills syncline s_{01} is parallel to bedding, where the latter can be recognised, but locally axial planar to small intrafolial, isoclinal B_1 folds, and has been folded about north-plunging B_2 axes (Fig. 8a). The axial plane of the Welwitsch Hills syncline dips steeply to the east but the axial plane foliation (s_2) is not well developed here, which is rather surprising in view of the tight nature of the folding.

Southeast of the Husabberg beacon structural work was carried out in the vicinity of the contact between the Husab and Witpoort Formations. Even in this small area several smaller subareas had to be separated because of the non-cylindrical nature of the folding. s_{01} has been folded during the F_2 phase and poles to s_{01}, which is very well developed in the porphyroblastic schists, define great circles in two of the subareas and indicate non-

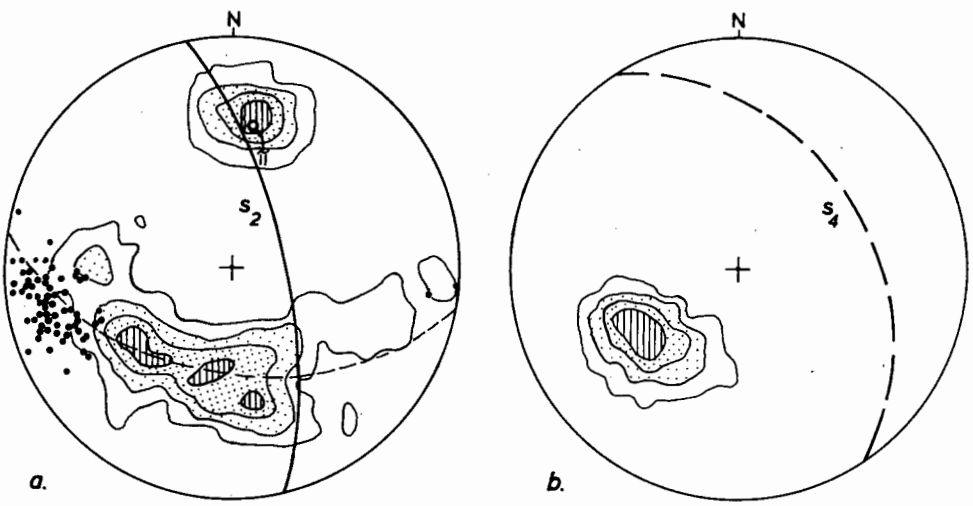

Figure 8. Structural data from the Welwitsch Hills subarea.

(a) 98 poles to bedding-/axial plane-foliation (s_{01}), contours 1-3-6-9 %
41 fold axes of minor B_2 folds and intersection s_{01}/s_2, contours 2-12-24-36 %
(•) poles to axial planes of minor B_2 folds and axial plane foliation (s_2)

(b) 46 poles to non-penetrative axial plane foliation (s_4), contours 3-6-13-20 %.

cylindrical folding in another (Fig. 9a). The fold axes generally plunge northeastwards but hinges of some minor, tight B_2 folds plunge in various directions within s_2 (Fig. 9b, Pl. 14). Slightly curved quartz rods, in places similar to those described by Wilson (1953), form linear structures in s_{01} parallel to B_2 folds and plunge generally to the northeast (Fig. 9b). The spread of plunges of B_2 folds and rods within s_2 is indicative of axial plane shearing, resulting from intense deformation during F_2 (Joubert and Kröner, 1972).

F_1 folding in the subarea at the Rote Adlerkuppe has already been mentioned. Axial planes to minor isoclinal B_1 folds (Fig. 10a), and s_1 surfaces (Fig. 10b) have been folded during F_2 and the hinges of minor B_1 folds (Fig. 10a) and the fold axes of superimposed B_2 folds (Fig. 10b) are coaxial in this small area, both plunging gently to the northeast. Axial planes (s_2) of minor B_2 folds strike northeast and dip at 60° to the southeast, which is less steep than in many other subareas.

Two small areas were investigated at the Vredelus anticline and the structural data are represented stereographically in Figures 11(a) and (b).

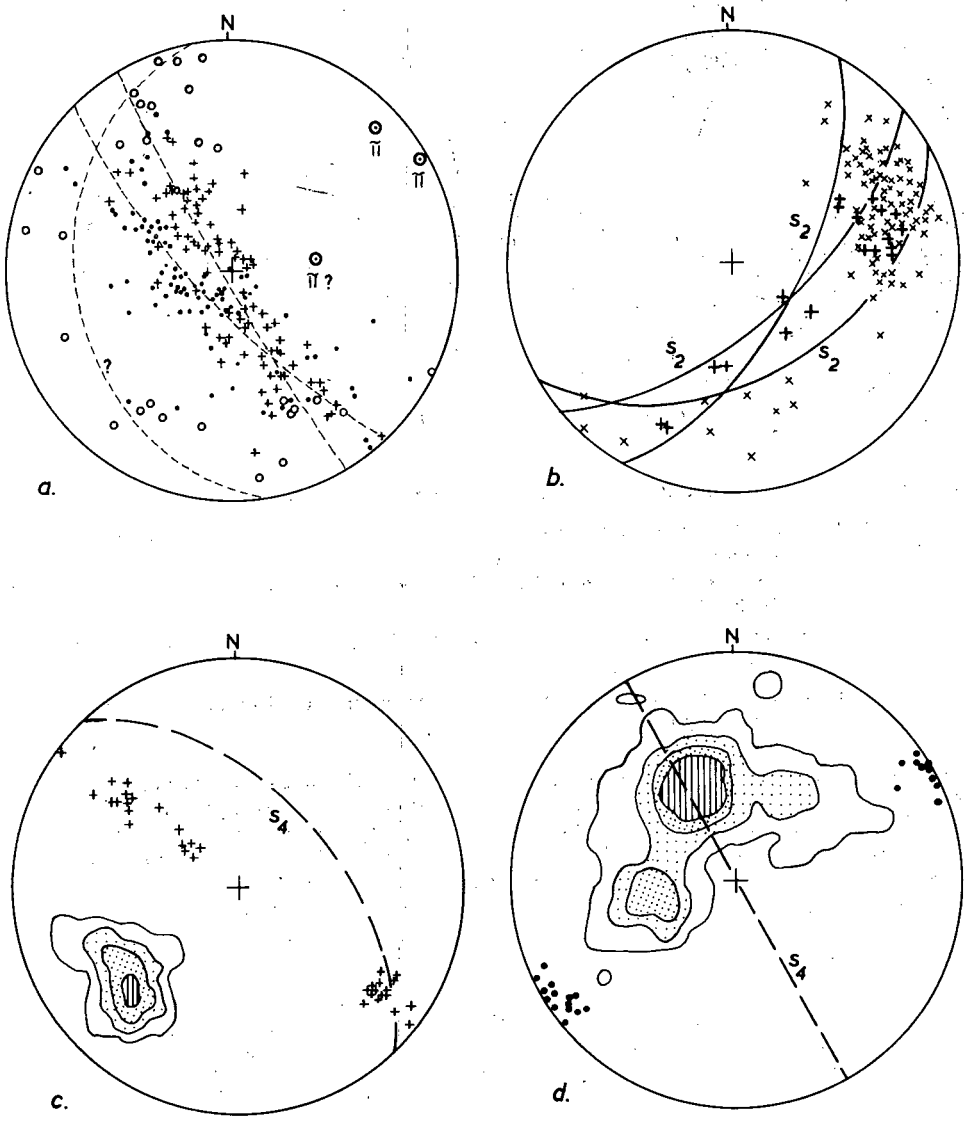
N
π
π
π ?
a.
N
S_2
S_2
S_2
b.
N
S_4
c.
N
S_4
d.

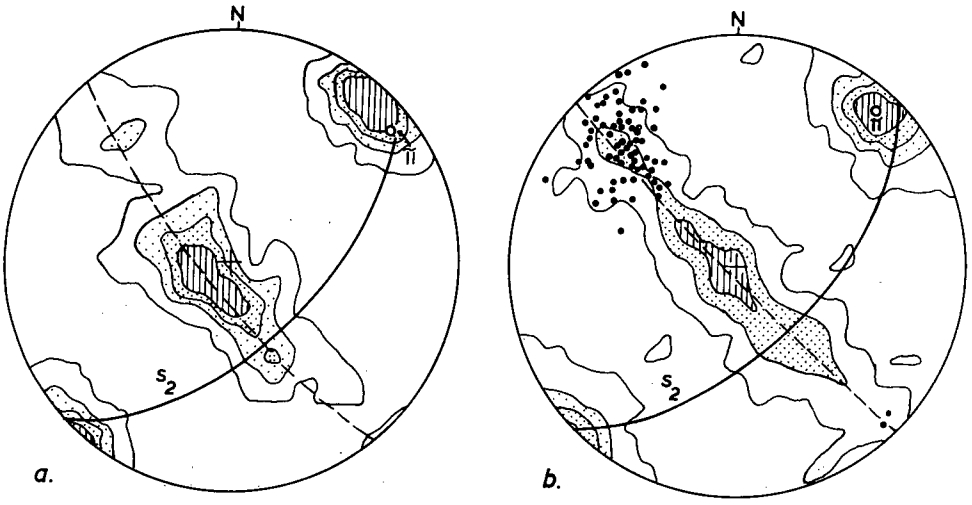

Figure 10. Structural data from Rote Adlerkuppe subarea.

(a) 100 poles to axial planes of minor B_1 folds, contours 1-4-7-10 %
80 fold axes and associated lineations of minor B_1 folds, contours 1-8-15-22 %

(b) 100 poles to s_1 , contours 1-4-7 %
101 lineations, intersection s_1/s_2, contours 1-8-15-22 %
(•) poles to axial planes of minor B_2 folds and axial plane foliation (s_2)

Figure 9. Structural data from Husabberg subareas.

(a) poles to ss and s_{01} from three small subareas (crosses, dots and circles). Dashed curves are great circles of best fit for each of the subareas
(b) linear structures from the subareas in (a)
(×) quartz rods
(+) fold axes of minor B_2 folds
(c) 29 poles to axial planes (s_4) of minor crenulation folds, contours 4-10-17-28 %
(+) necklines of microboudins on limbs of B_2 folds
(d) 175 poles to s_1 in biotite gneiss, contours 0,6-3-6-9 %
(•) poles to non-penetrative cleavage (s_4)

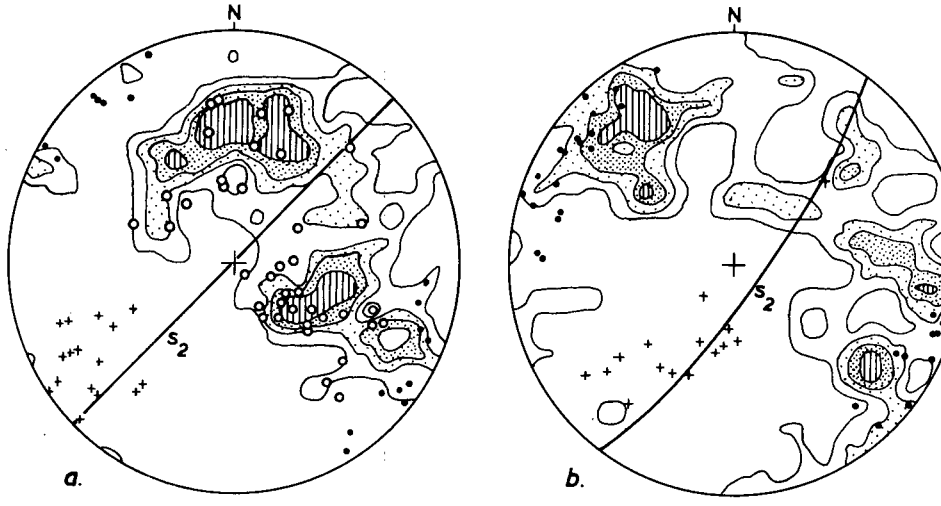

Figure 11. Structural data from subareas in the Vredelus anticline

(a) 106 poles to bedding-/axial plane-foliation (s_{01}), contours 1-2-3-4 %

(b) 100 poles to bedding (ss) and bedding foliation (s_0), contours 1-2-3-4 %

(o) poles to axial planes of minor B_1 folds
(•) poles to axial planes of minor B_2 folds and axial plane foliation (s_2)
(+) intersection lineation s_{01}/s_2 (a), s_0/s_2 (b)

In each of these subareas the pattern is that of non-cylindrical plane folding. In Figure 11(b) a unique great circle cannot be drawn through the contoured poles to the folded s_0 surfaces. Axial planes of minor B_2 folds strike approximately northeast and dip at $\pm 76^{\circ}$ to the southeast. The intersection of s_0 and s_2 generally plunges southwest but readings are spread out more or less within s_2, due to axial plane shearing and non-cylindrical plane folding. In the quartzites s_2 is found as a fracture cleavage which is axial planar to minor B_2 folds. In pelitic interbeds s_0 is folded to produce a crenulation foliation which is parallel to s_2 in psammitic rocks. According to Whitten (1966) crenulation foliations are generally formed late in the tectonic history of folded terrains but reports where crenulation foliation and axial plane foliation are closely associated in time, also exist, e.g. Jones (1959). The crenulation foliation is developed only in thinly bedded alternations of schists and quartzites and the heterogeneity of such successions is the reason for the presence of both crenulation and axial plane foliations.

At the nose of the Vredelus anticline s_{01} and axial planes of minor B_1

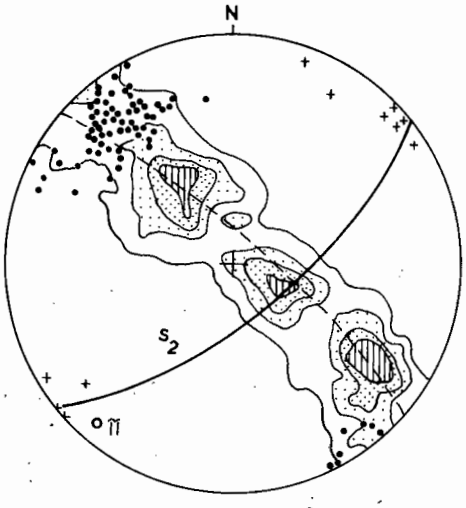

Figure 12. Structural data from the Rooikuiseb anticlinorium subarea.

103 poles to bedding (ss) and bedding foliation (s_0), contours 1-3-5-7 %
(•) poles to axial planes of minor B_2 folds and axial plane foliation (s_2)
(+) intersection lineation, s_0/s_2.

folds have been folded during F_2 (Fig. 11a). Here again B_2 folding is non-cylindrical so that the contoured plot of poles to s_{01} does not define a unique π-axis. Nevertheless, the contoured diagram and *b*-lineations indicate that the B_2 folds generally plunge southwestwards. The axial plane foliation and axial planes of minor B_2 folds strike northeast and are vertical.

Concentric, flexural and flexural-slip folding of F_2 age has affected quartzites of the Etusis Formation in the Rooikuiseb anticlinorium (Pl. 11). s_{01} is well developed in pelitic rocks, in quartzofeldspathic gneisses and in the augen gneisses of the Red Granite-Gneiss sequence. Structural data from an area of quartzites at the Achas River indicate that s_0 has been folded about almost horizontal northeast-trending axes (Fig. 12). The axial plane foliation and axial planes of minor B_2 folds dip southeast at 70°. Elsewhere in the core of the anticlinorium both slip and flexural folds occur side by side in interbedded pelites and psammites (Pl. 15). In places refolding of tight B_1 folds appears to have taken place (Pl. 16).

Along the southeastern margin of the mapped region, the most extensive outcrops of the Tinkas Formation are found from Rooikuiseb 109 to the Schieferberge and here F_2 structures are excellently preserved. The folds are normally almost isoclinal, with steeply-dipping axial planes overturned towards the southeast. The s_1 foliation in the schists is parallel to the

lithological layering but since the attitude of the strata is steep in most places and virtually parallel to axial planes of B_2 folds, s_0, s_1 and s_2 are often parallel to one another. In the schists transposition of s_{01} into the axial plane foliation of B_2 folds (s_2) has commonly occurred in the hinge areas of these folds. Transposition of interbedded calc-granofels layers has resulted in formation of elongated lens-like bodies that extend much farther in one dimension than in the other two and these effects are shown in Pl. 4. Generally, the calc-granofels layers themselves do not show the axial plane cleavage of the pelitic interbeds but appear to have flowed and a faint compositional banding parallel to s_2 can normally be recognised.

The style of folding in the Tinkas Formation is illustrated in Pl. 17, showing very tight slip folding with very narrow hinge areas and almost straight limbs. Left of the centre of the photograph the folding is almost isoclinal and, near the extreme right, transposition of s_{01} into s_2 has occurred. The very tight nature of the B_2 folding, and the axial plane foliation (s_2) are illustrated on a mesoscopic scale in Pl. 12, which shows a section perpendicular to the fold axis. Cordierite has crystallised syntectonically in the s_2 plane.

Linear structures of F_2 age are generally well preserved. Fold mullions (Pl. 18) on all scales from centimetre to metre "wavelength" are very common, and the lineations produced by intersection of s_0 and s_1 with s_2 are generally seen as fine lines on the folded surfaces and are caused by intersection of s_2-oriented biotite flakes with the older structures. In places hornblende crystals are oriented parallel to B_2 fold axes but at other places the hornblende has crystallised radially and without preferred orientation in either s_0 or s_1 planes.

Structural data from two subareas at the Schieferberge are shown in Figures 13(a) and (c). In Figure 13(a), contours to s_{01} poles define a great circle but the contoured diagram has a "tail" on the southern side which is due to later, minor F_3 folding; here s_2 is steep with a southerly dip of 85° and an east-northeast strike. The intersection of s_{01} and s_2 defines l_2, which is parallel to axes of minor B_2 folds and which plunges in various directions in the B_2 axial plane (Figs. 13a, c). The varying orientations of l_2 within s_2 are probably due to axial plane shearing during the intense F_2 deformation and sheared-out B_2 fold closures commonly occur (Joubert and Kröner, 1972).

Similar relationships are found south of the Aram Mountains (Fig. 14) where B_2 folds are almost isoclinal and l_2 plunges at different angles within s_2 which strikes northeast and dips to the northwest at 66°.

Figures 15(a), (b) and (c) show structural data from the Rabenrücken anticline at the southern corner of the area. During F_2, ss and s_{01} have been folded about southwest-plunging B_2 axes and the axial plane foliation and axial planes of minor folds (s_2) strike variously northeast and north-northeast and are almost vertical. s_{01} in the Chuos Formation is clearly folded about B_2 at the southern nose of the anticline.

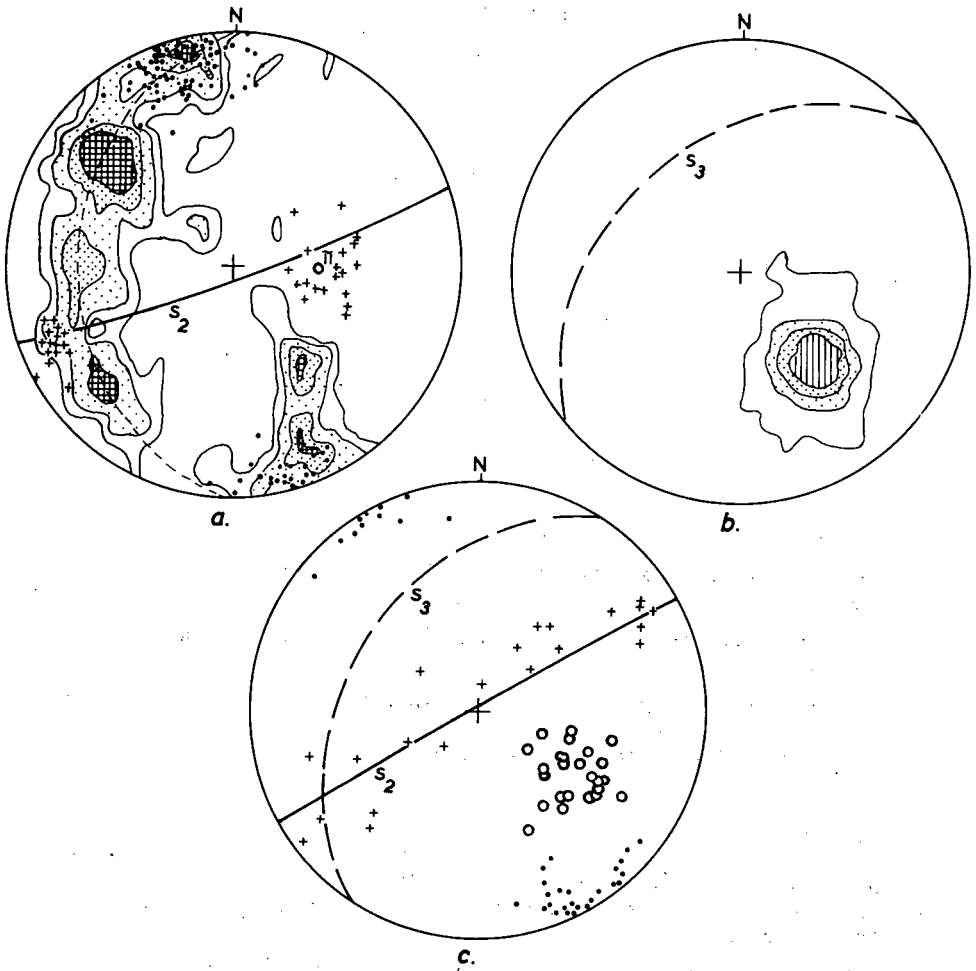

Figure 13. Structural data from Schieferberge subareas.

(a) 114 poles to bedding-/axial plane-foliation (s_{01}), contours 1-2-3-5 %

(b) 101 poles to axial plane foliation (s_3) contours 1-8-16-24 %; same locality as (a)

(c) Data from subarea northeast of (a) and (b)

(•) poles to axial planes of minor B_2 folds and axial plane foliation (s_2)

(o) poles to axial plane foliation of B_3 folds (s_3)

(+) l_2 lineations, intersection s_{01}/s_2

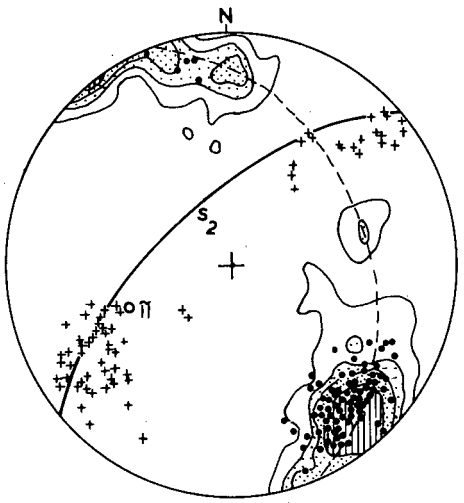

Figure 14. Structural data for B_2 folds from subarea south of Aram Mountains.

83 poles to bedding-/axial plane-foliation (s_{01}), contours 1-4-6-11 %

(•) poles to axial planes of minor B_2 folds and axial plane foliation (s_2)

(+) l_2 lineation, intersection s_{01}/s_2

3.2.3. F_3 structures

The data, insufficient for final conclusions about the number of post-F_2 phases, are indicative of at least two further fold phases of lesser intensity than F_1 and F_2.

An F_3 phase has been recognised only in the southeastern part of the area between Rooikuiseb 109 and the Schieferberge where it is represented by minor open B_3 folds on steep limbs of B_2 folds (Fig. 16).

An axial plane foliation (s_3), in the form of a slightly fanning cleavage, is associated with this folding and has partly obliterated and folded s_2 in the schists. The foliation is non-penetrative and in places is not observable. It is, however, more common than the associated minor folds. The axial planes of F_3 folds strike northeast and dip at 40-50° to the northwest (Fig. 13b, c).

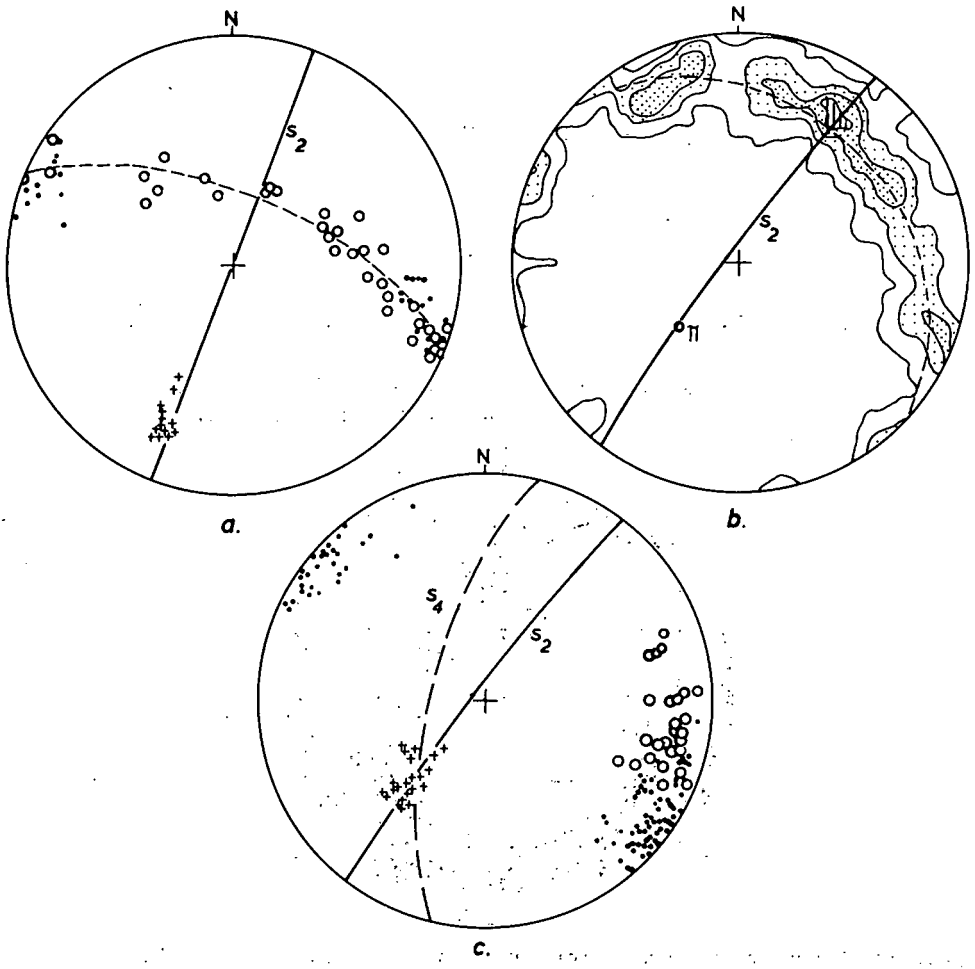

Figure 15. Structural data from subareas at the Rabenrücken anticline.

(a) (o) poles to bedding (ss) and bedding-/axial plane-foliation (s_{01})
(•) poles to axial planes of minor B_2 folds and axial plane foliation (s_2)
(+) B_2 lineations, intersection s_{01}/s_2

(b) 101 poles to bedding-/axial plane-foliation (s_{01}), contours 1-3-5-7 %

(c) (•) poles to axial planes of minor B_2 folds and axial plane foliation (s_2)
(o) poles to non-penetrative cleavage (s_4)
(+) B_2 lineations, intersection s_{01}/s_2

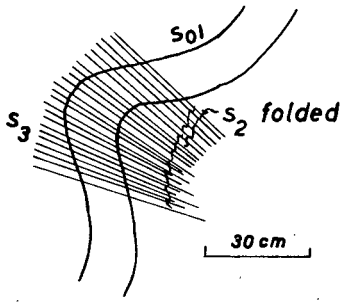

Figure 16. Minor B_3 fold showing axial plane foliation (s_3). s_2 is folded on a small scale; Gemsbok River, Schieferberge.

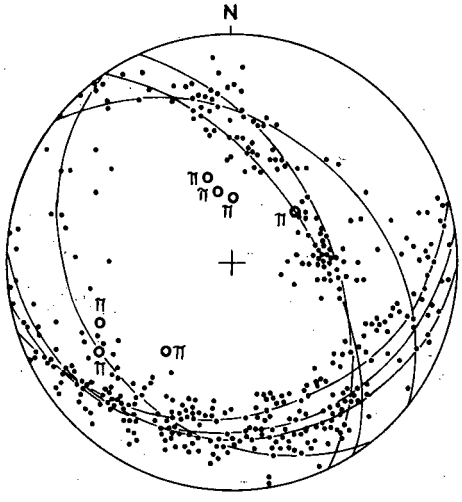

Figure 17. Synoptic stereogram for subareas around the Langer Heinrich.

(·) poles to bedding (ss) and bedding foliation (s_0).
The great circles shown are those of best fit for each of the subareas

---

Figure 18. Structural data from subareas on the northern and eastern sides of the Langer Heinrich dome.

(a) to (f) poles to axial planes of minor B_2 folds and axial plane foliation (s_2) (•)
(d) 95 poles, contours 1-7-14-26 %
(e) 40 poles, contours 2-13-25-37 %

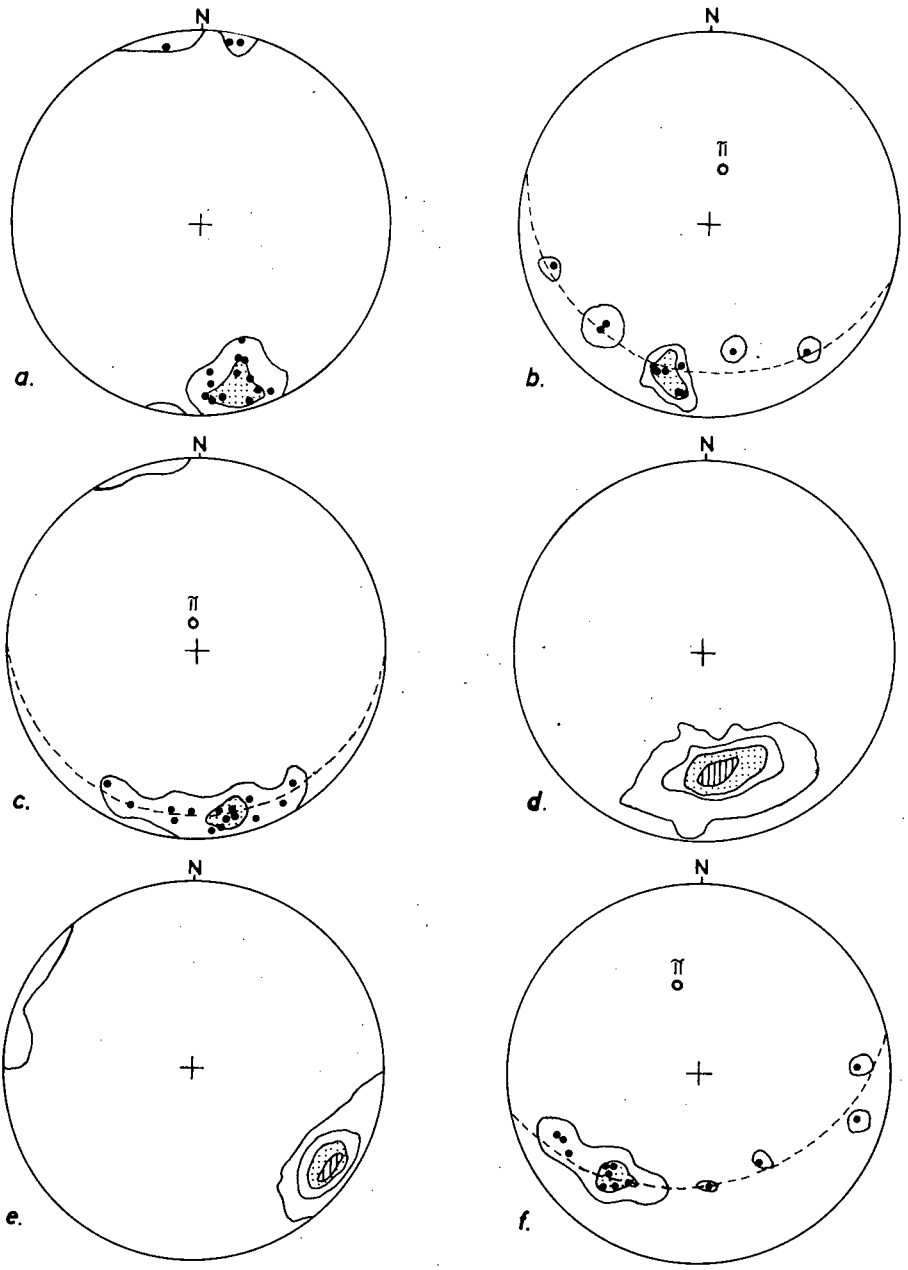
N
a.
N
π
b.
N
π
c.
N
d.
N
e.
N
π
f.

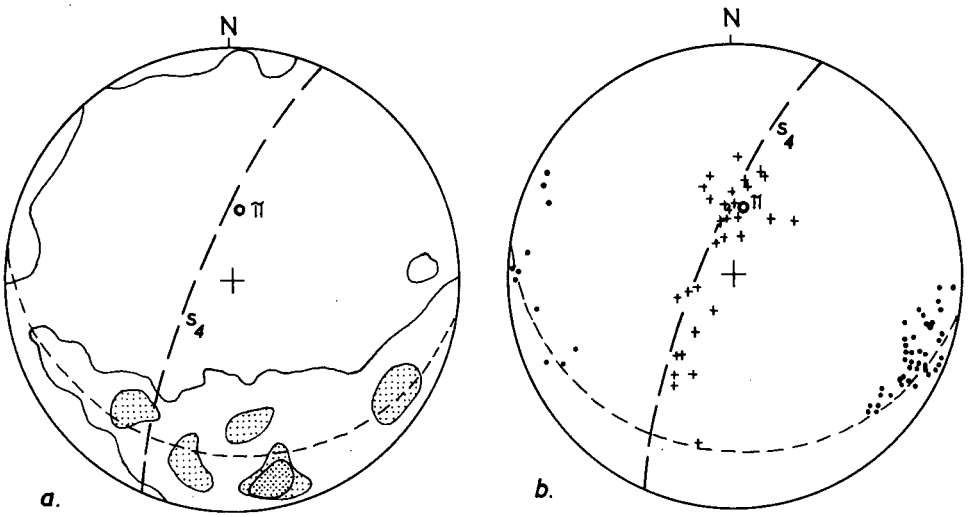

Figure 19. Synoptic stereograms, Langer Heinrich.

(a) Contour maxima and lower contour limits for poles to s_2 from Figure 18. s_4 plane from Figure 19(b)

(b) (•) poles to axial planes of minor B_4 folds and axial plane foliation (s_4).
(+) intersection lineation s_{01}/s_4 (l_4)
Great circle represents poles to folded s_2 , from Figure 19(a)

3.2.4. F_4 structures

At the Langer Heinrich dome F_4 structures have been superimposed on those of F_2 age. Several small subareas have been investigated in the general area of the dome and the structural data are to be found in Figures 17, 18 and 19. In Figure 17 poles to s_0 from all subareas around the dome have been plotted. The great circles shown are those of best fit for each of the subareas studied. Poles to s_2 , representing the F_2 axial planes and axial plane foliation, for the subareas on the northern and eastern sides of the dome, are plotted and contoured in Figures 18(a) to (f). It is apparent from Figures 18(b), 18(c) and 18(f) that s_2 is folded about N- to NNE trending axes of F_4 age. Mesoscopic structures in the field also attest to this (Fig. 20).

Figure 19(a) is a synoptic diagram of data from Figure 18, from which contour maxima and lower contour limits have been taken. A great-circle can be drawn through this girdle plot, defining a π-axis which plunges steeply to the north. Poles to s_4, the axial plane of B_4 folds, are shown in Figure 19(b). The lineation resulting from intersection of s_{01} with s_4 (l_4) plunges

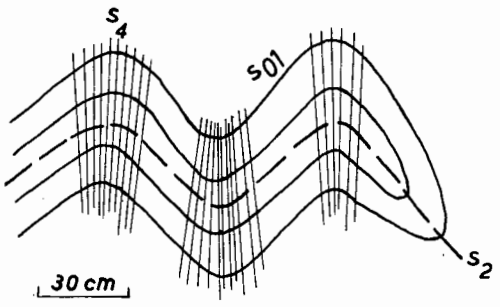

Figure 20. Isoclinal B_2 fold deformed during F_4. Small scale transposition effects occur along s_4, the axial plane foliation of B_4 folds; between Tinkas River and Langer Heinrich dome.

at varying angles in the s_4 plane as a result of superimposition of F_4 folds on the already-folded s-surface. Most s_4 planes strike north-northeast and dip steeply to the west-northwest at approximately 80°. B_4 folds are fairly open but some transposition of s_{01} into s_4 has occurred (see Fig. 20).

At the Rabenrücken (Fig. 15c) a non-penetrative cleavage (s_4) strikes north-northeast and dips steeply to the west-northwest. This orientation is fairly consistent with that at the Langer Heinrich (compare Fig. 15c with Fig. 19) and the cleavage is tentatively assigned to the F_4 phase. In the western part of the area, at the Gürtel Hills, a non-penetrative cleavage is found (Fig. 5b) striking just east of north and dipping to the east.

In many places in the west, however, axial planes of minor folds produced during late deformation strike north-northwest to northwest and dip northeast. At the Husabberg the prominent s_1 surfaces in Nosib gneisses have been folded non-cylindrically about axes plunging to the southeast (Fig. 9d). In the overlying basal schists of the Husab Formation a northwest-striking, non-penetrative vertical cleavage is developed. Quartz fills many of the planes and retrograde metamorphic alteration has occurred along this direction. It is not certain whether this cleavage is axial planar to the southwest-plunging structures. On the southeastern side of the Husabberg minor folds have been observed (Fig. 9c) which have axial planes striking northwest and dipping at 57° to the northeast. These folds are sporadic in occurrence and form small crenulations on s_{01} surfaces. On the limbs of B_2 folds fine grooves have been etched out between what appear to be microboudins, developed along bedding planes of calc-granofels layers (Fig. 9c). The linear structures defined by the necklines of these boudins are distributed in a vertical plane, which has a northwest strike. It is not certain whether this linear structure is related to F_2 folding (likely) or to the later northwest folds because the plane in which the lineations fall has no simple relationship either to the northwest-trending crenulation folds or to the axes of F_2 folds.

At the Welwitsch Hills a northwest-striking, non-penetrative cleavage,

which is axial planar to minor folds, dips to the northeast at an average angle of 42^{o} (Fig. 8b). Superimposition of the above folds on s_1, already folded during F_2, has caused the spread of s_1 poles in Figure 8(a). Near Arcadia 80 minor crenulation folding is associated with a north-northwest striking axial plane foliation which dips to the east-northeast at nearly 70^{o} (Fig. 7). The foliation, in the form of a fine cleavage, is non-penetrative.

Thus in the mapped area, in what are called F_4 structures, there are two distinct orientations in different parts of the region. In the east, a north-northeast-striking foliation and associated folding have been superimposed on earlier structures while in the west the general trend of minor folds, normally of crenulation type, is between north-northwest and northwest. The relative ages of the two directions are not known with certainty and they are both tentatively assigned to F_4.

Beyond the mapped area, to the northwest, Nash (1971) has described what he termed "F_3" structures. These are mesoscopic folds found as small crenulations in pelitic rocks also occurring as open folds whose wavelengths are rarely greater than a few metres. The axial planes of these folds strike east-west and dip to the south at 60^{o}. Nash (op. cit.) suggests that retrograde metamorphism may have accompanied this deformation. Smith (1961, 1965) makes no mention of similar structures but reports a group of north-trending linear structures as being of post-F_2 age. In the present area no measurements have been made on structures of similar orientation to those described by Nash. However, at the Zebraberge, gentle post-F_2 warping of banded gneisses of the Khan Formation about axes trending east-west has been observed. The warps have wavelengths of about 10 metres and amplitudes of about 1 metre. Since no definite F_3 or F_4 structures were found here it is not known with which fold phase this warping is associated.

3.2.5. Faults

Faulting has played a relatively minor role during deformation of the rocks and no major faults have been recognised. Near Arcadia 80 the contact between the Red Granite-Gneiss and the Witpoort Formation appears to be faulted, however, and south of the Swakop River fault gouge is locally present in a narrow rectilinear valley. The fault appears to have developed at a fairly early stage of deformation, during formation of a possible small overturned structure (see section C-D, Map 1).

At a later stage, during post-F_2 times, Etusis Formation psammites were thrust over the Witpoort Formation and Salem Granite at the Rote Adlerkuppe along a small undulating flat fault.

Most of the faults in the region strike approximately north-south. In the east the strikes are slightly east of north and towards the west they vary between north and north-northwest. The faults are generally tear faults with up to 400 m left lateral displacement. The horizontal movement on vertically-dipping beds is about the same as that on gently-dipping strata and confirms that these are tear faults. Thin zones of dark reddish-brown fault gouge are developed along the almost-vertical faults and within these zones biotite has retrograded to chlorite. The faults are younger than all folding and

displace late pegmatites associated with the Donkerhoek Granite; they are cut by dolerite dykes and sheets.

3.3. Discussion

As an introduction to the discussion a brief summary will be given of several structural studies which have been completed in different parts of the Damara orogen.

Approximately 100 km southeast of the present area, De Waal (1966) reported four phases of post-Damara folding in an area bordering on the southern margin of the orogen. He recognised an early phase (F_1) of north-east-trending folds followed by F_2 during which northwest-trending structures were formed. Northeast structures of F_3 age were then superimposed co-axially on F_1 structures which were in turn affected by north-south crenulation folding at a much later stage. The F_1 and F_3 phases were regarded as the most intense.

Farther to the northeast of the area studied by De Waal, Hälbich (1970) examined a profile between the Auas Mountains, south of Windhoek, and Okahandja. He also conducted a structural reconnaissance through the Khomas Hochland farther to the west and southwest. He recognised three deformational phases which he numbered B_1, B_2 and B_3 respectively. The B_1 phase has a northeast trend with axial planes, vertical near Okahandja, becoming inclined to the northwest as one proceeds southwards towards the margin of the orogen. The B_2 phase is not well developed near Okahandja but southwards B_1 structures are overprinted by the younger (B_2) fracture cleavage which grows in intensity southwards until the older structures are refolded co-axially during the B_2 phase. The B_2 cleavage and axial planes strike northeast and dip constantly to the northwest; their dips flatten as one moves southwards.

The area studied by von Groote-Bidlingmaier (1973) overlaps with those mapped by De Waal (1966) and Hälbich (1970). He recognised two northeast-trending sets of linear structures, ascribed to two fold phases, the later phase being associated with steep axial planes, and a later third phase represented by small crenulations of second-fold axial surfaces.

More than 200 km north of the area under investigation Frets (1969) described four phases of folding post-dating deposition of the Damara System (sic.). The area lies just to the south of the pre-Damara Welwitschia Ridge, which exerted a strong control over the structural trends. The F_1 phase produced folds parallel to this ridge (east-west). F_2 folds have variable orientation from north-south in the southeast to east-west near the ridge. The F_3 phase has a northerly trend and produced dome structures whereas F_4 is represented by north-northeast crenulations on earlier surfaces.

Miller (1972) worked south and southeast of the area mapped by Frets (op. cit.) and he described the following fold phases:

(i) Folds of the F_1 phase trend east-west
(ii) F_2 folds trend northwest in the western part, and north-northeast in the eastern part of the region; the variation

is controlled by the distribution of pre-Damara rocks which exerted a strong control over F_2 folds

(iii) East-northeast-trending crenulations of F_3 age were followed by

(iv) west-northwest-trending kink folds.

Guj (1970) mapped the area around Sesfontein, along part of the north-northwest branch of the Damara Orogen. He distinguished a period of post-Nosib/pre-Damara folding and a major phase of north-south to northwest-trending post-Damara folding (F_2S), as well as northeast and north-northeast-trending penecontemporaneous fold phases, F_3 and F_4 respectively.

Smith (1961) and Roering (1961) were two of the earlier workers to apply modern structural techniques in their investigations of the Damara rocks. Roering investigated the emplacement of pegmatites in the Karibib district and described three phases of folding with trends, from oldest to youngest: west-northwest, north-south and north-northeast. He stated (op. cit., p. 25-26), "Without more detailed knowledge of the regional geology, it is impossible to determine whether these three phases of folding are part of one act or if they are related to definitely different ages of folding".

Smith (1961, 1965) discussed three phases of folding which he ascertained in the Khan and Karub Gorges northwest of the present area. With respect to the first fold phase he states that "The original stress orientation cannot be accurately determined, but was apparently in a northeast-southwest direction" (1965, p. 73) and the resulting folds trend northwest. The second and major phase produced northeast-trending folds with upright axial surfaces. This was followed by a third phase of north-south-trending, non-penetrative structures.

The polyphase character of deformation has thus been well documented by a number of workers in different parts of the Damara belt. Figure 21 shows the various trends reported above together with those from the region discussed here. If one confines remarks to the northeast-trending branch of the Damara belt, the above review indicates that there have been two major phases of folding during the Damaran Orogeny. These two major phases resulted in fold trends approximately parallel to the long axis of the orogen. However, in the marginal regions the trends are strongly controlled by physical and topographic variations in the relatively immobile pre-Damara floor and have been deflected, in places by as much as 90° (Frets, 1969; Miller, 1972). The structural trends in the area studied by Roering (1961) cannot be extrapolated because they appear to be atypical of the regional structural grain. Smith (1961, 1965) was uncertain about the trend of the earliest folds (see above), but their postulated northwesterly trends are similar to the west-northwesterly-trending folds recognised by Roering (1961).

The two major phases were followed by development of small-scale structures such as crenulation folds. The trends of these later minor structures vary in different places but a general northerly alignment seems established in several areas (Fig. 21).

In the area under consideration two major phases of folding have been recognised. The original trend of B_1 folds is not known for certain but it

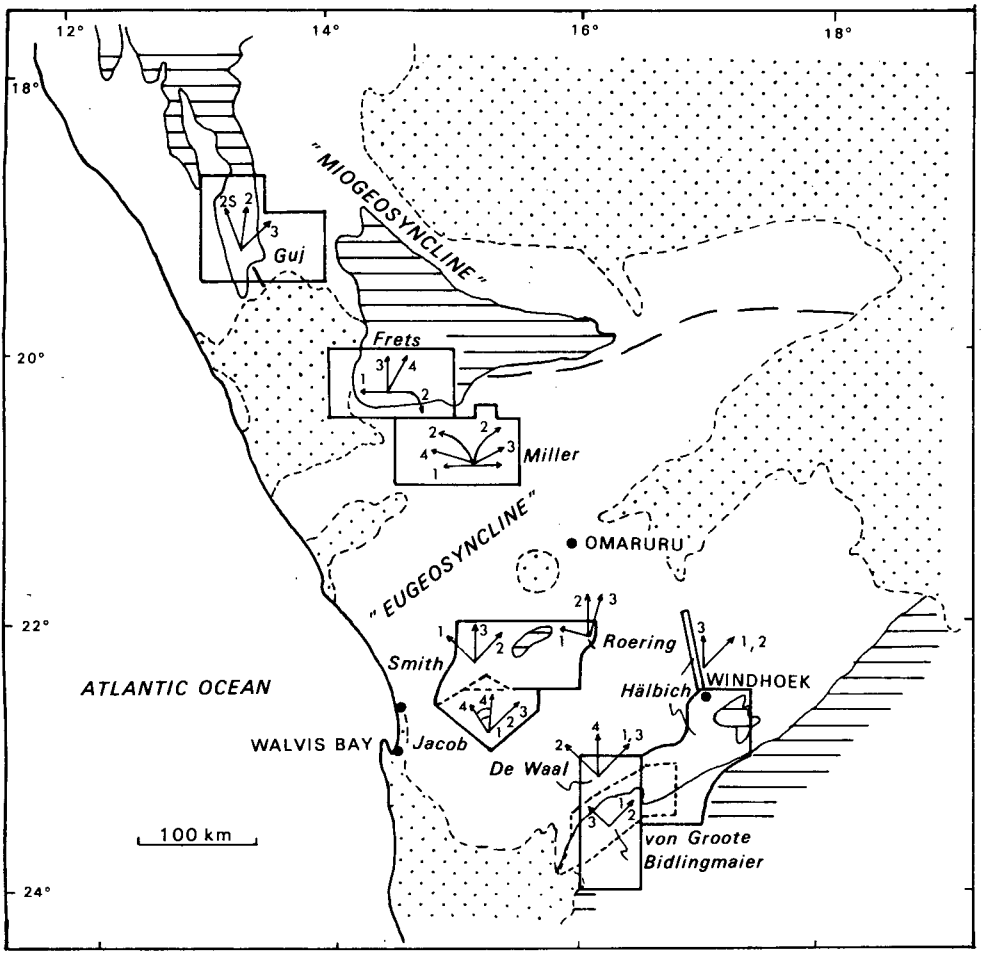

Figure 21. Map showing fold trends in the Damara belt. Fold phases are listed chronologically for each area studied. The arrows indicate fold trends. Geology modified after Martin (1965).

may well have been northeast similar to the trend of B_2 folds. F_3 is of minor importance and may represent a late stage of F_2. Later F_4 folding is generally on a small scale but may have contributed to the formation of dome structures. The orientation of the late B_4 folds is variable and

northerly trends are most common. Thus the structural orientations in this area accord with the regional findings of other workers as described above and are discussed further below.

The regional foliation (s_0) formed through flexural-slip processes during early F_1 folding and is a bedding foliation. Further deformation resulted in the formation of isoclinal B_1 folds and a penetrative axial plane foliation (s_1). As a result of this folding, s_0 and s_1 are frequently parallel to one another and indistinguisable. During F_1 major isoclinal structures were created and large recumbent folds probably formed whereas the F_2 deformation produced the major northeast-trending structures now exposed.

During F_2, competent psammitic rocks were deformed by flexural-slip- and incompetent pelitic rocks by slip-processes. An axial plane foliation (s_2) is developed in schists, in places very prominently as in the Schieferberge, where transposition of s_0 and s_1 into s_2 has occurred. In the west, incompetent marbles of the Rössing and Husab Formations have undergone flow folding (Wynne-Edwards, 1963). Flow processes have probably operated in pelitic rocks during F_2 at several of the localities investigated, where s_2 is either very weakly developed or not present at all. Smith (1961) postulated that the lack of s_2 in places is due to metamorphism outlasting deformation but this is unlikely because s_0 and s_1 are still well preserved. The constancy in orientation of B_2 axial planes (Fig. 22a) over the area, except where s_2 is clearly folded by later deformations, speaks against wild flow folding.

Smith (1961, 1965) has remarked on the orientation of B_2 fold axes, saying that they plunge consistently to the northeast in the area mapped by him. This is not the case in the present area, however, where B_2 axes plunge both towards northeast and southwest (Fig. 22b) but the author agrees with Smith (1965) that the maximum stress during F_2 was oriented northwest-southeast. F_1 and F_2 are not regarded as being contemporaneous because the respective axial planes do not fold one another (Ramsay, 1967). Whether F_1 and F_2 represent successive folding during a single continuous process of deformation or whether they represent separate episodes altogether can only be decided after more detailed work has been done and the original trend of B_1 folds is known with certainty.

The B_3 folds show a trend very similar to that of B_2 but their axial planes dip to the northwest at 40° to 50° (Fig. 23a) in contrast to the steeper (about 80°) dip of F_2 axial planes. The similarity in trend and the fact that porphyroblast growth has occurred along both s_2 and s_3, although less pronounced along s_3, indicates that F_3 followed closely on F_2. F_2 and F_3 are thus regarded as being part of the same period of folding, and the author is inclined to the view that the major phases, F_1 and (F_2 + F_3) correlate with the two major phases elsewhere.

After the F_3 folding two main cleavage directions developed in the rocks of the Khan/Swakop River area (Fig. 23b). In the east a north-northeast direction of folding is found which gave rise to B_4 folds. Interference of B_2 and B_4 folds is considered to have accentuated the Langer Heinrich dome structure. Farther to the west, north-northwest to northwest-striking s_4-surfaces dip to the east and northeast. With the possible exception of the southeast-plunging syncline at the Husabberg the associated folds are of

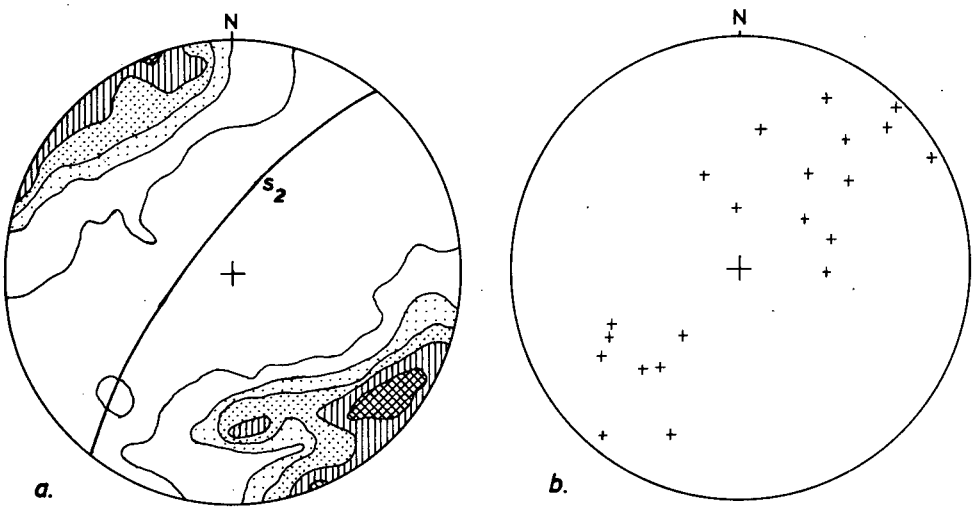

Figure 22. Synoptic stereograms for B_2 folds

(a) 700 poles to s_2, data from all subareas, contours 0,1-1-3-4-6 %

(b) B_2 axes; crosses represents π (ss), π (s_0) or π (s_{01}) of the various subareas

minor crenulation type.

Dome structures are not uncommon in the areas mapped by Smith (1961, 1965) and the writer and the problem of their origin has not yet been finally solved. Smith (1961) attributed dome formation to interference of B_1 and B_2 folds which should result in a pattern similar to Ramsay's Type 1 (Ramsay, 1962). Later, Smith (1965, p. 73) stated that "The third phase of folding is considered to have been caused by extension parallel to the second-fold axes resulting in many of the elongate dome structures found in the area". Although Smith regarded the B_1 folds as having been oriented northwest he states that B_1 and B_2 folds "were nearly always found to be co-axial" (1965, p. 72). It is very difficult to reconcile dome formation with co-axial refolding unless pre-F_1 folding is called upon. On the other hand co-axial refolding of B_1 folds is likely when the latter are recumbent, or nearly so, and the strike of F_2 axial planes is parallel to the direction of the earlier B_1 axes (as in the Type 3 pattern of Ramsay, 1962). In the area under consideration the highly variable, in places horizontal, attitude of s_1 and the lack of any reasonably consistent trend of B_1 axial planes speaks against formation of domes by interference of B_1 and B_2 folds. The pattern of interference folding at the Rote Adlerkuppe and the Rooikuiseb anticlinorium is similar to that of Ramsay's Type 3 and it is thus tentatively concluded that B_1 fold axes originally followed a general northeasterly trend and that

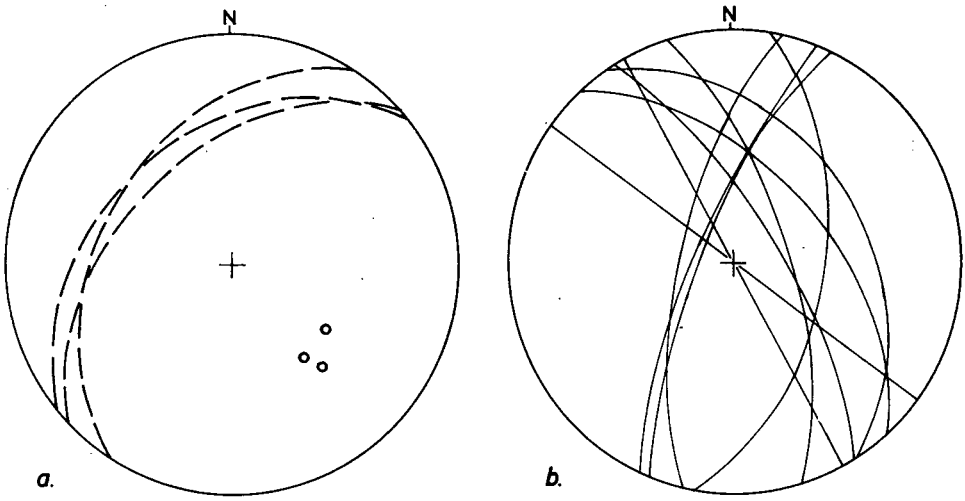

Figure 23. Synoptic stereograms for s-surfaces of F_3 and F_4 age.

(a) s_3 planes, derived from contour maxima from Schieferberge subareas

(b) s_4 planes, derived from contour maxima in all subareas

refolding about northeast-trending axes during F_2 produced the basic fold pattern as exposed today.

If this is so then an explanation for the formation of dome structures must call on processes other than interference of B_1 and B_2 folds. In a discussion on the origin of brachy-anticline and dome structures in the Damara belt, Gevers (1963, p. 225) stated that ".... it seems to the writer completely unlikely that his (Smith's) explanation ..... (by) crossfolding can receive general application throughout the geosyncline". He subscribes rather to Cloos' general concept of the vertical component of the stress field increasing in effectiveness with depth and with the degree of plasticity and mobility of transformed material (Cloos, 1935).

In the area between Otimbingwe and Okahandja Gevers (1963) distinguished between an infrastructure north of the Swakop River, where the fold pattern is one of brachy-anticlines and domes, and a suprastructure to the south where the relatively simple isoclinal folding of the Khomas Hochland is found. He believed that the two structural domains were separated by a marked shear zone. In the southeastern part of the present area there is a similar change in style of folding but it is considered that this is due, at least partly, to a change in the rock types exposed. Brachy-anticlines and domes are found where the competent Etusis quartzites are present, whereas strongly elongated anticlinal and synclinal structures are found in the southeast where the relatively incompetent rocks of the Tinkas Formation are developed. No

evidence for a shear zone, similar to that postulated by Gevers (1963) exists here and Hälbich (1970), likewise, found no evidence for a major zone of shearing in the area investigated by him.

Martin briefly discussed a tectonic synthesis of the Damara orogen in Roering's paper (Roering, 1961, pp. 28-32), pointing out that all fold belts show plunging folds and that attribution of the plunges to later folding at right angles is, "in most cases wrong" (p. 30). He envisaged a single major phase of folding during which axial plunges appeared at an early stage and became progressively more pronounced with increasing compression. Martin suggested that some of the larger anticlines may have become diapiric in form under conditions of very high grade metamorphism. Opinion, however, is divided as to whether a single phase of folding can produce structures exhibiting marked changes in fold plunges (Ramsay, 1962).

The author concurs with Martin's ideas about dome formation since it is significant that dome structures are only found in the axial zone of the Damara orogen where anatexis has occurred (see chapter on Metamorphism) and where the rocks must have reached a considerable degree of plasticity. The change in style of folding coincides closely with the "migmatite" isograd and could help to explain Gever's findings of infra- and suprastructures. Within the Damaran axial zone the immediate surroundings of several dome structures, e.g. Ida dome, SJ dome (Smith, 1965), are characterised by large concentrations of Alaskitic Pegmatitic Granite which attests to great mobility in these areas. An origin for the domes by means of a differential flattening in the a-b plane (Ramsay, 1962), accompanied by uprise of migmatitic material in the sense of Cloos (1935), Reesor (1970) and, perhaps, Eskola (1949) may well turn out to be the most satisfactory explanation.

It is emphasised that more work needs to be done on the structure but at this stage the conclusions can be summarised as follows. During F_1 intense isoclinal folding gave rise to the regional foliation s_0 and to major structures many of which were probably recumbent. The trend of B_1 axes has not been established with certainty but was probably approximately northeast. During F_2 northeast-trending folds and interference structures developed. Axial plunges that existed, or appeared at an early stage of F_2, became more pronounced and where anatexis occurred migmatitic uprise and differential flattening produced dome structures. F_3 appears to represent a late stage of F_2. Later folding during F_4 generally occurred on a minor scale but has locally accentuated pre-existing structures like that of the Langer Heinrich dome.

4. PETROGRAPHY AND METAMORPHIC PETROLOGY

The mapped area is situated in the west-central part of the Damara Orogen and the rocks have suffered high-grade metamorphism and partial anatexis. The mineral assemblages in metasediments are compatible with those of the amphibolite facies (Turner, 1968). Petrographic investigation shows that the metamorphic grade increases from the southeastern part of the area towards the west.

For the purposes of description and interpretation the rocks have been assigned to three compositional categories, calcareous, basic and pelitic and the mineral assemblages are discussed in terms of the metamorphic reactions which have produced them. The metapelites have proved most rewarding for determinations of temperature-pressure conditions and it has been possible to construct isograds based on the appearance of index assemblages in such rocks.

4.1. Carbonate and siliceous carbonate associations

A variety of marbles and calc-silicate rocks was found in the Rössing, Husab and Tinkas Formations. With the exception of a notable increase in grain size, the changes occurring in these rocks from east to west in the study area are not as pronounced as those in the pelitic metasediments. However, they have proved useful in demonstrating the effect of variable ratios of partial pressures of CO_2 and H_2O, and in the southeast, have aided in the determination of metamorphic temperatures.

4.1.1. Marbles

Marble horizons, though widespread, have their thickest development in the western parts of the mapped area. In the east they occur in the Tinkas Formation as generally impure beds between 1 cm and 2 m thick. The colour of the marbles varies from dark grey (graphitic types) through pale green (serpentine-rich types) to white.

The grain size of the marbles is generally coarser than that of the surrounding metasediments, usually about 2 mm, but grain sizes exceeding 2 cm are also found. In thin section, textures are granoblastic-polygonal to granoblastic with curved and embayed grain boundaries; monomineralic marbles, in particular, are granoblastic-polygonal. Whereas most carbonate grains have recrystallised, after deformation, into unstrained aggregates several samples (RJ392, RJ663) consist of grains which display deformation textures such as bent cleavages and deformation twins and lamellae.

Dolomite and calcite, the most abundant minerals, were distinguished by staining techniques (Wolf et al., 1967). The relative proportions of the two carbonates vary considerably in the rocks examined and essentially pure calcite marbles as well as pure dolomite marbles were found. The mineral assemblages are listed in Table 3.

Table 3. Mineral assemblages in marbles. Samples listed approximately in order of increasing metamorphic grade. X = major constituent, m = minor and accessory constituents, r = retrograde constituent.

Sample No	Cc	Dol	For/ Serp	Chond	Di	Tr	Phl	Graph	Other *	Locality
RJ423	X				X				qtzX, hb, sph, clz(r), plag	K23
RJ663	X						m	m	qtz	Q11
RJ373	X				X				ap, qtz, clz(r)	L18
RJ375	X				X				qtz, plag, scap, clz(r), sph	L18
RJ448	X					m	m	m		H20
RJ392	X					m		m		J18
RJ316		X								L11
RJ317	X	X	X	m			m		spinel, ap	L11
RJ349	X	X	m	X	m		m		plag, ap	H13
RJ320	X	X					m			L10
RJ338	X						m		ap, vesuv	M10
RJ538	X	m			X	m	m		ap, Fe-ore	D15
RJ298	X	X	X				m		Fe-ore	E12
RJ719	m	X				mr	m		ap, vesuv	I10
RJ 93	X	X	X						brucite	J9
RJ127	X	X	X				m		ap, chl(r)	L8
RJ 4	X	X	m		m	mr			ap	M8
RJ 5	m	X			m		m		scap, chl(r)	M8
RJ100	X		X				m			N9
RJ672	m	X			X	m		m	ap	O8
RJ233	X	m	m	X		mr	m	m	pyrite	M4
RJ208	X	m	X				m		spinel, chl, Fe-ore	J5
RJ105	X	X	X							H5
RJ191	X	X	X						brucite, spinel	J1

* all minor or accessory unless otherwise indicated.

At the Rote Adlerkuppe dome and in the Husabberg range, calcite contains exsolution lamellae and blebs of dolomite (Pl. 19); these intergrowths are confined to rocks which contain co-existing calcite and dolomite. Many of the samples contain subparallel rods of dolomite but the shapes are dependent on the orientation of the exsolution products, which appears as lenses and circular blebs. Between crossed nicols the exsolved blebs extinguish together and, in certain orientations, with the host. Apart from the blebs, larger grains of dolomite are found as globular forms within calcite grains with or partly surrounding them in much the same way that albite rims microcline (Ramberg, 1962; Miller, 1974). They are most probably completely exsolved from the host calcite but it is often difficult to distinguish between dolomite grains of such an origin and those which are primary. An exsolution origin is postulated here because of the general uniformity in size of the guest, the markedly parallel orientation of blebs and the similarity between these textures and those reported by Van der Veen (1965), Goldsmith et al. (1955) and Carpenter (1967), for which exsolution origins have been accepted.

Dolomite was not found to be a common constituent in marbles collected in the east and southeast, largely because these marbles are impure and dolomite has reacted with quartz to form calc-silicates. In no instance do dolomite and quartz occur in contact as a stable pair. Dolomite and tremolite are found together in some specimens although normally they are separated by silicate minerals such as diopside and forsterite. The occurrence of tremolite is of significance as its presence is unexpected in this relatively high-grade metamorphic environment. Smith (1965, p. 30) noted that tremolite is an accessory mineral in the marbles north of this area. Tremolite appears to exist as a stable mineral in only a few of the samples studied (e.g. RJ392), co-existing with calcite. In most samples it is found either as a retrograde phase after forsterite or diopside (RJ719, RJ4, RJ233), or as armoured relics within newly-formed grains, as for example in RJ672 where tremolite is surrounded by diopside, which insulates it from further reaction with dolomite (Pl. 20).

Diopside is not a common mineral in the marbles whereas serpentine is frequently present. Although unaltered forsterite occurs locally, generally it is more or less serpentinised, and this lends an attractive yellow-green to pale green speckling or banding to the rock. Forsterite is found around the Rote Adlerkuppe dome and farther to the west. At the Husabberg and near the confluence of the Khan and Swakop Rivers small amounts of brucite appear to have formed during serpentinisation of forsterite. Forsterite aggregates in dolomitic marbles usually are surrounded by masses of calcite which contain dolomite as an exsolution product (Pl. 21).

Chondrodite occurs in some marbles, generally in association with forsterite. It is most common in the vicinity of intrusive granites and is possibly of metasomatic origin in such cases; however it is also found away from intrusive contacts where it may have formed during regional metamorphism. Nash (1971, p. 59) has described textures showing replacement of forsterite by chondrodite. Similar relationships are found in some places in this area but in others chondrodite and forsterite co-exist stably and have apparently formed at the same time. Table 3 shows that certain samples contain co-existing

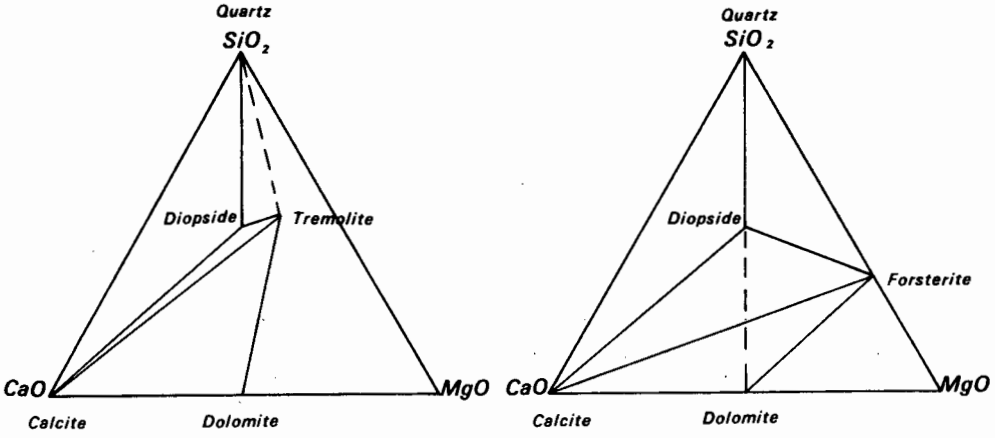

Figure 24. Possible three-phase assemblages co-existing with CO_2 and phlogopite; in the east (a) and west (b). Modified from Winkler (1967).

calcite-dolomite-tremolite-forsterite or chondrodite (RJ4, RJ233, RJ719). In these, tremolite is retrogressive after forsterite and/or chondrodite and occurs as partial reaction rims together with some dolomite which formed at the same time (Pl. 22).

Graphite is a very common accessory, occurring as macroscopic discrete flakes. Accessory phlogopite, easily confused with talc because of its lack of colour and similar optical properties, is equally common and in several samples is altered to chlorite. Small amounts of talc occur with serpentine as a retrograde phase after forsterite. Less common accessory minerals include apatite, pyrite, vesuvianite, scapolite and spinel.

The mineral assemblages in the east and west are graphically illustrated in Figure 24.

4.1.2. Calc-silicate rocks

Calc-silicate rocks constitute a significant part of the Tinkas Formation where they occur interbedded with pelitic schists and individual layers vary in thickness from a few millimetres to more than one metre. The rocks are normally massive and non-foliated but in fold closures a gneissic banding is developed in response to transposition. In thin calc-silicate layers there is conspicuous colour zoning from pale grey-green in the centre to almost black at contacts with schist layers (see p. 71). In the central and western parts of the area calc-silicate rocks are found in the Rössing-, Husab- and, to a more limited extent, in the Witpoort Formations.

In thin section the calc-granofelses of the Tinkas Formation are

Table 4. Representative mineral assemblages in calc-silicate rocks. The samples are listed in approximate order of increasing grade. X = major constituent, m = minor or accessory, r = retrograde.

Sample No.	Quartz	Microcline	Plagioclase	Hornblende	Diopside	Garnet	Calcite	Scapolite	Clinozois/epid	Sphene	Apatite	Fe-ore	Other	Locality
RJ 35	X	X	X	X	X		m		mr	m	m		biotite m	I25
RJ 37	X	m	X	m	X		X	X	m	m	m	m		I25
RJ429	X		X	X		X			X	m	m	m	tourm m	J24
RJ620	X		X	Xr	X		m		mr	m	m	m		N21
RJ614	X	sauss		X	X		X		mr	m	m			O19
RJ638	X		X	m	X		m		mr	m		m		P15
RJ586	m		X		X		X		mr	m	m	m		O13
RJ590	X	m	X	m	X		X	m	mr	m		m		P14
RJ664	X		m		X	X	m	m	Xr	m				Q12
RJ 65			m	m	X		m	X	mr	m		m	tourm m	P12
RJ657	X	m	X		X	X	mr			m			wollastoniteX	P12
RJ573	X	m	X	m	X		X	m	m	m	m		tourm m	G26
RJ404	X		X	X	X		mr		mr					H21
RJ449	X		X	X	X		m			m		m		H20
RJ489	X		X		X		m		mr	m		m		F20
RJ474					X			X	m	m				F20
RJ527	m		X	m	X		m		mr	m				H14
RJ327	X		X	m	X				mr	m				K14
RJ536	X		X	m	X					m		m		F12
RJ 94	X	X	X	X	X					m	m		chlorite r	J10
RJ268	X	X	m		X		m	X		m	m	m		L7
RJ274	m	X			X		X	X		m			wollastoniteX	J5
RJ210	X		X	m	X					m	m	m		J5
RJ223	X		m		X		X	X		m	m	m		K2
RJ218	m				X	X	mr			m	m	m	wollastoniteX	K1

generally fine grained but inequigranular, and either porphyroblastic or seriate in texture. The average grain size is close to 0,02 mm with larger grains exceeding 2 mm. Grain boundaries tend to be lobate and somewhat irregular although felsic patches are polygonal. Towards the west the grain size increases, the heteroblastic appearance is lost and grain boundaries straighten. The texture approaches granoblastic polygonal although the ideal triple-point arrangement is not universally developed because of different grain-boundary or interfacial energies of diopside, hornblende, quartz and feldspar (Spry, 1969; Stanton, 1972). In addition, gneissic structures become more common. Representative mineral assemblages are listed in Table 4.

Quartz is a constituent of most of the calc-silicate rocks where it forms clear, xenoblastic grains.

Slightly saussuritised and generally zoned plagioclase occurs occasionally as poikiloblastic grains but usually it is found as polygonal grains, with quartz. Although labradorite is most common the composition varies between andesine and bytownite. In the west, antiperthitic textures are developed. It has not thus far been possible to relate the Ca-content of plagioclase to metamorphic grade because crystal zoning, a lack of twinning and, in particular, the variability of associated mineral species militate against reliable correlation. The whole rock mineralogy exerts a greater control over plagioclase composition than does metamorphic grade. Wenk (1962) and Winkler (1970), have emphasised the importance of comparing the An-content of plagioclase only in rocks of similar mineralogy. During his work in the Alps, Wenk (1962) dealt only with assemblages where calcite and plagioclase are the Ca-bearing minerals. When this condition was not met, highly erratic results followed. Ghent and DeVries (1972) reported that regularity of change of plagioclase composition occurred only in rocks containing the assemblage quartz-plagioclase -hornblende-garnet-epidote and that where epidote was absent the An-content of plagioclase fell sharply. In the present area the mineral assemblages are too varied to permit reliable statistical data to be extracted.

Microcline occurs in small amounts in the calc-granofelses but is more common in para-amphibolite border zones (p. 71).

Scapolite is a common mineral in the calc-granofelses, co-existing stably throughout the area with other calc-silicate minerals although it is more abundant in the west. The polygonal grains and poikiloblastic plates, falling within the range of mizzonite (Table 5), have resulted from both regional and contact metamorphism. In many places the scapolite has altered to sericite/saussurite aggregates and occasionally to virtually isotropic material, possibly analcime.

Diopside is a common and characteristic mineral in the calc-granofelses and calc-silicate gneisses and usually gives rise to the pale green colouration of the rocks although it is colourless in thin section. The pyroxene has almost invariably crystallised before hornblende, which encloses it poikiloblastically or replaces it along cleavage planes.

2V-angle and refractive index measurements (Table 6, Fig. 25) indicate that the clinopyroxene in many cases contains some traces of Fe and would more correctly be termed salite, following the nomenclature of Poldervaart and Hess (1951).

Table 5. Refractive indices (±0,002) and birefringence of scapolite from calc-silicate rocks. Meionite content after Shaw (1960).

Sample No	n_ω	n_ε	$n_\omega - n_\varepsilon$	%Meionite	Rock type	Locality
RJ661	1,579	1,555	0,024	65	scapolite para-amphibolite	Q12
RJ377	1,586	1,556	0,030	72	scapolite-diopside amphibolite	K19
RJ474	1,586	1,558	0,028	74	diopside-scapolite granofels	F20
RJ241	1,585	1,556	0,029	72	skarn	M5
RJ223	1,578	1,556	0,022	65	diopside-hornblende gneiss	K2

Table 6. Refractive indices (n_β) and 2V-angles of clinopyroxenes from calc-silicate rocks.

	RJ601	RJ35	RJ578	RJ423	RJ65	RJ716	RJ210
n_β (± 0,002)	1,692	1,693	1,699	1,695	1,698	1,676	1,698
2V	59°	59°	59°	57°	57°	57°	56°
Locality	016	I25	H26	K23	P12	J10	J5

Figure 25 shows the plotted positions of the samples of Table 6 on a n_β/2V diagram (Muir, 1951). The compositions of the plotted points can be only approximate because neither the Al, Ti and Fe^{3+} contents, nor their structural sites, are known (Deer et al., 1962, vol. 2, p. 132).

The only carbonate found is *calcite*, which varies considerably in amount but shows a general decrease in a westerly direction. It occurs as polygonal grains slightly larger than the grains of other minerals in the rock. In places in the west, as in the Gürtel Hills, it has reacted with quartz to form wollastonite (RJ274), where thin calc-silicate layers are interbedded with schists. Wollastonite is normally more common in contact aureoles (p. 135).

Grossularite/andradite garnet is not common in the calc-granofelses, except in the vicinity of intrusive granites. In response to regional and contact metamorphism, it has grown as skeletal, fishnet-type grains poikiloblastically enclosing other minerals. Near the southeastern boundary

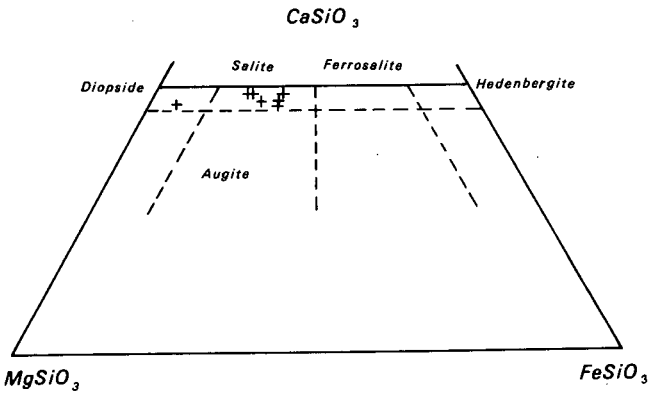

Figure 25. Composition of clinopyroxenes in calc-silicate rocks as determined by measurement of 2V and n_β

very clear examples are seen of the breakdown of clinozoisite/epidote to grandite (RJ429, Pl. 23) and in contact aureoles it has formed as a retrograde mineral, after wollastonite-plagioclase. West of the main outcrop area of the Tinkas Formation, grossularite has not been observed, but in the west large masses of andradite-rich garnet (e.g. RJ220) are not uncommon, particularly in skarn assemblages. In Table 7 cell-edge lengths and refractive indices of three specimens are listed, two from the southeast (RJ362, RJ618) and the other from the west, near Hildenhof 58 (RJ220).

When plotted on the determinative charts of Winchell (1958), the samples lie very close to the grossularite-andradite join, suggesting that they contain insignificant amounts of pyralspite.

Table 7. Refractive indices and cell edges of selected specimens of grossularite-andradite from calc-silicate rocks. Composition according to data of Winchell (1958).

	n (± 0,002)	a(Å)	Composition	Locality
RJ362	1,758	11,890	Gr_{86} And_{14}	M17
RJ618	1,768	11,889	Gr_{73} And_{27}	N20
RJ220	1,861	12,006	Gr_{17} And_{83}	K2

Representatives of the *epidote group* are found in the calc-silicate rocks but are seldom present in greater than accessory amounts. The composition of selected samples from the Tinkas Formation in the southeastern part of the area is given in Table 8.

Table 8. Refractive indices (n_β) and composition of clinozoisite/epidote from calc-silicate rocks. Compositions according to data of Holdaway (1972). r = retrograde.

	n_β (± 0,002)	Mol. % Pistacite	Locality
RJ664	1,717	Ps_{11} r	Q12
RJ590	1,715	Ps_{10} r	P14
RJ655	1,728	Ps_{17}	P12
RJ429	1,728	Ps_{17}	J24

Clinozoisite is in most samples present only as a retrograde phase replacing diopside, hornblende, scapolite, plagioclase and, particularly, grossularite where it occurs as xenoblastic, interstitial grains and as pseudomorphs. RJ429 is of particular interest because here epidote (Ps_{17}) is partially replaced by grandite in a prograde relationship (Pl. 23). While clinozoisite is of retrograde origin, it is clear that epidote still can be observed as a prograde mineral in the presence of quartz in the southeast and as far west as the Rooikuiseb anticlinorium. No prograde clinozoisite/epidote has been observed in the western parts of the area.

Hornblende is a common mineral in the calc-silicate rocks but description of it is delayed until the next section (p. 71).

Other constituent minerals occur in minor or accessory amounts. The most common of these is sphene which is normally found as small, acute rhombic cross-sections and larger irregular to rounded aggregates. In many samples the mineral is pleochroic in shades of red and yellow and where enclosed in hornblende or biotite, pleochroic haloes are found, indicating that the sphene contains rare-earth elements and that it is somewhat radioactive. Biotite, occasionally altered to chlorite, is found as scattered flakes in the calc-granofelses and becomes more common towards the margins of the layers, where it is poikiloblastically enclosed by hornblende. Idioblastic and rounded grains of apatite as well as small amounts of allanite, tourmaline and vesuvianite appear in some samples. Although commonly found as a contact metamorphic mineral (Winkler, 1967; Deer et al., 1962), vesuvianite is of regional metamorphic origin here. Pyrite, chalcopyrite and pyrrhotite occur in accessory amounts. The sulphides tend to be more common in rocks which have suffered extensive retrograde change, e.g. near Hildenhof 58. The retrogression in such cases may have been caused by sulphide-bearing hydrothermal solutions. Clinozoisite/epidote and pyrite are intergrown in some samples.

4.1.3. Quartz-microcline para-amphibolites

A characteristic feature of most calc-silicate layers in the Tinkas Formation is the presence of narrow para-amphibolite bands symmetrically distributed on either side of the calc-granofelses, along the contacts between the latter and the pelitic schists. These amphibole-rich layers are designated quartz-microcline para-amphibolites even although they do not consist essentially of plagioclase-hornblende. Plagioclase is usually present, but the major minerals are hornblende, microcline and quartz. The mafic layers vary in thickness from about 1 mm to several cm and they are thickest where granofels/schist contacts are gradational. The symmetrical distribution and generally similar thickness of such pairs of amphibolite layers is suggestive of a metamorphic origin for them.

Table 9 lists the mineral assemblages which are found in the mafic layers.

Table 9. Mineral assemblages in quartz-para-amphibolites associated with calc-silicate rocks of the Tinkas Formation.

	Qtz	Mcl	Plag	Hb	Di	Cc	Scap	Bi	Fe-ore	Sph	Locality
RJ601	X	X	X	X		X		X	X	X	016
RJ661	X	X		X	X		X		X	X	Q12
RJ666	X	X	X	X		X	X			X	Q11
RJ622	X	X	X	X				X		X	N21
RJ635	X	X	X	X					X	X	Q15
RJ593	X	X	X	X	X			X	X	X	014
RJ384	X	X	X	X	X	X	X	X	X	X	K20

The zonal arrangement of minerals from the centre of calc-granofels layers (a) through to the amphibole-rich layers (c) is illustrated as follows:

(a) Quartz - plagioclase - diopside - calcite - sphene
(b) Quartz - plagioclase - diopside - sphene ± calcite ± microcline ± hornblende
(c) Quartz - microcline - plagioclase - hornblende - sphene ± calcite ± biotite.

Thin-section studies show that quartz, calcite and biotite do not occur in contact with each other. Calcite and biotite are present in very minor amount and are of smaller size than other mineral grains. Hornblende and microcline occur as poikiloblastic grains, coarser in size than other minerals with the possible exception of scapolite. It is clear that microcline and hornblende have been produced by reaction between the non-compatible phases calcite, quartz and biotite; this is discussed further on p. 81.

In the calc-silicate rocks and quartz-microcline para-amphibolites, hornblende differs from the other minerals in that it forms large poikiloblastic grains, which are idioblastic to subidioblastic in form. The grains are elongated in the bedding or s_{01} but within this surface they may display no preferred orientation. However, as mentioned on p. 46, hornblende prisms are locally oriented parallel to B_2 fold axes. The mineral has formed after diopside and replaces it. In other mafic rocks such as amphibolites, hornblende has formed as a result of other reactions and displays different textural relationships. The γ-axial colour of the hornblende shows regional variation; it is blue-green in the east and south and deeper blue-green to green in the west. Rock composition appears to exert a greater control over the colour than metamorphic grade because the colours of hornblendes from schists and from amphibolites are different (p. 84).

4.1.4. Interpretation

During metamorphism of siliceous carbonate rocks minerals like talc, tremolite, diopside and forsterite may form over large temperature ranges, depending on P_T (total pressure), P_f (fluid pressure) and the composition of the fluid phase. The term fluid, as used here, encompasses both liquid and gaseous phases for, as Krauskopf (1967, pp. 434-440) has pointed out, under conditions of high pressures, supercritical phases and liquids have similar properties and unless the physical conditions and composition are accurately known, it is usually not possible to be certain whether such phases are liquids or gases. Because the effects of $P_f < P_T$ have not yet been adequately investigated by experimental work the assumption is made that $P_f = P_T$. P_f is the sum of the partial pressures of H_2O, CO_2 and other fluids like HF, SO_2 and so on. For metamorphism of siliceous carbonate rocks the effects of varying P_{H_2O} and P_{CO_2} have been evaluated for many relevant reactions but the effects of other fluids are again not well known. The composition of a fluid phase consisting of H_2O and CO_2 is normally expressed as the mole fraction, X_{CO_2}, and this is the terminology adopted here. H_2O and CO_2 are the only fluid phases involved in most of the important reactions; the possible effects of HCl, HF, SO_2, NH_3 etc have been neglected for they have not been adequately investigated in the laboratory.

Talc and tremolite can form under similar physical conditions, but which of these minerals forms first depends on the availability of water (Trommsdorff, 1966; Winkler, 1967; Metz et al., 1968; Metz and Puhan, 1970). Puhan and Hoffer (1973) have investigated the formation of these two minerals near the south-eastern margin of the Damara Orogen. In that area talc has crystallised first, through the reaction:

(1) 3 dolomite + 4 quartz + 1 H_2O = 1 talc + 3 calcite + 3 CO_2

This reaction has been investigated experimentally by Gordon and Greenwood (1970) and Metz and Puhan (1970, 1971). The experimentally established equilibrium curve, at 5 kb, of this and the reactions described below are shown in Figure 26. Tremolite has formed through the reaction:

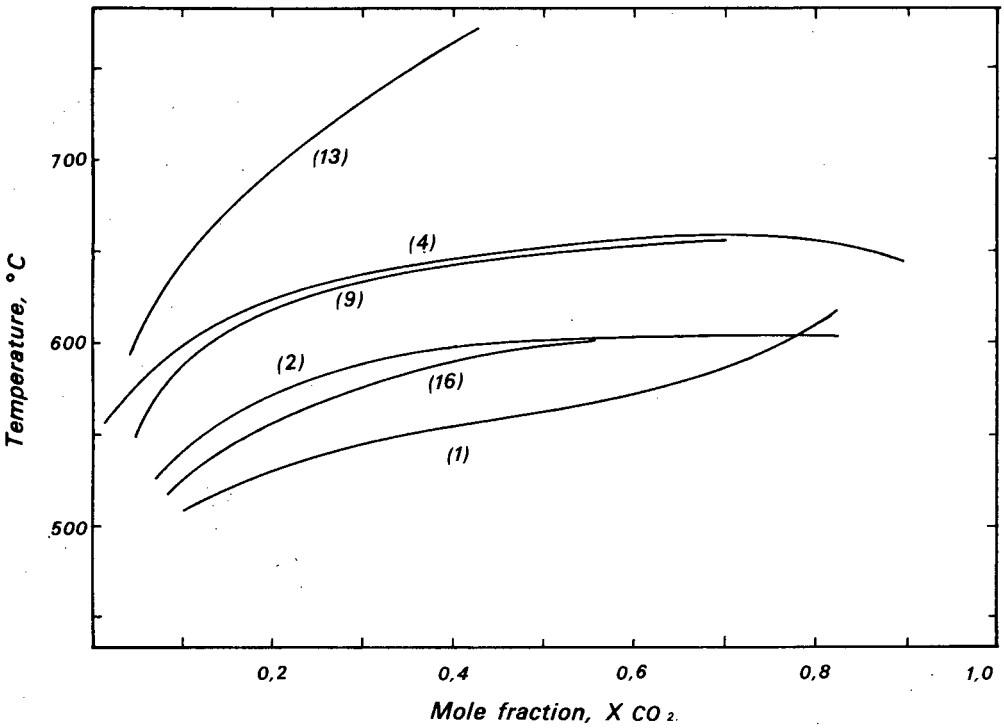

Figure 26. Reaction curves at P_f = 5 kb for reactions (1), (2), (4), (13) and (16). Reaction (9) is plotted at P_f = 4kb. Data from literature cited in the text.

(2) 5 talc + 6 calcite + 4 quartz = 3 tremolite + 6 CO_2 + 2 H_2O

From the stable co-existence of tremolite-talc-calcite-dolomite-quartz, metamorphic temperatures in the Damara belt southeast of Windhoek were estimated to be 590° C at a pressure of 5 kb (Fig. 26) (Puhan and Hoffer, 1973). The Khan/Swakop area is more than 200 km west of the region investigated by Puhan and Hoffer and considerably farther away from the southern margin of the orogen. Here temperature conditions exceeded those of the divariant reactions above. Talc is not found, except as a retrograde phase, but tremolite is locally preserved. Phlogopite, however, is a very common mineral and has probably taken the place of talc through the reaction:

(3) 1 talc + 1 K-feldspar = 1 phlogopite + 4 SiO_2

(Gordon and Greenwood, 1970) because phlogopite + quartz is stable over a much wider range of P-T conditions than talc + K-feldspar. Tremolite and talc, furthermore, have reacted with other phases (see below) to form new minerals. Diopside is present as a stable phase throughout the area and has formed

farther to the southeast. The most likely reaction for its formation is that investigated by Metz (1970):

(4) 1 tremolite + 3 calcite + 2 quartz = 5 diopside + 3 CO_2 + 1 H_2O

The reaction is divariant, being dependent on P_T and X_{CO_2} (Fig. 26). It is very difficult to estimate X_{CO_2} at the time of metamorphism. Metz (1970) has stated that X_{CO_2} is unlikely to be very low during metamorphism of siliceous dolomitic sediments because the preceding reaction forming tremolite consumes H_2O and liberates CO_2. Nevertheless, it is likely that the temperature of formation of diopside was different in the calc-granofelses and in the marbles. In the former, which are finely interbedded with pelitic rocks, X_{CO_2} was almost certainly lower than in the marbles. Metz gives the temperature of reaction as $630^{\circ} \pm 25^{\circ}$ at 5 kb for X_{CO_2} between 0,1 and 1,0, the maximum temperature being registered at $X_{CO_2} = 0{,}75$. X_{CO_2} values were high in the marbles but not high enough to have given rise to diopside before formation of tremolite or to have allowed reaction of dolomite and diopside, which co-exist stably throughout the area (see Metz and Trommsdorff, 1968, reactions 8 and 14).

The presence of diopside indicates that the metamorphism reached at least amphibolite facies (Winkler, 1967) or medium stage (Winkler, 1970) conditions in the southeastern part of the area mapped. This is confirmed by the presence of sillimanite, cordierite and staurolite in associated schists (see section on pelitic rocks, pp. 92-97). Where diopside and tremolite co-exist, the latter mineral is generally of retrograde origin but in the absence of quartz tremolite does, in places, still co-exist with calcite.

According to Winkler (1967) tremolite + calcite is not a stable assemblage in rocks metamorphosed to hornblende-hornfels facies conditions. The assemblage does, however, exist under amphibolite facies conditions of regional metamorphism, e.g. in the Barrovian-type facies series (Winkler, 1967, p. 109; Misch, 1964, p. 332) where calcite - diopside - tremolite parageneses occur. The above assemblage also exists within quartz-free marbles in the present area.

At the nose of the Vredelus anticline (RJ392) and at Vlakteplaas 110 (RJ538) the assemblage tremolite + calcite is stable, but at the Witpoortberge (RJ672, Pl. 20) and elsewhere tremolite and calcite have reacted to form diopside ± forsterite. The relevant reactions are:

(5) 1 tremolite + 3 calcite = 1 dolomite + 4 diopside + 1 CO_2 + 1 H_2O

and

(6) 3 tremolite + 5 calcite = 11 diopside + 2 forsterite + 5 CO_2 + 3 H_2O

Winkler (1967, p. 33) suggested that reaction (5) would occur under conditions similar to those of reaction (4) but Metz and Trommsdorff (1968) and Metz (1970) have shown that this reaction can be expected to occur only under conditions of high X_{CO_2} (Fig. 27). Furthermore, the calculated equilibrium curve is very steep on a T - X_{CO_2} diagram and thus it cannot be used for temperature determinations. A calculated reaction curve (Fig. 28) for reaction (6) has been presented by Skippen (1971). His curve, calculated for P_f = 2 kb shows a temperature maximum of 615° at $X_{CO_2} = 0{,}6 - 0{,}7$. The equilibrium curve lies at higher temperatures where $P_f > 2$ kb.

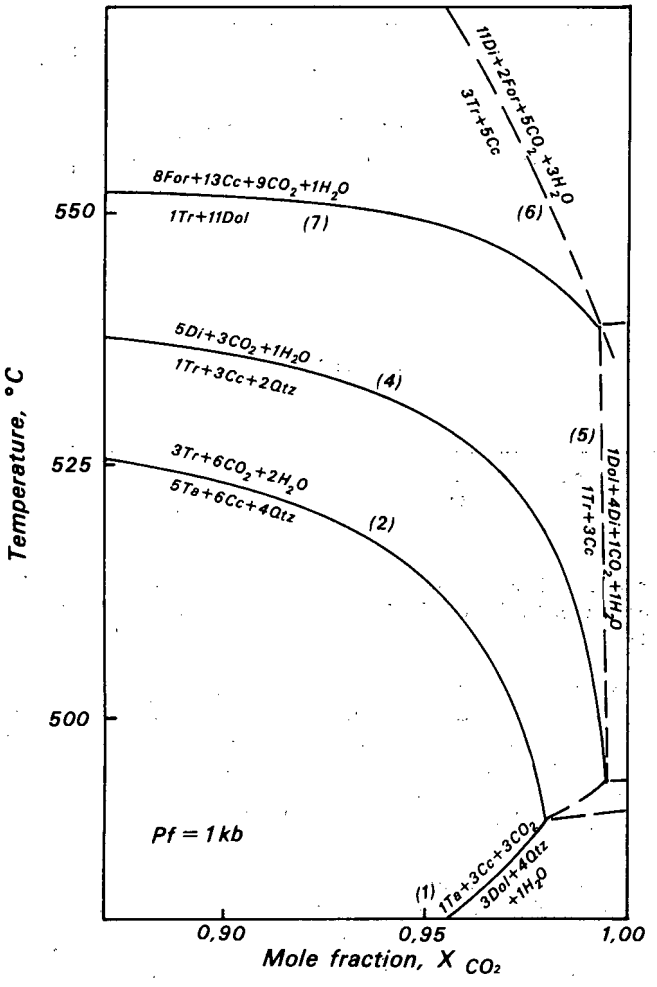

Figure 27. Isobaric T - X_{CO_2} diagram for metamorphosed siliceous dolomites at total fluid pressure (P_f) of 1 kb, after Metz and Trommsdorff (1968). Reactions are numbered as in text. Solid curves have been experimentally determined, dashed curves are based on calculations (Metz and Trommsdorff, op. cit.). Reaction (5) occurs only at very high X_{CO_2}.

Because of the strong control that X_{CO_2} exerts over the tremolite + calcite reaction, an "isograd", defined as "tremolite + calcite out", would be expected to show a different trend in many metamorphic terrains from

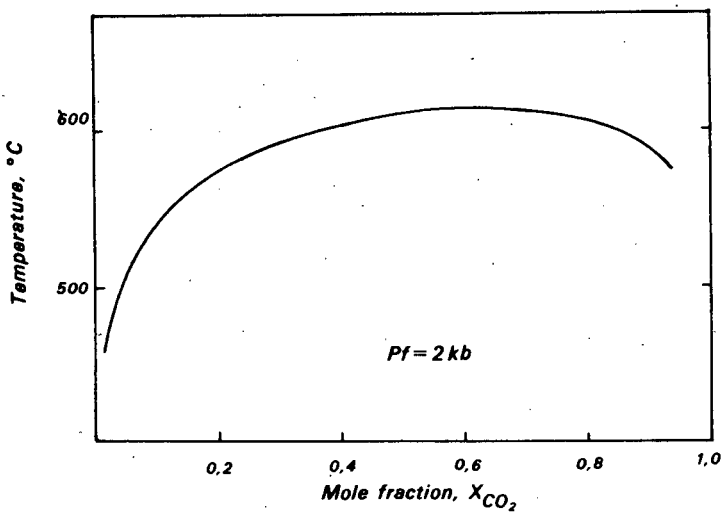

Figure 28. Isobaric T - X_{CO_2} diagram at total fluid pressure of 2 kb, showing the calculated equilibrium curve for reaction (6), after Skippen (1971).

isograds in pelitic or basic rocks. In the area mapped by the writer such an isograd would probably trend in a north-northwesterly direction from, approximately, the position of Riet 30, but the distribution of carbonate rocks in the central parts of the area is too sparse for its trend to be definitely established. The phenomenon of one isograd trending at a high angle across other isograds has been reported by Carmichael (1970) and Hutcheon and Moore (1973).

Tremolite and dolomite are not found in contact in prograde assemblages. They have reacted to form forsterite through reaction (7) which has been experimentally investigated by Metz (1967)

(7) 1 tremolite + 11 dolomite = 8 forsterite + 13 calcite + 9 CO_2 + 1 H_2O

Field studies elsewhere and experimental work have indicated that this reaction occurs at very nearly the same P - T conditions as reaction (4) (Metz, 1967, 1970; Trommsdorff, 1966; Winkler, 1970), although from purely thermochemical reasoning Turner (1967, 1968) concluded that forsterite should form after diopside unless P_{H_2O} was high and X_{CO_2} very low.

In the area under investigation, forsterite-bearing assemblages have not been observed east of the Rote Adlerkuppe dome. While this is suggestive of formation of forsterite subsequent to diopside, it is unlikely that this is the case. The lack of forsterite in the east may be due to:

(a) thin and siliceous marble bands not chemically suitable for forsterite formation,

(b) apparent lack of dolomite, so that reaction (7) could not take place,
(c) incomplete sampling.

Textures like those shown in Plate 21 are an expression of reaction (7), the forsterite (now serpentine) and calcite having formed at the expense of tremolite and dolomite. The formation of serpentine is a later feature. At, for example, the Husabberg brucite is found together with serpentine as an alteration product (RJ93), and probably formed through the reaction:

(8) $2\ \text{forsterite} + 3\ H_2O = 1\ \text{serpentine} + 1\ \text{brucite}$,

which has been investigated by Johannes (1968), who has shown that it occurs slightly above 400° C at 5 kb. In this case brucite has formed during serpentinisation and is not the result of hydration of periclase or breakdown of dolomite.

Where chondrodite is found it has probably formed from fluor-tremolite through a reaction similar to reaction (7), investigated by Becker and Hoschek (1973) (Fig. 3):

(9) (F,OH) tremolite + dolomite = (F,OH) clinohumite + forsterite + calcite + H_2O + CO_2.

These authors state that this reaction at 4 kb, and that investigated by Metz (1967) (i.e. reaction 7), occur at approximately the same temperature. Fluorine for the formation of fluor-tremolite and subsequent chondrodite has, in some places, probably been derived from adjacent intrusive granites, but in others, may have been derived from original, fluorine-bearing minerals in the marbles. Gevers (1931) has reported the presence of fluorite in the marbles of western Damaraland. The observed intergrowths of forsterite and chondrodite are easily explained, and are to be expected, if reaction (9) has occurred (but with chondrodite as a product in place of clinohumite).

During prograde metamorphism a limited amount of $MgCO_3$ is taken into solution in calcite in rocks that contain co-existing calcite and dolomite. The amount held can be used for purposes of geothermometry as shown by Harker and Tuttle (1955), Graf and Goldsmith (1955, 1958), Goldsmith and Heard (1961) and Goldsmith and Newton (1969), amongst others. The geothermometer has been applied to natural rocks by Greenwood (1967), Carpenter (1967) and Hutcheon and Moore (1973). However, its use is limited to moderate temperatures because microscopically visible exsolution occurs above about 600° (Verhoogen et al., 1970, p. 589). In the present area exsolution of dolomite from calcite in dolomitic marbles is a common feature from the Rote Adlerkuppe northwards and westwards. To the east the marble samples collected do not contain co-existing dolomite and calcite and thus do not display exsolution effects. It has not been possible to perform reliable determinations of the $MgCO_3$ content in the magnesian calcites because of considerable exsolution.

With regard to the calc-silicate rocks, petrographic observations indicate that certain of the assemblages present are useful for temperature determinations, especially those containing members of the epidote group.

Storre and Nitsch (1972) have shown that the stability field of zoisite is bounded by the reaction:

(10) 2 zoisite + 1 CO_2 = 3 anorthite + 1 calcite + 1 H_2O,

and that zoisite is stable with CO_2 - H_2O mixtures only at very low X_{CO_2} (about 6 mol. per cent at 5 kb). The equilibrium curve for this reaction is independent of temperature. Similar restrictions on the stability of clinozoisite and epidote are likely to apply. With increase of Fe_2O_3 in the place of Al_2O_3 the equilibrium curve moves to higher X_{CO_2} values and with increase of Na in plagioclase it moves to lower values. The relative effects of Fe_2O_3 in zoisite and Na in plagioclase are not yet known for this reaction but are possibly compensatory (Storre and Nitsch, 1972). The paucity of epidote-group minerals in carbonate-rich calc-silicate rocks can thus be readily explained because reaction (10) has gone to the right in many of the samples studied.

If X_{CO_2} is low, epidote and clinozoisite eventually break down to garnet + plagioclase ± Fe-oxide ± quartz ± corundum, depending on the prevailing oxygen fugacity (fO_2) (Holdaway, 1972). However, in quartz-rich rocks they will generally disappear before this through a reaction of the type:

(11) 4 zoisite + 1 quartz = 5 anorthite + 1 grossularite + 2 H_2O

This is the type of reaction applicable to the breakdown of clinozoisite/epidote in those siliceous rocks that contain garnet rather than calcite. Epidote still occurs as a stable prograde metamorphic mineral in calc-silicate rocks at the Vredelus anticline, but normally only in the absence of quartz.

Several studies of this reaction, in some cases with clinozoisite or epidote in the place of zoisite, have been published, notably by Nitsch and Winkler (1965), Newton (1966), Holdaway, (1966, 1972) Boettcher (1970) and Liou (1973). Equilibrium curves from several of these studies are shown in Figure 29.

In the calc-granofelses of this area, clinozoisite with a low pistacite (Ps) content is found nearly everywhere as a retrograde phase only. RJ429,

---

Figure 29. Calculated and experimental equilibrium curves for stability of epidote group minerals in the presence of quartz.

(a) Nitsch and Winkler (1965)
Epidote (Ps_{10-33}) (+ quartz) = anorthite + grandite + haematite + H_2O (+ quartz)

(b) Newton (1966)
4 zoisite + 1 quartz = 5 anorthite + 1 grossularite + 2 H_2O

(c) Boettcher (1970)
4 zoisite + 1 quartz = 5 anorthite + 1 grossularite + 2 H_2O

(d) Holdaway (1972)
4 clinozoisite (Ps_0) + 1 quartz = 5 anorthite + 1 grossularite + 2 H_2O

(e) Liou (1973)
Epidote (Ps_{25}) quartz = anorthite + grandite + magnetite + H_2O

The shaded field indicates likely P - T conditions during metamorphism in the southeastern parts of the present area.

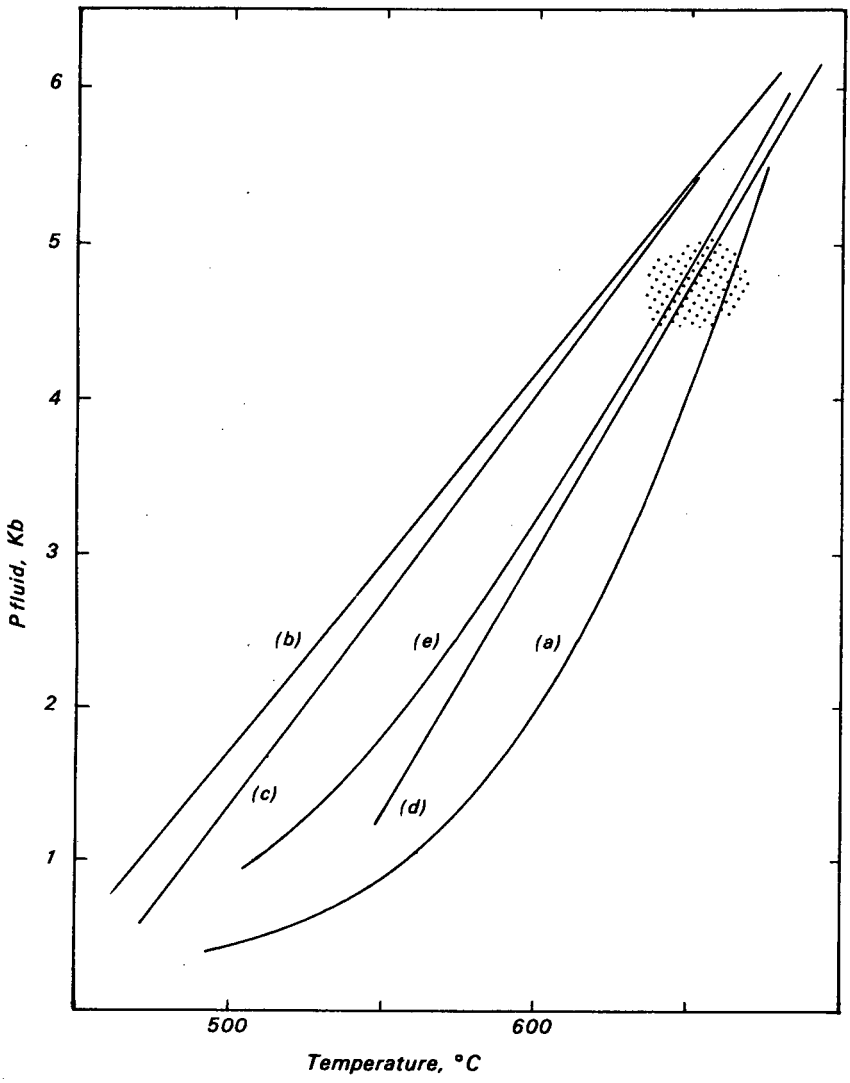
6
5
4
3
2
1
P fluid, Kb
(b)
(e)
(a)
(c)
(d)
500
600
Temperature, °C

collected close to the southeastern boundary of the mapped area along the southwestern boundary of Wilsonfontein 110, has epidote (Ps_{17}) in a reaction relationship with grandite (see Pl. 23). The relevant reaction for this relationship is:

(12) Epidote (Ps_{17}) + quartz = grandite + anorthite + magnetite + H_2O

In addition to the control exerted by bulk-rock composition, Holdaway (1972) and Liou (1973) have shown that the stability of epidote is dependent on its Fe_2O_3 content and this in turn is dependent on fO_2. As oxidising conditions change towards reducing the temperature of stability of epidote decreases and it becomes more Al-rich. The reaction is thus divariant. According to Eugster (1959), most metamorphic rocks appear to have crystallised within the magnetite fO_2 - T field. If the fO_2 exerts a very strong control on the composition of epidote, the value Ps_{17} suggests that fO_2 was in the vicinity of the quartz-fayalite-magnetite (QFM) and nickel-nickel oxide (NNO) buffers. Curve (e) in Figure 29 shows the equilibrium curve for reaction (12), at the fO_2 values of the NNO buffer, after Liou (1973). At P_f = 5 kb, the temperature is about 650° C ± 50° for the expected fO_2 values.

At P_f = 5 kb partial anatexis in gneisses begins at about 660° C. This has not occurred at the place where sample RJ429 was collected but is evident only 4 km northwest of this point. Thus a temperature estimate of about 650° C for the southeastern boundary area seems reasonable. To a certain extent this also confirms that fO_2 was close to that of the QFM and NNO buffers. A temperature much lower than 650° C seems unlikely in view of the widespread development of diopside. At P_f = 5 kb diopside will form through reaction (4) below 600° only if $X_{CO_2} < 0{,}1$ (Fig. 26). Extremely low CO_2 concentrations are not probable during progressive metamorphism of the pelitic/calcareous sequence of the Tinkas Formation because the previous reaction (2) consumes H_2O and releases CO_2. Furthermore, diopside has formed southeast of the mapped area and, therefore, the equilibrium temperature of reaction (4) must have been exceeded in the southeastern parts of the area. This temperature should be regarded as an approximation because the effects of other components cannot be taken into account at this stage. For example, the effect of Na in plagioclase would be to lower the equilibrium temperature; the effects of Mg and CO_2 are not known although, in the case of CO_2, the effects are probably small because clinozoisite/epidote will normally only be stable if X_{CO_2} is low (Storre, 1972).

In places, in the southeast and west, wollastonite has formed through the reaction:

(13) 1 calcite + 1 quartz = 1 wollastonite + 1 CO_2.

The reaction curve at P_f = 5 kb is shown in Figure 26, extrapolated from Greenwood (1967). From its position it can readily be seen why wollastonite is a very rare mineral in regionally metamorphosed rocks (Winkler, 1967). At high pressures and for a wide range of X_{CO_2}, very high temperatures are needed for its formation. However, wollastonite can form where the partial pressure of CO_2 in the fluid phase is very low. In the area studied, the occurrence of regional-metamorphic wollastonite is limited in all cases to thin calc-granofels layers, interbedded with pelitic schists, where X_{CO_2} was low. The co-existence of wollastonite and grossularite is further evidence for low

partial pressures of CO_2. Because of the very strong influence of P_{CO_2} the presence of wollastonite is not a suitable indicator of either temperature or pressure.

The quartz-microcline para-amphibolite bands along the contacts between calc-granofels and schist can be explained in terms of reaction (14):

(14) Biotite + calcite + quartz = hornblende + microcline + CO_2 + H_2O

The reaction was initiated southeast of the area, and has gone to the right in all of the samples studied because in none of them are all the reactants in mutual contact but separated by intervening hornblende or K-feldspar.

Carmichael (1970) has shown that the CO_2/H_2O ratio in the fluid phase exerted a control over the reaction temperature in the Whetstone Lake area, Ontario, such that an isograd defined by reaction (14) intersected those defined by other reactions in pelitic rocks. A chemical study of this isograd indicated that other phases probably took part in the reaction and that the actual reaction could be written as

(15) biotite + calcite + quartz + epidote + plagioclase = hornblende + K-feldspar + sphene + CO_2 + H_2O

In the para-amphibolites studied here sphene is more abundant and plagioclase less so than in the calc-granofels and schist layers on either side, which suggests that these phases may have taken part in the reaction.

A simplified reaction (16) has been studied by Hoschek (1973):

(16) 5 phlogopite + 6 calcite + 24 quartz = 3 tremolite + 5 K-feldspar + 2 H_2O + 6 CO_2

The reaction curve, at 5 kb, has been plotted in Figure 26 from the data supplied by Hoschek (op. cit.). From this it can be seen that the reaction temperature is lower than that of reaction (2) and considerably lower than that of reaction (4). The effect of adding Fe, Al, etc., to the system has not yet been investigated (Hoschek, op. cit.) and thus the significance of the temperatures defined by reaction (16), is not known in natural assemblages. In the calc-granofelses and quartz para-amphibolites, hornblende and microcline have unquestionably formed after diopside and the evidence suggests that reaction (14), or one similar to reaction (15), has occurred at a higher temperature than reaction (4) and not as indicated in Figure 26. The effect of adding other components to the system may thus be greater than anticipated.

The mineral assemblages in rocks of the siliceous carbonate association provide good examples of the importance of the composition of the fluid phase during regional metamorphism. In the area under study, certain of the mineral assemblages are controlled more by X_{CO_2} than by metamorphic grade. The predictions of Greenwood (1961, 1962) that isograds, when defined on the basis of reactions evolving different volatile components, could be expected to cross one another, have been confirmed by Carmichael (1970) and Hutcheon and Moore (1973). In the Khan-Swakop area there is a suggestion of a similar situation with the assemblage tremolite-calcite but there does not appear to be a continuous regional variation in the proportion of CO_2 and H_2O. The composition of the fluid phase was very variable and dependent on the mineralogy and thickness of the lithological units.

Besides the example of the tremolite-calcite assemblage, the presence of minerals like clinozoisite/epidote (in the absence of quartz) and grossularite is dependent on X_{CO_2}. Furthermore, the occurrence of wollastonite is restricted to local areas where X_{CO_2} was very low.

In summary the following points may be mentioned:

Diopside is present throughout the area as a stable mineral. Clinozoisite/epidote has reacted with quartz in the southeast to form grossularite/andradite which becomes enriched in andradite towards the west. Forsterite appears to have formed after diopside although unsuitable rock compositions have probably prevented its formation in the east. Wollastonite is more common in the west but is locally found in the southeast. The assemblage tremolite-calcite is not stable in the west and hornblende in calc-granofelses changes in colour from blue-green to deeper blue-green and green.

4.2. Basic- and banded-gneiss associations

4.2.1. Amphibolites

Nearly all of the basic metamorphic rocks in the Khan/Swakop area are amphibolites and these are more common in the Nosib- than in the Damara Group, occurring as tabular bodies rarely thicker than a few metres. They are found as boudinaged and disrupted layers in psammitic and pelitic gneisses, in some places concordant with s_0 and the lithological layering of the surrounding rocks, but discordant in others (Pl. 5).

In thin section the rocks occurring in the east of the study area exhibit granoblastic textures with curved grain boundaries which become straight in the west. The change towards a granoblastic-polygonal appearance is accompanied by a gradual increase in grain size from 0,5 mm to more than 1 mm. The foliated appearance of most rocks is clearly displayed in thin section by the preferred orientation of hornblende grains. Mineral assemblages in the amphibolites tend to be rather simple, representative examples of which are listed in Table 10.

Plagioclase varies in amount between 10 and 70 per cent and its grain size is somewhat smaller than that of the accompanying hornblende. It is normally partly saussuritised and is completely fresh in only a few thin sections. Zoning is a common feature with the anorthite content of the grains increasing outwards from the cores. A general increase in the anorthite content in rims of zoned plagioclase in mafic igneous rocks has been demonstrated in a number of studies of progressive regional metamorphism (Wiseman, 1934; Miyashiro, 1958; Wenk and Keller, 1969; Ghent and DeVries, 1972), and this is also apparent in the rocks of this area.

Determinations of plagioclase composition were carried out, by Universal Stage techniques, on twinned grains and on the rims of zoned grains (see Appendix). The differing effects of Ca-bearing minerals on the An-content of co-existing plagioclase (Wenk and Keller, 1959) were obviated by confining measurements to the following mineral assemblage: quartz-plagioclase-horn-

Table 10. Mineral assemblages in amphibolites. X = major constituent, m = minor, a = accessory.

Sample No.	Qtz	Plag	Hb	Bi	Sph	Ap	Fe-ore	Other	Locality
RJ 19	m	X	X	m	a	a	a		H23
RJ582	a	X	X	m	a	a	a		H24
RJ410	a	X	X	X	a	a	a	allanite (a)	I22
RJ491	a	X	X		m	a	m	chlorite (m)	E21
RJ692	m	X	X	a	a	a	m	vesuvianite (a)	M8
RJ128	a	X	X		m	a	m		L8
RJ102		X	X	X	a	a	a	diopside (m)	J7

blende-biotite-sphene-apatite-Fe-oxide.

As a result of the restrictions imposed by the mineral assemblage only 9 suitable samples could be investigated: 6 from the east and southeast, and 2 each from the central and western parts. The conclusions based on these measurements are tentative especially since Wenk and Keller (op. cit.) have demonstrated that valid interpretations must be based on a statistical treatment of an adequate number of samples. The results obtained here are listed in Table 11.

Table 11. Anorthite contents of plagioclase from amphibolites.

	Sample No.	No. of readings	Range in An-content	Mean
Southeastern part of the area,	RJ 19	4	36-40	38
east of Schieferberge and	RJ582	5	36-42	39
southeast of Swakop River	RJ 26	6	30-35	32
	RJ592	4	27-32	30
	RJ587	5	58-65	63
Vredelus anticline	RJ491	5	65-75	70
Rote Adlerkuppe	RJ313	5	75-90	82
West of Husabberg	RJ128	4	77-90	82
	RJ692	6	80-100	>80

These An-contents indicate high grades of metamorphism in the central and western parts of the area, but they are somewhat higher than those reported by Wenk and Keller (1969), although similar to values reported by Binns (1964).

Hornblende occurs as subidioblastic and xenoblastic grains showing preferred orientation and varying in amount between 30 and 90 per cent by volume. Poikiloblastic enclosure of minor and accessory minerals such as

sphene and Fe-oxide is a common feature. In many samples concentrations of tiny Fe-oxide grains are found in the cores of hornblende crystals, the rims being relatively free of them.

In the east and southeast the γ-axial colour of the hornblende is generally green to dark blue-green. In the centre of the region the mineral loses this blue-green shade and green prevails while in the west dark green is the dominant colour. A brownish-green colour was encountered in only one sample from the west. Miyashiro (1958) and Binns (1964) have used the change of colour in hornblende for the determination of metamorphic isograds but since basic rocks are relatively scarce in the Khan/Swakop area accurate isograds cannot be drawn on this basis.

Biotite is a common minor constituent of the amphibolites, and occurs as flakes in parallel orientation with, and poikiloblastically enclosed by, hornblende. Diopsidic clinopyroxene and scapolite have been observed in several samples and in the east small amounts of epidote occur. Opaque oxide is a most common accessory mineral, frequently surrounded by partial rims of sphene, which suggests that the oxide is ilmenite. Lesser amounts of sulphide are present in some samples while sphene, in addition to its occurrence with ilmenite, occurs as discrete rounded grains and granular aggregates displaying distinct pleochroism.

4.2.2. Origin

Where field relationships are inconclusive the origin of amphibolites constitutes one of the most vexing problems of metamorphic petrology. Distinction on major-element chemical grounds has been attempted (Evans and Leake, 1960; Leake, 1964) but this has proved inconclusive in many cases, mainly because all hornblende-plagioclase assemblages, however derived, have compositions very much like basic igneous rocks (Orville, 1969). The latter author has discussed the value of using Niggli c-mg variation diagrams in discussions on the origin of amphibolites, and he concluded that "It is clear .... that any possible composition variation in an amphibolitic hornblende-plagioclase ($An_{50 \pm 20}$) assemblage will fall within the range of differentiation trends of basic igneous rocks as represented on this type of diagram" (Orville, op. cit., p. 74).

Figure 30 is an ACF diagram showing the compositional field of basic igneous rocks and that of shale-carbonate mixtures. Although there is a small overlap of the two fields it is clear that most sedimentary rocks do not have the composition of amphibolites, whose composition field coincides with that of basic igneous rocks. Nevertheless, para-amphibolites are not uncommon rocks in metamorphic belts and this suggests that many, if not most, para-amphibolites have originated through metasomatic processes (Orville, 1969).

Where thin-layered amphibolites occur, Orville (op. cit.) has proposed that metasomatic reactions take place among incompatible assemblages of interbedded pelitic and carbonate layers under open system conditions. Direct reaction between carbonates and silicates occurs first with expulsion of CO_2, H_2O and probably K_2O. This is followed by leaching of excess $CaCO_3$ and reaction of Ca with silicate phases in adjacent rocks, accompanied by an

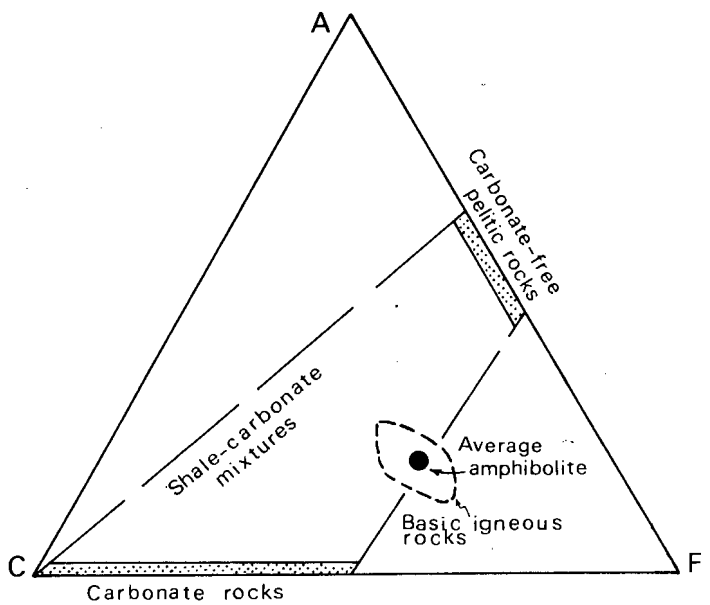

Figure 30. ACF diagram showing the composition fields of sedimentary shale-carbonate mixtures, basic igneous rocks and average amphibolite (after Orville, 1969).

exchange of Ca and Mg + Fe^{2+} between the Ca-rich and Ca-poor rocks. Experiments with synthetic carbonate/pelite mixtures in the presence of chloride solutions have shown that cations move down activity gradients with Ca and K migrating outwards from carbonate to pelite and Mg, Si, Al and H (Vidale, 1969). Metasomatic transport proceeded through the pore fluid, whose salt concentration greatly influenced differential movement.

Field relationships indicate that many of the amphibolites encountered in the study area are derived from originally intrusive rocks but the origin of the concordant bodies remains problematical. In the southeastern part of the area very little metasomatism appears to have occurred during the formation of the quartz-microcline para-amphibolites whereas in the west, where large-scale melting occurred, the mobility of elements was higher and here thin interbedded hornblende-plagioclase amphibolites are more common. These have biotite-rich selvedges suggestive of some metasomatic transfer. However, no definite conclusions can be drawn about their origin without chemical data.

Their limited thickness and association with carbonate-pelite sequences renders it unlikely that such interbedded amphibolites represent metamorphosed basic lava flows or tuffs. Although evidence for acid-volcanic activity exists in the Etusis Formation (p. 10), it has not yet been demonstrated that basic vulcanicity occurred in this part of the Damara Orogen. However, Smith (1965, p. 18) has described a group of amphibolitic rocks which he called the Amphibolite Facies of the Upper Stage of the Nosib Formation. These dense, dark rocks occur stratigraphically between the Etusis Formation and the Rössing Formation and are perhaps stratigraphically equivalent to the Khan Formation, although of different lithology. These rocks, together with others described by Gevers as having the appearance of massive plutonic rocks on weathered surfaces in an area west of the confluence of the Khan and Swakop Rivers (Gevers, 1931a; p. 48), may turn out to have volcanic affinities and need further study.

4.2.3. Banded gneisses

Banded gneisses in which individual lithological layers vary from less than 1 cm to several centimetres in thickness, characterise the Khan Formation (Pl. 1) and occur interbedded with quartzites in the Etusis Formation. The mineral composition of individual bands varies considerably and this is illustrated in Table 12.

In general, assemblages consisting of quartz-clinopyroxene-plagioclase alternate with quartz-K-feldspar-hornblende associations and transitional bands containing quartz-K-feldspar-hornblende-pyroxene (e.g. RJ203). Layers consisting almost entirely of feldspar, usually plagioclase, with minor clinopyroxene and accessory quartz (RJ107, RJ108) are not uncommon whereas bands of pyroxene-garnet gneiss are rare. The individual layers themselves may be granofelsic or gneissic in character, and small lenticular and rounded diffuse bodies of granitic and pegmatitic mobilisates, in places giving rise to stictolithic structure (Mehnert, 1968; p. 38), are ubiquitous. The mineral assemblages are illustrated graphically in Figure 31.

Textures are granoblastic-polygonal with most major constituents

Table 12. Representative mineral assemblages of individual layers in banded gneisses. X = major constituent, m = minor, a = accessory, r = retrograde.

Sample No.	Qtz	Kf	Plag	Hb	CPx	Gar	Epid	Sph	Ap	Fe-ox	Other	Locality
RJ488	a	X	a	X	X		a	a	a	m	calcite (a), allanite (a)	F20
RJ460	a		X	X	X	X	a	a	a	m	scapolite (m) allanite (a)	G21
RJ107	a	a	X		X			a	a	m		M6
RJ108		m	X		m			a	a	a		M6
RJ266	X		X		X	m	ar	a	a	m		L6
RJ541	X	X	X	X				a	a	a	biotite (m), allanite (a), tourmaline(a), calcite (m)	D11
RJ226	X	X	m	X	m			a	a	m	biotite	L4
RJ227	X	m	X	a	X		ar	a	a	a		L4
RJ203	X	a	X		X			a	a	a	calcite (m), allanite (a)	
RJ203	X	X	m	a	X			a	a	a	calcite (m), allanite (a)	K4
RJ203	m	X	a	X	a			a	a	a	calcite (m), allanite (a), chlorite (a)	

averaging between 0,3 and 1 mm in grain size. Quartz and feldspar normally make up most of the rock but in the pyroxene-garnet gneisses ferromagnesian minerals may be more abundant. Modal quartz varies between 0 and 40 per cent. The plagioclase is generally andesine (An_{30} - An_{45}); An_{77} occurs in the mafic pyroxene-garnet gneisses. It displays antiperthitic structures in places, particularly in those specimens from the west and zoning is not as pronounced as in those from the amphibolites. Myrmekitic intergrowths are developed along contacts with K-feldspar, and this mineral occurs as cross-hatch-twinned polygonal grains, normally perthitic in character.

The clinopyroxene differs from that in the calc-silicate rocks in that it is coloured, shows larger extinction angles (c/γ = 48-50° as against 44-46° in calc-silicate rocks) and generally has a higher 2V-angle (Table 13).

The colour of the pyroxene is usually pale green, in places pleochroic from very pale green (α) to yellow-green (γ). The pyroxene-garnet gneisses contain a more deeply coloured variety, pleochroic from bright green or blue-

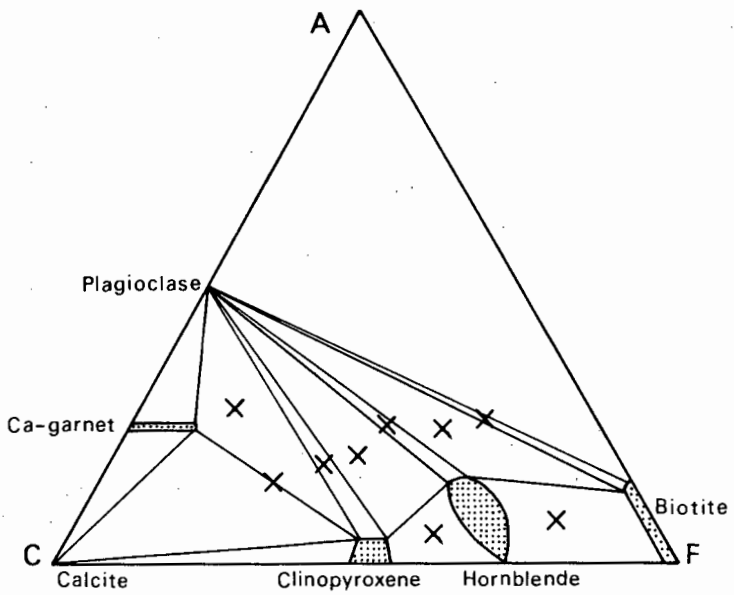

Figure 31. ACF diagram (modified from Orville, 1969) showing the compositional fields (X) occupied by the banded gneisses of the Khan and Etusis Formations. Quartz is generally present in excess and K-feldspar is an additional phase in many assemblages, particularly those to the right of the plagioclase-clinopyroxene join.

Table 13. Refractive indices (n_β) and $2V_\gamma$ angles for clinopyroxenes from selected samples of banded gneiss.

	RJ460	RJ488	RJ107	RJ202	RJ266	RJ730
n_β (±0,002)	1,702	1,687	1,692	1,688	1,720	1,700
$2V_\gamma$	68°	62°	69°	66°	70°	62°
Locality	G21	F20	M6	K4	L6	H5

green (α) to yellowish or brownish green (γ). Microprobe analyses of the two varieties of clinopyroxene from the banded gneisses are presented in Table 14. Details of the analytical procedures are given in the Appendix.

Both pyroxenes are aluminous but there is a significant difference in the Fe and Mg contents, the mineral from the pyroxene-garnet gneiss being higher in Fe and lower in Mg. While all Fe has been expressed as FeO, significant amounts of Fe^{3+} are probably present, which could account for the deep colour

Table 14. Chemical analyses (in per cent oxides) of clinopyroxenes from banded gneiss (RJ202) and pyroxene-garnet gneiss (RJ266). All Fe expressed as FeO.

	SiO_2	Al_2O_3	TiO_2	FeO	MnO	MgO	CaO	Na_2O	Total
RJ202	52,17	1,99	0,09	9,21	0,53	13,34	22,82	0,89	101,04
RJ266	47,46	3,50	0,22	18,77	0,37	6,89	23,47	0,60	101,28

and high 2V-angle.

The garnet occurring in the pyroxene-garnet gneisses is typically an andradite-rich variety (Tables 15 and 16). It appears to have formed later than the pyroxene, in places surrounding it poikiloblastically, but is also separated from it by a pyroxene-free halo of quartz and plagioclase grains. It occurs as irregular brownish to orange-coloured xenoblastic grains concentrated in layers parallel to the foliation. Unit cell values and refractive indices for two samples are listed in Table 15.

Table 15. Unit cell values (a) and refractive indices for garnets from pyroxene-garnet gneisses. Compositions estimated from charts in Winchell (1958), assuming that the garnets contain only andradite, grossularite and almandine components.

Sample	a (Å)	standard deviation	n	Composition	Locality
RJ460	11,988	0,004	1,858	$And_{78}Gr_{17}Alm_5$	G21
RJ266	11,971	0,013	1,867	$And_{80}Gr_9Alm_{11}$	L6

A microprobe analysis of the garnet in RJ266 is shown in Table 16, in which all Fe has been expressed as Fe_2O_3:

Table 16. Chemical analysis of garnet from pyroxene-garnet gneiss (RJ266).

SiO_2	Al_2O_3	TiO_2	Fe_2O_3	MnO	MgO	CaO	Na_2O	Total
36,12	4,41	0,44	27,78	0,55	0,17	31,65	0,02	101,14

Recalculation of the analysis to the most probable proportions of ferric and ferrous oxides, by assignment of molecular proportions of Al_2O_3 to CaO, FeO, MnO and MgO and conversion of excess FeO to Fe_2O_3, yields the following molecular percentages: $And_{80}Gr_{16}Alm_4Pyr_{tr}Sp_{tr}$.

Hornblende occurs as xenoblastic polygonal grains and as sub-idioblastic, poikiloblastic forms. It surrounds and replaces clinopyroxene. Wherever

the two are found in contact, hornblende appears to have crystallised later than the clinopyroxene, but generally the two minerals occur in separate bands. The colour of hornblende does not appear to be dependent on metamorphic grade and remains more or less constant throughout the area (α = yellow-green, β = green, γ = blue-green), mainly because there is probably no change in the bulk chemistry of the hornblende-bearing layers over the area and because the hornblende generally co-exists only with quartz and feldspar.

Pleochroic prograde epidote is found in small amounts in the pyroxene-garnet gneisses and, to a lesser extent, in the banded gneisses in the east and as far west as the Vredelus anticline. Elsewhere it occurs either as a retrograde mineral or as a constituent of granitic neosomes in the gneisses.

Nash (1972) has reported anhydrite from gneisses in the SJ Claims area, 8 km northwest of the northwestern boundary of the mapped area, but this mineral has not been observed in the gneisses here. Minor and accessory amounts of calcite, biotite/chlorite, scapolite and allanite occur in the gneisses. Opaque Fe-Ti oxide and sphene are very common, the oxide grains being partially surrounded by sphene which also occurs as discrete pleochroic grains. Ilmenite, martitised magnetite, haematite, pyrite and pyrrhotite have been identified in polished sections.

4.2.4. Discussion

The origin of the rocks west of the Khan River has been discussed in some detail by Nash (1971) who concluded that, with the exception of certain ortho-amphibolite bodies, the banded gneisses were derived from sediments. Similar conclusions had previously been reached by Gevers (1931, p. 47), who termed the original rocks calcareous sandstones, and by Smith (1965, p. 21), who called them calcareous, feldspathic sandstones.

The origin of the characteristic banding in the gneisses could be attributed to one or more of the following processes:

(i) Primary depositional layering,
(ii) Metamorphic differentiation,
(iii) Metamorphic differentiation in response to shearing.

Nash (1971) concluded that the banding originated as a result of metamorphic differentiation in response to shearing in a fairly homogeneous sequence of gneisses during the F_2 deformation. He based his conclusions on "the close relationship between the banding and the outline of the SJ dome structure" (op. cit., p. 34) in believing that the shearing, and hence the banding, was controlled by the formation of this dome. However, evidence from the area east of the Khan River does not support this conclusion. Firstly, the banded structure is a regional feature and is not only developed in the vicinity of dome structure; it is, for example, prominent at the Geisebberge and along the western boundary of the Welwitschia Flats. Secondly, the banding has been folded during F_2 and its development therefore pre-dates the formation of dome structures (see Pl. 1).

In the writer's opinion, Nash dismissed the first two alternatives

above on insufficient evidence. It is believed that both primary depositional structures and metamorphic differentiation, which occurred during F_1 flexural-slip folding, between layers of different chemical and mineralogical composition played important roles in the origin of the banding and that the orientation of bedding dictated the orientation of metamorphically differentiated bands. Where transposition of bedding occurred during F_1 the banding is nevertheless still a reflection of original inhomogeneities.

The banding in the gneisses is parallel to an original bedding where the latter can still be recognised as, for example, at the base of the Khan Formation and in the Vredelus anticline, where the banded gneisses occur in a sequence of feldspathic quartzites. An originally thinly-bedded sequence of alternating carbonate-bearing semipelitic/psammitic layers and siliceous Mg-Fe carbonate layers with the overall composition of a sandy marl or calcareous greywacke is envisaged for the parent rock of the gneisses.

During subsequent regional metamorphism the quartz-K-feldspar-hornblende assemblages formed through reactions (14) and/or (15) (see p. 81):

(14) biotite + calcite + quartz = hornblende + microcline + CO_2 + H_2O

(15) biotite + calcite + quartz + epidote + plagioclase = hornblende + microcline + sphene + CO_2 + H_2O

The siliceous Mg-Fe carbonate layers probably have produced calc-silicate minerals through reactions analogous to (4) (p. 74)

(4) 1 tremolite + 3 calcite + 2 quartz = 5 diopside + 3 CO_2 + 1 H_2O

The clinopyroxene found in the gneisses contains more Fe than that of the calc-silicate rocks and, judging from its greenish colouration and high 2V-angle, Fe was present largely in the Fe^{3+} form.

That a high oxygen fugacity must have prevailed in the banded gneiss sequence during metamorphism is evidenced by the presence of haematite in the gneisses and in associated granitic mobilisates. The existence of a high oxygen fugacity helps to explain why epidote and quartz still co-exist in a few places in these rocks, for Liou (1973) has shown that under conditions of high fO_2 epidote can remain stable up to 750° C at P_f = 5 kb.

The andradite-rich garnet of the pyroxene-garnet gneisses has probably formed through several reactions (12, 17, 18). In some places it was produced as a result of epidote-breakdown as follows:

(12) epidote + quartz = grandite + anorthite + magnetite + H_2O

(see p. 80, but with epidote having higher Fe^{3+}). Where quartz was not present originally, reaction (17) probably occurred:

(17) epidote = grandite + anorthite + Fe-oxide + quartz + H_2O

In both reactions the anorthite content of pre-existing plagioclase would be increased and this is seen in the pyroxene-garnet gneisses where the plagioclase is bytownite whereas oligoclase/andesine is present elsewhere.

It is significant that the pyroxene is most deeply coloured in the pyroxene-garnet gneiss layers. In these layers fO_2 was higher than in the

surrounding rocks and this has promoted incorporation of Fe^{3+} into the pyroxene during metamorphism through reaction (18), investigated by Huckenholz (1969):

(18) $(4\ CaFe^{2+}Si_2O_6 + 2\ CaMgSi_2O_6) + O_2$

clinopyroxene

$= \{CaFe^{3+}(Fe^{3+}Si)O_6 + 2\ CaMgSi_2O_6\} + Ca_3Fe_2^{3+}\ Si_3O_{12} + 4\ SiO_2$

ferri-diopside$_{ss}$ andradite quartz

The products of this reaction include strongly pleochroic ferri-diopside and andradite. The mottled structures seen in some hand specimens and thin sections, where segregations of andradite are separated from clinopyroxene by haloes of felsic minerals, are products of metamorphic differentiation and can be explained by reaction (18).

The metamorphic reactions and the mineral assemblages of the banded gneisses of the Khan and Etusis Formations are not of any great value for temperature or pressure estimates but they do show that at the time of metamorphism the oxygen fugacity was higher in these rocks than in the overlying pelitic sequences of the Damara Group (see p. 133).

4.3. Pelitic and psammitic associations

Pelitic and psammitic rocks make up the bulk of the Etusis, Rössing, Chuos, Witpoort and Tinkas Formations. Of these, the pelitic rocks in particular have proved useful in the determination of temperature and pressure conditions during metamorphism. Mineral assemblages throughout the area conform with those of the amphibolite facies (Turner, 1968); according to the classification of Winkler (1970) the physical conditions were those of the medium and high stages. These two stages are separated in the field by the boundary marking the beginning of anatexis in gneisses, which is observed close to the isograd "K- feldspar + sillimanite" in anatectic gneiss. Partial melting phenomena and the presence of a variety of index minerals indicate that the grade of metamorphism increases from the southeastern boundary of the area towards the west and northwest.

4.3.1. Medium stage

Rocks representative of this stage exist in the southeastern parts of the area where the Tinkas Formation is best developed and mineral assemblages are listed in Table 17. Although migmatitic structures are found along the southeastern boundary of the region, close to outcrops of the Donkerhoek Granite, these are related to intrusion of the granite and not to regional metamorphism. The area southeast of the Rooikuiseb anticlinorium, between the Hottentottenkirche and the Gawib stock, is devoid of partial melting

Table 17. Mineral assemblages in metapsammites and metapelites subjected to medium stage regional metamorphism. X = major constituent, m = minor constituent, a = accessory constituent, r = retrograde.

	Quartz	K-feldspar	Plagioclase	Biotite	Muscovite	Cordierite	Sillimanite	Andalusite	Garnet	Opaque	Apatite	Zircon	Tourmaline	Other	Locality
RJ774	X	m	X	X	a	X			m	a	a	a	a		I25
RJ773	X	m	X	X		X		a		a	a	a			J23
RJ 44	X		X	X	a	X			m	a	a	a			J23
RJ422	X	m	X	X	m	m	m	m		a	a	a	a	staurolite(m)	K23
RJ 48	X		X	X	m					a		a			L21
RJ625	X	m	X	X						a	a	a	a		M21
RJ745	X		X	X	mr					a	a	a		calcite(mr)	O19
RJ615	X	X	X	X						a	a	a	a		O19
RJ742	X	m	X	X	m	X				a	a	a	a		N17
RJ168	X	m	X	X		X			m	m	a	a	a	staurolite(m) chl(mr)graph	O16
RJ739	X	m	X	X		m			m	a	a	a	a		O14
RJ637	X		m	X						a	a	a	a		P15
RJ678	X		X	X						m	a			hornblende(X) sphene(a)	R14
RJ749	X	m	X	X		X		m		m	a	a		graph	Q11
RJ 34	X	X	m		m					m	a	a			I24

phenomena.

In contrast to the pelitic rocks the *psammitic* strata of the Nosib and Damara formations generally do not contain mineral associations of critical importance for the determination of metamorphic grade. The mineralogy of the psammites of the Etusis Formation is simple since the rocks are composed mainly of quartz, which has locally replaced feldspar, and microcline together with lesser amounts of plagioclase, biotite and muscovite with accessory magnetite and zircon. The conglomerates comprise quartz pebbles in a matrix of quartz, microcline, muscovite and minor biotite together with greater quantities of magnetite and zircon than are present in the quartzites.

Along the southeastern limb of the Rooikuiseb anticlinorium, northeast of the Onanis River, the top of the Etusis Formation consists of gneissic,

microcline-rich, quartzofeldspathic rocks which were probably originally quartz-feldspar porphyries. In thin section the rocks consist almost entirely of quartz and microcline together with minor amounts of muscovite and plagioclase and accessory pyrite, magnetite and biotite. The texture is inequigranular and appears to be blastoporphyritic (Pl. 24). Quartz and perthitic microcline occur as relict phenocrysts, each generally consisting of several grains of the particular mineral. They are set in a granoblastic-polygonal matrix of quartz and microcline in which the amount of microcline is greater than that of quartz (65:35). Recrystallisation has destroyed any possible diagnostic textures such as resorption effects. Muscovite occurs as oriented flakes in the matrix and it is perhaps significant that none is enclosed in the larger composite grains, a feature that would indicate a porphyroblastic origin for the larger grains rather than the interpretation favoured above that the larger grains are relict phenocrysts. Dr. Miller has provided the author with samples from the Naauwpoort Formation, northwest of Omaruru, for which a volcanic origin has been demonstrated (Miller, 1972). Texturally and mineralogically, Miller's samples are indistinguishable from those of the Etusis Formation.

In the Chuos diamictite the matrix is semipelitic in character and consists of quartz, plagioclase, microcline, biotite and muscovite. Near the contact with the Gawib Granite porphyroblasts of microcline have grown in the diamictite.

The *metapelites* are relatively fine-grained schists with average grain sizes between 0,02 and 0,1 mm. Porphyroblastic varieties are less common than equigranular types, the size of the porphyroblasts generally not exceeding 5 mm. In thin section the schists display well-developed lepidoblastic textures and in the felsic interstices between mica flakes grain boundaries are smoothly curved to polygonal. Biotite, quartz and feldspar are the most common constituents but important metamorphic minerals like cordierite, andalusite, sillimanite, staurolite and garnet also occur.

Quartz is present in nearly all samples as equidimensional to slightly elongated grains. Small amounts of microcline occur together with quartz and plagioclase and in places enclose andalusite poikiloblastically, as does plagioclase, which is the most common feldspar. The plagioclase ranges in composition from oligoclase to andesine but because of zoning, the generally fine grain and the paucity of twinning the composition is not readily determined.

The lepidoblastic texture of the schists is due to the strong parallel alignment of small biotite flakes which form the regional foliation s_{01}. In many places s_{01} and s_2 are parallel and indistinguishable, especially in the hinge zones of B_2 folds where transposition is a feature. During F_3 biotite was folded and has partially recrystallised along non-penetrative s_3 surfaces. A folded foliation defined by biotite flakes (s_{01}) is preserved in cordierite porphyroblasts in some thin sections together with biotite, aligned along s_2, (Fig. 32).

Retrograde alteration has resulted in chloritisation of some biotite together with formation of muscovite and of epidote and prehnite lenses along cleavage planes. Muscovite, less common than biotite, is also present as a

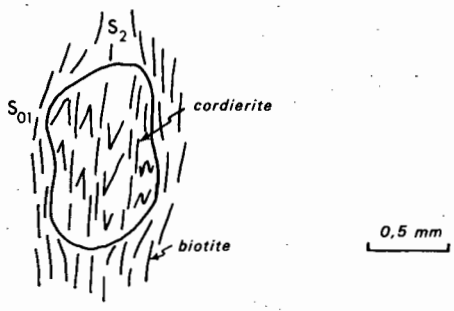

Figure 32. Cordierite porphyroblast helicitically enclosing folded s_{01} and transposition foliation s_2.

prograde metamorphic mineral co-existing with quartz. Much muscovite was consumed in earlier metamorphic reactions hence its concentration is low in the metapelites.

Andalusite occurs in the southeast in response to both regional and contact metamorphism. Near the Donkerhoek Granite it is found as elongated porphyroblasts reaching more than 5 cm in length, but away from the contacts both their size and number decrease. Beyond the thermal aureole of the Donkerhoek Granite the mineral occurs as small skeletal porphyroblasts and aggregates of tiny droplike grains. An early foliation defined by biotite is preserved in the porphyroblasts, which are themselves oriented within s_{01}. In many places replacement by later muscovite has occurred, particularly near the Donkerhoek Granite, where pegmatitic fluids were more active.

Andalusite persists almost to the boundary marked by partial anatexis in gneisses beyond which it is no longer found. From thin section evidence its disappearance is due to several reactions (see p. 125) In samples taken near the line of its final disappearance, it occurs as aggregates of small, rounded, droplike to dumb-shell-shaped grains poikiloblastically enclosed in cordierite, plagioclase and minor K-feldspar. Tiny grains of biotite are also enclosed.

Sillimanite, generally fibrolite, is common in the contact aureole of the Donkerhoek Granite. Away from here, to the northwest, its amount decreases and then increases once again. Prismatic sillimanite occurs as an inversion product of andalusite but this variety is less common than fibrolite, which shows no particularly close relationship with andalusite and is not normally in contact with it. Instead, it occurs as nests of fibres generally associated with biotite, having crystallised epitaxially in the manner described by Chinner (1961).

Staurolite is an uncommon mineral in the metapelites, partly because their composition is generally inappropriate for its formation (Hoschek, 1967;

Winkler, 1970), but mainly because it has largely disappeared through various breakdown reactions. It is found in the metapelites as small, isolated xenoblastic to subidioblastic grains usually enclosed in either cordierite or garnet. The high relief and pleochroism are distinctive. Chemical analysis of staurolite (Table 18) from a sample in which it co-exists with cordierite, garnet and biotite shows it to be relatively depleted in Mg if compared with other published analyses (Deer et al., 1962, vol. 1).

Table 18. Partial chemical analysis of staurolite in RJ168 in weight per cent oxides. All iron expressed as FeO; P_2O_5 and H_2O not determined. Electron microprobe analysis by Mr. J.P. Willis, Department of Geochemistry, University of Cape Town.

SiO_2	Al_2O_3	TiO_2	FeO	MgO	MnO	CaO	Na_2O	K_2O	Total
26,81	55,66	0,58	13,06	1,63	0,09	0,02	0,07	0,01	97,93

Cordierite is one of the most common and widespread metamorphic minerals in the pelitic rocks and is present as a stable phase throughout the area. It is found as poikiloblastic crystals which are easily confused with quartz or plagioclase except where pleochroic haloes and the characteristic sector twinning are present to facilitate identification. Recognition is easier where incipient pinitisation and sericitisation have occurred. In some sections the mineral has altered to a pale greenish-yellow isotropic substance of unknown composition.

Cordierite has crystallised at different times and appears to post-date the formation of s_0 and s_1. It has formed syntectonically during F_2, and is oriented preferentially along s_2 (Fig. 32). Crystallisation continued during F_3 when cordierite formed along s_3 surfaces.

The mineral is present in metapelites along the southeastern boundary of the area and occurs farther to the southeast, but beyond the mapped area interpretation is complicated by the presence of the Donkerhoek Granite and its thermal aureole. It is not known whether cordierite occurs southeast of the wide outcrop area of the Donkerhoek Granite, in the Khomas Hochland.

Almandine garnet is not particularly common in the schists of this stage and, where found, it generally co-exists with cordierite. Porphyroblastic grains displaying sieve texture enclose biotite, quartz, feldspar and staurolite but not cordierite even though these two minerals do occur in contact. Partial retrogression of garnet along grain boundaries to chlorite is visible in several samples.

In places garnet has crystallised syntectonically during F_2. While recognising that crystal form is a reflection of power of crystallisation and not necessarily of paragenesis (Spry, 1969), the idioblastic form and lack of deformation textures such as granulation indicate that garnet formed relatively late in the paragenetic sequence.

The garnets found in the metapelites are almandine-rich as shown by refractive index and lattice constant measurements (Table 19) and electron

microprobe analyses (Table 20).

Table 19. Refractive indices and lattice constants for garnets from pelitic schists and gneisses of the Witpoort and Tinkas Formations.

Sample No.	a(Å)	standard deviation	n(± 0,002)	Locality
RJ774	11,540	0,008	1,809	I25
RJ739	11,549	0,004	1,807	014
RJ389	11,531	0,005	1,808	J20
RJ754	11,563	0,003	1,805	M10

Table 20. Partial chemical analysis of the core and rim of a garnet porphyroblast in RJ774. The garnet co-exists with biotite, cordierite and Fe-oxide. All iron expressed as FeO. Data in weight per cent. Analyst : R.E. Jacob.

	SiO_2	Al_2O_3	TiO_2	FeO	MgO	MnO	CaO	Na_2O	Total
CORE	38,06	20,23	0,03	34,00	4,78	2,65	1,16	0,02	100,93
RIM	38,10	20,19	0,03	35,11	4,52	2,35	1,06	0,02	101,38

The slight increase in FeO towards the rim is in accordance with the changes to be expected during prograde blastesis (Sturt, 1962; Atherton, 1968; Brown, 1969; Hyndman, 1972; Miyashiro, 1973) as is the decrease in CaO and MnO.

Apatite, strongly pleochroic idioblastic tourmaline, opaque Fe-ore and zircon are usually present as accessory minerals and in many samples small amounts of sphene, hornblende (see p. 71) allanite and graphite occur. The mineral assemblages in metapelites of the medium stage are summarised in AKF and AFM diagrams in Figure 33. To facilitate comparison with high-stage assemblages the AFM diagram has been projected through the K-feldspar point.

4.3.2. High Stage

At the limit of the medium stage, staurolite and andalusite have disappeared from pelitic assemblages and the metapelites contain combinations of quartz, plagioclase, K-feldspar, biotite, muscovite, cordierite, garnet and sillimanite. The boundary between the two stages is marked by the first sign of anatexis in metasediments, i.e. the appearance of migmatites. This occurs close to the southeastern margin of the Etusis Formation in the Rooikuiseb anticlinorium (Fig. 50). The high stage extends westwards over the remainder of the area, and beyond. Mineral assemblages are listed in

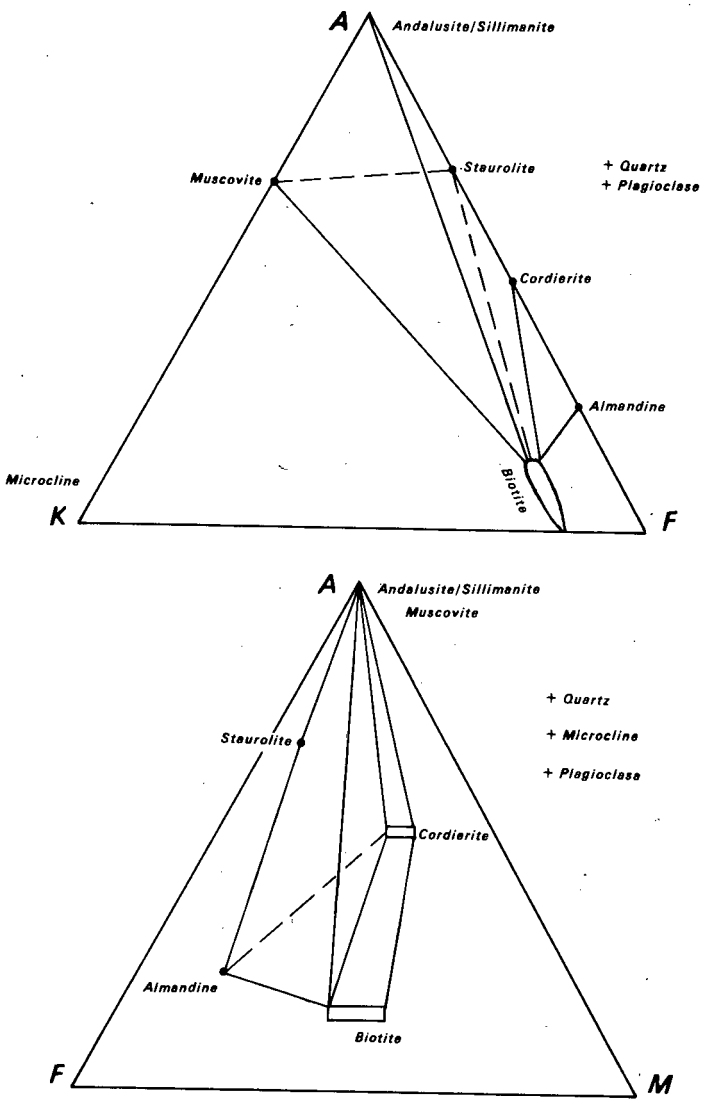

Figure 33. Medium-stage assemblages.

(a) AKF diagram

(b) AFM diagram, projected through the K-feldspar point to facilitate comparison with Figure 34(b). Mineralogical compositions derived from analytical data in text; tie lines derived from petrographic observations.

Table 21. Mineral assemblages in metapelites and metapsammites subjected to high stage metamorphism. X = major constituent, m = minor constituent, a = accessory constituent, r = retrograde.

	Quartz	K-feldspar	Plagioclase	Biotite	Cordierite	Sillimanite	Garnet	Muscovite	Opaque	Apatite	Zircon	Tourmaline	Other	Locality
RJ 68	X	X	m	m		X		m			a			F25
RJ568	X	m	m	X		X		Xr	a	a	a			F26
RJ388	X	m	X	X			m	Xr	a	a	a	a	chl(mr)	J20
RJ480	X	X	X	X	X	m		mr		a	a			E21
RJ476	X	m	X	X			X		a	a	a		hb(m)	F21
RJ473	X	X	X	X	m	m			a	a	a			F20
RJ469	X	X						ar	a		a			F20
RJ450	X	X	m	X	X	X	m		a	a	a			H19
RJ330	X	m	m	m		m		ar	a	a	a			K14
RJ305	a	X	m	a		m	m	mr	m	a	a			J12
RJ353	X	X	X	X	X	m		mr		a	a			H13
RJ499	X	X	X	X	X					a	a	a		D17
RJ539	X	X	m						a	a	a		amph(m)	D16
RJ 80	X	X	m	X	X			ar	a	a	a			G12
RJ354	X	X	m	X	X	a		mr	a					H12
RJ151	X	X	m	X	X		a		a	a		a		L9
RJ 7	X	m	m	m					a	a	a			M9
RJ106	X	X							a		a		amph(m), piem(a)	D11
RJ763	X	X	m	X	X			ar	a	a	a			H8
RJ103	X					X			a					H7
RJ283	X	X	m	m	X	X			m	a	a			H7
RJ269	m	m	m		X			ar	m	a				J7
RJ780	X	X	X	X					a	a	a		hb(m)	K6
RJ225	X	m	X						a		a			L4
RJ273	X	X	m	X	X		m	ar	a	a	a			J5
RJ767	X	X	X	X						a	a		hb(X)	J5
RJ183	X	m		m	X	X		ar	X		a			H4

4.3.2.1. Metapsammites

Metapsammites are found mainly in the Etusis Formation. In thin section the purer quartzites are seen to consist of quartz with minor amounts of microcline and plagioclase. Grain size is variable from 0,2 to 2,0 mm and averages about 1 mm. Some quartzites have granoblastic polygonal textures but, more commonly, large grains of quartz replace the feldspars. Microcline and oligoclase are in contact along polygonal grain boundaries but are normally almost wholly enveloped in the larger quartz grains which display lobate grain boundaries. Isolated islands of feldspar grains may still be in optical continuity.

Impure quartzites predominate and here quartz and red K-feldspar are found with plagioclase and variable amounts of biotite. In the southeastern part of the Rooikuiseb anticlinorium muscovite is still present but farther to the west and northwest sillimanite occurs in its place as small knots and smears along foliation planes. In the Vredelus anticline gradations occur into typical banded gneisses. There, and farther to the west, the psammites consist of quartz, K-feldspar, plagioclase, biotite and sillimanite, occasionally with minor amounts of weakly pleochroic amphibole. In places garnet and epidote were found, the latter generally occurring as a retrograde phase after garnet. Accessory minerals include zircon, apatite, Fe-oxides, allanite, sphene and, rarely, piemontite. All gradations occur between psammitic and pelitic rocks. The semipelitic varieties are now found as migmatitic quartzofeldspathic gneisses.

Conglomerates are similar to those already described (see p. 93) but contain sillimanite instead of muscovite and display partial melting effects. The petrographic changes occurring from east to west in the metapsammites are not pronounced, apart from a coarsening of grain and an increase in antiperthite and rutile. Gneissic textures and migmatitic structures are more conspicuous towards the west while the distinction between psammitic gneisses and the Red Granite-Gneiss becomes arbitrary here. Mica-poor sillimanite gneisses are conspicuous in the Rössing Formation and, although they appear to be psammitic in hand specimen, they have pelitic compositions (RJ764, RJ765 Table 22), the phyllosilicates having been broken down during prograde metamorphism. Psammitic and semipelitic rocks of the Rössing Formation in the west are gneissic and consist of lithotypes ranging from those comprising quartz with minor amounts of K-feldspar to those comprising quartz-K-feldspar-plagioclase-sillimanite and quartz-plagioclase-biotite.

4.3.2.2. Metapelites

Metapelites are less common than metapsammites in the Etusis Formation but are prominent in the Tinkas and Witpoort Formations. The schists differ from those of the medium stage in their coarser grain, different mineral assemblages and more or less migmatitic character.

Very close to, but on the high-temperature side of, the boundary

marking the beginning of anatexis in gneisses (see Fig. 50), muscovite and quartz no longer co-exist but have reacted to produce K-feldspar and sillimanite. In thin section, remnants of muscovite are seen to be preserved in K-feldspar porphyroblasts which are intergrown with, and rimmed by, sillimanite aggregates and needles. Beyond the isograd, marked by the formation of K-feldspar + sillimanite, the pelitic schists contain fairly simple assemblages consisting of quartz, plagioclase, K-feldspar (often missing because of its entry into melts), biotite and sillimanite with garnet or hornblende as additional phases in some samples. Accessory minerals include zircon, apatite, tourmaline, allanite, magnetite and pyrite, and sphene in rocks containing hornblende. Hornblende has generally crystallised after biotite, encloses it poikiloblastically and is usually oriented in the foliation.

Almandine is not common and large grains (1-2 cm) are often surrounded by quartzofeldspathic haloes depleted in biotite.

About 5 km beyond the sillimanite + K-feldspar isograd, cordierite becomes a conspicuous porphyroblastic mineral in the metapelites. The textural relationships in thin section are as follows:

(i) concentrations of sillimanite needles are poikiloblastically enclosed in the cores of cordierite porphyroblasts, which have sillimanite-free peripheries (Pl. 25),

(ii) very small, relict grains of biotite are also poikiloblastically enclosed in the cordierite,

(iii) the growth of cordierite has effectively protected the sillimanite from reacting with other phases,

(iv) K-feldspar has been produced by the same reaction which formed cordierite and, when in contact, the two minerals appear to have crystallised together,

(v) K-feldspar grains contain sillimanite-rich cores but, in places, the components of the feldspar have entered into anatectic melts,

(vi) in some samples garnet also is present as a product of the reaction which formed cordierite and K-feldspar.

The assemblage at this isograd is quartz-plagioclase-biotite-K-feldspar-sillimanite-cordierite ± garnet. In some of the rocks all the sillimanite was exhausted here but in many samples it remains preserved in cordierite. AKF and AFM diagrams illustrating the mineral assemblages in metapelites of the high stage beyond this isograd are presented in Figure 34.

Similar textural relationships are found farther to the west. However, at the Rote Adlerkuppe and east of the Husabberg garnet is not common. The cordierite porphyroblasts reach 2 cm in size and impart a knotty appearance to the migmatitic schists and gneisses which is particularly noticeable in the Witpoort rocks east of the Witpoortberge-Husabberg-Pforteberge range.

Small biotite flakes in parallel orientation are poikiloblastically enclosed within cordierite and K-feldspar. The flakes define an internal

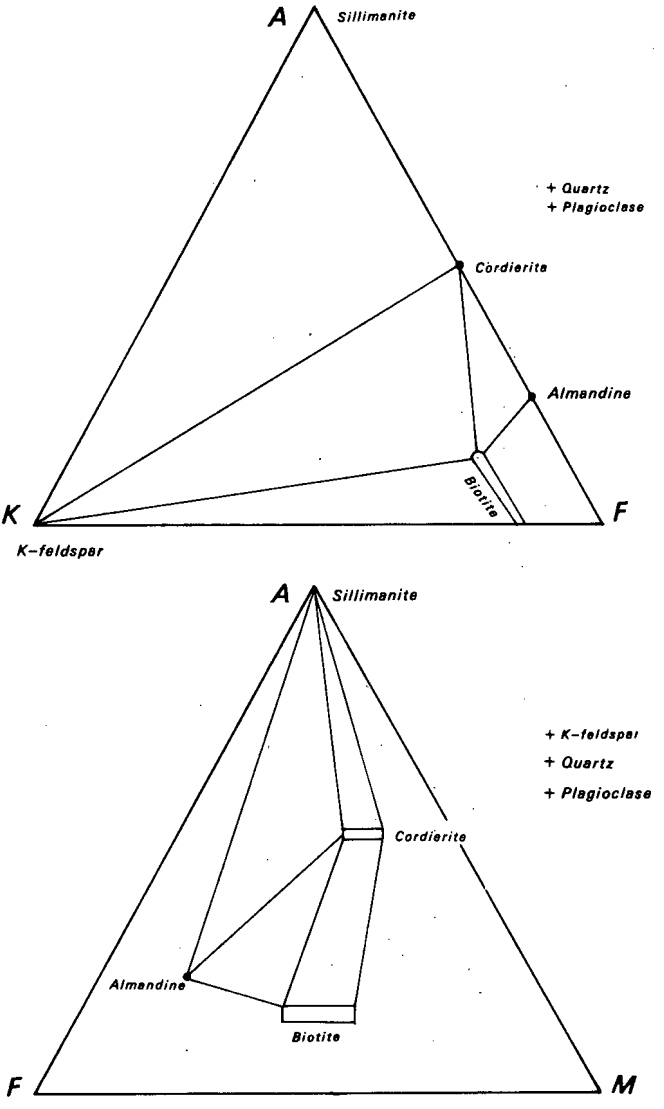

Figure 34. High-stage assemblages.

(a) AKF diagram

(b) AFM diagram, projected through the K-feldspar point as muscovite is not a stable phase in such rocks.

foliation (s_i) which is probably s_1, of F_1 age and which, in some samples but not in all, is parallel to the external foliation (s_e). The external foliation is s_1 in some samples but is s_2 in the hinges of B_2 folds. Where $s_i \neq s_e$, rotation of the porphyroblasts has occurred after their formation, as in Plate 26. s_e is flattened around the porphyroblasts, demonstrating that deformation outlasted their growth.

Some of the pelitic gneisses in the Rössing Formation west of the Husabberg, between the Welwitsch Hills and Arcadia 80, differ from the metapelites of the Witpoort Formation in that they contain small to almost negligible amounts of biotite, conspicuous amounts of opaque Fe-ore and substantial amounts of sillimanite, which is not confined to the cores of cordierite and K-feldspar grains but present throughout the samples. The typical mineral assemblage is

quartz - K-feldspar - cordierite - sillimanite - Fe-oxide
(- plagioclase - biotite)

Cordierite and K-feldspar are present in abundance and together with plagioclase and Fe-ore form large irregular grains of poikiloblastic character enclosing rounded inclusions of quartz, biotite and sillimanite prisms. Magnetite, ilmenite, haematite, pyrrhotite and pyrite constitute the opaque Fe-ore suite. In polished sections the sulphide grains are rimmed by oxides. Rutile and zircon are common accessory minerals.

4.3.2.3. Migmatites

Migmatites accompany high-grade metamorphism in many metamorphic terrains to which the Damara Orogen is no exception. They are first found at the boundary marking the start of anatexis in gneisses and become exceedingly common farther west. The degree of migmatisation of the metasediments is dependent on the grade of metamorphism and their composition (Winkler, 1967). The psammitic rocks contain irregular segregations of granitic and pegmatitic mobilisates but in pelitic and semipelitic rocks the effects are pervasive and migmatitic structures are very clearly displayed (Pl. 2). Pure quartzites have not been affected.

Most of the structures discussed by Mehnert (1968, pp. 7-42) are displayed by the migmatites in this area. Vein, layered, dilatation, ptygmatic and augen structures are very common; nebulitic and schlieren structures are very common towards the west. Palaeosomes, as defined by Mehnert (1968, pp. 7-8) can usually be distinguished from neosomes. The melanosomes, making up part of the neosomes, are generally dark in colour and form conspicuous mafic margins to leucosome segregations. While varying in composition, they normally consist of biotite with or without hornblende. The biotite is generally considerably coarser than in the palaeosomes and is not as lepidoblastic but nevertheless shows parallel orientation. Quartz and /or plagioclase also contribute towards the melanosomes, but only in small amount within interstices between mafic grains.

The leucosomes vary considerably in texture and composition. Grain sizes of several centimetres are attained in many leucosomes and an irregular

pegmatitic texture is then characteristic. They are thus not conveniently studied under the microscope. Many leucosomes, however, consist of equigranular intergrowths of felsic minerals, averaging less than 5 mm.

The texture of leucosomes is typically hypidiomorphic-granular (igneous) but occasionally it is granoblastic-polygonal (metamorphic). Nearly all contain quartz but the feldspar varies in different migmatites. In some it is microcline, in others plagioclase (usually oligoclase to andesine), while in others again microcline and plagioclase co-exist. The microcline is normally perthite which is occasionally surrounded by albite rims. Plagioclase generally shows better development of crystal faces than microcline and may be zoned. Muscovite is present in several leucosomes studied although it is not present in associated palaeosomes. It usually replaces biotite, which occurs as unoriented flakes.

The mineralogy of the leucosomes is related to that of the palaeosomes. Microcline is more abundant in leucosomes of feldspathic metapsammites, and plagioclase in metapelites without K-feldspar. Leucosomes in migmatitic metapelites may contain small amounts of cordierite and sillimanite as inclusions in quartz. Leucosomes in the banded gneisses of the Khan Formation display small amounts of clinopyroxene, hornblende, andradite and epidote.

In the Arysap Hills syncline gradational contacts make it difficult in places to fix the boundary between migmatites and the Salem Granite. Similar gradations are encountered on Geluk 116 and south and southwest of the Rote Adlerkuppe dome.

4.3.3. Petrochemical considerations

Major-element chemical analyses have been performed by the National Institute for Metallurgy on selected samples of metapelites from the area under investigation. Complete analyses are presented in Table 22, partial analyses in Table 23, and mineral assemblages in Table 24. The modal compositions (see Appendix) of the very fine-grained schists could not be determined satisfactorily. The compositions of co-existing cordierite and biotite were also investigated in an attempt to correlate variations in mineral chemistry with variations in metamorphic grade.

4.3.3.1. Whole-rock chemistry

Whole-rock composition generally exerts the major control over the presence or absence of index metamorphic minerals such as cordierite. Wynne-Edwards and Hay (1963) found that, under conditions of regional metamorphism, cordierite forms only in lime-poor, magnesia-rich rocks and that the chemical control exerted by rock composition was as important a factor as pressure in determining whether cordierite or garnet, or both, form in metapelites. Their composition diagram is reproduced as Figure 35, to which have been added the samples analysed in this study. As expected, most of the cordierite-bearing samples plot in the cordierite-biotite field, but several cordierite-free samples do likewise. The condition of low CaO and low

Table 22. Major-element chemical analyses for whole-rock samples.

	RJ743	RJ773	RJ774	RJ740	RJ741	RJ749	RJ742	RJ770	RJ736	RJ759	RJ735	RJ760
SiO_2	67,27	59,24	58,10	57,92	62,19	60,05	60,25	58,65	58,30	63,60	60,24	56,04
Al_2O_3	13,52	17,68	18,78	18,16	16,28	16,69	17,04	18,05	17,92	15,73	16,29	18,74
TiO_2	0,88	0,83	1,02	1,13	0,96	0,96	0,99	1,12	0,84	0,86	0,93	0,97
Fe_2O_3	0,64	1,03	0,89	0,94	0,74	1,30	0,84	0,62	0,96	0,91	0,65	0,88
FeO	6,37	7,36	7,24	8,13	7,16	6,75	7,89	7,56	6,57	5,25	6,53	6,84
MgO	3,58	4,77	5,08	4,79	5,61	4,89	4,94	4,92	4,38	4,62	4,68	4,79
MnO	0,05	0,07	0,08	0,08	0,07	0,04	0,07	0,10	0,13	0,10	0,16	0,18
CaO	0,97	1,26	1,70	1,14	0,68	1,35	0,89	0,86	2,27	1,90	1,99	1,68
Na_2O	2,09	2,04	2,10	1,86	1,72	2,50	1,69	1,15	1,62	1,92	1,55	1,34
K_2O	3,11	2,79	3,02	3,13	2,77	3,72	2,95	3,89	4,93	4,18	4,27	4,71
P_2O_5	0,13	0,12	0,14	0,15	0,12	0,13	0,12	0,15	0,15	0,14	0,14	0,18
Cr_2O_3	0,03	0,03	0,04	0,03	0,03	0,02	0,03	0,04	0,04	0,03	0,04	0,04
H_2O^-	0,21	0,21	0,34	0,23	0,17	0,19	0,27	0,28	0,20	0,25	0,25	0,42
H_2O^+	1,58	1,63	1,70	2,36	1,99	1,67	2,07	1,65	1,48	1,41	1,51	2,30
CO_2	0,01	0,07	0,09	0,04	0,03	0,02	0,09	0,08	0,01	0,10	0,04	0,06
TOTAL	100,44	99,13	100,32	100,09	100,52	100,28	100,13	99,12	99,80	101,00	99,27	99,17

	RJ753	RJ756	RJ757	RJ763	RJ764	RJ765	RJ748	RJ738	RJ776	RJ771	RJ767
SiO_2	60,20	62,20	55,85	57,36	57,52	61,79	57,43	46,30	57,61	58,46	56,79
Al_2O_3	18,51	15,80	18,76	18,72	18,79	17,71	17,44	21,49	16,80	17,03	17,15
TiO_2	0,89	0,91	1,19	0,99	1,04	1,33	1,04	1,22	0,96	1,00	1,18
Fe_2O_3	1,51	1,14	3,56	1,09	1,83	6,14	1,67	1,90	0,88	1,12	2,76
FeO	5,82	6,46	5,79	6,84	5,72	4,66	7,34	8,50	6,70	7,43	5,60
MgO	4,15	3,57	5,15	4,10	4,22	1,36	4,54	5,15	5,26	5,10	4,77
MnO	0,07	tr	0,16	0,11	0,11	0,04	0,10	0,23	0,13	0,13	0,11
CaO	0,62	0,23	1,44	0,55	0,57	0,12	1,26	3,77	2,52	2,28	2,22
Na_2O	1,54	1,50	1,91	1,26	1,16	1,49	2,72	2,23	2,33	2,24	2,31
K_2O	5,15	6,12	3,88	6,40	6,51	3,83	4,43	7,37	4,62	4,08	4,32
P_2O_5	0,06	0,04	0,13	0,10	0,10	0,07	0,20	0,23	0,19	0,21	0,21
Cr_2O_3	0,04	0,03	0,04	0,04	0,04	0,06	n.d.	n.d.	n.d.	n.d.	n.d.
H_2O^-	0,30	0,24	0,25	0,26	0,15	0,21	0,17	0,16	0,10	0,11	0,10
H_2O^+	1,74	2,46	1,81	1,89	1,07	0,84	2,24	2,22	1,56	1,40	0,92
CO_2	0,08	0,07	0,03	0,05	0,06	0,03	n.d.	n.d.	n.d.	n.d.	n.d.
TOTAL	100,68	100,77	99,95	99,76	98,89	99,68	100,58	100,77	99,66	100,59	98,44

Analyst: National Institute for Metallurgy. Analyses by X-Ray fluorescence except for FeO, H_2O^-, H_2O^+ and CO_2, which were titrimetrically and gravimetrically determined. TiO_2, FeO, MnO, P_2O_5, K_2O, Na_2O, H_2O^- and H_2O^+ in RJ748, 738, 776, 771 and 767 determined by R.E. Jacob by colourimetric, titrimetric and gravimetric methods. n.d. = not determined. tr = trace. Localities: see Table 24.

Table 23. Partial chemical analyses of whole-rock samples. All Fe expressed as Fe_2O_3.
Analyst: National Institute for Metallurgy. Analyses by X-ray fluorescence techniques.

	RJ747	RJ775	RJ737	RJ755	RJ751	RJ761	RJ762
SiO_2	57,85	42,60	62,99	60,42	58,53	60,66	63,31
Al_2O_3	19,98	16,37	18,03	17,36	17,90	17,84	22,79
Fe_2O_3	10,49	18,03	8,21	8,03	8,11	8,10	3,00
MgO	4,24	7,75	2,89	4,04	3,99	4,19	1,35
CaO	0,44	6,11	1,33	2,13	0,55	1,12	0,69
Locality	M21	H23	F20	M10	M8	G12	H7

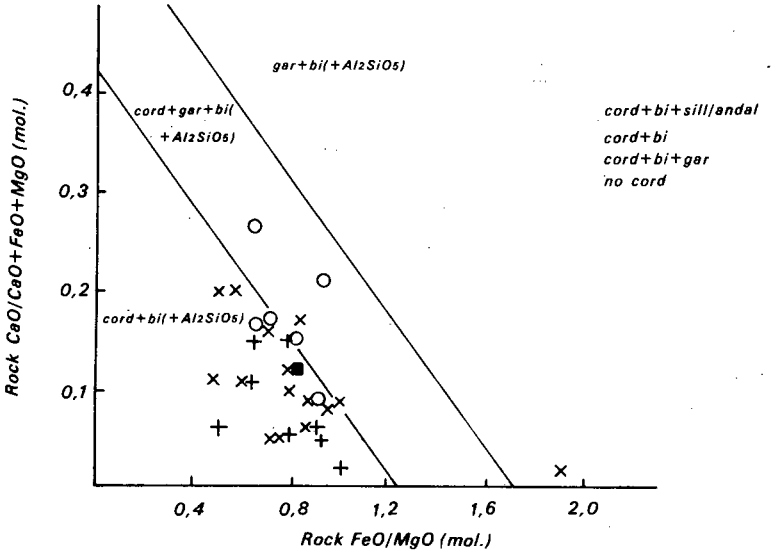

Figure 35. Combined effect of CaO, FeO and MgO on mineralogy of metapelites, after Wynne-Edwards and Hay (1963).

FeO/MgO ratio does not therefore necessarily ensure that the mineral will form.

The plot of Wynne-Edwards and Hay is better suited to the rocks of the Khan/Swakop region than that recommended by Dallmeyer (1972) for distinguishing between assemblages comprising cordierite + biotite + sillimanite,

Table 24. Mineral assemblages and modes (in volumetric per cent) of samples subjected to chemical analysis. X = major constituent, m = minor constituent, a = accessory constituent, r = retrograde.

Sample No.	Quartz	K-feldspar	Plagioclase	Biotite	Cordierite	Sillimanite	Andalusite	Muscovite	Fe-ore	Zircon	Apatite	Other	Locality
RJ743	X		X	X	X	m	m		a	a	a	tour(a)	018
RJ773	X	m	X	X	X		a		a	a	a		J23
RJ774	X	m	X	X	X			a	a	a	a	chl(r),gar (m),tour(a)	I25
RJ740	X	m	X	X	X	m	m	mr	a	a	a	tour(a),chl (r),graph(m)	014
RJ741	X	m	X	X	X		a		a	a	a	tour(a), graph(m)	P16
RJ749	X	m	X	X	X		m		a	a	a	graph(a)	Q11
RJ742	X	m	X	X	X			mr	a		a	tour(a), chl(r)	N17
RJ770	X	m	X	X	X	X		mr	a	a	a		J20
RJ736	24,5	19,5	5,5	27,3	20,8	1,7			— 0,7 —				F20
RJ759	26,3	21,8	7,4	24,2	20,0			ar	— 0,3 —				K12
RJ735	20,0	16,4	12,9	25,2	24,5			ar	— 1,0 —				D17
RJ760	26,9	1,8	27,5	27,4	13,8	0,3		2,2r	— 0,1 —				H12
RJ753	28,3		16,9	38,4	12,3			3,9r	— 0,2 —				N8
RJ756	20,7	14,7	18,9	30,1	14,7				— 0,7 —			chl(r)	J9
RJ757	23,0	tr	24,9	32,7	19,1				— 0,2 —				K9
RJ763	18,1	28,8	6,6	27,7	18,0			0,8r	a	a	a		H8
RJ764	16,4	36,2	4,9	14,4	5,7	18,6		1,7r	2,1	a	a		I7
RJ765	21,2	31,8	8,1	2,3	14,9	12,7		1,1r	7,7	a	a	rutile(0,2)	K6
RJ748	X		X	X			m	m	a	a	a	tour(a)	R15
RJ738	X	X	X	X				mr	a	a	a	tour(a), chl(r)	M15
RJ776	X		X	X				ar	a	a	a		E24
RJ771	X		X	X						a	a		H20
RJ767	m	X	X	X						a	a	hb(X)	J5

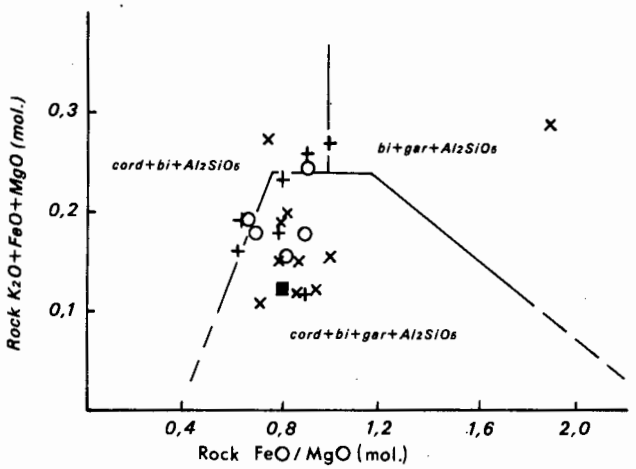

Figure 36. Combined effect of K_2O, FeO and MgO on mineralogy of metapelites, after Dallmeyer (1972). Symbols as in Figure 35.

cordierite + biotite + garnet + sillimanite and garnet + biotite + sillimanite (Fig. 36). Most of the samples from Table 22 plot in the cordierite + biotite + garnet + sillimanite field but do not contain garnet.

Compositionally, the cordierite-bearing schists are similar to geosynclinal shales (Wedepohl, 1969, p. 260) but contain more iron and magnesium, in which respect they are closer to pelagic clays. Figure 37 is an AKF diagram after Winkler (1967, p. 56) on which the cordierite-bearing samples are plotted. Their positions fall mostly within the greywacke field and cluster around the average for marine clays. It should be noted that most of the analyses presented are representative only of those rocks containing co-existing cordierite and biotite and they are thus not representative of the mass of pelitic and semipelitic schists in the various formations.

Figure 38 shows the percentages of whole-rock oxides plotted against metamorphic grade. The oxides are relatively consistent throughout the area although Fe_2O_3 and K_2O increase westwards. Figure 38 should be studied in conjunction with Figures 44 and 45, which show the changes in mineral chemistry with change in metamorphic grade.

4.3.3.2. Co-existing cordierite and biotite

One of the problems of metamorphic petrology is the difficulty of demonstrating whether equilibrium existed during metamorphism, since only equilibrium mineral assemblages have significance for the interpretation of physical conditions. The study of textures in thin section is often not definitive while conformation of the number of mineral phases with the requirements of Goldschmidt's mineralogical phase rule indicates an approach

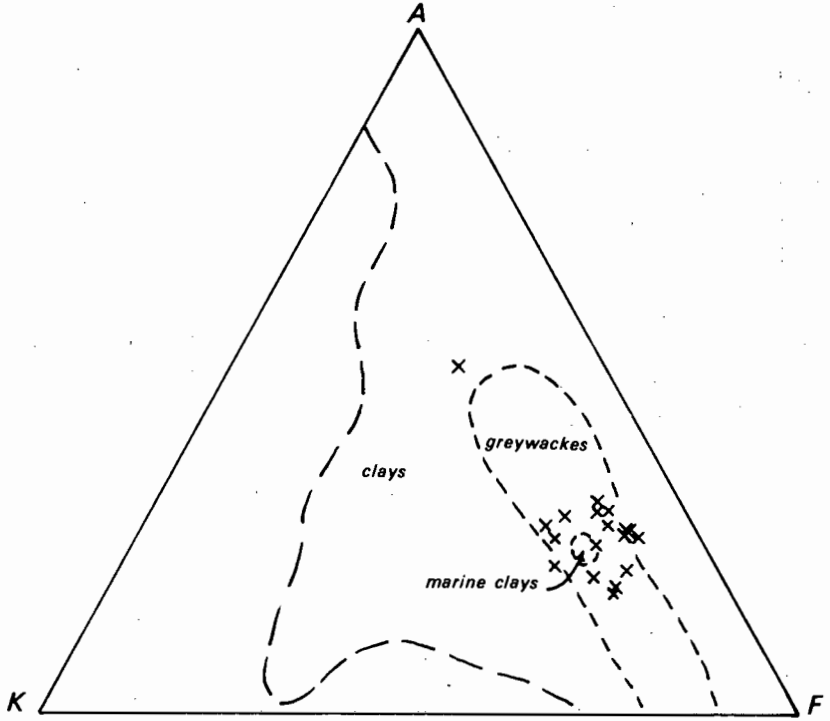

Figure 37. AKF diagram showing compositions of clays, marine clays and greywackes, modified after Winkler (1967, p. 56). Analysed samples (X) fall within the greywacke field and cluster around the field of marine clays.

to equilibrium.

The attainment of equilibrium is better demonstrated through the analysis of co-existing minerals since the regular distribution of an element between co-existing minerals implies equilibrium (Kretz, 1959; McIntire, 1963). If several elements show equilibrium distributions between co-existing phases it is generally assumed that equilibrium existed during metamorphism.

If the element in question exists in very dilute concentration, its distribution follows Nernst's Distribution Law (Kretz, 1959) and when the concentration of the element in one mineral is plotted against its concentration in a co-existing mineral, in a number of samples, the points will plot on a straight line if equilibrium exists. The slope of the line gives the distribution coefficient (K_D) for that element. At higher concentrations the distribution no longer follows Nernst's Law, but if a regular distribution

Table 25. Microprobe analyses of cordierites co-existing with biotite in metapelites. Samples listed approximately in order of increasing metamorphic grade. All Fe expressed as FeO.

	RJ743	RJ773	RJ774	RJ168	RJ740	RJ741	RJ749	RJ742	RJ770	RJ736
SiO_2	47,84	48,20	49,74	47,34	47,40	48,66	47,81	48,02	48,39	48,83
Al_2O_3	32,65	32,51	33,82	33,18	32,49	32,80	32,45	32,60	33,05	33,21
TiO_2	0,02	0,02	0,02	0,02	0,03	0,02	0,02	0,02	0,02	0,20
FeO	8,17	8,46	6,93	6,85	8,23	7,41	7,35	8,30	7,38	8,96
MgO	7,66	7,75	8,48	8,60	7,20	8,36	8,10	7,84	8,34	7,74
MnO	0,31	0,23	0,12	0,06	0,25	0,17	0,13	0,20	0,42	0,07
K_2O	0,01	0,01	0,01	0,01	0,01	0,01	0,01	0,02	0,01	0,01
Na_2O	0,33	0,32	0,37	0,49	0,73	0,34	0,37	0,32	0,24	0,21
TOTAL	96,99	97,50	99,49	96,55	96,34	97,77	96,24	97,32	97,85	99,23
	Number of ions on the basis of 18 oxygen anions									
Si	4,981	4,977	5,007	4,930	4,977	4,980	4,994	4,984	4,976	4,986
Al^{IV}	1,019	1,023	0,993	1,070	1,023	1,020	1,006	1,016	1,024	1,014
Al^{VI}	3,020	2,980	3,051	3,018	3,031	3,009	3,022	3,004	3,013	3,014
Ti	0,001	0,001	0,001	0,001	0,001	0,001	0,001	0,001	0,001	0,001
Fe	0,717	0,739	0,588	0,601	0,729	0,646	0,648	0,727	0,640	0,771
Mg	1,199	1,208	1,281	1,347	1,136	1,298	1,271	1,223	1,289	1,186
Mn	0,028	0,021	0,011	0,006	0,022	0,015	0,012	0,018	0,037	0,007
K	0,002	0,002	0,002	0,002	0,002	0,002	0,002	0,003	0,002	0,002
Na	0,067	0,012	0,073	0,099	0,150	0,067	0,074	0,064	0,048	0,041

	RJ759	RJ735	RJ760	RJ753	RJ756	RJ757	RJ763	RJ764	RJ765
SiO_2	48,18	47,89	47,96	49,12	47,56	47,51	47,76	48,10	48,50
Al_2O_3	32,75	32,73	32,83	33,53	32,63	32,36	32,70	33,18	32,98
TiO_2	0,02	0,02	0,02	0,02	0,02	0,02	0,02	0,02	0,02
FeO	8,34	8,90	7,53	6,13	7,28	8,44	8,54	9,48	8,03
MgO	7,95	7,41	8,18	8,99	8,22	7,65	7,71	7,09	8,04
MnO	0,39	0,27	0,50	0,66	0,45	0,42	0,40	0,36	0,21
K_2O	0,02	0,01	0,01	0,01	0,01	0,01	0,01	0,01	0,01
Na_2O	0,16	0,21	0,20	0,22	0,25	0,18	0,20	0,24	0,31
TOTAL	97,81	97,44	97,23	98,68	96,42	96,59	97,34	98,48	98,10
	Number of ions on the basis of 18 oxygen anions								
Si	4,978	4,977	4,970	4,992	4,966	4,977	4,965	4,961	4,977
Al^{IV}	1,022	1,023	1,030	1,008	1,034	1,023	1,035	1,039	1,023
Al^{VI}	2,998	3,019	3,012	3,033	3,012	3,004	3,004	3,026	3,006
Ti	0,001	0,001	0,001	0,001	0,001	0,001	0,001	0,001	0,001
Fe	0,727	0,780	0,658	0,524	0,641	0,746	0,749	0,825	0,677
Mg	1,235	1,157	1,273	1,370	1,289	1,203	1,204	1,100	1,288
Mn	0,034	0,024	0,044	0,057	0,040	0,038	0,036	0,032	0,017
K	0,003	0,002	0,002	0,002	0,002	0,002	0,002	0,002	0,002
Na	0,033	0,042	0,040	0,043	0,051	0,036	0,040	0,047	0,067

Figure 38. Variation of oxide percentages (whole-rock) of metapelites across mapped area. Samples listed from left to right in order of increasing metamorphic grade to facilitate comparison with Figures 44 and 45.

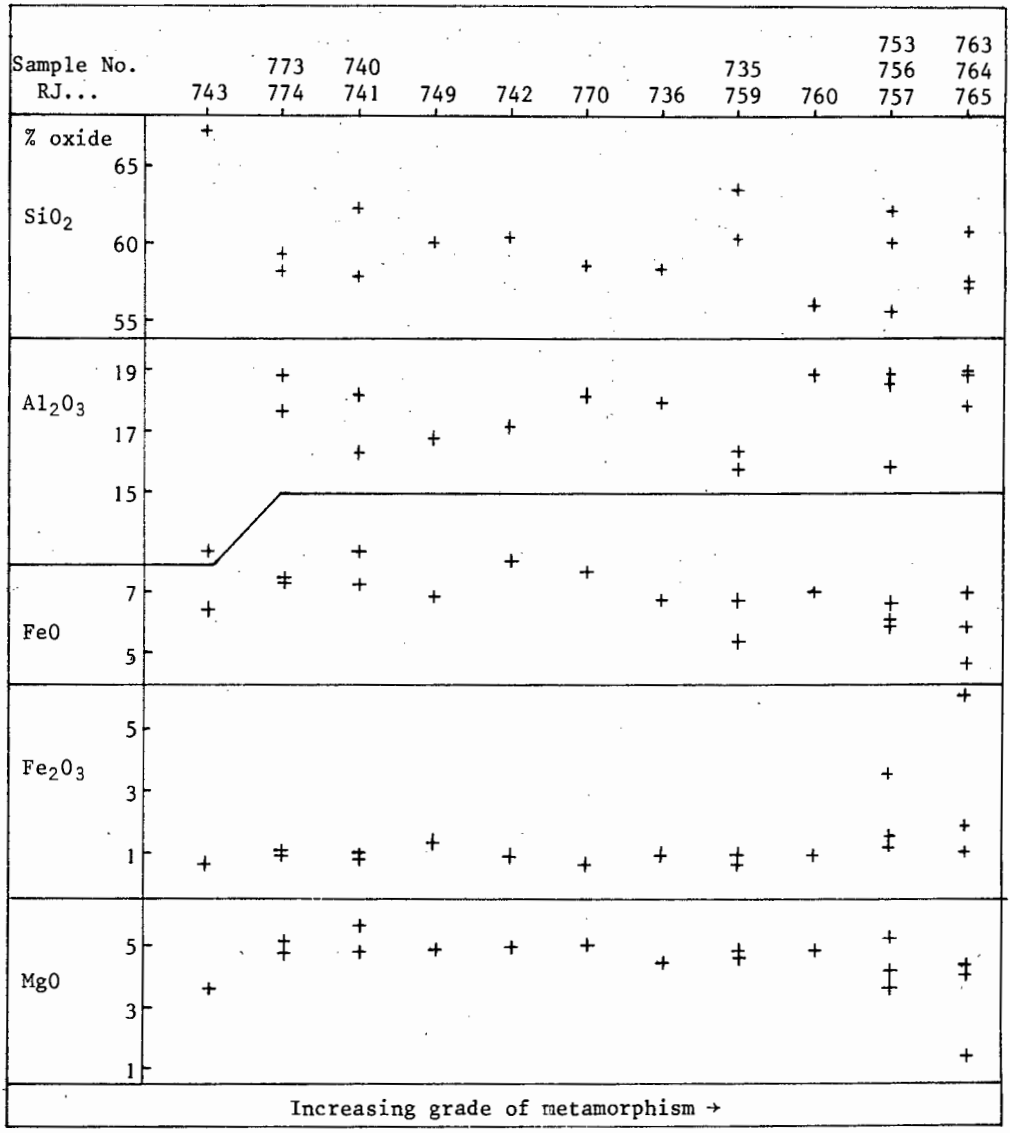

Figure 38 continued

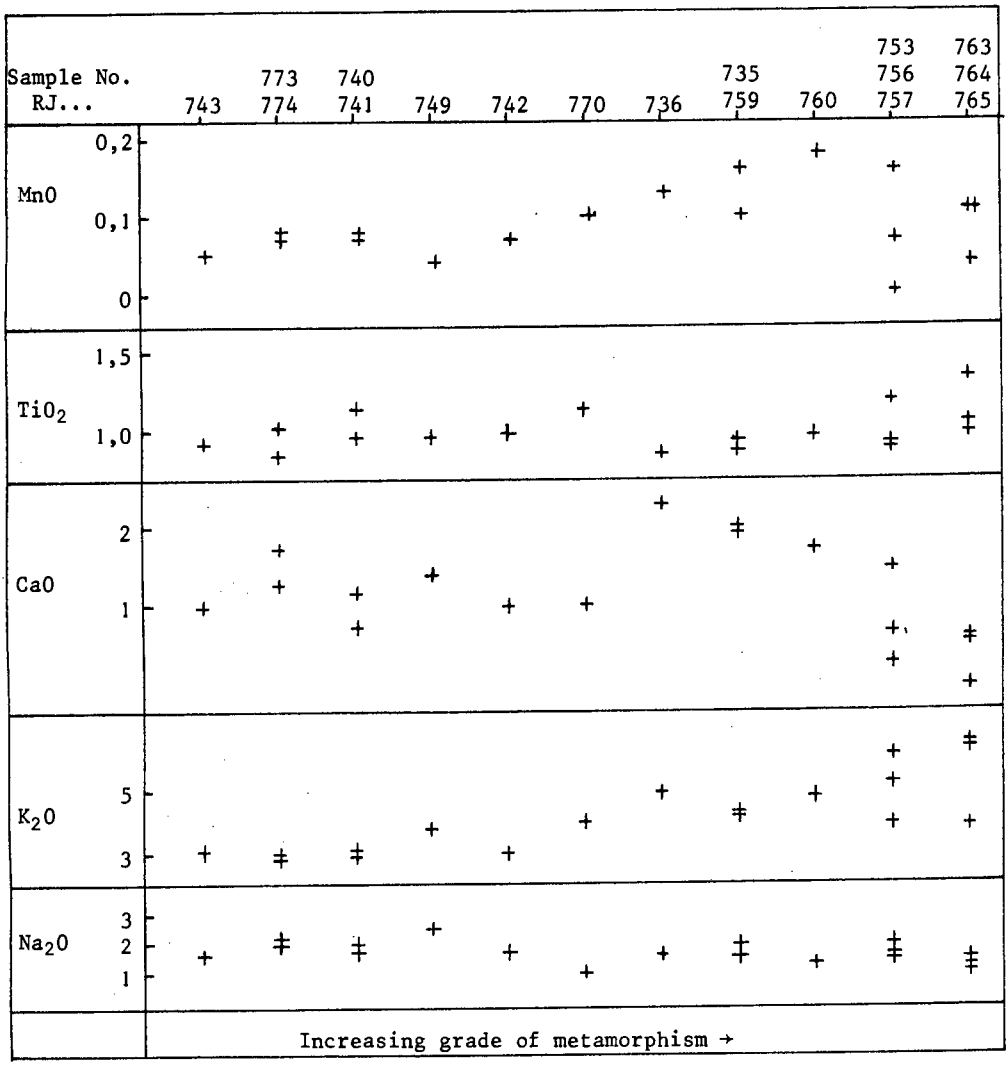

Table 26. Microprobe analyses of biotites co-existing with cordierite in metapelites. Samples listed approximately in order of increasing metamorphic grade. All Fe expressed as FeO.

	RJ743	RJ773	RJ774	RJ168	RJ740	RJ741	RJ749	RJ742	RJ770	RJ736
SiO_2	34,78	35,05	36,57	35,06	35,55	35,56	35,02	35,15	35,47	35,34
Al_2O_3	19,96	18,74	19,66	20,31	19,99	19,01	19,55	19,37	20,07	19,74
TiO_2	2,21	2,56	2,26	1,28	1,84	1,61	2,09	2,38	2,24	2,51
FeO	19,25	20,34	17,22	17,48	19,37	18,31	18,31	19,58	17,69	20,15
MgO	8,76	9,20	10,61	11,39	8,82	10,86	9,65	9,13	9,90	8,25
MnO	0,12	0,09	0,04	0,01	0,08	0,06	0,05	0,06	0,15	0,03
K_2O	8,92	8,64	8,89	8,48	8,87	8,45	8,79	8,89	9,22	9,89
Na_2O	0,28	0,41	0,27	0,59	0,33	0,30	0,29	0,29	0,26	0,14
TOTAL	94,28	95,03	95,52	94,60	94,85	94,16	93,75	94,83	95,00	96,05
	Number of ions on the basis of 22 oxygen anions									
Si	5,337	5,364	5,457	5,301	5,409	5,420	5,374	5,365	5,360	5,365
Al^{IV}	2,663	2,636	2,543	2,699	2,591	2,580	2,626	2,635	2,640	2,635
Al^{VI}	0,945	0,742	0,912	0,919	0,993	0,833	0,908	0,850	0,933	0,895
Ti	0,255	0,295	0,253	0,145	0,210	0,185	0,242	0,274	0,254	0,287
Fe	2,470	2,603	2,148	2,209	2,465	2,331	2,350	2,500	2,236	2,559
Mg	2,004	2,099	2,360	2,567	2,001	2,467	2,208	2,079	2,231	1,862
Mn	0,015	0,011	0,004	0,001	0,010	0,008	0,007	0,008	0,019	0,003
K	1,747	1,686	1,691	1,635	1,723	1,643	1,720	1,731	1,777	1,916
Na	0,084	0,121	0,077	0,173	0,092	0,088	0,086	0,086	0,075	0,042

	RJ759	RJ735	RJ760	RJ753	RJ756	RJ757	RJ763	RJ764	RJ765
SiO_2	35,05	35,20	34,86	36,00	34,53	34,76	35,22	34,81	35,01
Al_2O_3	19,01	20,09	19,56	19,60	19,34	19,17	20,06	20,46	19,11
TiO_2	2,96	2,73	2,27	1,96	1,94	2,55	2,87	2,39	2,68
FeO	19,35	19,25	17,44	16,82	18,05	18,60	18,05	19,74	19,30
MgO	8,82	8,24	9,59	10,99	9,59	9,15	8,82	7,99	8,86
MnO	0,15	0,10	0,24	0,23	0,19	0,17	0,16	0,11	0,10
K_2O	9,84	9,69	9,72	9,69	9,44	9,19	9,54	9,52	9,74
Na_2O	0,11	0,16	0,16	0,20	0,24	0,19	0,15	0,16	0,13
TOTAL	95,29	95,46	93,84	95,49	93,32	93,78	94,87	95,18	94,93
	Number of ions on the basis of 22 oxygen anions								
Si	5,356	5,338	5,359	5,402	5,352	5,363	5,352	5,315	5,366
Al^{IV}	2,644	2,662	2,641	2,598	2,648	2,637	2,648	2,685	2,634
Al^{VI}	0,778	0,941	0,900	0,868	0,883	0,847	0,941	0,995	0,815
Ti	0,340	0,312	0,263	0,221	0,226	0,296	0,328	0,274	0,308
Fe	2,473	2,449	2,242	2,111	2,339	2,399	2,294	2,520	2,473
Mg	2,010	1,870	2,198	2,459	2,217	2,104	1,998	1,818	2,024
Mn	0,020	0,013	0,031	0,029	0,025	0,021	0,020	0,014	0,013
K	1,918	1,881	1,905	1,855	1,866	1,808	1,848	1,854	1,903
Na	0,031	0,048	0,046	0,057	0,073	0,055	0,044	0,046	0,037

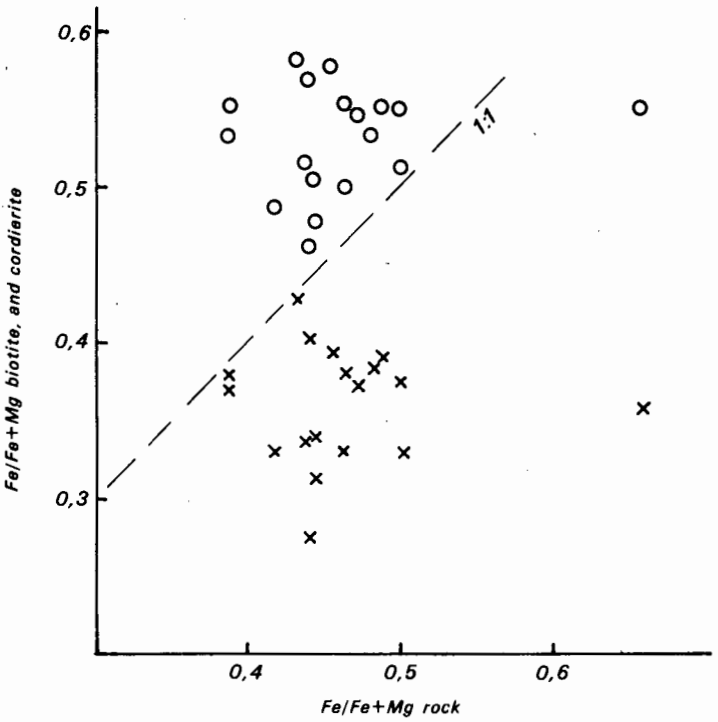

Figure 39. Iron concentration in rock plotted against iron concentration in biotite (O) and cordierite (X). Relative to the rock, biotite is enriched, and cordierite depleted in iron.

exists the points will still plot on smooth curves indicative of equilibrium (Kretz, 1959; Saxena 1968). K_D is dependent on temperature, pressure and the concentration of other elements. Its dependence on temperature has encouraged attempts to use it as a metamorphic geothermometer. (Albee, 1965; Gorbatschev, 1968; Saxena and Hollander, 1969; Saxena, 1969; Hess, 1971; Currie, 1971; Hensen and Green, 1973).

Most work on ferromagnesian silicates in pelitic rocks has been directed at co-existing garnet and biotite (Albee, 1965; Blackburn, 1968; Dahl, 1969; Fleming, 1972; Frost, 1962; Kretz, 1959, 1964; Saxena, 1968; Okrusch,1971; Fediukova, 1971). Less attention has been paid to co-existing cordierite and biotite (Gorbatschev, 1968; Gable and Sims, 1969; Saxena and Hollander, 1969; Dallmeyer and Dodd, 1971; Hess, 1971; Fediuk, 1971). The present writer elected to study co-existing cordierite and biotite because of their almost ubiquitous occurrence in the metapelites. Garnet was not included in the study, partly because of its less common occurrence but mainly because of a limited allocation of time on the electron microprobe. The zoning in garnet and the effects of Ca and Mn on K_D are complicating factors (Kretz,

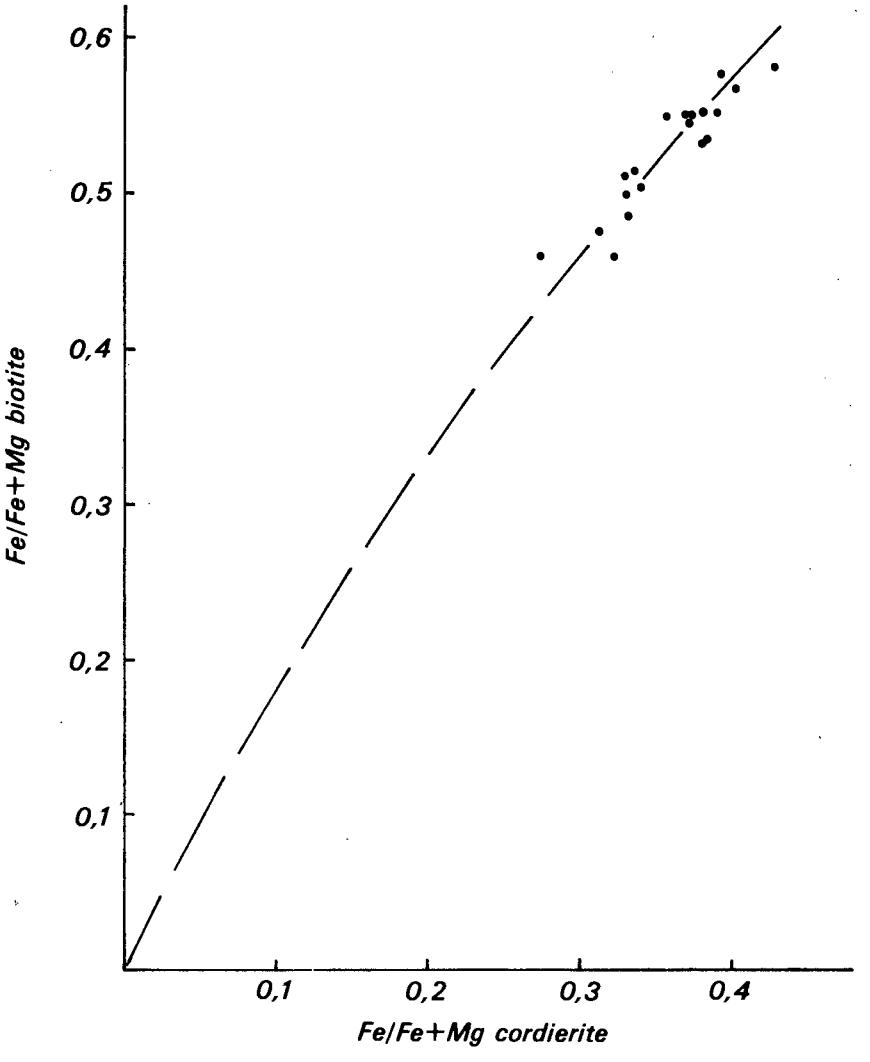

Figure 40. Distribution of iron between co-existing biotite and cordierite, base on microprobe analyses.

1959, 1964; Frost, 1962; Saxena, 1968) that were considered likely to be absent in cordierite. The purpose of the study was to test whether equilibrium existed in the metapelites, to determine whether K_D was temperature dependent and to ascertain whether systematic changes in mineral

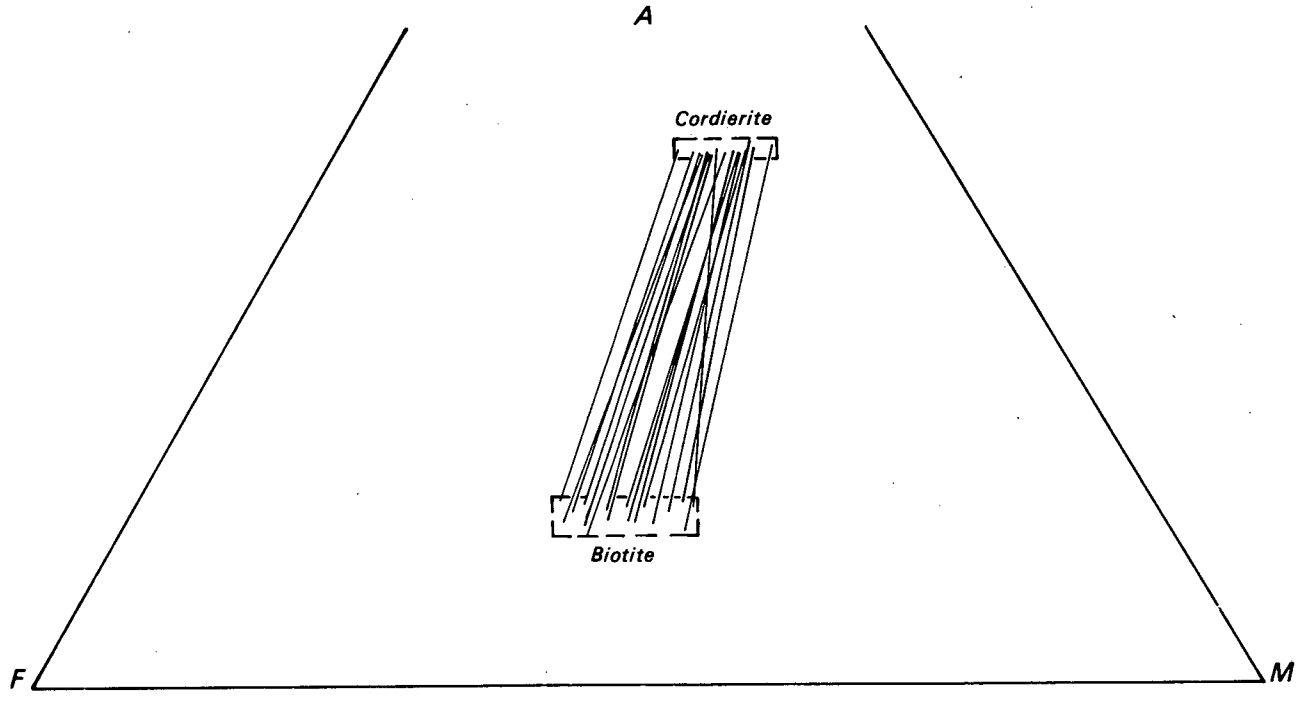

Figure 41. AFM diagram showing tie-lines between co-existing biotite-cordierite pairs. The general absence of crossing tie-lines is indicative of an equilibrium distribution of Fe and Mg.

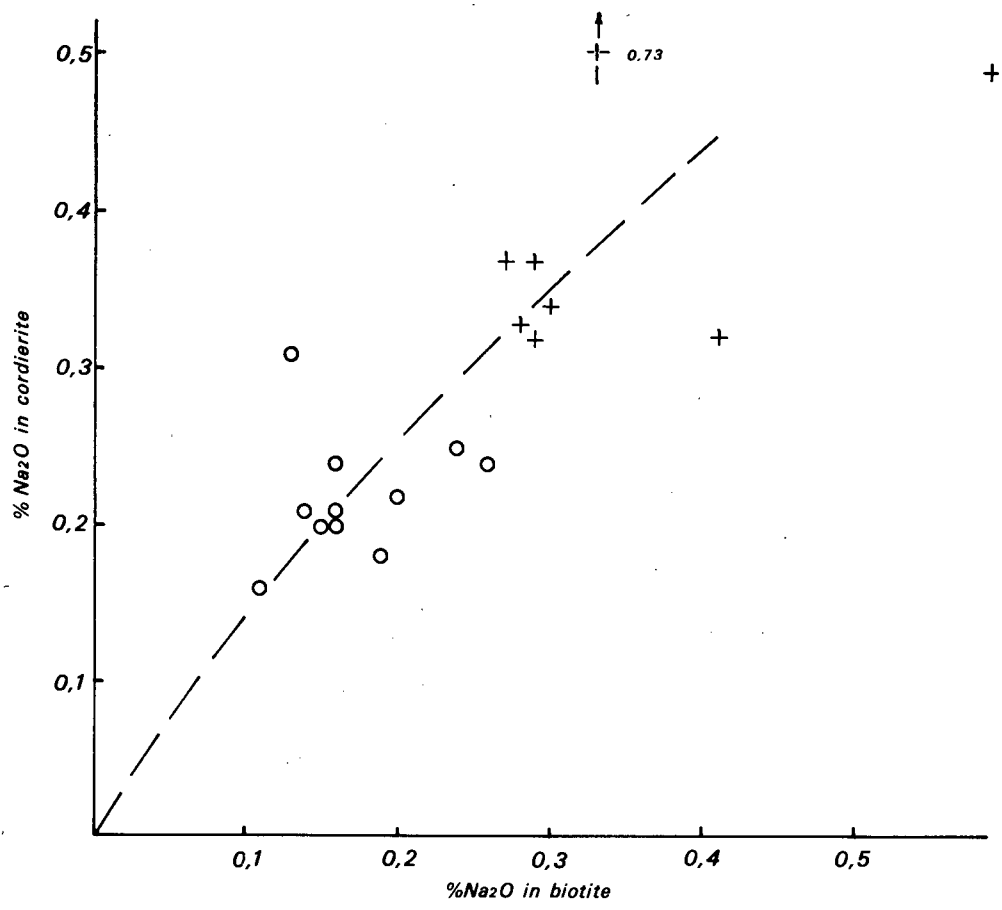

Figure 42. Distribution of Na between co-existing cordierite and biotite. Samples from the high stage rocks (O) contain less Na than those from medium stage rocks (+).

composition accompany increases of metamorphic grade.

Co-existing cordierite and biotite were analysed in 19 samples. With the exception of RJ168, whole-rock analyses for major elements were performed on the same samples (Table 22) in order to ascertain whether changes in mineral composition were governed by rock composition or whether they were controlled by the grade of metamorphism. In most of the samples, cordierite and biotite are the only ferromagnesian silicates but RJ774 contains garnet and RJ168 garnet and staurolite in addition. Neither cordierite nor biotite were found to be zoned.

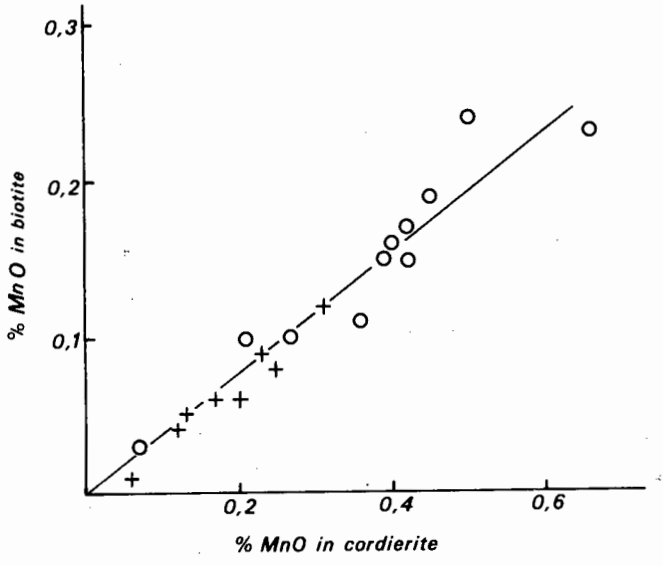

Figure 43. Distribution of Mn between co-existing biotite and cordierite. There is a tendency for high-stage samples (O) to contain more Mn than medium-stage samples (+).

Cordierite analyses are presented in Table 25 and biotite analyses in Table 26. All iron is expressed as FeO. The low totals are due to incomplete analysis since H_2O, CaO, P_2O_5, F etc. were not determined.

In comparison with whole-rock composition, cordierite is depleted in Fe while biotite is enriched (Fig. 39). The distribution between co-existing cordierite and biotite is shown in Figure 40. The plotted points fall on a smooth curve, indicating that equilibrium did in fact exist during metamorphism, at least with respect to Fe and Mg. The equilibrium distribution is also shown in Figure 41 where cordierite - biotite tie-lines run approximately parallel to one another. Regular distributions are also present for Na (Fig. 42) and Mn (Fig. 43). In both these figures there is a separation of medium- and high-stage samples. It is thus concluded that equilibrium was attained in the metapelites during metamorphism, at least between cordierite and biotite, and probably amongst other phases too.

It has been observed in several metamorphic terrains that an increase in the grade of metamorphism is often accompanied by a change in chemical composition of individual minerals in metapelites (Engel and Engel, 1960; Winkler, 1967, pp. 148-152; Hyndman, 1972, pp. 306-307; Miyashiro, 1973, pp. 198-233). The analyses of cordierite and biotite are plotted in Figures 44 and 45 respectively, in terms of number of ions in the structural formulae, in sequence (left to right) of increasing metamorphic grade. It is evident that the variation is not systematic. The erratic decrease of

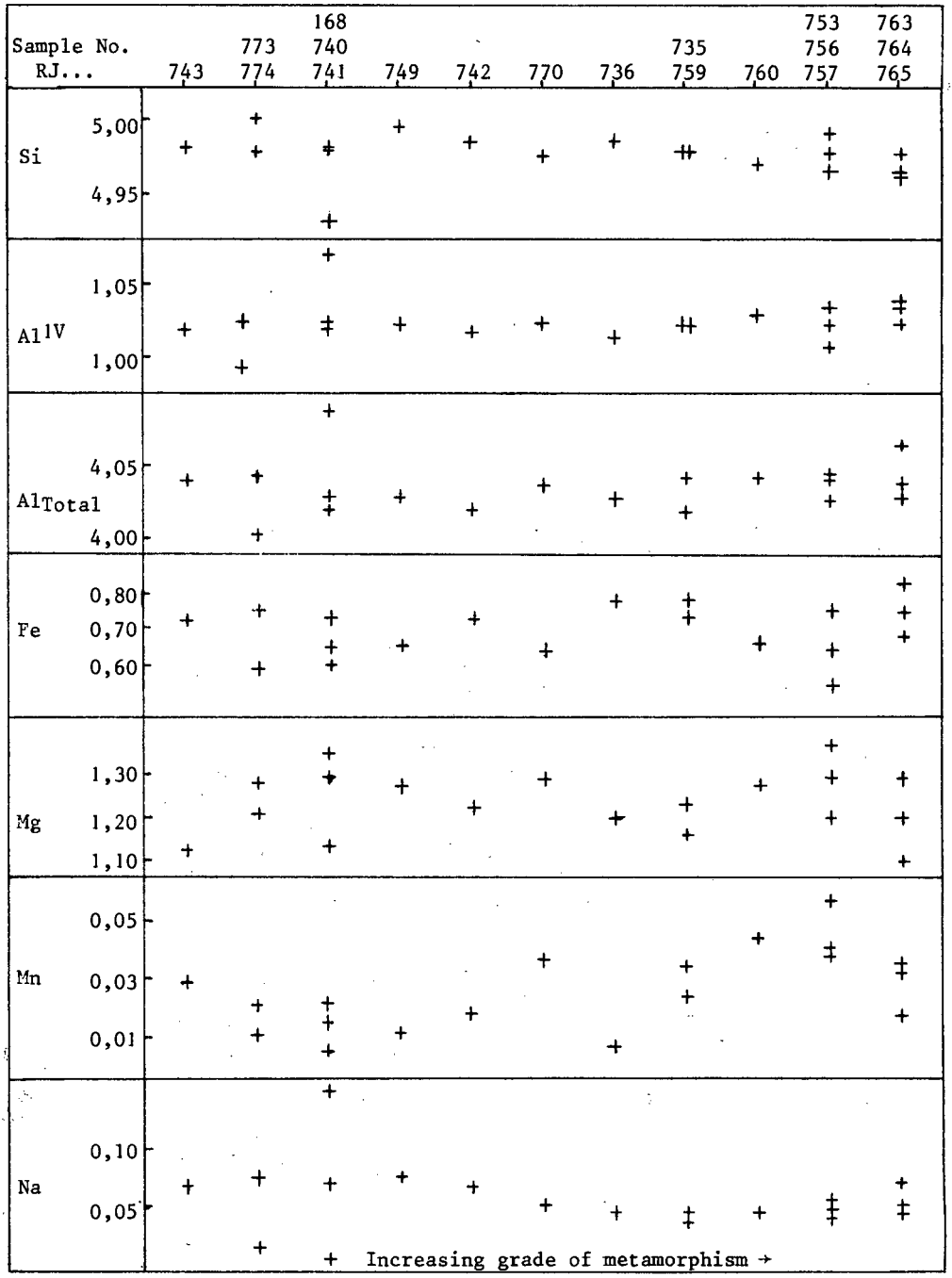
Sample No.
RJ...
743
773 774
168 740 741
749
742
770
736
735 759
760
753 756 757
763 764 765
Si
5,00
4,95
Al IV
1,05
1,00
Al Total
4,05
4,00
Fe
0,80
0,70
0,60
Mg
1,30
1,20
1,10
Mn
0,05
0,03
0,01
Na
0,10
0,05
Increasing grade of metamorphism →

Mg in biotite is paralleled by Mg in the whole rock. Engel and Engel (1960) have reported an increase in the Mg/Fe ratio in biotite with increasing metamorphic grade, substantiated elsewhere (Hyndman, 1972, p. 306), but in such cases biotite has usually co-existed with garnet, into which Fe is preferentially partitioned, leaving biotite enriched in Mg. An increase in the Mg/Fe ratio in biotite can also be expected under oxidising conditions where $Fe^{2+} \rightarrow Fe^{3+}$; Fe^{3+} forms oxide phases and the biotite becomes thus enriched in Mg. There is no significant change in the Mg/Fe ratio in biotite in the present writer's samples but this is not a unique circumstance (Butler, 1965; Ushakova, 1972; Evans and Guidotti, 1966).

Since the distribution coefficient for Fe ($K_{D_{Fe}}$)

$$K_{D_{Fe}} = \frac{(Fe/Fe + Mg)\ \text{biotite}}{(Fe/Fe + Mg)\ \text{cordierite}}$$

does not vary systematically with grade of metamorphism (Fig. 45) it cannot be used for the estimation of metamorphic temperatures. There is a roughly linear correlation of K_D with the Fe content of cordierite(but not of biotite) in Figure 46, which probably indicates a change in activity of the element with concentration. Thus KD_{Fe} is controlled by chemistry rather than by temperature. Gorbatschev (1968) found KD_{Fe} (biotite-cordierite) to be dependent on the proportion of Mg and/or Fe in biotite and related to the (Al^{VI} + Ti) content of biotite. A similar relationship was not found in the samples studied by the author.

Si and Al in biotite and cordierite show no regular change with metamorphic grade. The Al^{IV} content of biotite has received much attention in metamorphic studies with the general consensus being that it increases with increasing grade of metamorphism (Butler, 1965; Binns, 1969; Ushakova, 1972) but with the proviso that total Al in the rock modifies this relationship. In the biotites under discussion there is a slight increase in Al^{IV} with increasing grade but the overall change in the number of ions from 2,61 in the medium stage to 2,64 for the high stage is less than the variation among samples from equivalent grades of metamorphism.

The Ti-content of biotite shows a fairly regular increase with increasing grade of metamorphism (Fig. 45). This appears to be a characteristic of biotite in metamorphic belts (Binns, 1969; Ushakova, 1972; Miyashiro, 1973). An increase is also apparent in the Mn-contents of both biotite and cordierite (Figs. 43, 44 and 45). Biotite from rocks containing garnet (RJ168, RJ774) is depleted in Mn because this element is preferentially concentrated in garnet. The trend of Mn enrichment with increasing grade follows that found in non-garnetiferous schists elsewhere (Hyndman, 1972), but it may be significant that MnO (whole-rock) also shows a general increase with increasing grade.

Figure 44. Variation diagram showing change of composition of cordierite with increasing grade of metamorphism (from left to right). Elements expressed as numbers of ions on the basis of 18 oxygen anions.

Figure 45. Variation diagram showing change of composition of biotite with increasing grade of metamorphism (from left to right). Elements expressed as numbers of ions on the basis of 22 oxygen anions.

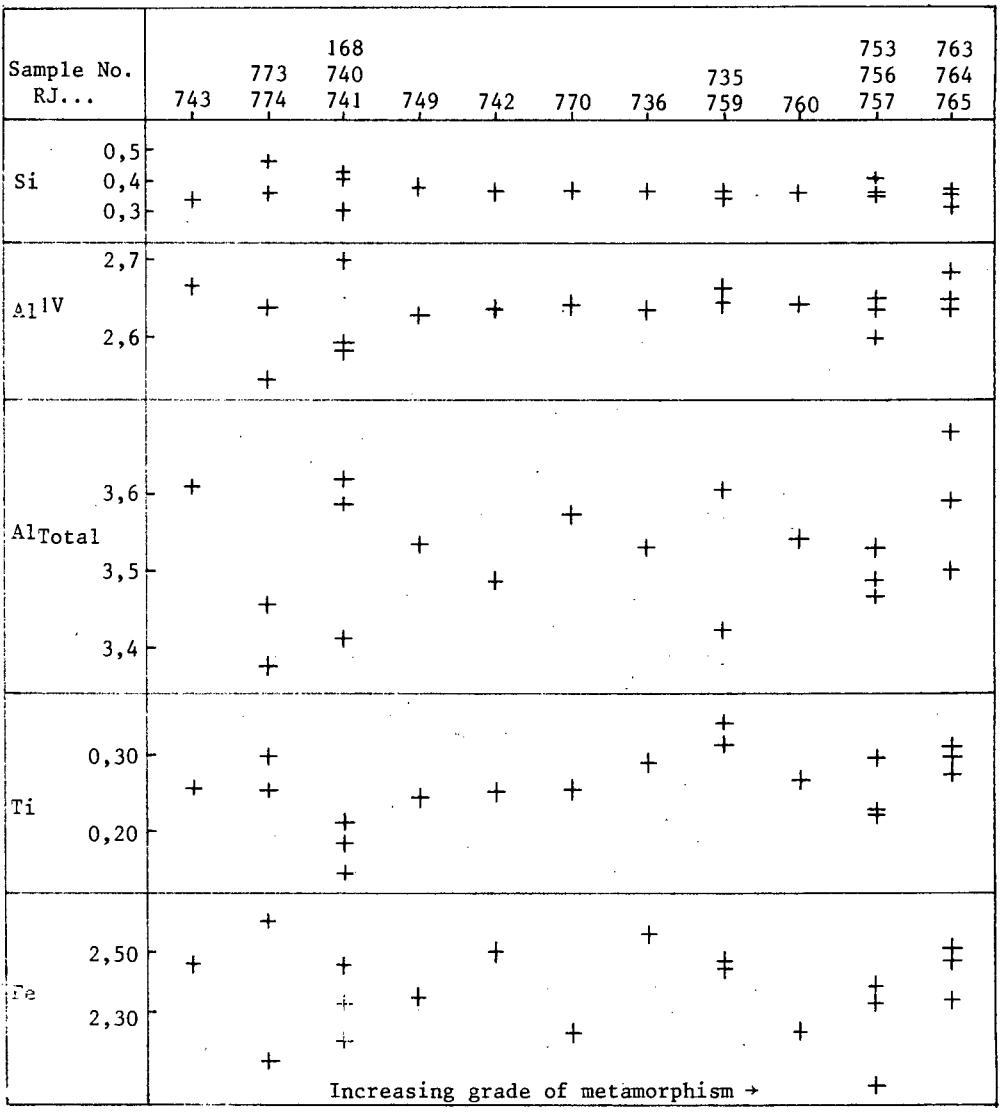

Figure 45 continued

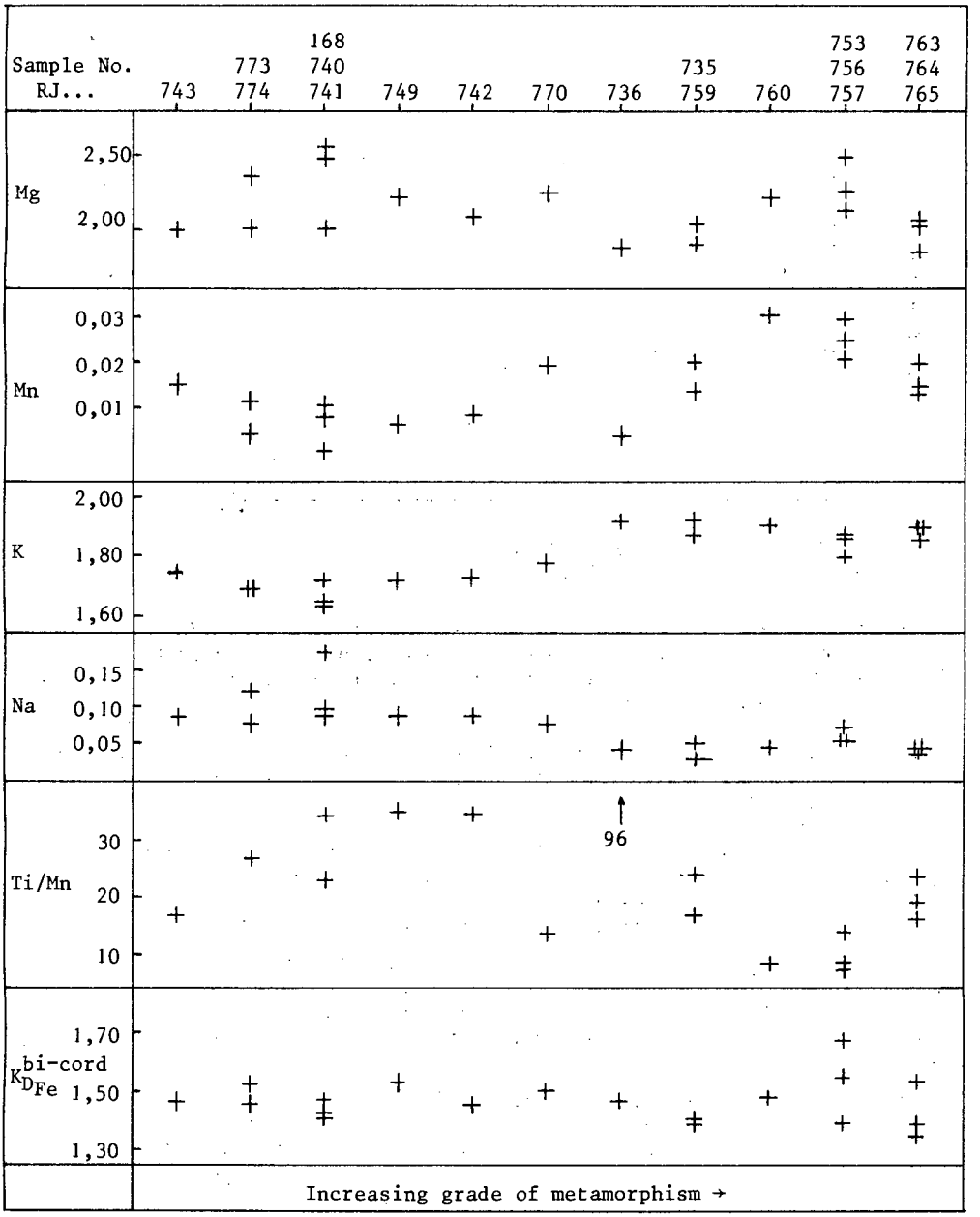

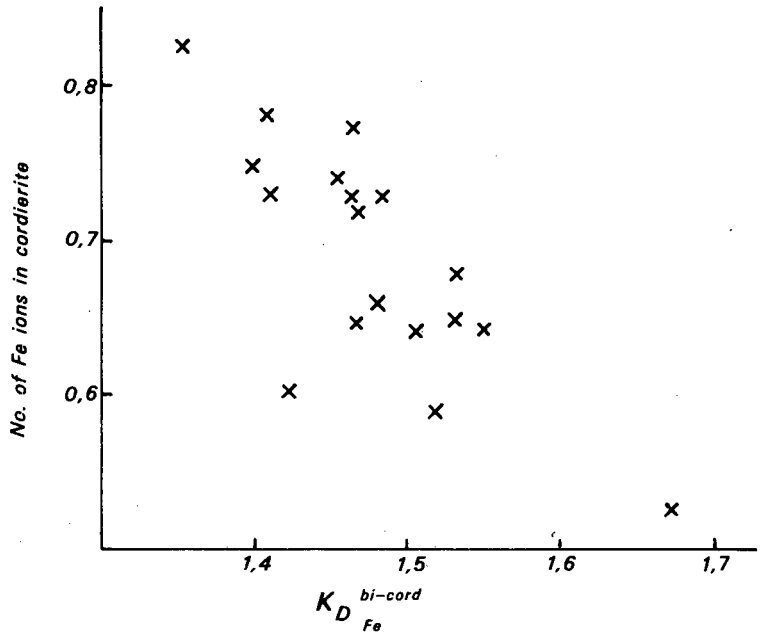

Figure 46. Near-linear relationship between concentration of Fe in cordierite and KD_{Fe}. The Fe and Mg contents of cordierite exert a greater control over the distribution coefficient than metamorphic grade.

Engel and Engel (1960) found the TiO_2/MnO ratio to be a useful indicator of metamorphic grade in garnetiferous metamorphites but whereas those workers found a substantial increase with increasing grade, the Ti/Mn ratio in the biotites from the area of the present study shows a general decrease (Fig. 45). Samples containing garnet have not been plotted in this particular diagram. Mn in biotite shows a complex relationship with Fe. In biotites from the medium stage Mn and Fe increase together but in those from the high stage the number of Mn ions decreases with increase of Fe (Fig. 47a, b).

There is a sympathetic variation of K in biotite and in the whole rock. In both, the K content increases with increasing metamorphic grade. In the case of Na, both biotite and cordierite contain smaller amounts at higher grades. There is also a slight decrease in Na_2O (whole-rock) with increasing grade.

Thus, with the possible exception of Ti, the compositions of co-existing biotite and cordierite do not appear to be controlled by the change in metamorphic grade and the chemical control exerted by rock composition is by far the most important factor. In this connection it is appropriate to cite the conclusions of Butler (1965, p. 295):

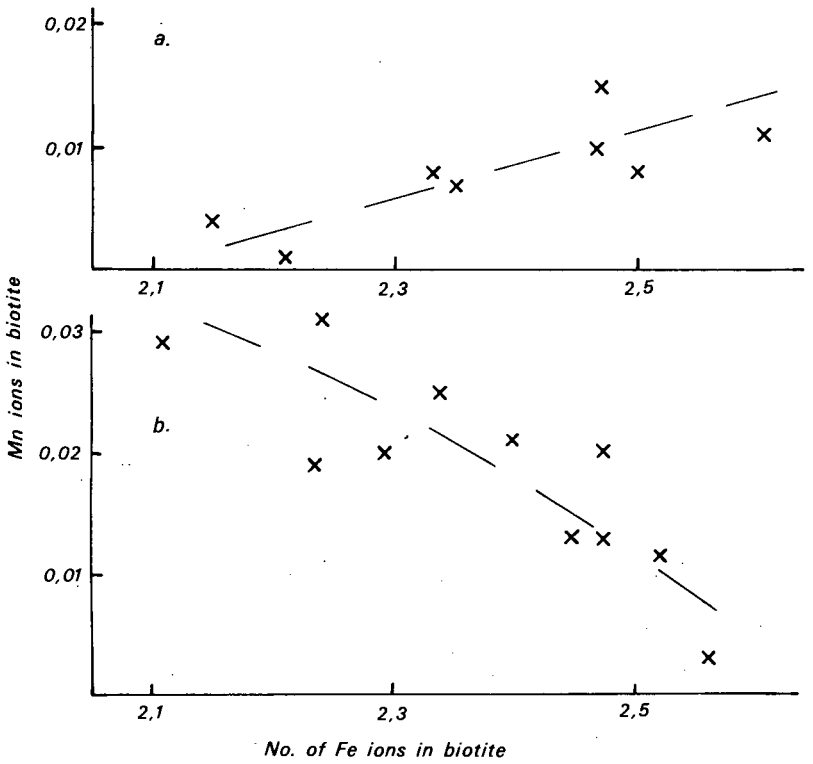

Figure 47. Fe-Mn relationships in biotites from
(a) medium-stage samples and from
(b) high-stage samples.

".... attempts to use the compositions of individual minerals as indices of variations in physical conditions of formation of metamorphic rocks are likely to be unsuccessful unless it is appreciated that the composition of any one mineral in a metamorphic rock is a function of the composition of the rock, and of the distribution relations between that mineral and any other that may be present; and that both of these may need to be determined before the significance of a single mineral analysis becomes apparent".

4.3.3.3. Co-existing cordierite and garnet

In only one sample were co-existing cordierite and garnet analysed (RJ774) and the analysis of the garnet is listed in Table 20 (p. 97). According to Chinner (1959) and Wynne-Edwards and Hay (1963) the compositional

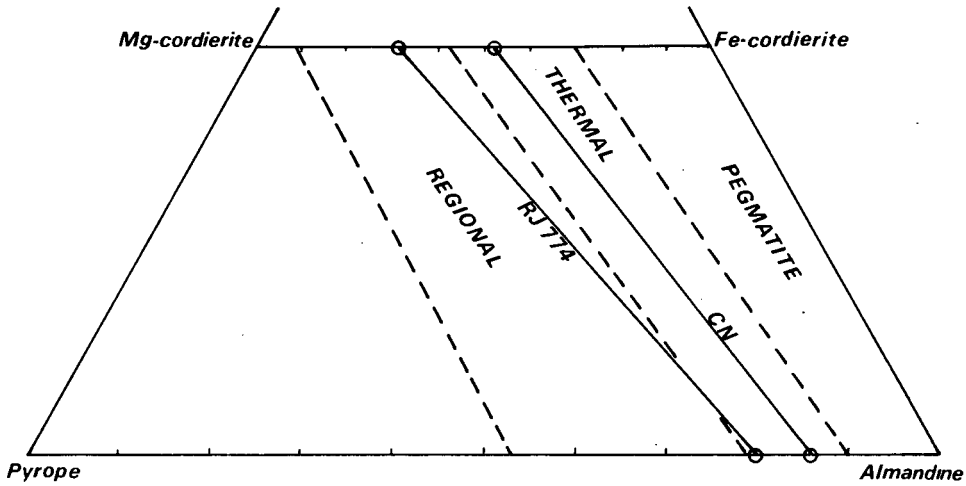

Figure 48. Triangular diagram showing the compositional ranges of co-existing cordierite and garnet in different environments (after Chinner, 1959). Tie-line labelled RJ774 is for an analysed cordierite-garnet pair from the Tinkas Formation. The compositions of co-existing cordierite-garnet (CN) in the SJ Area (Nash, 1971) are inserted for comparison.

ranges of co-existing garnet and cordierite vary in different environments. Figure 48, adapted from Chinner (op. cit.), shows the compositions of the two co-existing minerals in RJ774.

The use of the Fe content of cordierite in equilibrium with garnet as an indicator of metamorphic grade is discussed on p. 133.

4.3.4. Interpretation of the mineral assemblages and petrogenesis

The textural relationships, mineral assemblages and appearance and disappearance of metamorphic index minerals can be interpreted in terms of certain prograde metamorphic reactions.

Andalusite is not uncommon near the southeastern margin of the region but its amount decreases northwestwards. In several samples it is closely associated with sillimanite and its disappearance is partly due to inversion to the latter:

(19) andalusite = sillimanite

The andalusite/sillimanite boundary line is crossed somewhere near the south-eastern margin of the area but because andalusite often persists metastably

(Chinner, 1966; Greenwood, 1972), the two minerals are usually found together for some distance. The actual boundary may be situated beyond the mapped area. This inversion is not, however, the main cause of disappearance of andalusite short of anatexis. The textural evidence suggests that a reaction of the following type has occurred:

(20) biotite + andalusite + quartz = cordierite + K-feldspar ± garnet + H_2O

Reaction (20) is probably a simplification because, in thin section, plagioclase appears to be one of the products and it is furthermore more calcic than the "matrix" plagioclase. A closer approximation to the reaction is believed to be:

(21) biotite + andalusite + quartz + Na-plagioclase = cordierite + K-Na feldspar (perthite) + Ca-richer plagioclase ± garnet + H_2O

Additional Al, required for this reaction, is readily available; the released Na is incorporated within K-feldspar.

Staurolite is found in the lower metamorphic terrains well to the southeast of the mapped area where it probably formed through the common reaction discussed by Winkler (1967) and Hoschek (1969):

(22) chlorite + muscovite = staurolite + biotite + quartz + H_2O

There are several reactions to be considered for the breakdown of staurolite during progressive metamorphism in this area. According to Hoschek (1967) and Winkler (1970) the most common reactions in non-anatectic terrains are:

(23) staurolite + muscovite + quartz = Al_2SiO_5 + biotite + H_2O

and

(24) staurolite + muscovite + quartz = Al_2SiO_5 + biotite + almandine + H_2O

In anatectic areas, the reaction of Winkler (1970) is applicable:

(25) staurolite + quartz = Al_2SiO_5 + almandine + H_2O

This reaction has been experimentally investigated in the Mg-free system by Richardson (1968) and Ganguly (1972), while reaction (23) has been investigated by Hoschek (1969). According to the latter author and Winkler (1970), reaction (7) can be expected to occur at higher pressures than reaction (5), although this has been disputed by Ganguly (1972), and will normally only be found in anatectic areas.

In the area under consideration, cordierite appears to be one of the products of staurolite breakdown but textural evidence is somewhat ambiguous. The two most likely possibilities are reaction (26) and reactions (24) plus (21):

(26) staurolite + biotite + quartz = cordierite + almandine + muscovite + H_2O

This reaction is perhaps not applicable in the present case since it occurs under pressures of less than 3 kb (Hess, 1969), while >4 kb pressures are believed to have prevailed in the area under discussion (p. 135), and since muscovite does not appear as a product.

A series of coupled reactions, whereby cordierite is not in a direct

reaction relationship with staurolite, is more likely:

(24) staurolite + muscovite + quartz = biotite + almandine + Al_2SiO_5 + H_2O

followed by

(21) biotite + Al_2SiO_5 + quartz (+ Na-plagioclase) = cordierite + K-Na feldspar (+ Na-Ca plagioclase) ± garnet + H_2O

Cordierite has formed through reaction (21) and, if present further to the southeast, probably also through reactions (27) and (28) (Winkler, 1967, 1970; Hirschberg and Winkler, 1968):

(27) chlorite + muscovite + quartz = cordierite + biotite + Al_2SiO_5 ± garnet + H_2O

(28) chlorite + muscovite + quartz = cordierite + biotite ± garnet + H_2O

The reactions responsible for formation of garnet under amphibolite facies conditions are possibly those suggested by Hirschberg and Winkler (1968), here listed as reactions (27) and (28). Whether cordierite or garnet are formed or both depends on the Fe- and Mg-contents of the system and on the prevailing pressure. Garnet has formed also through reactions involving the breakdown of staurolite and andalusite (reactions (21) and (24).

Very close to, but on the high-temperature side of the boundary marking the start of anatexis in gneisses (see Fig. 50), muscovite and quartz no longer co-exist and have reacted as follows:

(29) muscovite + quartz = sillimanite + K-feldspar + H_2O.

Winkler (1970) has used this reaction to define the high stage of metamorphism because it has been recognised in many metamorphic terrains throughout the world.

According to Winkler (1970) the stability of the association muscovite + quartz up to anatectic conditions is indicative of pressures greater than 4 kb. The perthitic character of some of the K-feldspar may indicate that the actual reaction in some samples involves plagioclase (Evans and Guidotti, 1966; Winkler, 1970) as follows:

(30) muscovite + quartz + plagioclase = K-Na feldspar + sillimanite + Ca-richer plagioclase + H_2O

However, plagioclase was not observed as a product and the Na may have come from the paragonite component of muscovite.

About 5 km beyond the sillimanite + K-feldspar isograd, cordierite becomes a conspicuous mineral in the metampelites through the following reaction:

(31) biotite + sillimanite + quartz = cordierite + K-feldspar ± garnet + H_2O

This reaction has been discussed by Hietanen (1947) Schreyer and Yoder (1961), von Platen and Höller (1966) and Schreyer and Seifert (1969).

In some samples plagioclase has taken part in the reaction because it also occurs as porphyroblasts containing sillimanite in the cores:

(32) biotite + Na-plagioclase + sillimanite + quartz = cordierite + K-Na feldspar + Ca-richer plagioclase ± garnet + H_2O

Reaction (32) is essentially the same as reaction (21) except that sillimanite is a reactant here rather than andalusite (see p. 125).

The biotite-poor cordierite-sillimanite gneisses of the Rössing Formation, west of the Husabberg, contain significant amounts of Fe-oxide. In these rocks a modification of reaction (32) appears to be responsible for the formation of Fe-oxide rather than garnet:

(33) biotite + sillimanite (+ Na-plagioclase) + quartz = cordierite + K-Na feldspar (+ Na-Ca plagioclase) + Fe-oxide + H_2O

The presence of Fe-oxide instead of garnet is probably due to higher P_{O_2} in these rocks during metamorphism. Hsu (1968) has shown that almandine is stable only under conditions of relatively low oxygen fugacities (up to conditions of the quartz + fayalite-magnetite (QFM) buffer) above which it breaks down to oxide phases. Oxygen fugacities probably were too high for almandine to be stable in these rocks. Analysed samples of the gneisses (RJ764, RJ765) contain greater amounts of Fe_2O_3 than most of the metapelites analysed (Table 22) and contain modal haematite.

The possibility of biotite breakdown through a reaction of the type:

(34) biotite + oxygen = K-feldspar + magnetite + H_2O

(Wones and Eugster, 1965) is unlikely because the Mg released during the breakdown would be expected to enter the surviving biotite (and perhaps cordierite too) and thus increase its Mg/Fe ratio; microprobe analyses (see 4.3.3.2.) show that this cannot be demonstrated.

The cordierite - K-feldspar - sillimanite gneisses probably contained a larger amount of muscovite relative to biotite than other pelitic types. During progressive metamorphism reaction (29) produced sillimanite which then reacted with biotite according to reaction (33), leading to the destruction of biotite. Excess sillimanite remained after the reaction.

Nash (1971) postulated two episodes of high-grade metamorphism for the Damara orogen. According to him (Nash, op. cit., Fig. 19, pp. 54,68) the M_1 episode apparently experienced temperatures of about 700° C and pressures of 6-8 kb. After a considerable period of time the M_2 episode occurred at temperatures of 675° - 750° C and pressures of 3-5 kb. The present author originally accepted this conclusion (Jacob, 1971) but after further investigation it became obvious that there is at present no compelling evidence for the existence of two separate metamorphic episodes affecting Nosib and Damara Group rocks. In addition, no evidence was found to substantiate Guj's (1970) postulate of a post-Nosib/pre-Damara tectonothermal event. The absence of any widespread occurrence of typical anhydrous granulite facies assemblages in the Khan/Swakop area (e.g. orthopyroxene in place of biotite in metapelites) militates against two high-grade metamorphic episodes. Had an earlier high-grade metamorphic episode occurred, the rocks would have been dehydrated to a significant degree and thus subsequent metamorphism would have occurred under conditions of $P_{H_2O} < P_T$. At the temperatures believed to have prevailed during the "later" metamorphism, typically anhydrous assemblages of the

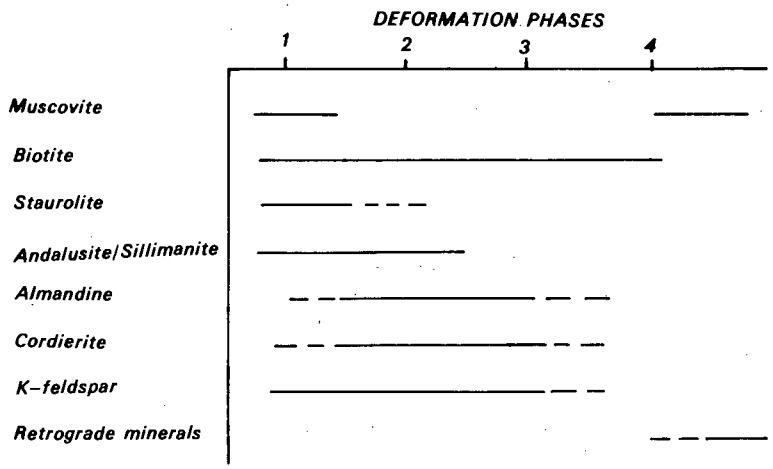

Figure 49. Paragenetic sequence of metamorphic minerals in metapelites.

granulite facies would almost certainly have formed (Wynne-Edwards, 1971; Hyndman, 1972, p. 363).

Nash (op. cit.) cited the paragenetic sequence of metamorphic minerals as evidence for two separate metamorphic episodes but in the area studied the sequence is quite compatible with a single prolonged metamorphic episode. It is possible, albeit with some uncertainty, to date mineral growth relative to other phases and relative to episodes of deformation (Johnson, 1962; Zwart, 1962) and it is to be expected that different minerals and mineral assemblages become stable at different times during progressive metamorphism.

The paragenetic sequence for metapelites in the region investigated is summarised in Figure 49. It is significant that biotite has recrystallised several times, that cordierite and garnet postdate the formation of s_1 and have outlasted F_2, and that migmatisation occurred during F_1 and continued until after F_2. Widespread retrograde metamorphism occurred in the rocks, resulting in the replacement of Al-silicates by muscovite, chloritisation of hornblende and biotite and pinitisation of cordierite.

The field and laboratory investigations have indicated that various metamorphic isograds can be recognised in metapelites and these are shown in Figure 50. From southeast to northwest the sequence is as follows:

(i) "Andalusite/sillimanite" (reaction 19, A in Fig. 50). The position of this isograd in the field is uncertain and may lie southeast of the mapped area although it is probably situated near the southeastern margin.

(ii) "Staurolite out in non-anatectic metamorphites" (Winkler, 1970)

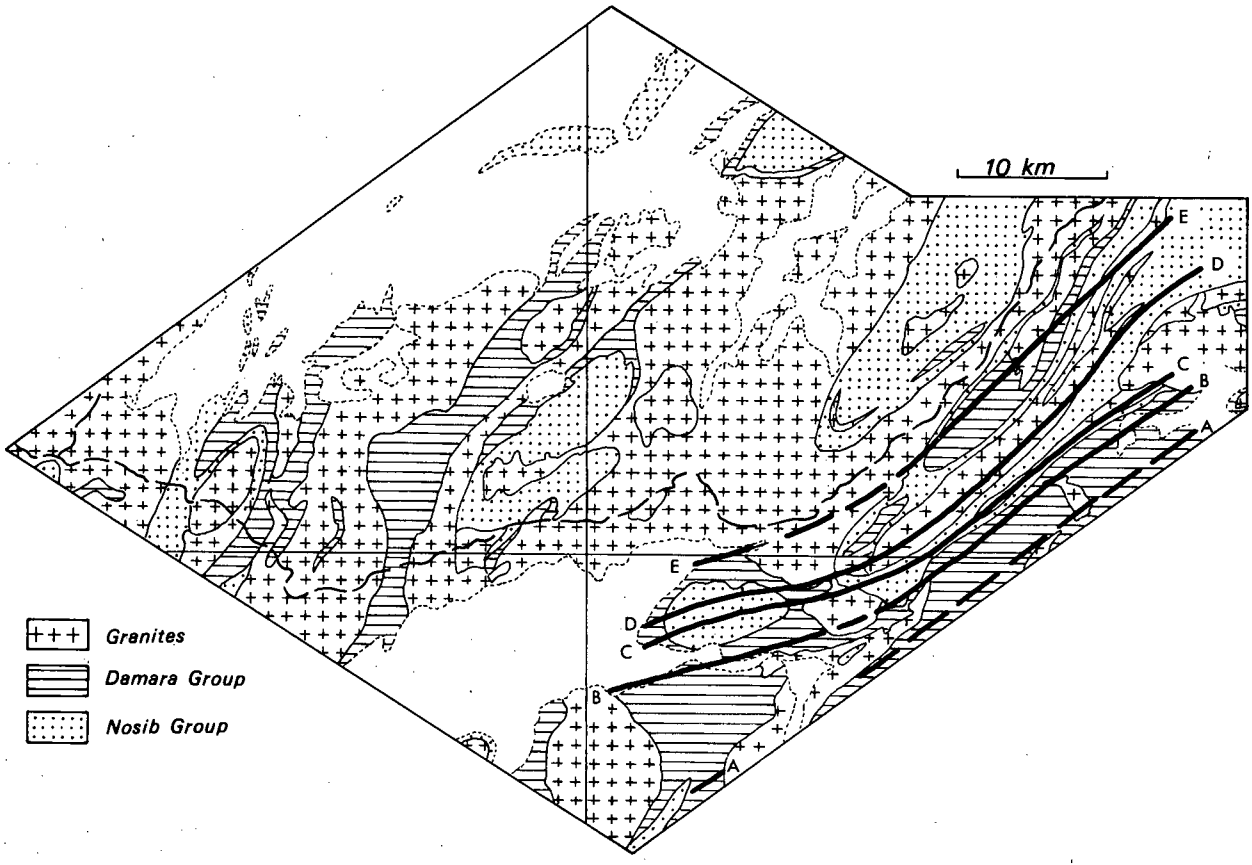

Figure 50. Isograd map, showing approximate positions of reactions discussed in the text. A = andalusite/sillimanite, B = staurolite out, C = anatexis in gneiss, D = K-feldspar + sillimanite, E = K-feldspar + cordierite.
The position of the andalusite/sillimanite isograd is uncertain and it is shown as a dashed line. The position of the first entry of cordierite lies further to the southeast.

(reaction 24, B in Fig. 50). The final disappearance of staurolite coincides, in the field, with the final disappearance of andalusite in pelitic rocks through reactions 19 and 21). The breakdown of both of these minerals is spread over a range of temperatures.

(iii) "Anatexis in gneisses" (C in Fig. 50). The beginning of anatexis in Nosib and Damara metamorphites can be located in the field and, for the purposes of this work, is regarded as an isograd although Winkler (1970) has not defined it as such. Its trend is parallel to other isograds.

(iv) "K-feldspar + sillimanite in anatectic gneiss" (Winkler, 1970) (reaction 29, D in Fig. 50). This isograd is found on the northwestern side of the "anatexis-in-gneiss" isograd.

(v) "K-feldspar + cordierite" (reaction 31, E in Fig. 50).

The position of the first entry of cordierite is uncertain but is not within the mapped area.

In order to correlate field findings with experimental work, the discussion will centre around Figure 51, which shows various experimentally determined and theoretical equilibrium curves.

The first appearance of cordierite and of staurolite in regional metamorphism is shown, approximately, as Curve (22, 27) (actually a divariant "band") after Hirschberg and Winkler (1968), Hoschek (1969) and Winkler (1970).

The position of the Al-silicate triple point and the stability fields of the three polymorphs kyanite, andalusite and sillimanite have received a great deal of attention from various laboratory workers, but are even now not well established. Two different sets of phase boundaries that have found acceptance in the literature are those of Richardson et al. (1969) and Althaus (1967). Both sets of data are shown in Figure 51. The fact that andalusite persists almost up to the anatexis isograd suggests that the andalusite/sillimanite boundary as determined by Richardson et al. (1969) is more appropriate to this area but ignores the possibility of metastable persistence of andalusite into the sillimanite field.

In the area under discussion pressure conditions were below those defined by the triple point because of the occurrence of andalusite and sillimanite. A further indication of the operative pressures is given by the position of the "K-feldspar + sillimanite" isograd relative to the isograd "anatexis-in-gneiss" (see below, p. 132).

The breakdown of staurolite is probably according to reaction (23) and/or (24). The reaction curve is shown as Curve 23 in Figure 51, after Hoschek (1969) and Winkler (1970). It has a positive slope and intersects the anatexis curve at about 5 kb. The reaction for the breakdown of staurolite in anatectic areas (reaction 25) is shown as Curve 25 in Figure 51, after Richardson (1968). From the isograd map (Fig. 50) it can be seen that staurolite breaks down before the anatexis isograd is reached but that its final disappearance occurs close to it. This indicates that reaction Curve 23 is more applicable to staurolite breakdown than Curve 25 and that pressures were probably near the intersection of Curve 23 and the anatexis curve,

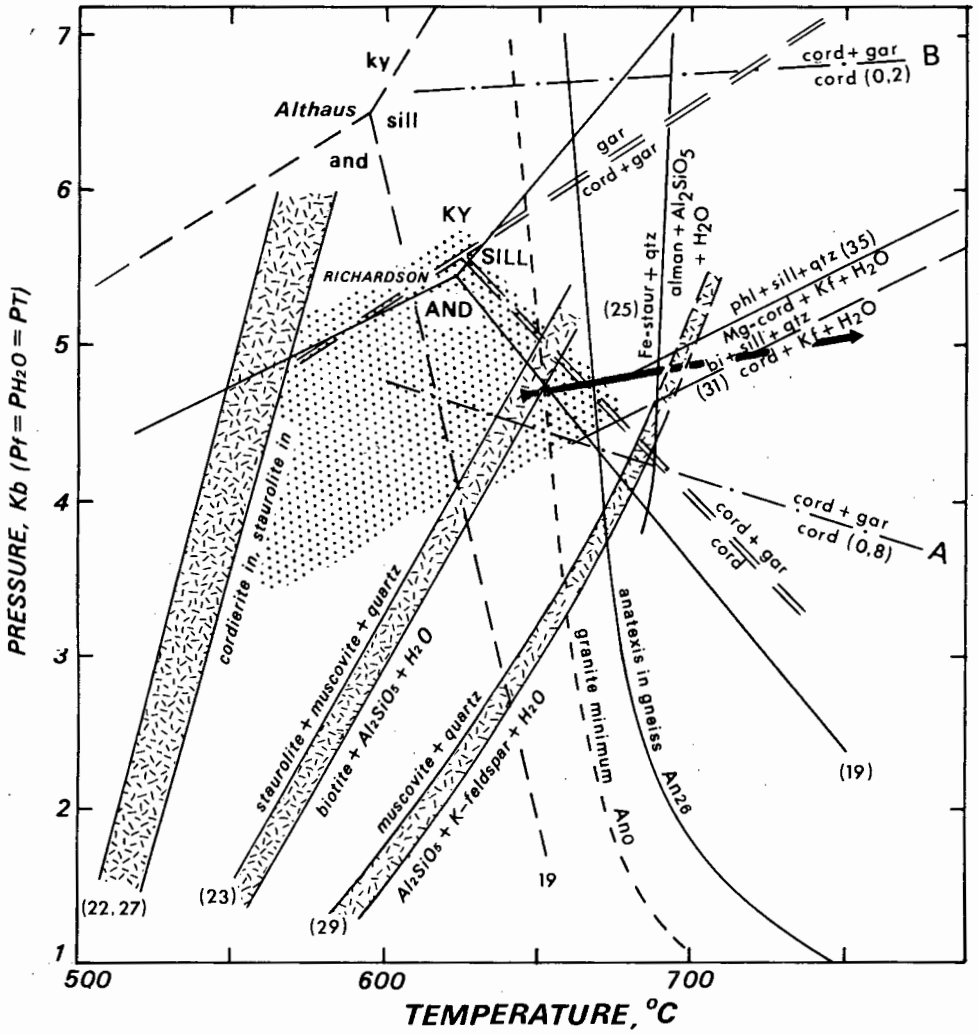

Figure 51. P-T diagram showing experimentally determined equilibrium curves for reactions discussed in text. Figures in brackets refer to reactions cited and dashed arrow indicates probable P-T conditions in the area studied.

= = = limits of the field of co-existence of cordierite and garnet after Hirschberg and Winkler (1968)

⁘⁘⁘ = field of co-existence of staurolite and cordierite after Ganguly (1972)

Several of the reaction curves are shown as divariant bands as reactions occur over a range of temperatures.

i.e. near 5 kb.

It is significant that in some samples staurolite and cordierite co-exist, seeing that it is likely that they occur together only over a restricted pressure interval. According to Richardson (1968) the pressure limits for overlap of the Mg-cordierite and Fe-staurolite fields are 1 and 8 kb which does not permit great precision, but in natural assemblages the two extreme end members will not be found because cordierite will contain a certain amount of Fe and staurolite a certain amount of Mg. This will have the effect of raising the lower-pressure limit and dropping the upper limit. The field of co-existence of the two minerals has been discussed by Ganguly (1972) and he has placed it in the vicinity of the Al_2SiO_5 triple point, mainly in the andalusite field. This field is shaded in Figure 51.

The curve for anatexis in gneiss has been taken from Winkler (1970) for the situation where the rocks contain oligoclase. The curve for water saturated melting of rocks containing albite with An_0 is also shown. It is important to note that muscovite and quartz co-exist up to the anatexis isograd. This indicates that pressures were above 4 kb because the intersection of Curve 29 with the melting curve is in the vicinity of 4 kb. Reaction (29) has been investigated by Evans (1965) and by Althaus et al. (1970). The two sets of results are in good agreement except at low water pressures. The curve shown in Figure 21 is that of Althaus et al. (1970). Later redeterminations by Kerrick (1972) using hydrothermal techniques produced results in agreement with Evans (1965) while experiments by Day (1973) confirmed the results of Althaus et al. (1970).

The important reaction for the breakdown of biotite + sillimanite + quartz (reaction 31) has not, to the author's knowledge, yet been experimentally investigated although its validity is indicated by field and laboratory observations. According to von Platen and Höller (1966) and Winkler (1967) the reaction occurs at higher temperatures than the breakdown reaction of muscovite + quartz (29) and according to Schreyer and Seifert (1969) the reaction curve will have a positive slope in a P-T diagram and will be confined to relatively high pressures. The theoretical reaction curve for the pure Mg-system (Schreyer and Seifert, op. cit.) is shown as Curve (35) in Figure 51:

(35) phlogopite + sillimanite + quartz = cordierite + K-feldspar + H_2O

The actual position of the curve for reaction (31) in a P-T diagram, where both Mg and Fe are present, however, is not yet known, although Hess (1969) has indicated that an increase in the Fe-content of the system will reduce the pressure at which the reaction occurs. For this reason Curve (31) is drawn parallel to Curve (35) in Figure 51, but at a lower pressure.

The compositions of co-existing cordierite and garnet are potential indicators of temperature and pressure conditions and have been investigated by several researchers, e.g. Hirschberg and Winkler (1968), Hensen and Green (1971, 1972, 1973) and Currie (1971, 1974). The field of co-existence in the Fe-rich system after Hirschberg and Winkler (1968) is shown in Figure 51. It is wedge-shaped and opens towards higher temperatures. Projections of garnet-cordierite equilibria, after Currie (1971), for varying Fe/Fe + Mg ratios of cordierite are shown as curves A and B. According to the data of

Hensen and Green (1973) the field of co-existence of cordierite and garnet covers most of the area of Figure 51 and is therefore not shown. There is still much uncertainty about the slopes of various curves for cordierite-garnet equilibrium. The above authors all agree that the lower-pressure limit of the field has a negative slope on a P-T diagram but disagreement exists over the upper limit. Currie (1971, 1974) has determined the equilibrium curve at high pressures as having a positive slope whereas Hensen and Green (1973) found a negative slope. Agreement also has not been reached over the variation of the distribution coefficient with temperature. Currie (1971, 1974) believes it to increase with increasing temperature while Hensen and Green (1973) believe it to diminish. Wood (1973) has attempted to reconcile the conflicting experimental data in terms of variation of P_{H_2O} during the experiments. Analytical data from RJ774 have been applied to both Currie's and Hensen and Green's results but in neither case were acceptable P-T estimates obtained (Currie, 800° C; Hensen and Green, less than 600°, P about 8 kb).

Before attempting to estimate temperature and pressure conditions from the data in Figure 51, two points merit brief discussion.

(i) The first point concerns the effects of fO_2 on the equilibrium data. It is unlikely that there is a shift in the position of the Al_2SiO_5 phase boundaries and the position of Curve 29 is also unlikely to be affected. The equilibrium conditions for reaction (29) were determined under fO_2 conditions of the graphite-water buffer (Althaus et al., 1970). The positions of Curves 23 and 25 for the breakdown of staurolite are sensitive to fO_2 and Hoschek (1969) reported shifts of ±20° C between the C and QFM buffers. Curves 23 and 25 were determined at QFM buffer conditions (Hoschek, 1969; Richardson, 1968). The anatexis curve is unlikely to be displaced through variation of fO_2. The effects on the breakdown of biotite + andalusite + quartz are not known.

Miyashiro (1964) pointed out that graphite in pelitic schists acts as a redox buffer and, where this is the case, fO_2 is likely to be low during metamorphism (Eugster, 1969), probably in the vicinity of the QFM buffer (Hoschek, 1969; Miyashiro, 1973). Fairly low fO_2 conditions have already been postulated from a consideration of the calc-silicate assemblages (p. 80) and the presence of almandine is also suggestive of relatively low fO_2 values (Hsu, 1968). If, as seems likely, fO_2 was in the vicinity of the QFM buffer then the curves will be in their correct positons as shown.

(ii) A more important effect concerns the relationship between P_{H_2O} and P_T. In the southeastern part of the area pelitic schists are interlayered with calc-silicate rocks, which were probably originally impure dolomitic limestones. During progressive metamorphism both H_2O and CO_2 were released. The presence of carbonaceous material probably also caused CO and CH_4 to be constituents of the fluid phase. Thus, although P_{fluid} was probably equal to P_T, it is very likely that P_{H_2O} was less than P_T; The effect of $P_{H_2O} < P_T$ on dehydration reactions is to reduce the temperatures of reaction. Thus some equilibrium curves, determined under conditions of $P_{H_2O} = P_T$, can be displaced to

considerably lower temperatures when $P_{H_2O} < P_T$ (Yoder, 1955; Hoschek, 1969; Hyndman, 1972).

Hoschek (op. cit.) has pointed out that X_{H_2O} lies between 0,7 and 1 in graphite-bearing pelitic rocks under most metamorphic conditions. Furthermore, the occurrence of clinozoisite/epidote, wollastonite and grossularite in calc-granofelses interbedded with the schists is indicative of a high X_{H_2O} in the Tinkas Formation. It may be recalled that reaction (21):

(21) biotite + andalusite + quartz (+ Na-plagioclase) = cordierite + K-feldspar (+ Na-Ca plagioclase) ± garnet + H_2O

occurs in the medium stage, well before the similar reaction

(31) biotite + sillimanite + quartz = cordierite + K-feldspar ± garnet + H_2O

in the high stage. The principal reason for the early occurrence of reaction (21) is probably the participation of plagioclase, which may have the effect of lowering the equilibrium temperatures for this reaction. The condition of $P_{H_2O} < P_T$ in the southeast, however, may be partly responsible for the occurrence of this reaction in the medium stage. Reaction (31) almost certainly occurred under conditions of $P_{H_2O} = P_T$, and this is indicated by the intense migmatisation and the paucity of calcareous assemblages.

Reaction (29), involving the breakdown of muscovite + quartz, does not appear to have occurred at lower temperatures, perhaps because X_{H_2O} was very near 1. Calcareous horizons are absent in the area where the beginning of anatexis and reaction (29) occur and therefore no CO_2 was present to dilute the fluid phase. The anatexis curve and Curve (29) in Figure 51 are probably in their correct positions ($P_f = P_{H_2O} = P_T$).

If, in the field, P_{H_2O} were less than P_T then the equilibrium curve for reaction (29) would have been displaced towards lower temperatures and the anatexis curve would have been displaced towards higher temperature. This would almost certainly have resulted in the K-feldspar + sillimanite isograd being found at a lower temperature than the anatexis isograd, but this is not the case (see Wyllie, 1971, pp. 180-181). The situation of $P_{H_2O} < P_T$ typifies the southeastern part of the area but over the rest of the region, in the high stage of metamorphism, anatectic phenomena like migmatisation, the abundance of pegmatites and the lack of anhydrous granulite-facies assemblages indicate that P_{H_2O} was equal to P_T;

From a consideration of the mineral assemblages, the pattern of isograds and the configuration of equilibrium curves in Figure 51, it is possible to estimate the metamorphic temperatures and pressures at the peak of the Damaran metamorphism (i.e. that corresponding to the M_2 metamorphism of Nash, 1971). The postulated P-T conditions for the southeastern and western parts of the study area are shown in Figure 51 and are compatible with the field findings and experimentally determined equilibrium data. In the east and southeast the temperatures reached 650° C and in the west, where widespread anatexis is evident, temperatures were probably around 750° C. The prevailing pressures

were above those of the intersection of Curve (29) with the "anatexis-in-gneiss" Curve, below that of the Al-silicate triple point and near the intersection of Curve (23) and the "anatexis-in-gneiss" Curve. The pressure is thus estimated as being between 4 and 5 kb. The P-T conditions postulated to have existed during metamorphism are indicated in Figure 51.

4.4. Contact Metamorphism

Thermal metamorphic effects, caused by intrusion of granitic rocks, have in places been superimposed on regionally metamorphosed metasediments. These effects can only be resolved in the southeastern parts of the area, where the regional metamorphic grade is slightly lower than that resulting from intrusion.

No marked contact metamorphic effects were observed along the border of the *Red Granite-Gneiss* although metasomatism and assimilation have resulted in the granitisation of surrounding metasediments. Very close to the western corner of the area a band of partly assimilated dolomite-calcite-forsterite marble contains small amounts of brucite.

The *Salem Granite* has no thermal aureole along its western contact with metapelites near the Witpoortberge - Husabberg - Pforteberge range and the contact itself is gradational in places. Typical intrusive contacts are developed in the southeast, especially in the vicinity of the Tinkas River, where the granite cuts the Tinkas Formation. Although the thermal aureole in this area is not more than a few metres wide, large xenoliths in the granite, measuring many tens of metres in length and width, are partly recrystallised. In the metapelites, metasomatic K-feldspar and plagioclase blastesis has occurred close to granite contacts.

Biotite has recrystallised to produce a decussate texture and almandine garnet is common in the contact zone. The mineral assemblages are similar to those of the regionally metamorphosed pelites but with the addition of hypersthene.

Subidioblastic to xenoblastic grains of hypersthene and K-feldspar poikiloblastically enclose remnants of biotite and quartz which were not completely destroyed by the following reaction:

(36) biotite + quartz = hypersthene + K-feldspar + H_2O

Reaction between K-feldspar, produced through reaction (36), and plagioclase has resulted in conspicuous myrmekitic intergrowths of these two minerals.

Calc-silicate rocks make up an important part of the succession along the Tinkas River and the presence of hypersthene in the metapelites is ascribed to reaction (36) occurring under conditions of $P_{H_2O} < P_T$, which would have the effect of causing it to take place at lower temperatures than would be the case if $P_{H_2O} = P_T$. This conclusion is supported by the apparent absence of hypersthene from metapelites immediately adjacent to contacts of the Salem Granite in the west, e.g. in the vicinity of the Rote Adlerkuppe and Witpoort, where calc-granofelses are virtually absent from the

Witpoort Formation and where $P_{H_2O} = P_T$.

In the vicinity of the Tinkas River and within a few metres of the Salem Granite contact, calc-granofelses contain diopside, wollastonite and grossularite-rich garnet. Diopside is poikiloblastically enclosed within wollastonite and grossularite porphyroblasts. Xenoliths of calc-granofels contain wollastonite, scapolite, diopside and grossularite, the latter having formed at the expense of wollastonite. The significance of this relationship is discussed below (p. 138).

The emplacement of the *Bloedkoppie Granite* has had very little metamorphic effect on the country rocks. In places biotite has recrystallised to coarser, disoriented flakes and cordierite has formed. Little change was found in calc-granofelses near the contact other than local growth of wollastonite and subsequent formation of grossularite at the expense of wollastonite.

The mechanical effects of the intrusion of the *Achas Granite* are more clearly displayed. Within several metres of the contact the Red Granite-Gneiss and psammitic lithotypes of the Etusis Formation have been brecciated and veined by the granite and biotite has recrystallised. The contact with the metapelites of the Tinkas Formation is generally poorly exposed but has been observed in places. Within several metres of the contact the metapelites are crumpled and have largely lost their foliated character. The rocks become coarser grained towards the contact and, in thin section, somewhat disoriented porphyroblasts of cordierite containing concentrations of sillimanite needles in their cores cut across, and are clearly younger than, lepidoblastic biotite. Reaction (31) has occurred in the metapelites close to the contact:

(31) biotite + sillimanite + quartz = cordierite + K-feldspar + H_2O

It should be noted that this reaction took place under the influence of thermal metamorphism before the appropriate regional isograd is reached. Close to the contacts zoned, antiperthitic andesine porphyroblasts have grown by replacement in the schists. The constituents of the plagioclase have been derived from the adjacent granite.

No effects of intrusion were noted in calc-granofelses although the granite has a bleached appearance, due to lower biotite content, where in contact with them.

Contact metamorphic effects around the *Gawib Granite* are limited to minor growth of cordierite and K-feldspar porphyroblasts in metapelites. Calc-silicate rocks close to the contact contain grossularite or wollastonite, or occasionally both; in places grossularite has grown partly at the expense of wollastonite.

The Donkerhoek Granite and its aureole have not been studied in detail because only a very small portion of this large body falls within the mapped region. According to Faupel (1973) the Donkerhoek Granite has no contact aureole but the present writer cannot agree with this statement as far as this area is concerned because the intrusion of the Donkerhoek Granite has affected the mineral assemblage of the older regional metamorphism in the southeast. The width of the aureole is difficult to ascertain but it appears

to reach up to 0,5 km in places.

The most obvious effect of intrusion is a crumpling of the invaded schists and the emplacement of vast amounts of pegmatitic material as veins, dykes and plugs. On a mesoscopic scale this has locally produced migmatites. Thermal effects of intrusion on the pelitic rocks include the following: recrystallisation of biotite to coarser, disoriented flakes; the formation of andalusite and masses of fibrolitic sillimanite and, near the contacts, the growth of a second generation of cordierite. The latter mineral has formed mainly through the reaction:

(21) biotite + Al_2SiO_5 + quartz + plagioclase = cordierite + K-feldspar + Ca-richer plagioclase + H_2O

but apparently also through the reaction:

(31) biotite + Al_2SiO_5 + quartz = cordierite + K-feldspar + H_2O

In some thin sections the later generation of cordierite and feldspar porphyroblasts encloses earlier, altered cordierite poikiloblastically. Emplacement of water-rich pegmatitic material has resulted in muscovitisation of sillimanite and andalusite, an effect previously noted by Gevers (1963).

The effects of thermal metamorphism on the calc-granofelses are best displayed in xenoliths in the granite and in large pegmatite bodies. Diopside, grossularite and wollastonite are common minerals in the xenoliths. Diopside is a product of regional metamorphism and in thin section it is seen to be poikiloblastically enclosed by grossularite and wollastonite. In some samples containing both wollastonite and grossularite, the textures are inconclusive in determining their age relationship. In other samples wollastonite is poikiloblastically enclosed by, and has broken down to form, grossularite (Pl. 27). The two minerals are not always found and individual samples may contain one or the other phase. Later calcite is pseudomorphous after wollastonite along joint planes in the rocks. The paragenetic sequence in the calc-granofels xenoliths is thus: diopside followed by grossularite and/or wollastonite, and also diopside followed by wollastonite and then by grossularite. It is possible to explain the paragenetic relationships between wollastonite and grossularite by reference to experimental work. The following discussion is applicable to thermal assemblages found around the Salem, Bloedkoppie, Gawib and Donkerhoek Granites.

The stability of grossularite has been investigated recently by Storre (1970) and Gordon and Greenwood (1971). Reference will be made to Figure 52, adapted from the latter authors for P_f = 2 kb on the assumption that the curves maintain their relationships at higher pressures, as suggested by Gordon and Greenwood's application of the data to the assemblages described by Misch (1964) from an area of relatively high pressures.

Figure 52 shows equilibrium curves for the following reactions:

(37) grossularite + quartz = anorthite + wollastonite

(38) calcite + anorthite + quartz = grossularite + CO_2

(39) calcite + anorthite + wollastonite = grossularite + CO_2

(13) calcite + quartz = wollastonite + CO_2

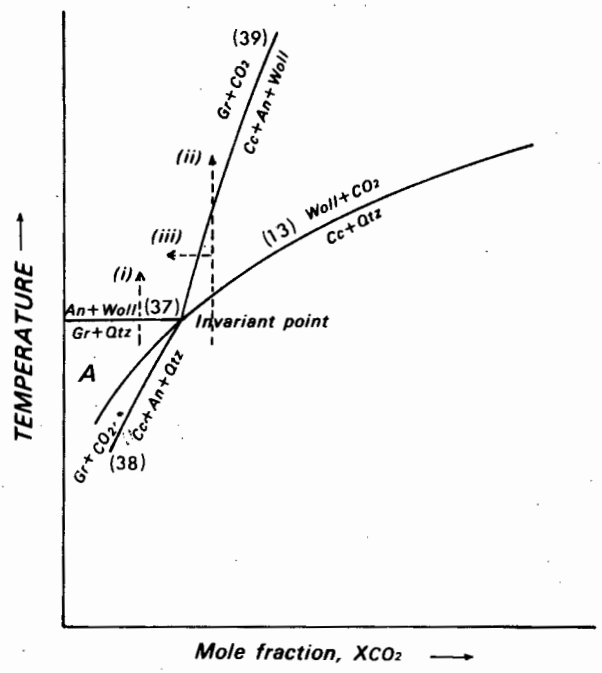

Figure 52. T-X_{CO2} diagram, adapted from Gordon and Greenwood (1971), showing phase relations involving wollastonite and grossularite. Possible paths followed during metamorphism and discussed in text are shown as (i) (ii) and (iii). Cc = calcite, Woll = wollastonite, Gr = grossularite, Qtz - quartz, An = anorthite.

In those samples where grossularite has formed before wollastonite, T-X_{CO2} conditions were probably those of field A in Figure 52 and in some cases metamorphism has followed path (i). The formation of plagioclase + wollastonite from grossularite + quartz is, however, not common and most of the plagioclase in the rocks is a product of regional rather than thermal metamorphism.

In the assemblages where grossularite has formed at the expense of wollastonite, one of two paths of Figure 52 may have been followed during contact metamorphism, but in both cases X_{CO2} was to the right of the invariant point. In the first case (path ii), calcite and quartz react to form wollastonite (Curve 13); with further rise in temperature, excess calcite reacts with plagioclase and wollastonite to form grossularite (Curve 39). In the second case (path iii) calcite and quartz react to form wollastonite (Curve 13). This is followed by diminution of X_{CO2} through dilution with H_2O derived from the water-rich melt in contact with the rocks. This, in turn, results in the reaction of calcite + plagioclase + wollastonite to

produce grossularite (Curve 39) without further rise in temperature. This is the interpretation favoured here because the fluid phase would become enriched in water, derived from the intrusive melt during its crystallisation, thus leading to a decrease of X_{CO_2}. Furthermore, in the case of path (ii) the temperatures required to cross Curve (39) might be too high if X_{CO_2} should lie well to the right of the invariant point.

The temperature must have been above the invariant point for grossularite to have formed after wollastonite. The position of this invariant point is subject to some uncertainty. Gordon and Greenwood (1971) place it at $T = 590^{\circ}$ C, $X_{CO_2} = 0{,}15$ at 2 kb and Storre (1970) places it at $T = 630^{\circ}$ C, $X_{CO_2} = 0{,}3$ at the same pressure. Boettcher (1970) has determined the effect of pressure on the reaction:

(37) grossularite + quartz = anorthite + wollastonite

in the system $CaO - Al_2O_3 - SiO_2 - H_2O$. According to his investigations the reaction will occur at about 700° C at a pressure of 5 kb.

The situation is complicated by the presence of Na in plagioclase and of Fe in grossularite. The effect of Na is to reduce the equilibrium temperature of the reaction and that of Fe to raise it (Kerrick, 1970) but the relative effects are not known. Thus the position of the invariant point and, therefore, the temperature necessary to convert the wollastonite-anorthite-calcite assemblage to grossularite are not precisely fixed. If the data from the system $CaO-Al_2O_3-SiO_2-H_2O$ are applied to the textural relationships as found in xenoliths of the study area, a minimum temperature of intrusion of about 700° C at 5 kb is indicated.

Very little need be added here to the observations of Nash (1971) concerning contact metamorphism caused by the *Alaskitic Pegmatitic Granite*. K-feldspar, of replacement origin, has formed in metapelites adjacent to the alaskite contacts and hornblende has been converted to biotite in basic gneisses.

Metasomatic skarn deposits are commonly developed along the contact between the alaskites and calcareous rocks. The skarn bodies vary in width from a few centimetres to several metres and may attain several hundred metres in length. They consist essentially of hedenbergitic clinopyroxene, andradite, scapolite and plagioclase, together with variable amounts of wollastonite and retrogressive tremolite/actinolite. Minor amounts of apatite, vesuvianite and melilite are common. Local radioactive mineralisation is associated with some of the skarns.

5. GRANITIC ROCKS

The granitic rocks form an integral part of the metamorphic history of the Damara Orogen and have been emplaced at different times. They can be broadly classified into syntectonic and late- to post-tectonic categories on the basis of field relationships and internal structural characteristics. The two most widespread types, the Red Granite-Gneiss (Gn_1) and the Salem Granites (Gn_2), are essentially syntectonic, and older than the crosscutting intrusive granites, although there probably is an overlap in time between the late members of the Gn_1 and Gn_2 suites and the late- to post-tectonic varieties.

5.1. Petrography

5.1.1. Red Granite-Gneiss (Gn_1)

The above term is a sack-name for a variety of granitic gneisses and gneissic granites, occuring below the base of the Husab Formation. Modal analyses (see Appendix) of samples are listed in Table 27. Recognition of the various rock types is best done in the field because they are essentially mineralogically similar in thin section. Compositionally, the Gn_1 is generally granitic, but granodioritic and alkali-feldspar-rich compositions are also found (Fig. 53). The constituent minerals are quartz, K-feldspar and plagioclase (oligoclase) together with lesser amounts of biotite and a variety of accessory minerals, the most common of which are zircon, apatite and magnetite. Small amounts of retrograde muscovite are usually present.

West of the Witpoortberge - Husabberg - Pforteberge range the Gn_1 consists mainly of red augen gneiss and red gneissic granite. The augen gneisses (RJ109, RJ196 in Table 27) are the oldest of the granitic rocks and have been severely deformed during F_1 and F_2. They are medium- to coarse-grained, strongly foliated rocks, the augen being composed of deformed individual grains, or aggregates, of microcline or strained quartz. The augen are surrounded by a finer-grained matrix containing biotite, which makes up a small proportion of the rock. In thin section, both metamorphic and igneous textures are found, the former being more common. The K-feldspar is microcline-microperthite and is diffusely twinned. Albite rims are usually developed along plagioclase/microcline contacts. Biotite occurs as fox-red, subhedral grains and schlieren with which are associated concentrations of heavy minerals. Garnet and sillimanite are present in some samples. The augen gneisses have the appearance of orthogneisses and are very similar to those of the Abbabis Formation, described by Gevers (1931a). Essentially similar augen gneisses crop out along the southwestern boundary of the region, 5 km west of the Gawib stock.

In the western parts of the region the augen gneisses are subordinate to foliated, medium-grained, red granites (RJ120, RJ700, RJ686 in Table 27) which are less deformed with smaller amounts of biotite and heavy minerals. Igneous textures are well-preserved and myrmekitic textures are not uncommon although

Tab e 27. Modes of samples of Red Granite-Gneiss (volumetric percentages).

Sample No.	Quartz	Microcline	Plagioclase	Biotite	Hornblende	Accessories	Accessories present	Locality
RJ412	35	39	23	2		1	zrn, ap, ore, musc, chl.	I23
RJ571	37	41	20	1		1	ore, musc.	G26
RJ409	27	42	15	15		1	zrn, ap, ore, musc.	I22
RJ442	29	23	30	16		2	ap, ore, musc, all, epid.	H19
RJ 72	22	40	27	9		2	zrn, ap, musc.	H19
RJ408	33	16	47	4		<1	ap, musc, chl, ore.	I22
RJ120	26	44	20	8		2	zrn, ap, ore, musc.	M8
RJ700	40	51	5	3		1	zrn, ap, musc, ore.	M7
RJ686	26	50	20	3		1	ap, musc, ore.	K3
RJ109	31	44	19	4		2	zrn, ap, ore, musc.	J7
RJ196	22	45	20	6	4	3	ap, ore, sphene.	I3

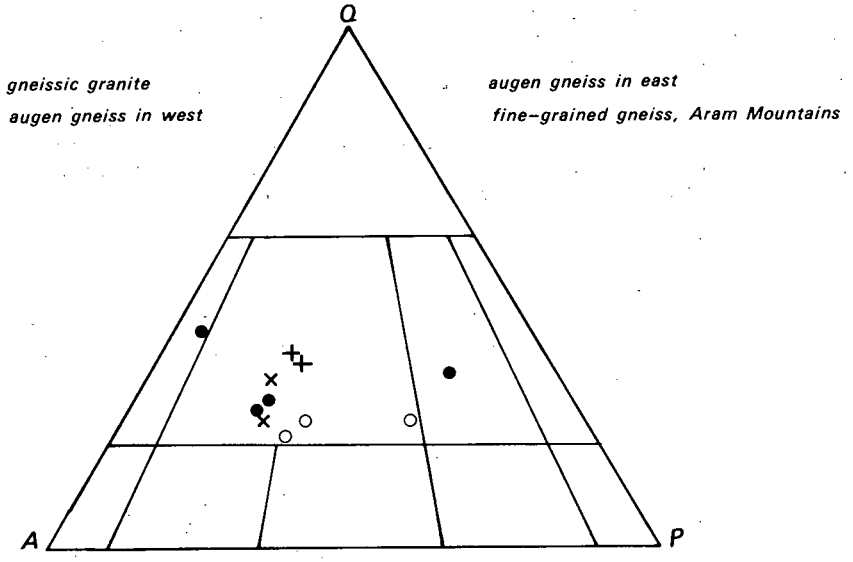

Figure 53. Modal composition of the Red Granite-Gneiss plotted on the classification diagram for plutonic rocks (Streckeisen et al., 1973).

graphic intergrowths are not prevalent. Biotite is altered to chlorite in many samples.

Plagioclase exists as zoned grains, generally occupying interstices. When enclosed in microcline, plagioclase is completely surrounded by albite rims, in optical continuity, and these rims form a conspicuous feature of the gneissic granites. The lack of perthitic textures in the enclosing microcline suggests migration of its albite component to grain boundaries (Tuttle and Bowen, 1958). In addition to the accessory minerals mentioned above, small amounts of sphene, rutile, allanite and epidote are sometimes present. With a decrease in ferromagnesian minerals the gneissic granites become alaskitic in character.

In the Vredelus anticline and the Rooikuiseb anticlinorium, in the eastern parts of the region, the Gn_1 comprises augen gneisses, gneissic granite and fine-grained gneisses. The augen gneisses differ from those in the west in that they appear to be migmatitic paragneisses. Metamorphic, granoblastic textures are well developed and the rocks consist of granitic augen and clots in a lepidoblastic, biotite-rich matrix. The growth of microcline porphyroblasts outlasted the two early phases of deformation F_1 and F_2. The augen gneisses (RJ409, RJ442, RJ72 in Table 27) found in the eastern part of the study area contain more biotite than those in the west. These rocks grade into, and are intruded by, red gneissic granite (e.g. RJ408 in Table 27).

Along the Aram mountains and southeast of the Horebisberg beacon the Gn_1 consists of deep-red, inequigranular, fine-grained granitic gneisses of possibly volcanic antecedents (see p. 10). The blastoporphyritic textures have been virtually obliterated. Highly perthitic microcline and strained quartz phenocrysts (?) are set in a finer-grained granoblastic matrix. In places, the textures are similar to those of true granulites (Spry, 1969, p. 294); these rocks are strongly foliated due to the streaky elongation of lenticular grains and aggregates of quartz "ribbon" set in a finer grained granoblastic-polygonal matrix of quartz, microcline and oligoclase. The matrix-microcline is less perthitic than the larger grains.

5.1.2. Salem Granite Suite (Gn_2)

Members of the Salem family crop out over a large area in the central part of the region. Modal compositions are presented in Table 28 and Figure 54.

5.1.2.1. Non-porphyritic gneissic granite

Between 5 and 6 km southeast of the Husabberg trigonometrical beacon a very early phase of the gneissic granite is found as a hybrid granitoid, formed more or less *in situ*. In thin section, the rock exhibits crystalloblastic textures and consists of quartz, microcline, plagioclase, biotite, cordierite and sillimanite. Albite rims are frequently developed along microcline/plagioclase boundaries and sillimanite grains occur

Table 28. Modes of samples of the Salem Granite Suite (volumetric percentages). Tr = <0,5 per cent.

Sample No.	Quartz	Microcline	Plagioclase	Biotite	Hornblende	Accessories	Accessories present	Locality
Non-porphyritic gneissic granite								
RJ457	27	23	34	11	4	1	ap, ore, sph, all.	I19
RJ391	25	21	34	15	3	2	ap, ore, sph, all	K18
RJ325	28	25	31	12	2	2	zrn, ap, ore, sph, epid, all.	L12
RJ358	26		41	32		1	ap, ore, epid.	G14
RJ355	27	16	40	16		1	zrn, ap, ore, all.	H12
RJ 91	31	1	47	19		2	ap, ore, sph.	I11
RJ137	22	28	39	6	4	1	ap, ore, sph, epid.	K10
Porphyritic biotite granite								
RJ513	25	19	37	15		4	ap, ore, sph, epid, all, cc.	K15
RJ519	18	9	41	31	Tr	1	zrn, ap, ore, sph.	J17
RJ 76	27	35	23	14		1	zrn, ap, ore, all.	G19
RJ332	20	15	37	27	Tr	1	zrn, ap, ore, sph, all.	K14
RJ326	22	15	33	29	Tr	1	zrn, sph, ap.	L12
RJ155	32	25	30	12		1	ap, sph.	L9
RJ 9	33	25	30	11		1	zrn, ap, ore, musc.	M9
Leucogranite								
RJ333	30	34	30	6		Tr	ap, ore, sph, musc.	K14
RJ514	28	37	27	8		Tr	zrn, ap, ore, sph, all.	K15
RJ522	27	36	28	8		1	zrn, ap, ore, all, musc.	G17
RJ511	32	33	26	8		1	zrn, ore, musc.	G16

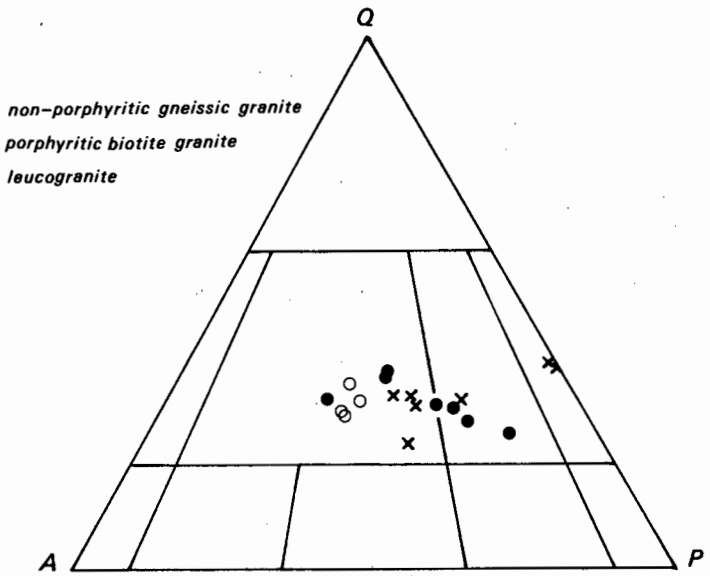

Figure 54. Modal composition of the Salem Granite Suite plotted on the classification diagram for plutonic rocks (Streckeisen et al., 1973).

poikiloblastically enclosed in the cores of cordierite and microcline grains. The cordierite is very extensively pinitized.

More common and widespread than this, however, is the gneissic granite, which is a medium grained, foliated rock of granitic to tonalitic composition (Fig. 54) intrusive into the country rocks. Contacts are sharp in places but gradational in migmatites. In thin section, the rocks have hypidiomorphic-granular or crystalloblastic textures. Plagioclase has crystallised before microcline and is poikilitically enclosed by it. In several samples more than one generation of plagioclase is present. The plagioclase is zoned and is more calcic (An_{36-44}) here than in later members of the suite. Biotite is subhedral and dark brown in colour, with a very slight greenish tint, and hornblende occurs as subhedral, very dark bluish-green grains. Accessory minerals are more abundant than in other members of the suite and include Fe-Ti oxide, pleochroic sphene, apatite, zircon, tourmaline, allanite, epidote and occasional garnet.

5.1.2.2. Porphyritic biotite granite

This member of the suite intrudes the non-porphyritic gneissic granite but also exhibits locally gradational contacts with the latter. A gneissic texture is developed near the margins but this is less pronounced than in the non-porphyritic variety. It is a medium- to coarse-grained, biotite-rich,

porphyritic igneous rock whose composition varies between granodiorite and granite (Fig. 54) (Streckeisen et al., 1973). The phenocrysts consist of microcline-perthite, exhibiting Carlsbad twinning; they reach 5 cm in length and are aligned parallel to the foliation. The phenocrysts enclose small, zoned grains of plagioclase and are themselves occasionally mantled by myrmekitic plagioclase intergrowths, producing a Rapakivi-type texture. A second generation of microcline occurs as a late crystallisation product in the matrix. The plagioclase is zoned oligoclase/andesine (An_{27-35}) and occurs as subhedral grains with albite rims when in contact with microcline. Accessory minerals are usually less abundant than in the gneissic granite except for allanite. Small amounts of hornblende occur. The biotite content is relatively high and many samples could be classed as melagranites (Streckeisen et al., 1973). Biotite occurs as dark brown grains with a very slight greenish tint. Typical metamorphic index minerals are absent, except in a strongly-foliated, slightly porphyritic body which occurs 4 km southeast of the Husabberg trigonometrical beacon. Highly pinitised cordierite and small amounts of sillimanite are found here.

5.1.2.3. Leucogranite

The leucogranite is a medium-grained, locally somewhat porphyritic granite. It is later than the biotite granite and intrudes it with either sharp or gradational contacts. It differs from the porphyritic variety in having a lower biotite and higher microcline content (Table 28). Its composition is granitic (Fig. 54) (Streckeisen et al., 1973). Where present, microcline phenocrysts are smaller than in the biotite granite and the subhedral plagioclase is less calcic (An_{25-29}). Myrmekitic intergrowths and albite rims are developed along microcline/plagioclase contacts. Allanite is a conspicuous accessory mineral in the leucogranite and is more abundant than in the other granite varieties. Small, irregular pegmatite bodies and veins are commonly developed.

The three members of the suite form a sequence in time and probably represent a differentiation sequence (Miller, 1972, 1973). Through the sequence, from oldest to youngest, the amount and Ca-content of plagioclase decrease more or less regularly while the microcline content increases. The biotite content decreases in the youngest member.

5.1.3. Bloedkoppie Granite (G_1)

In the field the Bloedkoppie Granite is very similar in appearance to the leucogranite of the Salem Suite but it contains more microcline (Table 29, Fig. 56) and is locally slightly porphyritic. In thin section the granite is medium-grained (grain size 1-3 mm) and hypidiomorphic-granular. The composition of zoned and subhedral plagioclase varies between An_{24} and An_0 (albite rims), although most samples contain An_{12}. Graphic and myrmekitic textures are prominent in the slides examined and antiperthite occurs locally. The accessory minerals include those listed in Table 29; of these allanite is most common while small amounts of garnet and fluorite may occur.

Table 29. Modes of samples (volumetric percentages) of late- and post-tectonic granites. Tr = <0,5 per cent.

Sample No.	Quartz	Microcline	Plagioclase	Biotite	Hornblende	Muscovite	Accessories	Accessories present	Locality
Bloedkoppie Granite									
RJ 57	37	42	15	5		Tr	1	zrn, all.	M20
RJ 51	29	45	21	5			1	zrn, ap, sph, all.	N18
RJ598	35	43	18	3		Tr	1	zrn, ap, ore, sph, all.	P16
RJ169	29	36	27	7			1	zrn, ap, ore, sph.	P17
Achas Granite									
RJ 27	24	5	51	14	5		1	zrn, ap, sph, all, epid.	H24
RJ433	27	10	44	15			4	ap, sph, ore, all, epid.	I25
RJ577	29	18	41	9	1	Tr	2	ap, sph, ore, all, epid.	H26
RJ 69	35	35	24	5		Tr	1	zrn, ap.	G25
Gawib Granite									
RJ 60	25	20	37	9	6		3	ap, ore, sph, all, epid, cc.	P14
RJ588	30	9	42	10	6		3	ap, ore, sph, all, epid.	P13
RJ643	18	12	37	11	15		7	ap, ore, sph, all, epid.	Q14
RJ 62	28	27	36	8			1	zrn, ap, ore, sph, all, epid.	Q12
RJ651	27	14	46	13			1	zrn, ap, ore, sph, all, epid.	P13
RJ 81	31	19	35	12	1		2	ap, ore, sph, all, epid, cc.	G12
RJ397	23	8	44	17	6		2	ap, ore, sph, all, epid.	H12
Horebis Granite									
RJ376	32	28	37	Tr		3	Tr	zrn, ap.	K19
RJ366	37	26	31	4		1	1	zrn, ap, ore, rutile.	M18
RJ367	14	43	33	7		2	1	zrn, ap, ore, all.	M18
Donkerhoek Granite									
RJ 40	35	36	24	3		2	Tr	zrn, ap.	J25
RJ 41	38	32	20	4		6	Tr	zrn.	I26
RJ629	34	24	39			3	Tr	zrn.	P18

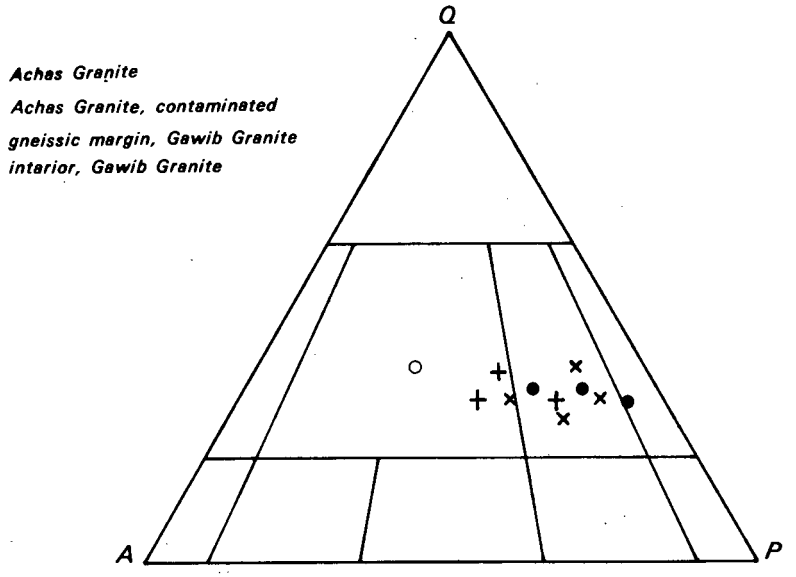

Figure 55. Modal composition of the Achas and Gawib Granites plotted on the classification diagram for plutonic rocks (Streckeisen et al., 1973).

5.1.4. Achas Granite (G_2)

The Achas Granite displays sharp, intrusive contacts against its country rocks. It is a medium-grained rock of tonalitic to granodioritic composition (Table 29, Fig. 55). In appearance it resembles the Salem biotite granite but contains smaller rounded "phenocrysts" of plagioclase and, less commonly, microcline. There is a seriate variation in size from coarse to fine constituents. The largest grains (maximum 1 cm) are zoned plagioclase, whose composition varies between An_{40} and An_{25}. Albite rims are locally developed. The textures in thin section are suggestive of emplacement of the Achas Granite as a crystal mush of low fluidity. The granite is contaminated near its contacts and contains more quartz and microcline where it intrudes the Red Granite-Gneiss and Etusis metapsammites (e.g. RJ69 in Table 29), but more biotite when intrusive into the Tinkas Formation. The accessory minerals are similar to those in the Gawib Granite (Table 29) but sulphides are more common.

5.1.5. Gawib Granite (G_3)

The stock near the Rabenrücken in the southern part of the area consists of an outer, gneissic granodioritic envelope (RJ60, RJ588 and RJ643 in Table

29) and a locally porphyritic, granodioritic to granitic interior. The smaller body, east of Marmor Pforte 37 (RJ81, RJ397) is similar in its composition to the gneissic margin in the southern stock but it does not display the pronounced gneissic texture. The rocks are also similar in appearance and composition to the Achas Granite. In thin section the rocks are medium-grained and exhibit seriate to porphyritic textures although the gneissic margin is generally free of phenocrysts.

Plagioclase occurs as subhedral, zoned grains. Its average composition in the gneissic margin of the southern stock is An_{41} but An_{30} towards the interior. The plagioclase composition in the northern stock is An_{40}. Microcline is locally perthitic and occurs as phenocrysts reaching 2 cm in size and as later, anhedral grains with quartz. Hornblende is common in the gneissic granodiorite but less common in the interior of the southern stock. A feature of the Gawib Granite is the abundance and variety of accessory minerals (Table 29); of these, epidote is probably the most common.

5.1.6. Alaskitic Pegmatitic Granite (G_4)

Early members of this group are sheared and contain small amounts of sillimanite; locally, the distinction between these and the Gn_1 is arbitrary. Compositionally, the G_4 bodies are granites and alkali-feldspar granites (Streckeisen et al., 1973) in which the grain size varies from fine (0,5 mm) to very coarse (>3 cm). Some of the coarser bodies may be classed as homogeneous pegmatites, whereas others are aplitic in character.

The most common mineral is microcline-microperthite, which is occasionally developed to the exclusion of plagioclase. Plagioclase varies from An_{20} to pure albite. Many alaskitic bodies contain plagioclase in the range An_{0-10}. Antiperthitic textures occur locally while graphic intergrowths of albite and microcline with quartz are common. Myrmekitic textures are also common and, in some samples, significant albitisation of microcline has occurred. Quartz is more common than plagioclase and exists as anhedral grains.

Biotite, frequently chloritised, is present in very small amounts in most samples or absent in others. Accessory minerals include apatite, zircon, magnetite, ilmenite, haematite, muscovite and, less commonly, garnet and sphene. A variety of accessory radioactive minerals, including uraninite and uranophane, is found locally.

5.1.7. Horebis Granite (G_5)

A variety of intrusive, post-tectonic granites has been included into this group. Their colour varies from white to red, their grain size is variable and on Horebis Nord 61 and Horebis Süd 108 the granite is locally pegmatitic with small pegmatite lenses and blows. West and east of the Rote Adlerkuppe dome the granite exhibits allotriomorphic, aplitic textures. The Horebis Granite is normally distinguished from the similar but older Gn_1 by a lack of foliation and by field relationships, but their distinction may

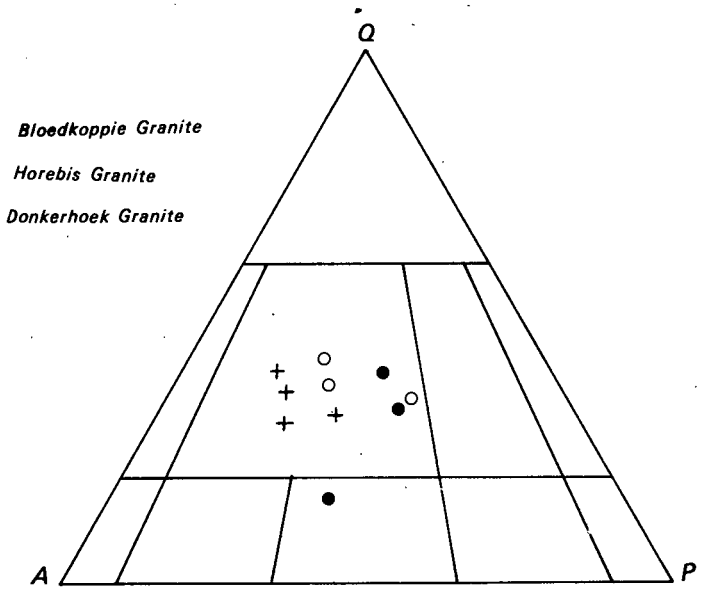

Figure 56. Modal composition of Bloedkoppie, Horebis and Donkerhoek Granites plotted on the classification diagram for plutonic rocks (Streckeisen et al., 1973).

locally be difficult.

The granites consist of quartz, microcline-microperthite, subhedral zoned plagioclase (An_{30-10}) and phyllosilicates. Myrmekitic intergrowths and albite rims around more calcic plagioclase grains are locally developed. Biotite is common in some samples, but absent in others, whereas muscovite is more common than in previously mentioned granites and may form nests up to several centimetres in diameter. Compositionally, most of the rocks are granitic (Table 29, Fig. 56) but syenite, monzonite, quartz syenite and quartz monzonite are all represented in minor amounts.

5.1.8. Donkerhoek Granite (G_6)

The Donkerhoek Granite was intruded post-tectonically into Damara Group metasediments (Faupel, 1973). It is a medium-grained (1-2 mm) to pegmatitic, leucocratic rock with roughly equal amounts of potash- and plagioclase feldspar (Table 29, Fig. 56). Plagioclase forms subhedral grains, often poikilitically enclosed in strongly twinned microcline-microperthite. Its composition is An_{12-15} and albite rims are locally developed. Myrmekitic intergrowths along microcline/plagioclase contacts are common. Minor biotite is present but muscovite is much more common than in other granites.

Accessory amounts of zircon, apatite, garnet and rare sillimanite occur.

5.2. Petrogenesis

It was not possible during the time available for this project to undertake a detailed geochemical study of the granitic rocks and the conclusions below have therefore been drawn mainly from field and microscopic evidence.

The largest masses of granitic rocks found in the region are representatives of the syntectonic, autochthonous and para-autochthonous Red Granite-Gneiss and Salem Granite suites. Smith (1965) favoured an origin for these rocks through "granitisation" processes and, although he did not explain what was meant by the term, he stated that the evidence is "..... generally indicative of granitisation resulting in the production of magmatic rocks on a minor scale" (Smith, 1965, p. 63).

Important features are the virtual confinement of these rocks to certain stratigraphic levels and the superbly conformable contacts on a regional scale. Furthermore, the paucity of regionally crosscutting relationships in this area, as well as in that mapped by Smith (1965), and the differences in character and composition between Gn_1 and Gn_2, also point to the derivation of these granites from different stratified rocks. Most rocks of the Gn_1 and Gn_2 suites occur on the high-temperature side of the "anatexis-in-gneiss" isograd (Fig. 50) so that an origin through anatexis of pre-existing rocks is feasible.

Gevers (1963) has drawn attention to the "Abbabis swell", within the Damara geosyncline, which he describes as a median geanticline with a northeasterly trend in the Karibib region. The rudaceous and arenaceous sediments of the Nosib Group were deposited upon the crest and flanks of this swell whereas away from this positive feature finer-grained sediments were deposited. The main outcrop area of the Red Granite-Gneiss is in the vicinity of the confluence of the Khan and Swakop Rivers (Smith, 1965; this work, Map 1), situated along the southwesterly extension of the Abbabis swell. Smith (1965) has shown that the thickness of the Nosib Group metasediments varies considerably in this region and it is therefore not unlikely that a significant proportion of the Gn_1 is pre-Nosib in age; indeed Smith (1965) has mapped a small outcrop of possible Abbabis gneiss southwest of the Khan Mine.

The author believes that the very strongly gneissic and sheared granitic rocks, such as the augen gneisses in the Gn_1, may be of pre-Nosib age and are possibly correlatives of the Abbabis Formation. The presence of strongly deformed augen gneisses adjacent to Damara metasediments that have not suffered anatexis, 5 km west of the Gawib Granite in the southern part of the region, is suggestive of an early age for these rocks. The Gn_1 in the cores of dome structures in the Khan/Swakop region (see also Smith, 1965) probably represents the pre-Nosib "basement" which was reactivated through anatexis during the Damaran orogeny and are found today as eroded mantled gneiss domes (Eskola, 1949).

Much of the Gn_1 is, however, less strongly foliated and was emplaced during the Damaran orogeny. The Etusis Formation consisted of psammitic, semi-pelitic and pelitic lithotypes, largely derived from weathering of granitic rocks, as shown by the presence of meta-arkoses and feldspar-rich metapsammites, together with volcanic products. During subsequent metamorphism these rocks, together with parts of the underlying Abbabis Formation, probably suffered fairly widespread anatexis with the production of granitic melts. Some of these crystallised more or less *in situ* prior to F_2 and the products are now seen as foliated, red gneissic granites. Fractionation during crystallisation eventually led to residual potash-rich siliceous melts, enriched in volatile constituents. These melts intruded, partly syntectonically but largely post-tectonically, into tensional fractures, or were dammed up against impermeable horizons such as the Damara marbles, and finally crystallised as the Alaskitic Pegmatitic Granite.

The rocks of the Salem Granite Suite are virtually confined to stratigraphic levels above the Chuos Formation. On a regional scale they are conformable but crosscutting relationships are found at the Rote Adlerkuppe dome and east of the Langer Heinrich. On a local scale, the granites are clearly intrusive into the country rocks although gradational contacts are found in migmatitic areas thus suggesting a subtle emplacement.

Petrographic evidence indicates that the non-porphyritic gneissic granite, the porphyritic biotite granite and the leucogranite are members of a single suite. Similar rocks in the Omaruru area, more than 200 km north of the region described here, have been geochemically investigated by Miller (1973), who concluded that the diorite, monzonite and adamellite in that area form part of a single suite, and were produced during *in situ* crystallisation differentiation processes.

Experimental work has shown that partial anatexis of geosynclinal sediments under high-grade metamorphic conditions may result in the production of melts (Tuttle and Bowen, 1958; Winkler and von Platen, 1960, 1961a, 1961b; von Platen, 1965; Winkler, 1967; Brown and Fyfe, 1970; Robertson and Wyllie, 1971 and others). Miller (1973) has suggested that the Salem Granite Suite originated through partial anatexis of Khomas schist.

Evidence from the area under investigation also suggests an origin for the Salem Granites through partial anatexis of Khomas Subgroup rocks, mainly of the Witpoort Formation. This conclusion, as outlined below, is based entirely on field evidence, since the chemical composition of the Witpoort rocks that produced the melts is not known at present. Chemical analyses of Khomas Subgroup schists (Table 22) have been performed on selected samples that contain cordierite and are thus not representative of the schists as a whole. They have compositions akin to shales (Wedepohl, 1969, p. 260) but are relatively enriched in MgO. Most of these samples have been collected close to the base of the Witpoort Formation, the place of the originally overlying rocks now being occupied by the Salem granites. Miller (1973) estimated that 50 per cent of the Khomas schist succession in the Omaruru area is composed of metagreywackes and, accepting this to be correct, the assumption is made, in the following discussion, that the basal pelitic Witpoort rocks were more greywacke-like upwards in their original succession prior to metamorphism and anatexis.

Most of the rocks of the Salem Granite Suite occur on the high-temperature side of the "anatexis-in-gneiss" isograd, the "K-feldspar + sillimanite" isograd and the "K-feldspar + cordierite" isograd (Fig. 50). During progressive metamorphism, melting first began in quartzofeldspathic layers (Winkler and Lindemann, 1972). Some interstitial water was probably present originally and more water was released during various dehydration reactions. Thus melting occurred under saturated conditions and, under the relatively high-temperatures and medium pressures that prevailed, significant quantities of melt were produced. At higher temperatures, some biotite melted incongruently, perhaps to form hornblende (Winkler, 1967), but it is unlikely that temperatures were sufficiently high for considerable melting of biotite; much of it must have remained crystalline.

During anatexis of mica-bearing metamorphites various refractory minerals are produced (Winkler, 1967; von Platen and Höller, 1966). Sillimanite, originally present in the schists and possibly produced during melting, would probably have been eliminated through further reaction with biotite and quartz (Reaction 31, p. 152) and its alumina content incorporated eventually into Ca-rich plagioclase. Small amounts of garnet are found in the Salem rocks and probably represent refractory residues. Cordierite, however, is common in the schists but virtually absent from the Salem suite except for local bodies mentioned before (pp. 142 and 145). The cause of its disappearance is still a problem. Cordierite may, of course, never have been present in the stratigraphically higher levels of the Witpoort Formation, if the chemical composition was that of a greywacke as postulated above; near the base, however, it is very common. All the cordierite-bearing samples of Salem Granite that were examined contain very highly altered cordierite and it is likely that its disappearance is due to hydration reactions which produced components for hornblende and for Mg-enrichment of biotite. The only available analyses of Salem biotites are those given by Miller (1973); they are considerably enriched in Mg relative to those from metapelites in the area under investigation (Table 26).

With increasing temperature and pressure most of the melt was produced at greater depths and this melt then moved upwards although the coarse grain size of the Salem rocks indicates that these melts were probably saturated and therefore did not move very far before crystallising (Cann, 1970; Fyfe, 1970). Granite emplacement occurred before the cessation of folding; this is indicated by the foliated structure of the gneissic granite and part of the porphyritic biotite granite as well as by local pinch-and-swell structures and folding of biotite granite veins. During crystallisation of the main biotite granite, the remaining melt became enriched in potash, silica and volatile constituents, and depleted in Ca and ferromagnesian constituents. Through differentiation, probably by filter-press action, this melt accumulated at higher levels and in lower pressure areas, and eventually crystallised as the leucogranite and associated small pegmatites. This final crystallisation was post-tectonic.

The Bloedkoppie Granite may represent a portion of this "residual" melt which was intruded into the surrounding country rocks. A point in favour of correlating the Salem leucogranite with the Bloedkoppie Granite is their similar levels of radioactivity (p. 166), substantially higher than that of

the Achas, Gawib and Donkerhoek Granites.

The Achas and Gawib Granites are possible derivatives of the magma that produced the Salem Suite and were intruded at a later stage. Their compositions are indicative of generation at greater depths and at higher temperatures (Brown, 1973). The inequigranular textures and deformed crystals are indicative of emplacement as viscous mushes at temperatures not high enough to produce pronounced contact metamorphic effects. Distortion of the regional foliation around the Gawib and Pforte bodies and the dearth of associated pegmatites are also suggestive of a viscous magma. No distortion, however, if found in the country rocks surrounding the Achas stock. This body was emplaced along a zone of weakness represented by the contact between the Nosib and Damara Groups.

Residual melts derived from a variety of magmas (Red Granite-Gneiss, Salem Granite and perhaps melts associated with the Donkerhoek Granite) crystallised post-tectonically under more brittle conditions, to form the Horebis Granite. Post-tectonic crystallisation of the Donkerhoek Granite probably occurred at about the same time. According to Faupel (1973) the Donkerhoek magma formed through anatexis of geosynclinal sediments during metamorphism and it ascended along a northeast-trending thrust fault within the overturned limb of a large syncline.

6. PEGMATITES

Previous studies on pegmatites in the Damara belt include those by Reuning (1923), Gevers and Frommurze (1929), Cameron (1955), Roering (1961, 1966) and Roering and Gevers (1964), most of which dealt mainly with pegmatites north of the area described in this report.

Several thousand of the larger pegmatite bodies have been plotted on the accompanying geological map (Map 1) although many more exist, too numerous and too small to be shown. Inspection of the map reveals their non-uniform distribution although they have not been shown in areas of Red Granite-Gneiss because of difficulties encountered in recognition, both in the field and on aerial photographs. The greatest concentrations exist in the southeastern parts of the area, in the vicinity of the Donkerhoek Granite.

6.1. Classification

A brief and reasonably accurate definition for the pegmatites of this region is that given by Andersen (1931, p. 3): "Pegmatites are mineral associations crystallised *in situ*, decidedly more coarse-grained than similar assemblages in the form of ordinary rocks and differing from these in having a more irregular fabric of the mineral aggregate."

The pegmatites in the area under consideration have crystallised over an extended period of metamorphism and granite emplacement; they have formed through a variety of processes and have different characteristics. It is possible to classify them in terms of age, genesis and/or internal features. At present, however, a chronological classification is unsatisfactory because the relative ages of the various granitic rocks, the source for many of the pegmatites, have not been established beyond doubt. A broad genetic classification can be applied as it is usually possible to distinguish between those pegmatites formed through metamorphic processes and those derived from intrusive melts. Where the pegmatites have suffered metamorphism, however, evidence is sometimes ambiguous. A classification based on internal structural and textural features which could readily be extended should more detailed work require it, is adopted here.

Homogeneous pegmatites

- Bodies with constituents derived from the surrounding rocks
- Bodies with constituents derived from intrusive granites

Inhomogeneous pegmatites

- Zoned pegmatites
- Layered pegmatites

The following grain size classification is used for the pegmatites:

Fine	grain size less than 3 cm
Medium	grain size 3-10 cm
Coarse	grain size 10-30 cm
Very coarse	grain size greater than 30 cm

6.2. Homogeneous Pegmatites

These pegmatites display no form of zoning, either textural or mineralogical, and are thus clearly distinguished from the inhomogeneous varieties.

6.2.1. Bodies with constituents derived from the surrounding rocks

Pegmatites of this category are found only on the high-temperature side of the "anatexis-in-gneiss" isograd and are very common in the metamorphites. They generally form tabular and lenticular bodies lying within the regional foliation and are thinner and more irregular than the inhomogeneous types. Their form and structures have been discussed in the section on migmatites (p. 103). Most have been produced during high-grade regional metamorphism and now occur as migmatitic leucosomes. Ptygmatic and pinch-and-swell structures are characteristic features (Pl. 28). While many of the bodies were generated prior to F_2, some are unaffected by it because metamorphism and migmatisation outlasted this phase of deformation. In general, however, the pegmatitic leucosomes are earlier than and cut by the inhomogeneous varieties. They are also older than many of the granites, such as the mobilised portions of the Red Granite-Gneiss, the Salem Granite and the late- and post-tectonic granites. A distinction between granitic leucosomes and pegmatitic leucosomes is made on grain size; a grain size of 1 cm has been accepted as the division but this is somewhat arbitrary since continuous variations exist. A metasomatic origin for many of the veins is evidenced by the preservation of "ghost stratigraphy" in them.

Although most of these pegmatites exhibit irregular veinlike forms, their shape is controlled by the structures in the host rocks and they show a tendency to accumulate in low-pressure areas, such as the crests of small folds. Small, irregular bodies commonly occur in the necks of boudins of calc-granofels, amphibolite or quartzite. A zone of "basification" can often be observed in the gneisses surrounding the pegmatite and flanking the boudins, thus proving that the constituents of the pegmatite have been derived from the immediately adjacent area. Similar relationships have been described by Ramberg (1956), Reitan (1958, 1959) and many others. The irregular pegmatite veins also show zones of "basification", the melanosomes (Pl. 29) referred to in the description of migmatites. However, several of the larger bodies do not show this feature and it is likely that the pegmatite-forming fluids were removed from their place of origin and transported to lower-pressure areas during deformation prior to crystallisation (Pl. 28). The pegmatites display sharp and/or gradational contacts, in places along opposing contacts (Pl. 29).

The mineralogical composition of the pegmatites can usually be predicted from the composition of the host rocks. This correlation of country-rock mineralogy with that of the pegmatites is peculiar to this category of pegmatite. Quartz, with plagioclase and microcline in widely varying proportions, is the most common assemblage.

The early pegmatites in the Etusis Formation are pink to white in colour and contain more microcline than those in the Damara Group. Pegmatitic mobilisates in the Khan Formation occur as lenticular veins and rounded to

irregular stictolithic segregations. They are granodioritic to granitic in composition, depending on the immediate country rock, and contain small amounts of diopside, hornblende, sphene, epidote, andradite, ilmenite and haematite.

Pegmatitic granite veins in the biotite gneisses, on the northern and western slopes of the Husabberg, have been folded during F_1. s_1 is axial planar to these folded veins, which exhibit metamorphic textures and contain nests of sillimanite.

6.2.2. Bodies with constituents derived from intrusive granites

The Alaskitic Pegmatitic Granites discussed in sections 2.4.7. and 5.1.6. could be classed as members of this group but, since many of the bodies exhibit granitic rather than pegmatitic textures, they have been discussed separately.

The homogeneous pegmatites in this category have similar origins and trends to the zoned and layered pegmatites but tend to be smaller and probably represent only a single zone (or layer) of the latter at the level of exposure. Many of the zoned pegmatites contain well developed wall zones and the homogeneous pegmatites are those that consist entirely of wall-zone material.

Homogeneous, dyke-like pegmatites are common in the Witpoort Formation, east of the Witpoortberge - Husabberg - Pforteberg range, where they are associated with layered varieties. They display pinch-and-swell structures and are usually concordantly emplaced along s_1-surfaces, although crosscutting relationships are also observed. Texturally, they are fine- to medium-grained and consist of quartz, microcline-perthite, plagioclase, biotite, apatite, garnet, schorl and minor muscovite. In places, small amounts of cordierite and sillimanite are found. The cordierite occurs as clots and may be of xenolithic origin. Biotite schlieren and xenoliths of country rocks are found and at one locality a xenolith of folded nebulitic Salem gneiss is preserved within a dyke-like pegmatite.

Thin boudinaged homogeneous pegmatites, of pre-layered pegmatite age (Pl. 30), occur in the vicinity of the Donkerhoek Granite. They are generally less than 1 m thick, contain muscovite in addition to quartz, plagioclase and perthite and are preferentially oriented parallel to s_{01}.

6.3. Inhomogeneous Pegmatites

6.3.1. Zoned Pegmatites

The zoned pegmatites are the most common of those shown in Map 1. They are found in the Red Granite-Gneiss, west of the Husabberg, as crosscutting dyke-like and irregular bodies and in many places their trend is similar to that of the G_4 granite. Some bodies are concentrated below overlying marble bands which have acted as structural traps (see also Smith, 1965) along the northern and western slopes of the Husabberg. Large numbers of reddish-

coloured, zoned pegmatites occur in the Etusis Formation at the Rote Adlerkuppe dome and on both sides of the Swakop River, between Witpoort and the Nabas River. Both the Salem anticline and the Rooikuiseb anticlinorium contain many such bodies. Along the southeastern margin of the area, zoned pegmatites occur but are subordinate in number to layered bodies.

The pegmatites exhibit a great variation in size and shape but tabular bodies are by far the most common. Their maximum length is more than 1 km and width about 50 m but most are considerably smaller, being only several tens of metres long and less than 5 m wide.

There is a considerable variation in trends and dips, although a large proportion run northwest to west-northwest, approximately at 90° to the structural grain of the area, i.e. at right angles to the F_2 trends. However, in strongly-foliated schists west of the Rote Adlerkuppe and very close to the Donkerhoek Granite the pegmatites lie in the foliation.

With respect to the age of the zoned pegmatites, the following generalisations are applicable to most bodies. They post-date the migmatitic, homogeneous pegmatites and the G_4 veins situated along the axial planes of B_2 folds. They are younger than associated aplite veins and occasionally occupy fault planes which have displaced such aplites. Boudinage effects and pinch-and-swell structures are generally absent. Although the pegmatites have been affected by the north- and north-northwest-trending faults they are generally younger than all other structures and are thus post-tectonic with respect to F_2. The zoned pegmatites, although similar in appearance, have originated from different granites of various ages, and thus differ in age. This is also revealed by northerly trending bodies cutting those trending northwest and west-northwest.

The pegmatites occupy faults and joints and normally have sharp contacts, with matching features along the side-walls, indicating that they have been emplaced in dilation structures. Their emplacement has had very little effect on the country rocks; most commonly the Salem Granite is reddened for several centimetres. Where marble bands are cut at the Husabberg and Arysap Hills syncline, thin skarn zones containing diopside, scapolite and wollastonite are developed. The mineralogy of the pegmatites is not clearly related to that of the country rocks but biotite is more abundant in those emplaced into schists and Salem Granite; sphene, hornblende and epidote are present in several pegmatites in the Tinkas Formation. The pegmatites are pink to red in colour where they cut the Etusis Formation and the Salem Granite, due to finely disseminated haematite in the perthite; they are white when emplaced into metapelites, as in the Arysap Hills syncline. Small xenoliths of country rock are not uncommon near contacts; in some pegmatites these have obviously been derived from underlying lithotypes. For example, on the western slopes of the Husabberg, pegmatites situated in the Husab marbles contain xenoliths of biotite schist and calc-granofels from the immediately underlying metasediments.

Cameron et al. (1949) summarised earlier work on pegmatites and suggested that granitic pegmatites have certain textural and mineralogical patterns of zoning which are of wide application. They subdivided the material of pegmatites into zones, fracture fillings and replacement bodies

and suggested a further subdivision into border, wall, intermediate and core zones. They concluded that a very large number of pegmatites not only have similar zonal structures, but also show similar sequences of assemblages of essential minerals from the contacts inwards. They recognised a general sequence of 11 dominant-mineral assemblages, which would rarely be encountered together in any one body, but parts of which would be illustrated by most bodies. The zonal structures and the sequence have been found to be applicable to a large number of pegmatite districts (Jahns, 1955) including southern Africa (von Backström, 1964; Hugo, 1970; Roering, 1966).

The many pegmatites that have been studied in detail by the author reveal a general pattern of zoning which, in certain respects, is very similar to that of Cameron et al. (1949). For the most part, they are "simple pegmatites" insofar as they consist of relatively few zones (2 to 5) and lithium mineralisation, characteristic of complex pegmatites, is absent from all but one of those studied.

Border zones (fine-grained chill zones according to some interpretations) are generally absent from the pegmatites although discontinuous aplitic selvedges are sometimes found. Fine- to medium-grained wall zones are usually well developed and make up an important part of the pegmatites. Medium- to coarse-grained intermediate zones are absent in many pegmatites but present in others. Where present, there is usually only one intermediate zone and only rarely more than two.

An investigation of the zoned pegmatites has revealed the following sequence. Locally the border and wall zones consist of quartz-plagioclase-muscovite and plagioclase-quartz. The wall zones generally consist of quartz-plagioclase-perthite ± muscovite ± biotite. The plagioclase is zoned (An_{20} to An_5) and graphic intergrowths of quartz and perthite exist. In pegmatites where plagioclase is not present the wall zones comprise quartz-perthite-muscovite or quartz-perthite-biotite. Accessory amounts of schorl, magnetite, garnet, apatite and zircon are common; rare sillimanite is encountered mainly along minor shear planes.

Intermediate zones generally contain less plagioclase and consist of perthite-quartz-muscovite or, less commonly, perthite-quartz-biotite. At many localities, phyllosilicates are absent and the common assemblage is perthite-quartz, in which graphic textures may be conspicuous. Where more than one intermediate zone is present the perthite-quartz assemblage occurs on the core side of the perthite-quartz-muscovite ± biotite zone. Beryl and tourmaline are found in the intermediate zones but in only one pegmatite was lithium mineralisation encountered, in the form of lepidolite, accompanied by cleavelandite.

Many of the pegmatites have cores of massive quartz, usually milky, but in places rose-coloured. These are generally situated near the centres of the bodies but in gently dipping bodies they are offset towards the hanging-wall side. Several pegmatites exhibit interrupted cores along their length and a few contain several cores which are not necessarily found at the same structural position. In those pegmatites not showing quartz cores, the core contains a quartz-perthite intergrowth which is often graphic. In others, the core is not exposed at the level of exposure.

Table 30. Mineral assemblages of pegmatites in the Karibib and Khan-Swakop areas which correspond to those reported by Cameron et al. (1949).

Cameron et al. (1949)	Roering (1966)	This study
1. Plagioclase-quartz-muscovite	✓	✓
2. Plagioclase-quartz		✓
3. Quartz-perthite-plagioclase ± muscovite ± biotite	✓	✓
4. Perthite-quartz	✓	✓
5. Perthite-quartz-amblygonite -spodumene		
6. Plagioclase-quartz-spodumene		
7. Quartz-spodumene		
8. Lepidolite-plagioclase-quartz	✓	
9. Quartz-microcline		
10. Microcline-plagioclase-lithia micas-quartz	✓	
11. Quartz	✓	✓

The mineral assemblages in pegmatites from the Karibib (Roering, 1966) and Khan-Swakop areas which match those of Cameron et al. (1949) are shown in Table 30. In general, the correlation is good. The main difference in this region seems to be the presence of the assemblage quartz-perthite ±muscovite±biotite (i.e., without plagioclase) which is not represented in the sequence of Cameron et al. (op. cit.). The general sequence for the zoned pegmatites in the study area is a decrease in the amount of plagioclase and mica from the walls inwards, accompanied by an increase in the amount of perthite and, finally, quartz.

The mineralogy of the zoned pegmatites has not been studied in detail but the following minerals have been identified, in addition to the essential rock-forming minerals: cleavelandite, muscovite, biotite, lepidolite, apatite, zircon, schorl, dravite, chrysoberyl, beryl, magnetite, ilmenite, haematite, pyralspite garnet, davidite, allanite, euxenite, sillimanite, epidote, hornblende, sphene, fluorite, amazonite, cassiterite, rutile and calcite.

Although the zonal pattern can usually be recognised, all gradations into homogeneous bodies on the one hand and layered bodies on the other can be found. A commonly encountered variety consists of large wedge-shaped perthite crystals (megacrysts) up to 50 cm in length, orientated at right angles to the walls and set in a fine-grained matrix (<2 cm) of plagioclase-quartz-muscovite ±biotite±perthite. Such bodies are not zoned but the term homogeneous gives a misleading impression of their textures.

Some of the pegmatitic bodies associated with the Horebis Granite along the Swakop River are more difficult to categorise. Irregular pods of pegmatitic material occur within branching veins illustrating agmatic structures. In some cases the pegmatitic material is concentrated in the central portions of the veins, in others it is offset to one side and in yet others the veins are composite and consist of granitic or aplitic central parts with pegmatitic borders. Similar features can be found at the Rote Adlerkuppe, along Skeleton Gorge, where boudinaged lenses of Salem Granite have pegmatitic margins.

Replacement bodies are not easily recognised and, where present, generally occupy positions between the wall zone and core. They are small in size, volumetrically unimportant and consist of irregular pods of sugary albite and sericitic greisen. Beryl and tourmaline may be present. Late-stage replacement bodies are associated with fluorite mineralisation.

Fracture fillings are always narrow, less than 10 cm across, and normally trend at high angles to the strike of the pegmatites. Most commonly they consist of quartz and tourmaline or muscovite and occasionally of cleavelandite. The fracture fillings generally terminate against the contacts but some continue for short distances into the country rocks.

6.3.2. Layered Pegmatites

The layered pegmatites are inhomogeneous bodies which consist of alternating bands of pegmatitic and aplitic material (Pl. 31). The aplitic layers themselves contain thin layers of ferromagnesian minerals. The layering is not symmetrical about the centres of the bodies. Very similar pegmatites have been described by Jahns and Tuttle (1963), as "layered pegmatite-aplite intrusions", and by Redden (1963) and Windley and Bridgwater (1965).

Layered pegmatites are confined to two regions in the area under investigation:

(i) Witpoort Formation, east of the Witpoortberge - Husabberg - Pforteberge range, west of the main outcrop area of the Salem Granite.

(ii) Tinkas Formation, between the eastern boundary of the area and the Schieferberge, northwest of the outcrop area of the Donkerhoek Granite.

In the area west of the Salem Granite the pegmatites are concordantly emplaced into the Witpoort Formation and follow a well-defined north-northeasterly to northeasterly trend. Some do not conform in detail with the foliation (s_1) but cut across it at varying angles. In general, however, s_1 conforms to the contacts of the pegmatites and follows the pinch-and-swell structures, which are a common feature of these bodies. Several pegmatites have been folded during F_2 while others were not affected. Their emplacement probably began in pre-F_2 times and continued until after the cessation of this phase. These pegmatites are earlier in age than the post-tectonic bodies in the east and southeast.

The layered pegmatites in the west reach up to 1 km in length and 20 m in width but are usually smaller. Small xenoliths of country rock and biotite schlieren are common. The layering in these pegmatites is not as well developed as in the east and gradations into homogeneous or zoned pegmatites were observed. The layered pegmatites are not found in the immediately adjacent Salem Suite, which is intruded instead by much smaller, zoned pegmatites.

In the east and southeast a vast number of layered pegmatites was found to be genetically related to the Donkerhoek Granite. According to Faupel (1973), who has studied the Donkerhoek Granite to the east and southeast of this area, the pegmatites constitute 30 per cent of the rock volume in places. Near the granite intrusions, the pegmatites are disposed concentrically about the plutons and are more or less concordantly emplaced along s_1-surfaces. They are too numerous to be shown individually but their general northeasterly trend is indicated on the accompanying geological map. Farther to the northwest, away from the granite, the trend of pegmatites in the Tinkas Formation changes rapidly to one approximately at right angles to the structural grain, i.e. across the F_2 trend. The pegmatites dip at various angles to the southwest. Relatively few layered pegmatites are found in the Etusis Formation, although they are common in the Achas Granite, where they are preferentially oriented east-west.

The form of the layered pegmatites is normally tabular but larger bodies are plugs rather than dykes or sheets. The largest body in the mapped area measures approximately 4 km x 1 km but this is exceptional. Away from the Donkerhoek Granite the size of layered bodies decreases.

The layered pegmatites in the east cut across all fold structures (Pl. 32) and are post-F_4 in age (Faupel, 1973). Contacts are usually very sharp and indicative of subtle intrusion (Pl. 32). They are faulted by later north-trending faults. No baking effects are observed in the country rocks although xenoliths in some of the larger plugs have suffered contact metamorphism, as shown by formation of wollastonite and grossularite in calc-granofels xenoliths.

The layered bodies are characterised by pegmatite-aplite layering, parallel to the walls of the intrusions. This is their most conspicuous feature and can readily be observed from a distance. The aplites themselves are internally layered, due to concentrations of tourmaline, garnet and muscovite.

A variety of internal features is displayed and gradations into zoned and homogeneous types exist. The previously mentioned porphyritic variety (p. 159), comprising perthite megacrysts in a fine grained matrix, also occurs near the Donkerhoek Granite. Pegmatites with shallow dips may be layered near the base but zoned in the upper portions, as described by Jahns and Burnham (1963).

The thickness of the pegmatitic layers is normally 5 cm to 1 m but may reach several metres, and the grain size ranges between 10 and 100 cm. The most common minerals are perthite, quartz (usually in graphic intergrowth with perthite) and plagioclase. Those pegmatites associated with the

Donkerhoek Granite contain a considerable amount of muscovite, in places having a radiating, almost "feathery" appearance. The pegmatites west of the Salem Granite, however, contain mostly biotite, although minor muscovite is also found in them. The long axes of larger perthite crystals lie normal to the layering and some project into the aplite layers, either preserving the fine layering as ghost structures or causing the aplite layering to curve or loop around the terminations of the megacrysts. Minor and accessory amounts of schorl, garnet, beryl and andalusite are found in the pegmatitic layers.

The aplitic layers are less than 1 m thick, usually varying between 5 and 50 cm, and may be internally homogeneous or segregated into thinner alternating dark and light layers. The dark layers consist of schorl or garnet and occasionally of fine-grained muscovite. Each dark layer is uniform in thickness at about 2 mm but some are 10 mm thick. The very small crystals of garnet and tourmaline are euhedral, the long axes of the tourmaline crystals being oriented perpendicular to the layers. Redden (1963) has applied the term "line rock" to aplite units displaying similar internal layering. The aplitic layers consist very largely of albite (An_{0-10}) and quartz with only small amounts of perthite.

Later fracture-filling veins are not uncommon; they consist of quartz-schorl, quartz-muscovite or cleavelandite.

6.4. Origin

The pegmatitic mobilisates of the migmatitic metamorphites are of syntectonic age with respect to F_2 and display the characteristic features of leucosomes. Many have remained at their place of origin while others have moved to lower-pressure regions and crystallised there. Their mineralogy and the fact that they antedate the intrusive granites indicate that they originated within their immediate surroundings. The preservation of ghost structures in some bodies is evidence for a replacement origin. These pegmatites are of metamorphic origin and would be classed as metamorphic-metasomatic in Ramberg's (1956) terminology. His ideas, or those of Gresens (1967a, 1967b), may be applicable to such bodies but, since they are found on the high-temperature side of the "anatexis-in-gneiss" isograd, an anatectic origin is more likely.

Zoned pegmatites have been interpreted as products of *in situ* metamorphic-metasomatic processes by Ramberg (1956) and Gresens (1967a, 1967b) but this origin is not accepted for the zoned pegmatites in the Khan-Swakop area, for the following reasons. They generally have sharp contacts against the country rocks, occupy dilation features and were emplaced after the peak of metamorphism (muscovite + quartz is a common assemblage in them throughout the area, but is not a stable assemblage in metamorphites west of the Rooikuiseb anticlinorium). Furthermore, their mineralogy is uniform and not necessarily related to that of the country rocks; for example, pegmatites in banded gneisses, marbles, quartzites and amphibolites have similar composition to those in schists and granites. Their distribution relative to igneous intrusives, and the similarity in zonal arrangement to granitic pegmatites of

igneous origin (Cameron et al., 1949) are indicative of a magmatic origin.

Jahns and Burnham (1957, 1961, 1969) have formulated a model for the derivation and crystallisation of granitic pegmatites and two particularly important conclusions may be drawn from their study. The first is that a large variety of structural and textural relationships can be explained in terms of the stage that the pegmatite melt is drawn off from a crystallising granitic magma. The second is that for true pegmatites (i.e. those exhibiting coarse crystal growth) to form, a separation of aqueous fluid (probably supercritical) and melt must occur. This separation can have a profound effect on the textures of the pegmatites, depending on the scale and degree to which it takes place.

In the region under investigation, brittle deformation prevailed after the peak of metamorphism and tension fractures developed more or less across the structural grain during the final stages of movement. Pegmatite-forming melt, rich in volatiles, was emplaced into these openings and subsequent crystallisation proceeded under more or less closed-system conditions. Early loss of volatiles along the contacts resulted in rapid crystallisation of what are now found as border zones.

Continued crystallisation produced the fine-grained wall zones until the melt was saturated with H_2O (together with other mineralisers). Second boiling (Jahns and Burnham, 1957, 1961, 1969; Krauskopf, 1967) then occurred. The effect of this was to provide space for crystal growth and to facilitate the supply of material to allow the crystals to grow to large size. At this point there is a change from fine- to medium- and coarse-grained textures. With progressive crystallisation, relatively greater amounts of perthite and quartz precipitated, culminating in formation of the quartz core. The problem of late formation of quartz cores in pegmatites is beyond the scope of this study but is one which has not yet been satisfactorily solved.

The magma which eventually crystallised as the Horebis Granite was probably emplaced in a slightly water-undersaturated condition. Saturation and resultant resurgent boiling at a late stage produced the pegmatitic pods and streaks so commonly encountered. In those pegmatites having medium- to coarse-grained wall zones, the pegmatitic melt was probably water-saturated at the time of emplacement, after having been drawn off from a granitic melt at a late stage (Jahns and Burnham, 1969).

The layered pegmatites are likewise of igneous origin and exhibit a spatial relationship with the Donkerhoek Granite. The layering is not due to crystal settling processes since both vertical and gently dipping pegmatites are layered parallel to their walls with the long dimensions of schorl crystals oriented perpendicular to this. The different relationship between perthite crystals and the aplitic layers noted above (p. 162) suggests that they formed at approximately the same time but were influenced by local variations in the rate of growth.

The fine laminations in the aplite layers are indicative of rhythmic primary *in situ* crystallisation. The author is in agreement with Jahns and Tuttle (1963, p. 87) that the fine laminations of garnet, schorl and muscovite "may well have resulted from alternating periods of undersaturation and supersaturation with respect to these minerals, perhaps in response only to

University of Cape Town

a very slowly dropping temperature gradient, but perhaps also in response to slight fluctuations in confining pressure on a magma saturated with volatile constituents".

Any theory for the origin of the aplite-pegmatite layering should take account of the contrasting compositions of the pegmatite (K-rich) and aplite (Na-rich) layers. Special conditions, not realised in the zoned pegmatites, must have pertained during their formation. Several hypotheses have been put forward; San Miguel (1969) postulated that sheared and crushed granite recrystallised to aplite which was then later metasomatically altered to pegmatite. There is no evidence for such an origin in the layered pegmatites of the study area. Redden (1963) proposed that the alternation of fine and coarse layers is caused by periodic loss of volatiles from the system but it is difficult to envisage why this should occur more or less rhythmically. Furthermore, obvious evidence of the expected metasomatic activity in the immediate country rocks is usually missing.

A further theory involves segregation of major alkalies which can occur to a significant degree if a pegmatitic magma becomes saturated with volatile constituents such that both melt and vapour are present. Experiments show that potassium is extracted from the melt and partitions into the vapour phase, thus leaving the melt relatively enriched in sodium (Jahns and Tuttle, 1963; Jahns and Burnham, 1969). If the composition of the magma corresponded to that of the thermal minimum at the existing confining pressure, preferential transfer of K-feldspar components into the aqueous fluid to form potash minerals would promote crystallisation of albite-rich rock from the melt, perhaps as aplite. (Jahns and Tuttle, 1963; Jahns and Burnham, 1969). The reason for rhythmic repetition of the pegmatite and aplite layers is, however, not clear but may be related to the composition of the melt being very close to the thermal minimum at the existing confining pressure.

The origin of the pegmatite magmas, which crystallised to form the zoned and layered bodies, can be sought in the various granites of the region. The Salem Granite has provided material for those along its western contact and within its outcrop area but a lack of complete separation of a pegmatitic residue from the main magma has resulted in the coarse-grained character of the suite rather than many large pegmatites.

The pegmatites west of the Husabberg were probably derived from residual anatectic melts which remained mobile after formation of the Red Granite-Gneiss; in some cases the Alaskitic Pegmatitic Granite was formed, in others, zoned pegmatites.

Very little pegmatitic activity is associated with the Achas and Gawib Granites and only small internal pegmatites are related to the Bloedkoppie Granite. The bulk of the pegmatite melts was derived from the post-tectonic Horebis and Donkerhoek Granites. Small bodies of post-tectonic granite are common in the area and large volumes are found to the north and east (Smith, 1965). Roering (1966) concluded that the zoned pegmatites around Karibib have their origin in the late to post-tectonic granites.

7. CONCLUSIONS

A noteworthy feature of the eugeosynclinal (Martin, 1965) part of the northeast-trending Damara belt is the existence of a median ge-anticline, the Abbabis swell (Gevers, 1963), which coincides approximately with the area of maximum metamorphic grade. The ridge, marked by the presence of rocks of the Abbabis Formation, exerted a strong influence on sedimentation in the Khan/Swakop area and was present from early times as a positive feature.

The Etusis sediments were deposited in a shallow-water, non-marine, high-energy environment as shown by the prevalence of conglomerates and crossbedding. The bulk of the sediments consist of granitic detritus and comprised feldspathic sandstones and arkoses. Their variable thickness is due partly to topographic relief but probably mainly to variable rates of subsidence. Away from the Abbabis swell, towards the southeast, finer-grained sediments were deposited and, locally, there is evidence that silicic-volcanic activity occurred. In the western parts of the area, sandstone deposition was followed by deposition of calcareous semipelites alternating with thin layers of impure siliceous carbonate. This assemblage was eventually metamorphosed to form the banded gneisses of the Khan Formation.

Shallow-water conditions continued to prevail during deposition of the sediments of the Rössing Formation, which is characterised by rapid changes of lithology, both vertically and laterally. The extreme lithological variations are indicative of sedimentation along a mixed clastic : carbonate shoreline (Selley, 1970) encompassing fluviatile coastal plain, tidal flat and lagoonal environments. Erosion took place during an ensuing hiatus, and thereafter glacial conditions prevailed, during which the glacial-marine Chuos diamictite was deposited with transgressive overlap on a variety of older rocks.

This was followed, in the west, by carbonate shelf sedimentation (Husab Formation). Algal growths may have existed at this time but subsequent deformation and metamorphism have destroyed any such original structures and textures. Further to the southeast, beyond the area of the Rote Adlerkuppe, sedimentation occurred under quiet conditions below wave base where fine grained shales and impure limestones of the Tinkas Formation were deposited. Yet further to the southeast, in the vicinity of the Khomas Hochland, pelitic and semipelitic sediments were laid down while in the west, the pelitic sediments of the Witpoort Formation followed on the carbonates of the underlying Husab Formation.

It is not known from existing evidence what period of time elapsed before orogenic movements and accompanying metamorphism were initiated. Early flexural-slip folding during F_1 produced a regional bedding foliation, which was folded together with the bedding to form isoclinal structures. Although the original trend of B_1 folds is uncertain, it is possible that it was northeast-southwest and similar to that of superimposed B_2 folds. The B_2 folds have steep axial planes and are slightly overturned to the southeast. Axial plunges became pronounced during F_2 and elongated brachyanticlines and dome structures were initiated. Towards the end of this phase minor B_3 folds were locally superimposed on earlier structures in the southeast. Axial planes of B_4 folds strike north-northeast to northwest and the F_4 folding

appears to have played an active part in the formation of some of the dome structures. Whether the F_4 phase is related to deformation in the north-northwest-trending "coastal branch" of the Damara belt is, at this stage, an open question which awaits detailed structural work farther to the west and northwest.

The earliest metamorphic episode in the Khan/Swakop area affected the rocks of the Abbabis Formation prior to deposition of the Nosib Group (Smith, 1965, p. 10). No evidence was found to support Guj's postulate (for the Sesfontein area) of a post-Nosib/pre-Damara tectonothermal event (Guj, 1970) since the Nosib and Damara Groups in the area under study have been deformed and metamorphosed to the same degree. Nash (1971) concluded that two high-grade metamorphic pulses had affected the Nosib and Damara rocks in the SJ area. No evidence confirming this conclusion was found during the present study and the mineral assemblages and textural relationships are indicative rather of a single prolonged period of metamorphism.

The main pulse of the Damaran orogenic episode occurred during the period 500-550 Ma ago (Clifford, 1967). Although most age determinations in the central Damara belt fall between 450 and 550 Ma (Smith, 1965; Burger et al., 1965; Burger and Coertze, 1973), there are exceptions. Rb-Sr determinations on lepidolites from post-tectonic pegmatites in the Karibib area yield ages varying between 600 and 850 Ma (Burger and Coertze, 1973) but these are clearly unreliable. Furthermore, Burger et al. (1965) reported an age of 600±20 Ma for sphene from the Khan Mine pegmatite and Clifford (1967) related this to the Katangan orogenic episode (580-680 Ma). The calculated ages for this specimen, however, vary between 460 and 660 Ma. The accepted age of 600 Ma is thus open to question and need not contradict the present findings of a single post-Nosib/Damara metamorphic episode in this part of the Damara Orogen.

The F_1 and F_2 deformations were accompanied by high-grade regional metamorphism which reached its peak after the cessation of F_2, but prior to F_4. The area is situated to the southeast of, but close to, the area of highest metamorphic grade and mineral assemblages are compatible with those of the amphibolite facies (Turner, 1968). The metamorphic grade increases from the southeastern margin, where the rocks have been subjected to medium-stage regional metamorphism, towards the west and northwest, where high-stage conditions were attained. With increasing grade of metamorphism staurolite and andalusite disappeared from metapelites, partial anatexis and migmatisation became widespread, sillimanite and K-feldspar formed from the reaction of muscovite and quartz; biotite, sillimanite and quartz reacted to form K-feldspar and cordierite (± almandine).

In addition to the controls exerted by temperature, total pressure and whole-rock composition on the mineral assemblages developed, other controls existed. In siliceous carbonate rocks the composition of the fluid phase (X_{CO2}) determined the stabilities of wollastonite, grossularite and epidote-group minerals. Oxygen fugacity varied between different lithological layers and controlled the stability of almandine, grossularite-andradite and epidote. Over most of the area P_{H2O} was equal to P_T in metapelites but where P_{H2O} was less than P_T dehydration-reaction temperatures were lowered.

A consideration of mineral assemblages, metamorphic reactions and experimentally derived phase equilibria has allowed estimates of metamorphic temperatures and pressures to be made. The evidence of the co-existence of andalusite and sillimanite, cordierite and staurolite, and cordierite and garnet together with the final disappearance of staurolite just short of the anatexis boundary, and the breakdown of muscovite + quartz beyond the same boundary, indicate that pressures were between 4 and 5 kb and depths between 14 and 17 km. Metamorphic temperatures are estimated to have attained 650° C in the southeast and approximately 750° C in the west. This is indicative of a geothermal gradient of 40-50° C per km and of metamorphic conditions transitional between low-pressure (Abukuma) and medium-pressure (Barrovian) "baric types" (Miyashiro, 1973).

During the high-grade regional metamorphism, reactivation of the pre-Nosib basement and anatexis of Nosib Group metamorphites produced melts of granitic composition parts of which crystallised more or less *in situ* before the cessation of folding. Final crystallisation of uraniferous Alaskitic Pegmatitic Granite outlasted deformation.

During the period of high-grade regional metamorphism, rocks of the Khomas Subgroup were subjected to partial anatexis. It is probably significant that all outcrops of the Salem Granite Suite occur on the high-temperature side of the "anatexis-in-gneiss" boundary; judging from the composition of these granites, relatively high temperatures would have been necessary to have formed the anatectic melts from which the granites eventually crystallised (Wyllie, 1971; Winkler, 1967). The rather calcic nature of the plagioclase, the relatively high ferromagnesian mineral content and the fact that the Khomas Subgroup rocks contain significant quantities of calc-silicates indicate that much of the melt was generated only at greater depths where temperatures were higher. Derivation of the melts from Khomas Subgroup rocks and subtle, passive emplacement resulted in the virtual confinement of these granites to the stratigraphic level of the Khomas Subgroup. Crystallisation differentiation and filter-press action displaced the remaining melts to higher levels where they crystallised as the leucogranite and, perhaps, Bloedkoppie Granite. Crystallisation of the Salem granites occurred over an extended period of time and outlasted the F_2 deformation. The late- to post-tectonic Achas, Gawib and Donkerhoek plutons were emplaced while the country rocks were still hot and have deformed earlier structures so as to cause them to wrap around the intrusive bodies at outcrop. Residual melts intruded the country rocks along zones of weakness and crystallised as zoned and layered pegmatites.

The origin of Pan-African-type orogenic belts has been ascribed to *in situ* large-scale upwelling and remobilisation of sialic material along zones of weakness within cratonic blocks (Clifford, 1968; Shackleton, 1969, 1973) and to continental collision following plate movements and subduction of oceanic crust (Burke and Dewey, 1970, 1973). Reasons for regarding these orogenic belts as more or less *in situ* zones of weakness include the matching of cratonic fabrics across the younger mobile belts, the apparent continued activity over great periods of time, the partial and in some cases complete encircling of cratons by mobile belts of approximately the same age, the high geothermal gradients and the relict and reactivated masses of basement (Shackleton, 1969, 1973; Hurley, 1972).

The northeastern arm of the Damara belt appears to be of ensialic character since pre-Nosib "basement" rocks in the form of the Abbabis Formation occur in the central parts. Furthermore, there is a lack of evidence for mafic vulcanicity which would be expected in an ensimatic, or ocean floor, environment. Martin (1965) has referred to the prominent amphibolite belt (Friedenau or Matchless belt) in the Khomas Subgroup as representing mafic and ultramafic volcanics but this remains speculative at present as no detailed work has as yet been done on these rocks. Ophiolite assemblages, characteristic of ocean floor environments (Coleman, 1971; Dewey and Bird, 1971; Dickinson, 1971) have not yet been reported from the Damara belt. The evidence of high T/P metamorphism in the central part of the belt does not necessarily favour the *in situ* orogenic belt theory, because such metamorphism has been shown to occur above the central parts of Benioff zones (Miyashiro, 1973). However, evidence for high pressure metamorphism in the Damara belt has yet to be found and this would be an essential feature for the acceptance of a plate tectonic model, whether it be cordilleran-, island arc- or collision-type (Dewey and Bird, 1970).

If a plate tectonic model were to be applied to the northeastern branch of the Damara belt the orogeny would be of the collision-type (Dewey and Bird, 1970; Burke and Dewey, 1973). The necessary geosuture, along which two continental masses collided, would probably have to be sought in the Matchless (Friedenau) amphibolites (Hartnady, 1974) or along the zone where the Donkerhoek Granite batholithic masses are now found. A northward-dipping subduction zone would be necessary to explain the high T/P metamorphism in the central granite zone. In such a model the Abbabis rocks and mantled gneiss (Gn_1) domes would consitute the reactivated basement similar to the reactivated Dahomeyan gneisses of west Africa as postulated by Burke and Dewey (1973, p. 1043).

The available published evidence for the Damara belt is more in favour of an ensialic, *in situ*, orogeny rather than a collision-type orogeny but there are large gaps in our knowledge and much information remains to be accumulated. In the present stage of knowledge it is appropriate to conclude with the words of Hurley (1972, p. 313) "It is clear that almost all of the characteristics of the Pan-African belts can be explained by both hypotheses, and that the conclusion must await secure evidence from a matching of pre-existing features between cratons, or from acceptable paleomagnetic data".

University of Pretoria

APPENDIX

Microprobe Analytical Procedure

Cordierite, biotite, pyroxene and garnet were analysed on a Cambridge Microscan 5 electron probe micro-analyser in the Department of Geochemistry, University of Cape Town, under the guidance of Mr. J.P. Willis. A variety of natural silicate mineral standards was used. The standards were natural silicate minerals, obtained from the Smithsonian Institution, currently used in the Department of Geochemistry and known to give satisfactory results. The raw data were corrected and reduced using ABFAN, a computer programme written by Boyd et al. (1968).

K_α lines were measured at 15 KV with a total beam current of 0,15 x 10^{-6} amps. For Si, Al, Mg and Na a RbAP analysing crystal was used, and for Ti, Fe, Mn, Ca and K, a quartz crystal.

Whole-rock Chemical Analysis

Complete major-element analyses of 18 samples, and partial chemical analyses of 12 samples were performed by X-ray fluorescence methods by the National Institute for Metallurgy. TiO_2 (Rigg and Wagenbauer, 1961), MnO (Maxwell, 1968), CaO (Bennett and Hawley, 1965) and P_2O_5 (Shapiro and Brannock, 1962) were determined by the writer on 5 samples by rapid colourimetric techniques. Other oxides were determined as follows: FeO - titrimetrically against $K_2 Cr_2 O_7$ (Maxwell, 1968); K_2O and Na_2O - flame photometer (Maxwell, 1968); H_2O^+ and H_2O^- - gravimetrically (Maxwell, 1968).

Determinative Mineralogy

Unknown minerals were identified from X-ray diffraction traces with the help of ASTM Data Cards. Unit-cells were determined with a 57.3 mm diameter Philips X-ray camera. Refractive indices were measured in Na-light and are correct to ± 0,002. The composition of plagioclase was determined on a universal stage by the Federov method and from the extinction angle of albite twin lamellae in sections perpendicular to the intersection of the (010) and (001) cleavages. Curves given by Tröger (1971, Part 1) have been used. Wenk and Keller (1969) discussed the measurement of zoned plagioclase grains and recommended investigation of the broad zone between the core and the rim, or the rim itself. Measurement of the broad zone between the core and rim is safer but the latter is more sensitive to the maximum temperature attained during metamorphic crystallisation. The An-content of plagioclase rims was determined in samples of amphibolites, whereas the zone between the core and rim was investigated in the granitic rocks. 2V angles were determined conoscopically on a 4-axis universal stage. Corrections for refractive index differences and angles of tilt were made from charts supplied by Muir (1967). Modal compositions were determined on samples of schists and granites: Fine-grained rocks were measured in thin section with a Swift automatic point

University of Cape Town

counter whereas coarser-grained rocks were measured on large polished and stained slabs under a binocular microscope. Point spacings were similar to the average grain size of the rocks and 2000 counts per sample were found to be adequate.

REFERENCES

ALBEE, A.L. (1965) Distribution of Fe, Mg and Mn between garnet and biotite in natural mineral assemblages. *Jour. Geol.*, 73, 155-164.

ALTHAUS, E. (1967) The triple point andalusite - sillimanite - kyanite. *Contrib. Mineral. Petrol.*, 16, 29-44.

_____, KAROTKE, E., NITSCH, K.H. & WINKLER, H.G.F. (1970) An experimental re-examination of the upper stability limit of muscovite plus quartz. *Neues Jahrb. Mineral. Monatsh.*, 1970, 325-336.

ANDERSEN, O. (1931) Discussions of certain phases of the genesis of pegmatites. *Norsk Geol. Tidsskr.*, 12, 1-56.

ATHERTON, M.P. (1968) The variation in garnet, biotite and chlorite composition in medium-grade pelitic rocks from the Dalradian, Scotland, with particular reference to the zonation in garnet. *Contrib. Mineral. Petrol.*, 18, 347-371.

BECKER, P. & HOSCHEK, G. (1973) Experimentelle bildung von klinohumit. *Neues Jahrb. Mineral. Monatsh.*, 1973, 281-287.

BENNETT, H. & HAWLEY, W.G. (1965) Methods of silicate analysis. *Academic Press, London*, 334p.

BINNS, R.A. (1964) Zones of progressive regional metamorphism in the Willyama Complex, Broken Hill district, New South Wales. *Jour. Geol. Soc. Australia*, 11, 283-330.

_____(1969) Ferromagnesian minerals in high-grade metamorphic rocks. *Geol. Soc. Australia, Spec. Publ.* 2, 323-332.

BLACKBURN, W.H. (1968) The spatial extent of chemical equilibrium in some high-grade metamorphic rocks from the Grenville of southeastern Ontario. *Contrib. Mineral. Petrol.*, 19, 72-92.

BOETTCHER, A.L. (1970) The System $CaO-Al_2O_3-SiO_2-H_2O$ at high pressures and temperatures. *Jour. Petrol.*, 11, 337-379.

BOYD, F.R., FINGER, L.W. & CHAYES, F. (1968) Computer reduction of electron-probe data. *Carnegie Inst. Washington, Yearbook* 67, 210-215.

BROWN, E.H. (1969) Some zoned garnets from the greenschist facies. *Amer. Mineral.*, 54, 1662-1677.

BROWN, G.C. (1973) Evolution of granite magmas at destructive plate margins. *Nature Phys. Sci.*, 241, No. 106, 26-28.

_____& FYFE, W.S. (1970) The production of granitic melts during ultrametamorphism. *Contrib. Mineral. Petrol.*, 28, 310-318.

BUDDINGTON, A.F. (1959) Granite emplacement with special reference to North America. *Geol. Soc. America Bull.*, 70, 671-747.

BURGER, A.J. & COERTZE, F.J. (1973) Radiometric age measurements on rocks from southern Africa to the end of 1971. *Geol. Surv. South Africa, Bull.* 58, 46p.

University of Cape Town

BURGER, A.L., VON KNORRING, O. & CLIFFORD, T.N. (1965) Mineralogical and radiometric studies of monazite and sphene occurrences in the Namib Desert, South West Africa. *Mineral. Mag.*, 35, 519-528.

BURKE, K.C. & DEWEY, J.F. (1970) Orogeny in Africa. In: Dessanvagie, T.F.J. & Whiteman, A.J. (Eds.), *Conference on African geology*. University of Ibadan, 583-608.

_____ _____ (1973) An outline of Precambrian plate development. In: Tarling, D.H. & Runcorn, S.K. (Eds.), *Implications of continental drift to the earth sciences*, 2. Academic Press, London, 1035-1045.

BURNHAM, C.W. (1967) Hydrothermal fluids at the magmatic stage. In: Barnes, H.L. (Ed.), *Geochemistry of hydrothermal ore deposits*. Holt, Rinehart and Winston, New York, 34-76.

BUTLER, B.C.M. (1965) Compositions of micas in metamorphic rocks. In: Pitcher, W.S. and Flinn, G.W. (Eds.), *Controls of Metamorphism*. Oliver and Boyd, London-Edinburgh, 291-298.

CAMERON, E.N. (1955) Concepts of the internal structure of granitic pegmatites and their applications to certain pegmatites of South West Africa. *Trans. Geol. Soc. South Africa*, 58, 45-70.

_____, JAHNS, R.H., MCNAIR, A.H. & PAGE, L.R. (1949) Internal structure of granitic pegmatites. *Econ. Geol., Monog.* 2, Econ. Geol. Publ. Co., Illinois, 115p.

CANN, J.R. (1970) Upward movement of granitic magma. *Geol. Mag.*, 107, 335-340.

CARMICHAEL, D.M. (1970) Intersecting isograds in the Whetstone Lake area, Ontario. *Jour. Petrol.*, 11, 147-181.

CARPENTER, A.B. (1967) Mineralogy and petrology of the system $CaO-MgO-CO_2-H_2O$ at Crestmore, California. *Amer. Mineral.*, 52, 1341-1365.

CHINNER, G.A. (1959) Garnet-cordierite parageneses. *Carnegie Inst. Washington, Yearbook* 58, 112-114.

_____(1961) The origin of sillimanite in Glen Clova, Angus. *Jour. Petrol.*, 2, 312-323.

_____(1966) The significance of the aluminium silicates in metamorphism. *Ear. Sci. Rev.*, 2, 111-126.

CLIFFORD, T.N. (1967) The Damaran episode in the Upper Proterozoic - Lower Palaeozoic structural history of southern Africa. *Geol. Soc. America, Spec. Paper* 92, 100p.

_____ (1968) Radiometric dating and the pre-Silurian geology of Africa. In: Hamilton, E.I. & Farquhar, R.M., *Radiometric dating for geologists*. Interscience, London, 299-416.

CLOOS, H. (1935) Die Kartierung des Grundgebirges in Südwest Afrika. *Geol. Rundsch.*, 26, 241-247.

COLEMAN, R.G. (1971) Plate tectonic emplacement of upper mantle peridotites along continental edges. *Jour. Geophys. Res.*, 76, 1212-1222.

CURRIE, K.L. (1971) The reaction 3 cordierite = 2 garnet + 4 sillimanite + 5 quartz as a geological thermometer in the Opinicon Lake region, Ontario. *Contrib. Mineral. Petrol.*, 33, 215-226.

_____(1974) A note on the calibration of the garnet-cordierite geothermometer and geobarometer. *Contrib. Mineral. Petrol.*, 44, 35-44.

DAHL, O. (1969) Irregular distribution of Fe and Mg among co-existing biotite and garnet. *Lithos*, 2, 311-322.

DALLMEYER, R.D. (1972) Compositional controls on cordierite-bearing assemblages in high grade regional metamorphism. *24th Internat. Geol. Congr.*, 2, 52-63.

_____& DODD, R.T. (1971) Distribution and significance of cordierite in paragneisses of the Hudson Highlands, southeastern New York. *Contrib. Mineral. Petrol.*, 33, 289-308.

DAY, H.W. (1973) The high temperature stability of muscovite plus quartz. *Amer. Mineral.*, 58, 255-262.

DEER, W.A., HOWIE, R.A. & ZUSSMAN, J. (1962) *Rock forming minerals*, vols. 1-5. Longmans, Green and Co., London.

DE WAAL, S.A. (1966) *The Alberta Complex, a metamorphosed layered intrusion north of Nauchas, South West Africa, the surrounding granites and repeated folding in the younger Damara System.* Unpubl. D.Sc. Thesis, Univ. Pretoria, 207p.

DEWEY, J.F. & BIRD, J.M. (1970) Mountain belts and the new global tectonics. *Jour. Geophys. Res.*, 75, 2625-2647.

_____ _____ (1971) Origin and emplacement of the ophiolite suite : Appalachian ophiolites in Newfoundland. *Jour. Geophys. Res.*, 76, 3179-3206.

DICKINSON, W.R. (1971) Plate tectonics and geologic history. *Science*, 174, 4005, 107-113.

ENGEL, A.E.J. & ENGEL, C.G. (1960) Progressive metamorphism and granitisation of the major paragneiss, northwest Adirondack Mountains, New York. Part II, mineralogy. *Geol. Soc. America Bull.*, 71, 1-58.

ESKOLA, P. (1949) The Problem of Mantled Gneiss Domes. *Quart. Jour. Geol. Soc. London*, 104, 461-476.

EUGSTER, H.P. (1959) Reduction and oxidation in metamorphism. In: Abelson, P.H. (Ed.), *Researches in Geochemistry*. John Wiley & Sons, New York, 397-426.

_____(1969) Oxygen. In: Wedepohl, K.H. (Ed.), *Handbook of Geochemistry*, 1. Springer-Verlag, Berlin, 8-C-1 to 8-P-2.

EVANS, B.W. (1965) Application of a reaction-rate method to the breakdown equilibria of muscovite and muscovite plus quartz. *Amer. Jour. Sci.*, 263, 647-667.

University of Cape Town

_____ & GUIDOTTI, C.V. (1966) The sillimanite-potash feldspar isograd in western Maine, U.S.A. *Contrib. Mineral. Petrol.*, 12, 25-62.

_____ & LEAKE, B.E. (1960) Composition and origin of the striped amphibolites of Connemara, Ireland. *Jour. Petrol.*, 1, 337-363.

FAUPEL, J. (1973) Geological and mineralogical investigation of the Donkerhoek Granite, Karibib district, South West Africa (Preliminary Report). *Neues Jahrb. Geol. Paläont. Monatsh.*, 1973, 327-341.

FEDIUK, F. (1971) Cordierite in Moldanubian gneisses. *Krystalinikum*, Czechoslovak Acad. Sci., 7, 183-202.

FEDIUKOVA, E. (1971) Distribution of FeO, MgO and MnO in the minerals of some Moldanubian metamorphic rocks. *Krystalinikum*, Czechoslovak Acad. Sci., 7, 7-25.

FLEMING, P.D. (1972) Mg-Fe distribution between co-existing garnet and biotite, and the status of fibrolite in the andalusite-staurolite zone of the Mt. Lofty Ranges, South Australia. *Geol. Mag.*, 109, 477-482.

FLINT, R.F., SANDERS, J.E. & RODGERS, J. (1960) Diamictite : a substitute term for symmictite. *Geol. Soc. America Bull.*, 71, 1809-1810.

FRETS, D.C. (1969) Geology and structure of the Huab-Welwitschia area, South West Africa. *Precambrian Res. Unit, Univ. Cape Town, Bull.* 8, 235p.

FROST, M.J. (1962) Metamorphic grade and Fe-Mg distribution between co-existing garnet-biotite and garnet-hornblende. *Geol. Mag.*, 99, 427-438.

FYFE, W.S. (1970) Some thoughts on granitic magmas. In: Newell, G. and Rast, N. (Eds.), *Mechanisms of igneous intrusion.* Seel House Press, Liverpool, 201-216.

GABLE, D.J. & SIMS, P.K. (1969) Geology and regional metamorphism of some high grade cordierite gneisses, Front Range, Colorado. *Geol. Soc. America, Spec. Paper* 128, 87p.

GANGULY, J. (1972) Staurolite stability and related parageneses : theory, experiments and applications. *Jour. Petrol.*, 13, 335-365.

GEVERS, T.W. (1931a) *The Fundamental Complex of Western Damaraland, South West Africa.* Unpubl. D.Sc. Thesis, Univ. Cape Town, 163p.

_____ (1931b) An ancient tillite in South West Africa. *Trans. Geol. Soc. South Africa*, 34, 1-17.

_____ (1934a) Untersuchungen des Grundgebirges im westlichen Damaraland. I. Zur Gliederung des Grundgebirges im westlichen Damaraland Südwestafrikas. *Neues Jahrb. Mineral. Geol. Paläont.*, Beil.-Bd., 72, Abt. B, 283-330.

_____ (1934b) Untersuchungen des Grundgebirges im westlichen Damaraland. II. Die alten Granite des Grundgebirges. *Neues Jahrb. Mineral. Geol. Paläont.*, Beil.-Bd., 72, Abt. B, 399-428.

University of Cape Town

_____(1935) Untersuchungen des Grundgebirges im westlichen Damaraland. III. Tektonik des Grundgebirges und Intrusions-mechanismus der alten Granite in westlichen Damaralande. *Neues Jahrb. Mineral. Geol. Paläont.*, Beil.-Bd., 73, Abt. B, 27-41.

_____(1963) Geology along the northwestern margin of the Khomas Highlands between Otjimbingwe-Karibib and Okahandja, South West Africa. *Trans. Geol. Soc. South Africa*, 66, 199-258.

_____& FROMMURZE, H.F. (1929) The tin-bearing pegmatites of the Erongo area, South West Africa. *Trans. Geol. Soc. South Africa*, 32, 111-149.

GHENT, E.D. & DEVRIES, C.D.S. (1972) Plagioclase-garnet-epidote equilibria in hornblende-plagioclase bearing rocks from the Esplanade Range, British Columbia. *Canad. Jour. Ear. Sci.*, 9, 618-635.

GOLDSMITH, R. (1959) Granofels, a new metamorphic rock name. *Jour. Geol.*, 67, 109-110.

GOLDSMITH, J.R., GRAF, D.L. & JOENSUU, O.I. (1955) The occurrence of magnesian calcites in nature. *Geochim. Cosmochim. Acta*, 7, 212-230.

_____& HEARD, H.C. (1961) Subsolidus phase relations in the system $CaCO_3$-$MgCO_3$. *Jour. Geol.*, 69, 45-74.

_____& NEWTON, R.C. (1969) P-T-X relations in the system $CaCO_3$-$MgCO_3$ at high temperatures and pressures. *Amer. Jour. Sci.*, 267A, 160-190.

GOODSPEED, G.E. (1948) Origin of granites. *Geol. Soc. America, Mem.* 28, 55-78.

GORBATSCHEV, R. (1968) Distribution of elements between cordierite, biotite and garnet. *Neues Jahrb. Mineral. Abh.*, 110, 57-80.

GORDON, T.M. & GREENWOOD, H.J. (1970) The reaction : dolomite + quartz + water = talc + calcite + carbon dioxide. *Amer. Jour. Sci.*, 268, 225-242.

_____ _____ (1971) The stability of grossularite in H_2O/CO_2 mixtures. *Amer. Mineral.*, 56, 1674-1688.

GRAF, D.L. & GOLDSMITH, J.R. (1955) Dolomite-magnesian calcite relations at elevated temperatures and CO_2 pressures. *Geochim. et Cosmochim. Acta*, 7, 109-128.

_____ _____ (1958) The solid solubility of $MgCO_3$ in $CaCO_3$: a revision. *Geochim. et Cosmochim. Acta*, 13, 218-219.

GREENWOOD, H.J. (1961) The system $NaAlSi_2O_6$-H_2O-Argon : total pressure and water pressure in metamorphism. *Jour. Geophys. Res.*, 66, 3923-3946.

_____(1962) Metamorphic reactions involving two volatile components. *Carnegie Instn. Washington, Year Book* 61, 82-85.

_____(1967) Wollastonite : Stability in H_2O-CO_2 mixtures and occurrence in a contact aureole. *Amer. Mineral.*, 52, 1669-1680.

_____(1972) Al^{IV}-Si^{IV} disorder in sillimanite, and its effect on phase relations of the aluminium silicate minerals. *Geol. Soc. America, Mem.* 132,

University of Cape Town

GRESENS, R.L. (1967a) Tectonic-hydrothermal pegmatites; I. the model. *Contrib. Mineral. Petrol.*, 15, 345-355.

_____(1967b) Tectonic-hydrothermal pegmatites; II. an example. *Contrib. Mineral. Petrol.*, 16, 1-28.

GUJ, P. (1970) The Damara mobile belt in the southwestern Kaokoveld, South West Africa. *Precambrian Res. Unit, Univ. Cape Town, Bull.* 8, 168p.

GÜRICH, G. (1892) Deutsch - Südwestafrika. *Mitt. d. geog. Ges. zu Hamburg.*

HÄLBICH, I.W. (1970) *The geology of the western Windhoek and Rehoboth districts : a stratigraphic-structural analysis of the Damara System.* Unpubl. D.Sc. Thesis, Univ. Stellenbosch, 199p.

HARKER, R.I. & TUTTLE, O.F. (1955) Studies in the system CaO-MgO-CO_2, part 2, limits of solid solution along the binary join $CaCO_3$-$MgCO_3$. *Amer. Jour. Sci.*, 253, 274-282.

HARLAND, W.B., HEROD, K.N. & KRINSLEY, D.H. (1966) The definition and identification of tills and tillites. *Earth Sci. Rev.*, 2, 225-256.

HARTNADY, C.J. (1974) Structural investigations in the Naukluft Mountains, South West Africa : a preliminary report. In: Kröner, A. (Ed.), *Tenth and eleventh Ann. Reps. for 1972 and 1973. Precambrian Res. Unit, Univ. Cape Town,* 83-88.

HAUGHTON, S.H. (1969) *Geological History of Southern Africa.* Geol. Soc. South Africa, Johannesburg, 535p.

HEDBERG, H.D. (Ed.) (1961) Stratigraphic classification and terminology. Internat. Subcomm. Stratigr. Classif., *Rep. 21st Internat. Geol. Congr.*, 25, 38p.

_____(1970) Preliminary report on lithostratigraphic units. Internat. Subcomm. Stratigr. Classif., *24th Internat. Geol. Congr., Rep.* 3, 30p.

HENSEN, B.J. & GREEN, D.H. (1971) Experimental study of the stability of cordierite and garnet in pelitic compositions at high pressures and temperatures. Part I. Compositions with excess alumino-silicate. *Contrib. Mineral. Petrol.*, 33, 309-331.

_____ _____ (1972) Experimental study of the stability of cordierite and garnet in pelitic compositions at high pressures and temperatures. Part II. Compositions without excess alumino-silicate. *Contrib. Mineral. Petrol.*, 35, 331-354.

_____ _____ (1973) Experimental study of the stability of cordierite and garnet in pelitic compositions at high pressures and temperatures. Part III. Synthesis of experimental data and geologic applications. *Contrib. Mineral. Petrol.*, 38, 151-166.

HESS, P.C. (1969) The metamorphic paragenesis of cordierite in pelitic rocks. *Contrib. Mineral. Petrol.*, 24, 191-207.

_____(1971) Prograde and retrograde equilibria in garnet-cordierite gneisses in south central Massachusetts. *Contrib. Mineral. Petrol.*, 30, 177-195.

University of Cape Town

HIETANEN, A. (1947) Archaean geology of the Turku district in southwestern Finland. *Geol. Soc. America Bull.*, 58, 1019-1084.

HIRSCHBERG, A. & WINKLER, H.G.F. (1968) Stabilitätsbeziehungen zwischen chlorit, cordierit und almandin bei der metamorphose. *Contrib. Mineral. Petrol.*, 18, 17-42.

HOLDAWAY, M.J. (1966) Hydrothermal stability of clinozoisite and quartz. *Amer. Jour. Sci.*, 264, 643-667.

_____(1972) Thermal stability of Al-Fe epidote as a function of fO_2 and Fe content. *Contrib. Mineral. Petrol.*, 37, 307-340.

HOSCHEK, G. (1967) Untersuchungen zum Stabilitätsbereich von Chloritoid und Staurolith. *Contrib. Mineral. Petrol.*, 14, 123-162.

_____(1969) The stability of staurolite and chloritoid and their significance in metamorphism of pelitic rocks. *Contrib. Mineral. Petrol.*, 22, 208-232.

_____(1973) Der Reaktion Phlogopit + Calcit + Quarz = Tremolit + Kalifeldspat + H_2O + CO_2. *Contrib. Mineral. Petrol.*, 39, 231-238.

HSU, L.C. (1968) Selected phase relationships in the system Al-Mn-Fe-Si-O-H : a model for garnet equilibria. *Jour. Petrol.*, 9, 40-83.

HUCKENHOLZ, H.G. (1969) Oxidation of Ca-rich clinopyroxenes. *Carnegie Instn. Washington, Year Book* 67, 94-96.

HUGO, P.J. (1970) The pegmatites of the Kenhardt and Gordonia districts, Cape Province. *Geol. Surv. South Africa, Mem.* 58, 94p.

HURLEY, P.M. (1972) Can the subduction process of mountain building be extended to Pan-African and similar orogenic belts? *Ear. Planet. Sci. Lett.*, 15, 305-314.

HUTCHEON, I. & MOORE, J.M. (1973) The tremolite isograd near Marble Lake, Ontario. *Canad. Jour. Ear. Sci.*, 10, 936-947.

HYNDMAN, D.W. (1972) *Petrology of igneous and metamorphic rocks*. McGraw-Hill Book Co., New York, 533p.

JACOB, R.E. (1972) Preliminary report on the geology of an area east of the confluence of the Khan and Swakop Rivers, South West Africa. In: de Villiers, J. (Ed.), *Seventh, eighth and ninth Ann. Reps. for 1969, 1970, 1971. Precambrian Res. Unit, Univ. Cape Town*, 58-67.

JAHNS, R.H. (1955) The study of pegmatites. *Econ. Geol.* 50th Anniv. vol., 1025-1130.

_____& BURNHAM, C.W. (1957) Preliminary results from experimental melting and crystallisation of Harding pegmatite. *Geol. Soc. America Bull.*, 68, 1751-1752.

_____ _____ (1961) Experimental studies of pegmatite genesis : a model for the crystallisation of granitic pegmatites. *Geol. Soc. America, Spec. Paper* 68, 206-207.

University of Cape Town

_____ _____ (1969) Experimental studies of pegmatite genesis : 1. a model for the derivation and crystallisation of granitic pegmatites. *Econ. Geol.*, 64, 843-864.

_____ & TUTTLE, O.F. (1963) Layered pegmatite-aplite intrusives. *Mineral. Soc. America, Spec. Paper* 1, 78-92.

JOHANNES, W. (1968) Experimental investigation of the reaction forsterite + H_2O = serpentine + brucite. *Contrib. Mineral. Petrol.*, 19, 309-315.

JOHNSON, M.R.W. (1962) Relations of movement and metamorphism in the Dalradians of Banffshire. *Trans. Edinburgh Geol. Soc.*, 19, 29-64.

JONES, A.G. (1959) Vernon map-area, British Columbia. *Geol. Surv. Canada, Mem.* 296, 1-186.

JOUBERT, P. (1971) The regional tectonism of the gneisses of part of Namaqualand. *Precambrian Res. Unit, Univ. Cape Town, Bull.* 10, 220p.

_____ & KRÖNER, A. (1972) The Stinkfontein Formation south of the Richtersveld. *Trans. Geol. Soc. South Africa*, 75, 47-54.

KERRICK, D.M. (1970) Contact metamorphism in some areas of the Sierra Nevada, California. *Geol. Soc. America Bull.*, 81, 2913-2938.

_____ (1972) Experimental determination of muscovite + quartz stability with $P_{H_2O} < P_{total}$ *Amer. Jour. Sci.*, 272, 946-958.

KRAUSKOPF, K.B. (1967) *Introduction to Geochemistry.* McGraw-Hill Book Co., New York, 721p.

KRETZ, R. (1959) Chemical study of garnet, biotite and hornblende from gneisses of southwestern Quebec, with emphasis on distribution of elements in co-existing minerals. *Jour. Geol.*, 67, 371-402.

KRETZ, R. (1964) Analysis of equilibrium in garnet-biotite-sillimanite gneisses from Quebec. *Jour. Petrol.*, 5, 1-20.

KRÖNER, A. (1971) Late-Precambrian correlation and the relationship between the Damara and Nama Systems of South West Africa. *Geol. Rundsch.*, 60, 1513-1523.

_____ & RANKAMA, K. (1972) Late Precambrian glaciogenic sedimentary rocks in southern Africa : a compilation with definitions and correlations. *Precambrian Res. Unit, Univ. Cape Town, Bull.* 11, 37p.

_____ (Ed.) (1974) Proposal for the stratigraphic classification and nomenclature of rocks presently considered to be of post-Waterberg/pre-Cape age. *Unpubl. Rep., S.A. Comm. Stratigr. working group post-Waterberg/pre-Cape*, 10p.

LEAKE, B.E. (1964) The chemical distinction between ortho- and para-amphibolites. *Jour. Petrol.*, 5, 238-254.

LIOU, J.G. (1973) Synthesis and stability relations of epidote, $Ca_2Al_2FeSi_3O_{12}(OH)$. *Jour. Petrol.*, 14, 381-414.

MARTIN, H. (1965) *The Precambrian geology of South West Africa and Namaqualand.* Precambrian Res. Unit, Univ. Cape Town, 159p.

University of Cape Town

MAXWELL, J.A. (1968) *Rock and mineral analysis.* Interscience Publishers, New York, 584p.

MCINTIRE, W.L. (1963) Trace element partition coefficients - a review of theory and applications to geology. *Geochim. Cosmochim. Acta,* 27, 1209-1264.

MEHNERT, K.R. (1968) *Migmatites and the origin of granitic rocks.* Elsevier Publ. Co., Amsterdam, 393p.

METZ, P. (1967) Experimentelle Bildung von Forsterit und Calcit aus Tremolit und Dolomit. *Geochim. Cosmochim. Acta,* 31, 1517-1532.

_____(1970) Experimentelle Untersuchung der Metamorphose von kieselig dolomitischen Sedimenten. II. Die Bildungsbedingungen des Diopsids. *Contrib. Mineral. Petrol.,* 28, 221-250.

_____& PUHAN, D. (1970) Experimentelle Untersuchung der Metamorphose von kieselig dolomitischen Sedimenten. I. Die Gleichgewichtsdaten der Reaktion 3 Dolomit + 4 quarz + 1 H_2O = 1 Talk + 3 Calcit + 3 CO_2 für die Gesamtgasdrucke von 1000, 3000 und 5000 Bar. *Contrib. Mineral. Petrol.,* 26, 302-314.

_____ _____ (1971) Korrektur zur Arbeit "Experimentelle Untersuchung der Metamorphose von kieselig dolomitischen Sedimenten". *Contrib. Mineral. Petrol.,* 31, 169-170.

_____ _____& WINKLER, H.G.F. (1968) Equilibrium relations in the formation of talc and tremolite by metamorphism of siliceous dolomite. *Naturwissenschaften,* 55, 225-226.

_____& TROMMSDORFF, V. (1968) On phase equilibria in metamorphosed siliceous dolomites. *Contrib. Mineral. Petrol.,* 18, 305-309.

MILLER, R. McG. (1972) *The geology of a portion of southern Damaraland, South West Africa, with particular reference to the petrogenesis of the Salem Granite.* Unpubl. Ph.D. Thesis, Univ. Cape Town, 246p.

_____(1973) The Salem Granite Suite, South West Africa : genesis by partial melting of the Khomas schist. *Geol. Surv. South Africa, Mem.* 64, 97p.

_____(1974) The implication of albite rims in granite studies. *Geol. Soc. South Africa, Spec. Publ.* 3, 443-446.

MISCH, P. (1964) Stable association wollastonite - anorthite, and other calc-silicate assemblages in amphibolite-facies crystalline schists of Nanga-Parbat, northwest Himalayas. *Beitr. Mineral. Petrol.,* 10, 315-356.

MIYASHIRO, A. (1958) Regional metamorphism of the Gosaisyo-Takanuki district in the Central Abukuma Plateau. *Jour. Fac. Sci., Univ. Tokyo,* 11, Sec. 2, 219-272.

_____(1964) Oxidation and reduction in the earth's crust with special reference to the role of graphite. *Geochim. Cosmochim. Acta,* 28, 717-720.

_____(1973) *Metamorphism and metamorphic belts.* George Allen and Unwin, London, 492p.

University of Cape Town

MUIR, I.D. (1951) The clinopyroxenes of the Skaergaard intrusion, eastern Greenland. *Mineral. Mag.*, 29, 690-714.

_____(1967) Microscopy : transmitted light. In: Zussman, J. (Ed.), *Physical Methods in Determinative Mineralogy*. Academic Press, London, 31-102.

NASH, C.R. (1971) Metamorphic Petrology of the S.J. Area, Swakopmund district, South West Africa. *Precambrian Res. Unit, Univ. Cape Town, Bull.* 9, 77p.

_____(1972) Primary anhydrite in Precambrian gneisses from the Swakopmund district, S.W.A. *Contrib. Mineral. Petrol.*, 36, 27-32.

NEL, L.T. (1954) *Geol. Surv. South Africa, Ann. Rep.*

NEWTON, R.C. (1966) Some calc-silicate equilibrium relations. *Amer. Jour. Sci.*, 264, 202-222.

NITSCH, K.H. & WINKLER, H.G.F. (1965) Bildungsbedingungen von Epidot und Orthozoisit. *Beitr. Mineral. Petrol.*, 11, 470-486.

OKRUSCH, M. (1971) Garnet-cordierite-biotite equilibria in the Steinach aureole, Bavaria. *Contrib. Mineral. Petrol.*, 32, 1-23.

ORVILLE, P.M. (1969) A model for the metamorphic differentiation origin of thin-layered amphibolites. *Amer. Jour. Sci.*, 267, 64-86.

PARK, R.G. (1969) Structural correlation in metamorphic belts. *Tectonophysics*, 7, 323-338.

POLDERVAART, A. & HESS, H.H. (1951) Pyroxenes in the crystallisation of basaltic magma. *Jour. Geol.*, 59, 472-489.

PORADA, H. (1973) Tektonisches Verhalten und geologische Bedeutung von Kalksilikatfels - Lagen und -Spindeln im Damara-Orogen Südwest-Afrikas. *Geol. Rundsch.*, 62, 918-938.

PUHAN, D. & HOFFER, E. (1973) Phase relations of talc and tremolite in metamorphic calcite-dolomite sediments in the southern portion of the Damara Belt (South West Africa). *Contrib. Mineral. Petrol.*, 40, 207-214.

RAMBERG, H. (1956) Pegmatites in West Greenland. *Geol. Soc. America Bull.*, 67, 185-213.

_____(1962) Intergranular precipitation of albite formed by unmixing of alkali felspar. *Neues Jahrb. Mineral. Abh.*, 98, 14-34.

RAMSAY, J.G. (1962) Interference patterns produced by the superposition of folds of similar type. *Jour. Geol.*, 60, 466-481.

_____(1964) The uses and limitations of beta-diagrams and pi-diagrams in the geometrical analysis of folds. *Quart. Jour. Geol. Soc. London*, 120, 435-454.

_____(1967) *Folding and fracturing of rocks*. McGraw-Hill Book Co., New York, 568p.

REDDEN, J.A. (1963) Geology and pegmatites of the Fourmile Quadrangle, Black Hills, South Dakota. *U.S. Geol. Surv., Prof. Paper* 297D, 199-291.

REESOR, J.E. (1970) Some aspects of structural evolution and regional setting in part of the Shuswap metamorphic Complex. *Geol. Assoc. Canada, Spec. Paper* 6, 73-86.

REITAN, P. (1958) Pegmatite veins and the surrounding rocks. II. Changes in the glivine gabbro surrounding the pegmatite veins, Risør, Norway. *Norsk Geol. Tidsskr.*, 38, 279-311.

_____(1959) Pegmatite veins and the surrounding rocks. III. Structural control of small pegmatites in amphibolite, Rytterholmen, Kragerøfjord, Norway. *Norsk Geol. Tidsskr.*, 39, 175-196.

REUNING, E. (1924) Pegmatite und Pegmatitmineralien in Südwestafrika. *Zeitsch. Kristallogr.*, 58, 448-460.

RICHARDSON, S.W. (1968) Staurolite stability in a part of the system Fe-Al-Si-O-H. *Jour. Petrol.*, 9, 467-488.

RICHARDSON, S.W., GILBERT, M.C. & BELL, P.M. (1969) Experimental determination of kyanite-andalusite and andalusite-sillimanite equilibria; the aluminium silicate triple point. *Amer. Jour. Sci.*, 267, 259-272.

RIGG, T. & WAGENBAUER, H.A. (1961) Spectrophotometric determination of titanium in silicate rocks. *Anal. Chem.*, 33, 1347-1349.

ROBERTSON, J.K. & WYLLIE, P.J. (1971) Rock-water systems, with special reference to the water deficient region. *Amer. Jour. Sci.*, 271, 252-277.

ROERING, C. (1961) The mode of emplacement of certain Li- and Be-bearing pegmatites in the Karibib district, South West Africa. *Econ. Geol. Res. Unit, Univ. Witwatersrand, Inform. Circ.* 4, 38p.

_____(1966) Aspects of the genesis and crystallisation sequence of the Karibib pegmatites, South West Africa. *Econ. Geol.*, 61, 1064-1089.

_____& GEVERS, T.W. (1964) Lithium- and beryllium-bearing pegmatites in the Karibib district, South West Africa. In: Haughton, S.H. (Ed.), *The geology of some ore deposits in southern Africa*, 2, Geol. Soc. South Africa, 463-495.

SAN MIGUEL, A. (1969) The aplite-pegmatite association and its petrogenetic interpretation. *Lithos*, 2, 25-37.

SAXENA, S.K. (1968) Distribution of elements between co-existing minerals and the nature of solid solution in garnet. *Amer. Mineral.*, 53, 994-1014.

_____(1969) Silicate solid solutions and geothermometry, part 3: distribution of Fe and Mg between co-existing garnet and biotite. *Contrib. Mineral. Petrol.*, 22, 259-267.

_____& HOLLANDER, N.B. (1969) Distribution of iron and magnesium in biotite, garnet and cordierite. *Amer. Jour. Sci.*, 267, 210-216.

University of Cape Town

SCHALK, K.E.L. (1973) Some late Precambrian formations in central South West Africa. *Geol. Surv. South Africa Annals*, 8 (for 1970), 29-47.

_____& HÄLBICH, I.W. (1965) The Geology of the area around Windhoek, Rehoboth and Dordabis. *Geol. Surv. South Africa, Unpubl. Explan. Sheets 2217C, 2217D, 2317A and 2317B.*

SCHMERMERHORN, L.J.G. (1966) Terminology of mixed coarse-fine sediments. *Jour. Sedim. Petrol.*, 36, 831-835.

SCHREYER, W. & SEIFERT, F. (1969) Compatibility relations of the aluminium silicates in the systems $MgO-Al_2O_3-SiO_2-H_2O$ and $K_2O-MgO-Al_2O_3-SiO_2-H_2O$ at high pressures. *Amer. Jour. Sci.*, 267, 371-388.

_____& YODER, H.S. (1961) Petrographic guides to the experimental petrology of cordierite. *Carnegie Inst. Washington, Year Book* 60, 147-152.

SELLEY, R.C. (1970) *Ancient sedimentary environments.* Chapman and Hall, London, 237p.

SHACKLETON, R.M. (1969) Displacement within continents. In: Kent, P.E., Satterthwaite, G.E. & Spencer, A.M. (Eds.), *Time and place in orogeny.* Geol. Soc. London, London, 1-7.

_____(1973) Correlation of structures across Precambrian orogenic belts in Africa. In: Tarling, D.H. & Runcorn, S.K. (Eds.), *Implications of continental drift to the earth sciences*, 2. Academic Press, London, 1091-1094.

SHAPIRO, L. & BRANNOCK, W.W. (1962) Rapid analysis of silicate, carbonate and phosphate rocks. *U.S. Geol. Surv., Bull. 1144A.*

SHAW, D.M. (1960) The geochemistry of scapolite. *Jour. Petrol.*, 1, 218-285.

SIEDNER, G. & MILLER, J.A. (1968) K-Ar age determinations on basaltic rocks from South West Africa and their bearing on continental drift. *Ear. Plan. Sci. Lett.*, 4, 451-458.

SKIPPEN, G.B. (1971) Experimental data for reactions in siliceous marbles. *Jour. Geol.*, 79, 457-481.

SMITH, D.A.M. (1961) *The geology of the area around the Khan and Swakop Rivers in South West Africa.* Unpubl. Ph.D. thesis, Univ. Witwatersrand, 173p.

_____(1965) The geology of the area around the Khan and Swakop Rivers in South West Africa. *Geol. Surv. South Africa, Mem.* 3 (S.W.A. Series), 113p.

SOUTH AFRICAN COMMITTEE FOR STRATIGRAPHY (1971) South African code of stratigraphic terminology and nomenclature. *Trans. Geol. Soc. South Africa*, 74, 111-129.

SPRY, A. (1969) *Metamorphic Textures.* Pergamon Press, London, 350p.

STANTON, R.L. (1972) *Ore Petrology.* McGraw-Hill Book Co., New York, 713p.

STORRE, B. (1970) Stabilitätsbedingungen Grossular-führender Paragenesen im System $CaO-Al_2O_3-SiO_2-CO_2-H_2O$. *Contrib. Mineral. Petrol.*, 29, 145-162.

_____& NITSCH, K. (1972) Die Reaktion 2 zoisit + 1 CO_2 = 3 anorthit + 1 calcit + 1 H_2O. *Contrib. Mineral. Petrol.*, 35, 1-10.

STRECKEISEN, A. (Ed.) (1973) Classification and nomenclature of plutonic rocks : recommendations. I.U.G.S. Subcomm. on the systematics of igneous rocks. *Neues Jahrb. Mineral., Monatsh.*, 1973, 149-164.

STURT, B.A. (1962) The composition of garnets from pelitic schists in relation to the grade of metamorphism. *Jour. Petrol.*, 3, 181-191.

TOBISCH, O.T. (1966) Large-scale basin-and-dome pattern resulting from the interference of major folds. *Geol. Soc. America Bull.*, 77, 393-408.

TRÖGER, W.E. (1971) *Optische Bestimmung der gesteinsbildenden Minerale, Teil 1*. E. Schweizerbärtsche Verlagsbuchhandlung, Stuttgart, 188p.

TROMMSDORFF, V. (1966) Progressive Metamorphose kieseliger Karbonatgesteine in den Zentralalpen zwischen Bernina und Simplon. *Schweiz. Mineral. Petrog. Mitt.*, 46, 431-460.

TRUSWELL, J.F. (1967) A critical review of stratigraphic terminology as applied in South Africa. *Trans. Geol. Soc. South Africa*, 70, 81-116.

TURNER, F.J. (1967) Thermodynamic appraisal of steps in progressive metamorphism of siliceous dolomitic limestones. *Neues Jahrb. Mineral. Monatsh.*, 1967, 1-22.

_____(1968) *Metamorphic Petrology*. McGraw-Hill Book Co., New York, 403p.

_____& WEISS, L.W. (1963) *Structural analysis of metamorphic tectonites*. McGraw-Hill Book Co., New York, 545p.

TUTTLE, O.F. & BOWEN, N.L. (1958) Origin of granite in the light of experimental studies in the system $NaAlSi_3O_8$ - $KAlSi_3O_8$ - H_2O. *Geol. Soc. America, Mem.* 74, 1-153.

USHAKOVA, E.N. (1972) The biotites. In: Sobolev, V.S. (Ed.), *The facies of metamorphism*. Austr. Nat. Univ. Press, Canberra, 352-362.

VAN DER VEEN, A.H. (1965) Calcite - dolomite intergrowths in high temperature carbonate rocks. *Amer. Mineral.*, 50, 2070-2076.

VAN EYSINGA, F.W.B. (1970) Stratigraphic terminology and nomenclature; a guide for editors and authors. *Ear. Sci. Rev.*, 6, 267-288.

VERHOOGEN, J., TURNER, F.J., WEISS, L.E., WAHRHAFTIG, C. & FYFE, W.S. (1970) *The Earth : an introduction to physical geology*. Holt, Rinehart and Winston, Inc., New York, 748p.

VIDALE, R. (1969) Metasomatism in a chemical gradient and the formation of calc-silicate bands. *Amer. Jour. Sci.*, 267, 857-874.

VON BACKSTRÖM, J.W. (1964) The geology of an area around Keimoes, Cape Province, with special reference to phacoliths of charnockitic adamellite-porphyry. *Geol. Surv. South Africa, Mem.* 53, 218p.

VON GROOTE-BIDLINGMAIER, M. (1973) Tectonics and metamorphism along the border between the Damara and pre-Damara terrains, S.W. of Windhoek, South West Africa (Preliminary Report). *Neues Jahrb. Geol. Paläont. Monatsh.*, 1973, 342-350.

VON PLATEN, H. (1965) Experimental anatexis and the genesis of migmatites. In: Pitcher, W.S. and Flinn, G.W. (Eds.), *Controls of Metamorphism*. Oliver and Boyd, Edinburgh-London, 203-218.

University of Cape Town

_____ & HOLLER, H. (1966) Experimentelle Anatexis der Stainzer Plattengneises von der Koralpe, Steiermark, bei 2, 4, 7 und 10 kb H_2O-druck. *Neues Jahrb. Mineral. Abh.*, 106, 106-130.

WEDEPOHL, K.H. (1969) Composition and abundance of common sedimentary rocks. In: Wedepohl, K.H. (Ed.), *Handbook of Geochemistry*, 1. Springer-Verlag, Berlin, 250-271.

WENK, E. (1962) Plagioklas als Indexmineral in den Zentralalpen. *Schweiz. Mineral. Petrog. Mitt.*, 42, 139-152.

_____ & KELLER, F. (1969) Isograde in Amphibolitserein der Zentralalpen. *Schweiz. Mineral. Petrog. Mitt.*, 49, 157-198.

WHITTEN, E.H.T. (1966) *Structural geology of folded rocks*. Rand McNally & Co., Chicago, 663p.

WILSON, G. (1953) Mullion and rodding structures in the Moine Series of Scotland. *Proc. Geol. Assoc.*, 64, 118-145.

WINCHELL, H. (1958) Composition and physical properties of garnet. *Amer. Mineral.*, 43, 595-600.

WINDLEY, B. & BRIDGWATER, D. (1965) The layered aplite-pegmatite sheets of Kinalik, south Greenland. *Grönl. Geol. Unders., Bull.* 60.

WINKLER, H.G.F. (1967) *Petrogenesis of Metamorphic Rocks*. Springer-Verlag, New York, 237p.

_____ (1970) Abolition of metamorphic facies, introduction of the four divisions of metamorphic stage, and of a classification based on isograds in common rocks. *Neues Jahrb. Mineral. Monatsh.*, 1970, 189-248.

_____ & LINDEMANN, W. (1972) The System Qz-Or-An-H_2O within the granitic system Qz-Or-Ab-An-H_2O. Application to granite magma formation *Neues Jahrb. Mineral. Monatsh.*, 1972, 49-61.

_____ & VON PLATEN, H. (1960) Experimentelle Gesteinsmetamorphose III: Anatektische Ultrametamorphose kalkhartige Tone. *Geochim. Cosmochim. Acta*, 18, 294-316.

_____ _____ (1961a) Experimentelle Gesteinsmetamorphose IV: Bildung anatektischer Schmelzen metamorphisierten Grauwacken. *Geochim. Cosmochim. Acta*, 24, 48-69.

_____ _____ (1961b) Experimentelle Gesteinsmetamorphose V: Experimentelle anatektische Schmelzen und ihre petrogenetische Bedeutung. *Geochim. Cosmochim. Acta*, 24, 250-259.

WISEMAN, J.D.H. (1934) The central and southwest Highlands epidiorites: a study in progressive metamorphism. *Quart. Jour. Geol. Soc. London*, 90, 354-417.

WOLF, K.H., EASTON, A.J. & WARNE, S. (1967) Techniques of examining and analysing carbonate skeletons, minerals and rocks. In: Chilingar, G.V., Bissell, H.J. and Fairbridge, R.W. (Eds.), *Carbonate Rocks, Physical and Chemical Aspects*. Elsevier, Amsterdam, 253-341.

WONES, D.R. & EUGSTER, H.P. (1965) Stability of biotite : experiment, theory and application. *Amer. Mineral.*, 50, 1228-1272.

WOOD, B.J. (1973) Fe^{2+} - Mg^{2+} partition between co-existing cordierite and garnet - a discussion of experimental data. *Contrib. Mineral. Petrol.*, 40, 253-258.

WYLLIE, P.J. (1971) *The Dynamic Earth.* John Wiley and Sons, New York, 415p.

WYNNE-EDWARDS, H.R. (1963) Flow folding. *Amer. Jour. Sci.*, 261, 793-814.

_____(1971) Plutonites, gneisses and granulites of the granulite facies. *Freiberger Forschungshefte*, Leipzig, C268, 11-24.

_____& HAY, P.W. (1963) Co-existing cordierite and garnet in regionally metamorphosed rocks from the Westport area, Ontario. *Canad. Mineral.*, 7, 793-814.

YODER, H.S. (1955) The role of water in metamorphism. *Geol. Soc. America, Spec. Paper* 62, 505-524.

ZWART, H.J. (1962) On the determination of polymetamorphic mineral associations, and its application to the Bosost Area (central Pyrenees). *Geol. Rundsch.*, 52, 38-65.

Plate 1. Minor B_2 fold in banded gneiss of the Khan Formation. The lighter bands in the gneiss consist of quartz–plagioclase–clinopyroxene while the darker bands comprise quartz–K-feldspar–hornblende. Small migmatitic mobilisates are irregularly developed. Thin dykes and veins of G_4 granite occur parallel to the axial planes (s_2) of B_2 folds; Zebraberge.

Plate 2. Migmatite in the Witpoort Formation. The hammer head rests on the palaeosome; Rote Adlerkuppe.

Plate 3. Alternation of biotite schist (darker grey) and calc–granofels (light grey) in Tinkas Formation; Gemsbok River. Height of face above intrusive pegmatite vein is 1,5 m.

Plate 4. Transposition of calc–granofels layers, interbedded with biotite schist, into s_2 (parallel to hammer handle) during F_2. The upper band has not been transposed to the same extent as that at ground level; Tinkas Formation, Gemsbok River.


2

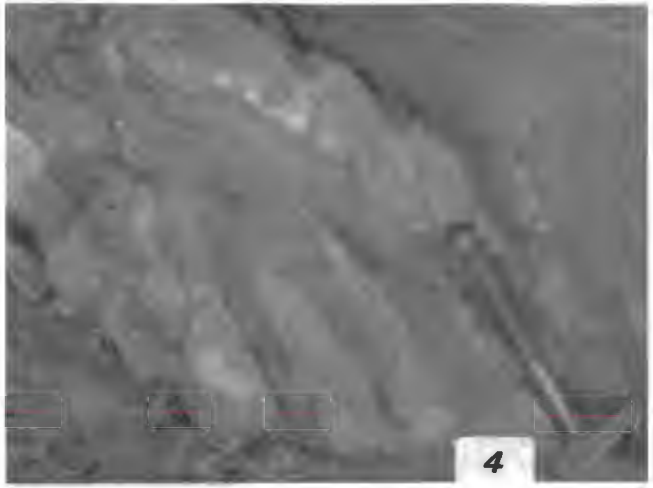
4

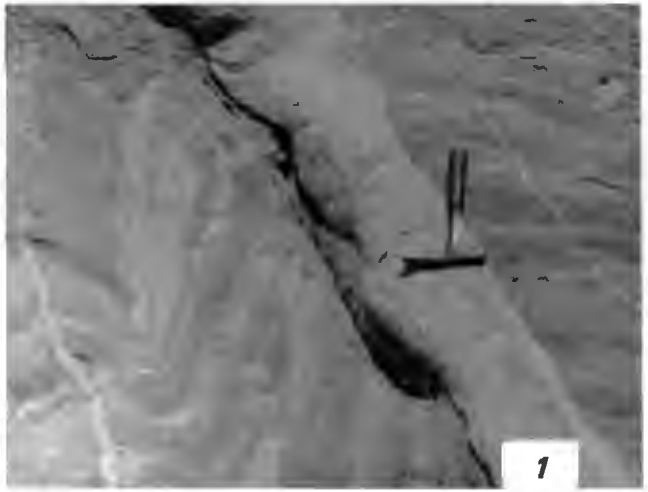
1


3

Plate 5. Disrupted amphibolite bodies in Red Granite-Gneiss which is heavily veined by gneissic granite (also part of the Gn_1 suite) and pale-coloured G_4 granite. Height of face approximately 30 m; Swakop River near Husab Gorge.

Plate 6. Intrusive contact of Salem Granite into Witpoort Formation. Note sharp contacts and pinch-and-swell structure of a vein of this granite. Height of cliff approximately 16 m; Swakop River, 1,5 km east of the Witpoort.

University of Cape Town

Plate 7. View of the Bloedkoppie from the east. The calcrete-covered flats in the foreground are locally uraniferous.

Plate 8. Agmatic structure. The Salem Granite (dark) is intruded by veins of Horebis Granite; Horebis Süd 108. Photo by courtesy of Atomic Energy Board.

5

6

7

8

Plate 9. Migmatitic foliation (s_1), axial planar to isoclinal, mesoscopic folds of F_1 age; Vredelus anticline, Vredelus 112.

Plate 10. Recumbent isoclinal fold of F_1 age, in Etusis paragneiss, deforming s_0. s_1 is axial planar to the fold and is almost horizontal. Note ptygmatic folding and pinch-and-swell structure of thin pegmatite vein; Vredelus 112.

Plate 11. Concentric disharmonic flexural slip folding of Etusis quartzites; Rooikuiseb 109. Height of cliff face about 13 m.

Plate 12. Tight, similar B_2 folds of slip-type developed in biotite schist/calc-granofels sequence, Tinkas Formation. Axial plane foliation (s_2) is visible in pelitic layers; Achas River, Wilsonfontein 110.


9


10

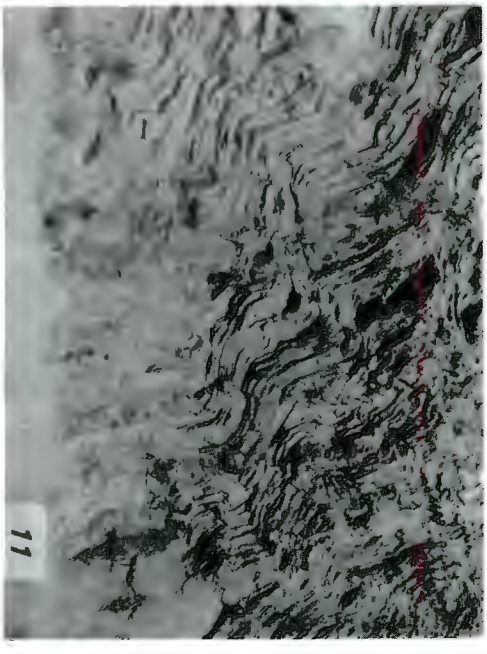
11


12

Plate 13. "Wild" ptygmatic folding in migmatite; Rooikuiseb 109.

Plate 14. Isoclinal B_2 folds in interbedded calc-granofels/biotite schist, showing axes plunging in different directions within s_2; contact between Husab and Witpoort Formations, southeast of Husabberg.

Plate 15. Similar, slip folds and concentric, isoclinal folds, of F_2 age, occurring side by side in migmatitic Etusis Formation; Rooikuiseb 109.

Plate 16. Flow fold of F_2 age, Etusis Formation. Fold closures of F_1 age can be seen in leucocratic layers; Rooikuiseb 109.


13

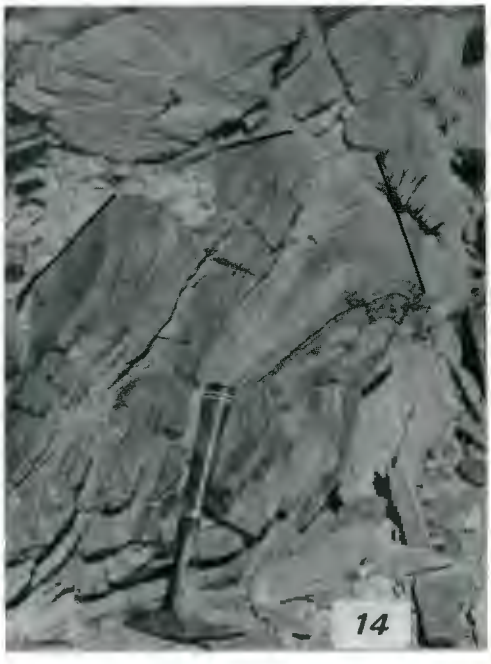
14


15


16

Plate 17. Very tight, almost isoclinal slip folding in the Tinkas Formation. The B_2 folds have narrow hinge areas; Tinkas River. Cliff face is approximately 30 m high.

Plate 18. Fold mullions of F_2 age plunging steeply northwards in a stream section just north of the Langer Heinrich. Height of cliff is 10 m.

Plate 19. Photomicrograph showing calcite (dark between crossed nicols) with exsolution lamellae of dolomite; RJ93.

Plate 20. Photomicrograph showing armoured relic of tremolite (dark, fibrous) protected from reaction with dolomite (white) by diopside (light grey, high relief). Crossed nicols; RJ672.

University of Cape Town

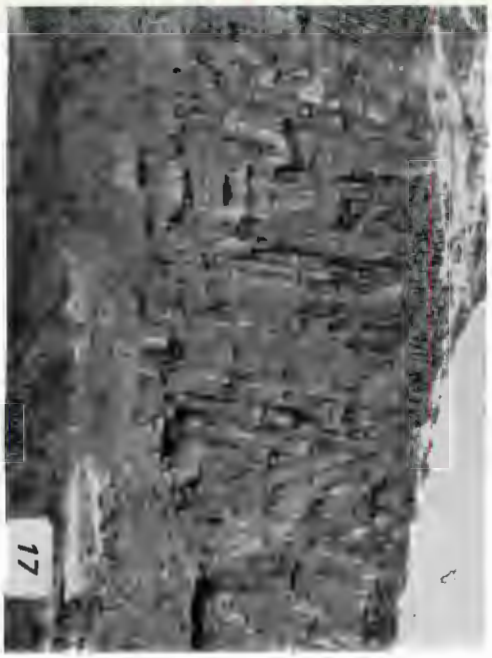

17

18

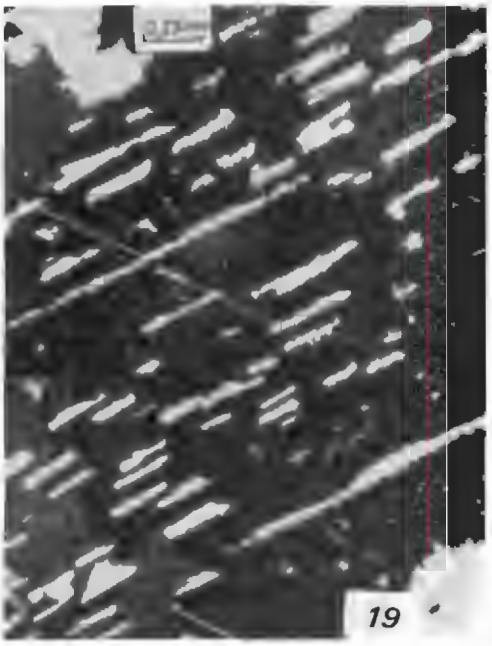

19

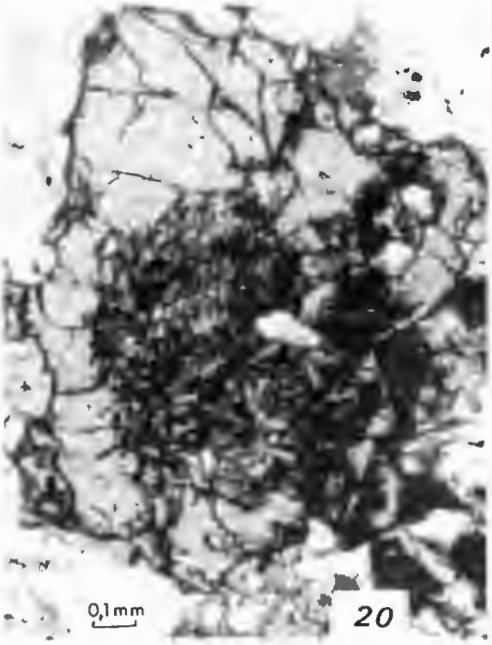

20

Plate 21. The reaction of tremolite and dolomite (reaction 7) has produced aggregates of forsterite (now serpentine) and calcite. The surroundings consist of calcite and dolomite. Stained slab, RJ93.

Plate 22. Central grain of chondrodite (dark, twinned) surrounded by a retrograde-reaction rim of tremolite (grey and white, medium relief) and dolomite (dark grey). Crossed nicols, RJ233.

University of Cape Town

Plate 23. Photomicrograph showing the petrographic evidence for reaction (12): reaction of epidote (light grey, in centre) and quartz has produced grandite which is seen as the isotropic mineral enclosing epidote. Crossed nicols, RJ429.

Plate 24. Photomicrograph showing blastoporphyritic texture in fine-grained quartzofeldspathic gneisses of possible volcanic parentage. Minerals are quartz, microcline and plagioclase. Crossed nicols, RJ785.

21

22

23

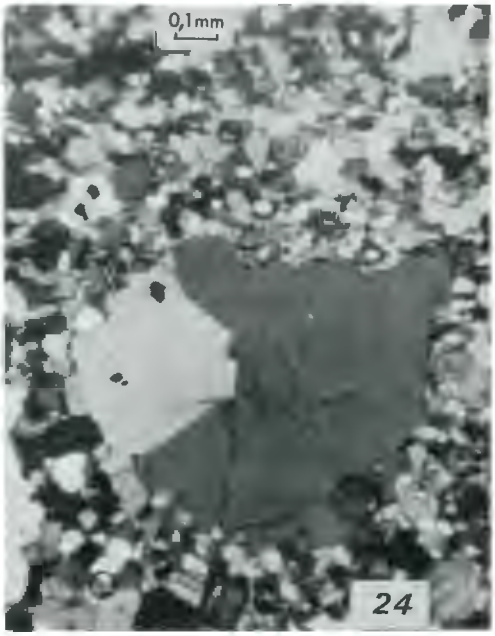

24

Plate 25. Photomicrograph showing an aggregate of sillimanite needles in the core of a cordierite porphyroblast whose growth has prevented further reaction between biotite, sillimanite and quartz (see reaction 31). Crossed nicols, RJ736.

Plate 26. Photomicrograph showing a rotated K-feldspar porphyroblast containing an internal foliation, defined by small flakes of biotite, which is oriented at an angle to the external biotite foliation. The external foliation is flattened around the porphyroblast. Crossed nicols, RJ8.

University of Cape Town

Plate 27. Photomicrograph showing wollastonite grains (white) poikiloblastically enclosed within later grossularite (black). Crossed nicols, RJ618.

Plate 28. Syntectonic homogeneous pegmatite of metamorphic origin showing pinch-and-swell structure; Swakop River, just west of the Witpoort.

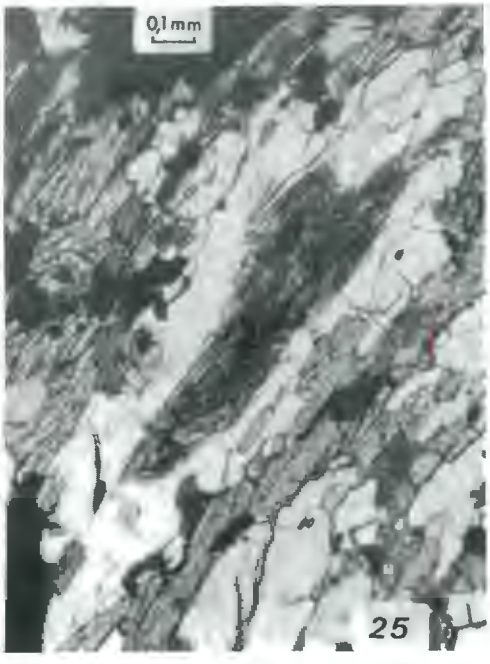
0,1 mm
25


0,3 mm
26


0,2 mm
27

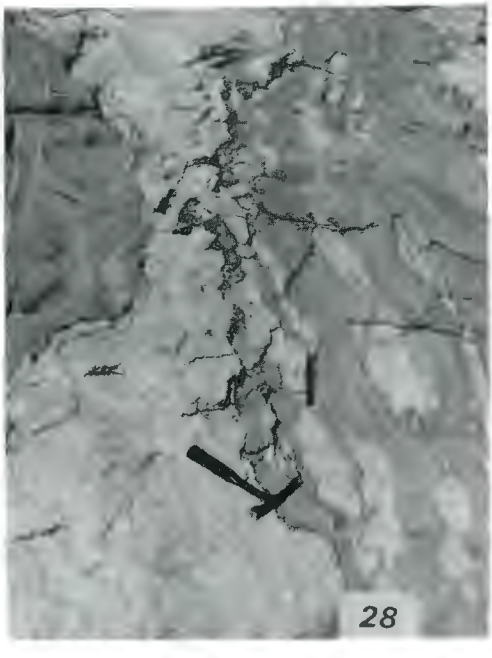
28

Plate 29. Biotite-bearing homogeneous pegmatite showing both sharp and gradational contacts. Biotite-rich selvedges are present in the country rock at the margins of the pegmatite. Witpoort Formation, Rote Adlerkuppe dome.

Plate 30. Boudinaged, homogeneous pegmatite in Tinkas Formation, near Donkerhoek Granite at the Onanis River.

University of Cape Town

Plate 31. Layered pegmatite showing alternation of fine-grained aplite and coarser-grained pegmatite; between Bloedkoppie and Langer Heinrich.

Plate 32. Passively emplaced post-tectonic layered pegmatite (layering not shown) in sharp intrusive contact with folded calc-granofels and biotite schist of the Tinkas Formation. The pegmatite cuts across an isoclinal B_2 fold; Tinkas River.

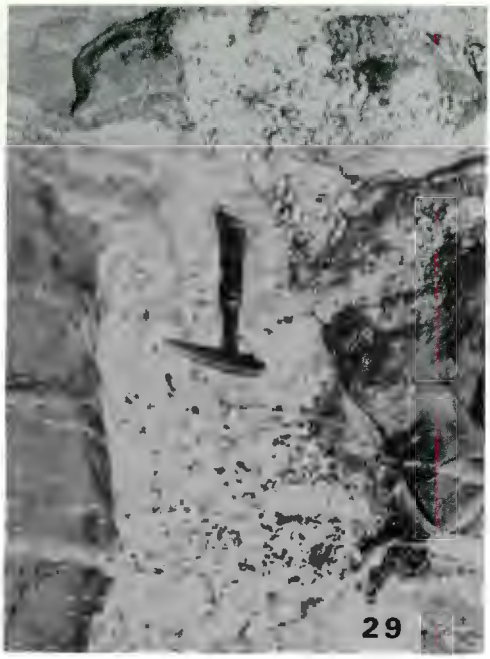
29


30


31


32

GEOLOGY AND METAMORPHIC PETROLOGY OF PART OF THE DAMARA OROGEN ALONG THE LOWER SWAKOP RIVER, SOUTH WEST AFRICA

by

R. Jacob

APPENDIX 2

RADIOACTIVE MINERALIZATION

University of Cape Town

EXPLANATION

The section on radioactive mineralization presented in this Appendix was originally included as chapter 7 of the thesis which was to be published as a Bulletin of the Precambrian Research Unit.

However, permisssion to publish this chapter was not granted by the Atomic Energy Board and it has therefore been removed from the main thesis prior to printing.

All references relating to radioactive mineralization are given at the end of this Appendix but general references already cited earlier in the thesis are not repeated here.

CAPE TOWN
September, 1974

R. Jacob

7. RADIOACTIVE MINERALISATION

The west-central part of the Damara Orogen is characterised by a widespread occurrence of radioactive minerals and may prove to be an important uranium province although its potential has not yet been fully assessed. The discovery of radioactive minerals dates from the early 1920's, when davidite was found near Rössing, northwest of the area under consideration (Smith, 1965; von Backström, 1970). Officers of the Geological Survey undertook brief reconnaissance work in 1939 and 1940 during which time samples of opaque, heavy minerals were collected from pegmatoids at various localities between Rössing Mountain and the Rooikuiseb anticlinorium. Most of these were identified as ilmenite and magnetite and proved to be non-radioactive but small amounts of yttrochrasite were found (Schwellnus and Kuschke, 1940; Schwellnus, 1941).

Radioactive mineralisation at the Ida copper mine was briefly described by Martin (1949) and later by von Backström (1967). Prospecting activity by a mining company was reported by Smith (1965). This activity was concentrated in the Louw's Claims- and SJ Claims areas in the general vicinity of the Khan Mine, northwest of the Khan River. At present the only economically viable deposit is the Rössing uranium deposit in the SJ area. According to von Backström (1970) the mineralised body is a very coarse-grained leucocratic granite, intrusive into high-grade metasediments, and which consists of quartz and microcline-perthite and minor amounts of biotite. The most important primary radioactive mineral is uraninite, which occurs together with a variety of yellow, secondary uranium minerals (von Backström, 1970, p. 147).

In 1968 the Geological Survey carried out an airborne radiometric survey over western Damaraland on behalf of the Atomic Energy Board. Follow up groundwork in the area under consideration was conducted by the author during the geological mapping programme by using a portable scintillation monitor.

7.1. Classification and distribution

An investigation of anomalous areas has resulted in the following classification of radioactive mineral occurrences:

Granites and granitic gneisses
Pegmatitic granites, pegmatites and aplites
Country rocks close to intrusives
Metasediments and sediments

7.1.1. Occurrences in granites and granitic gneisses

The *Red Granite-Gneiss* consists of several different granitic rocks and gneisses but the radioactivity is highest over strongly gneissic, biotite-rich, augen gneisses of deep red colour. The radioactivity is apparently related to the biotite content since biotite schlieren show even higher count rates than the augen gneisses while Red Granite-Gneiss of lower biotite

content is less radioactive. The biotite schlieren contain greater quantities of magnetite, ilmenite and monazite. Yellow secondary uranium minerals have been found in the biotite schlieren. Smoky quartz is a common feature in both the augen gneisses and in the later, less gneissic red granites. It is more easily observed in pegmatoid mobilisates, where the grain size is coarser. The anomaly highs over the Red Granite-Gneiss are partly due to good exposures of the augen gneisses and partly, near the Swakop River, to heavy mineral sands (p. 169). Investigations by the National Institute for Metallurgy indicate that monazite is responsible for much of the radioactivity in the Gn_1 (pers. commun. Dr. E.J. Oosthuysen).

The radioactivity in rocks of the *Salem Granite Suite* is highest over the central parts of the outcrop area of this rock association where the late leucogranite phase is developed. In the field this rock displays a spotting or speckling caused by radioactive metamict allanite which is black when fresh, with a vitreous to metallic lustre and conchoidal fracture. This occurs as tabular and irregular grains up to 1 cm in size and its surface generally has a rusty, reddish-brown appearance. Normally it is surrounded by a red-stained "halo" (haematite?) on weathered surfaces, or on fresh surfaces by reddened feldspar and cracked, smoky quartz. It is more abundant in coarser pegmatoid lenses and irregular segregations with gradational contacts where it seems to be associated with concentrations of magnetite. Allanite also occurs in the porphyritic biotite granite but to a lesser extent. However, because of the darker colour of this rock it is not so noticeable here. Certain other radioactive minerals have been identified in the Salem suite. Smith (1965, p. 70) reported that age determinations (falling in the range 510 ± 40 Ma) had been carried out on yttrocolumbite and yttrotantalite from the vicinity of the old Jakalswater station, standing on the leucogranite. Measurements on samarskite and davidite from the porphyritic biotite granite in the vicinity of Salem 102 yielded ages of 480 ± 20 and 550 ± 20 Ma (Burger and Coertze, 1973).

The radioactivity of the *Bloedkoppie Granite* is up to 3 times greater than that of the country rocks (Tinkas Formation) and is comparable with that of the leucogranite of the Salem suite. The radiation of the Bloedkoppie Granite is uniform but increases over thin, internal pegmatites. This granite is nowhere at present of potential ore grade but constitutes the protore of the uranium mineralisation in the overlying calcretes. No anomalous radioactivity readings or radioactive minerals were observed in the *Achas*, *Gaxib* and *Horebis* granites and the airborne radiometric contours fall to background levels over them.

Radioactive occurrences in *Migmatites* (early pegmatitic mobilisates of anatectic origin) were found in the Vredelus anticline. Here a biotite gneiss of the Etusis Formation has been migmatised and comprises quartz-rich pegmatoid and granitic leucosomes with biotite-rich melanosomes. Within the leucosomes pods and lenses of strongly radioactive davidite are irregularly distributed. In hand specimen the mineral is opaque and dark grey with a metallic lustre and conchoidal fracture and it occurs together with haematite and ilmenite. The feldspar is reddish-purple in colour around the davidite concentrations.

7.1.2. Occurrences in pegmatitic granites, pegmatites and aplites

Within this group of rocks the *Alaskitic Pegmatitic Granite* (G_4) is of major importance and the Rössing uranium deposit belongs to this category. Smith (1965) referred to the host rock as pegmatite but the term pegmatitic granite may be more appropriate. The mineralised alaskites are confined to the western parts of the region where a large number are radioactive. They display certain features which help to distinguish them from those that are barren. They tend to be more deeply coloured on weathered surfaces than unmineralised bodies and are normally of reddish to buff colour in contrast to the white to very pale pink colour of the barren intrusives. In a general way the intensity of colour is proportional to the degree of mineralisation. There are exceptions, however, because almost white, mineralised alaskites have been found. The mineralised bodies usually contain smoky quartz and darkened feldspar. Again, generally speaking, those bodies which are mineralised tend to contain more biotite and less muscovite than the barren varieties. Garnet-bearing pegmatitic granites are usually less radioactive but here it is difficult to generalise because the mineralised pegmatitic granites at Louw's Claims, northwest of the Khan River, are garnetiferous. The alaskites are of different ages and the late phases show the highest mineralisation. With respect to the structural and stratigraphic positions, the well-mineralised bodies show a tendency to occur around dome structures close to, and generally just below, the prominent marbles of the Damara Group, either those of the Rössing Formation or the Husab Formation, depending on which of these is present immediately above either the Nosib Group or the Red Granite-Gneiss. The mineralised bodies are never far from the Red Granite-Gneiss, and occur also within it. The economically most promising area investigated during the mapping is in the vicinity of the Ida dome, on the southern, southeastern and eastern sides. Mineralised G_4 occurs along the contact between the Khan Formation and marbles of the Husab Formation and is radioactive, in places patchily, over a distance of about 9 km along strike, on either side of the Swakop River. The mineralised body is part of a wide zone of alaskites and can easily be recognised in the field due to its reddish colour. In the vicinity of the Ida Mine cupriferous biotite-hornblende schists are preserved as xenoliths in the alaskite and are preferentially mineralised.

Gradations exist between the G_4 and the *zoned pegmatites* and the classification of a particular body may occasionally be arbitrary. The zoned pegmatites are smaller than most of the G_4 intrusives and radioactive mineralisation is very erratic. None of those investigated appear to have potential as "ore-bodies".

No radioactivity or only low-order anomalies were found in *layered pegmatites* in the area under investigation.

Radioactive *quartz-fluorite* veins, similar to the calcite-apatite-fluorite vein dykes described by Satterly (1957) and Heinrich (1958), occur at the Husab Mine as an *en echelon* set of lenses and short dykes over a distance of 4 km. In places pegmatites and fluorite veins appear to be contemporaneous but elsewhere the fluorite cuts across earlier structures and post-dates at least parts of the pegmatites. Irregular blebs and patches of fluorite

are found forming part of the pegmatites. These associated pegmatites are generally somewhat sheared and extensively replaced by greisen, consisting of sericite, sericitised biotite, calcite and albite. Besides quartz and fluorite, the following minerals have been recognised in the veins: anti-perthitic, schillerised plagioclase, magnetite, ilmenite, barytes, galena, wulfenite, garnet, muscovite, biotite and calcite. In thin sections fluorite and calcite show replacement relationships towards other minerals; calcite displays prominent growth zoning. The association of greisen and the veins suggests that the veins represent a late, probably hydrothermal phase of pegmatitic activity. During this phase uranium minerals were deposited with fluorite.

Aplites associated with the Salem granites and the Red Granite-Gneiss generally have the same levels of radioactivity as these rocks.

7.1.3. Occurrences in country rocks close to intrusives

Occurrences in this category are of hydrothermal and metasomatic origin. The intrusive rocks are normally the G_4 bodies.

Biotite schist xenoliths in the mineralised alaskitic pegmatitic granites are normally preferentially enriched in uranium relative to the alaskites and have acted as precipitants or sponges for radioactive minerals. Similar effects characterise the immediate country rocks of mineralised G_4 and in many places the schists surrounding the G_4 bodies are more heavily mineralised than the intrusives for distances up to one or two metres from the contacts. The presence of isolated porphyroblasts of K-feldspar, derived from the alaskite melts, and abundant quartz veining in the schists attest to metasomatic activity. It is postulated that the melts underwent "second boiling" during crystallisation of the alaskites (Krauskopf, 1967; Burnham, 1967) and that silica and alkali-rich aqueous fluids entered the country rocks, more or less under open system conditions. Uranium contained in these fluids was precipitated by biotite and hornblende. Occurrences of the above type are common in the area between the Ida dome and Holland's Gorge.

Skarn bodies are developed along the contacts between intrusive granitic rocks, generally G_4, and calcareous metasediments. They are normally small and sporadically developed but southeast of the Ida dome some of them reach several hundred metres in length and more than 10 metres in width where they form resistant knolls and ridges. The skarns consist essentially of andradite, scapolite, hedenbergite and wollastonite together with lesser amounts of quartz, plagioclase, sphene, calcite and apatite. Where the skarn bodies have formed adjacent to mineralised G_4 they are mineralised and small amounts of secondary uranium minerals are visible. The presence of yellow to orange-coloured calcite is often indicative of radioactivity in the skarns. Metasomatic activity, associated with the final stages of crystallisation of the alaskite melts, has produced the skarns. The metasomatising fluids, derived through "second boiling", have carried U in solution into the carbonate rocks where reaction has changed the composition and chemical properties of the fluids, resulting in precipitation of radioactive minerals.

7.1.4. Occurrences in metasediments and sediments

Conglomerates of the Etusis Formation at the Langer Heinrich form an important part of the succession. The conglomerates contain significant amounts of heavy minerals, mostly magnetite and they are more radioactive than the surrounding quartzites due to a varying content of monazite.

Very large areas of *calcrete*-covered flats exist in the Namib Desert Park and these are locally mineralised by secondary uranium compounds. The most significant anomaly area in the region mapped is that along the Gawib valley between the Schieferberge - Bloedkoppie and the Langer Heinrich where anomalies extend over a length of 12 km. The mineralisation is confined to consolidated grits and conglomeratic material cemented by calcareous material, the whole being here termed calcrete. The gritty fragments and pebbles are composed of feldspar, quartz and fragments of pegmatite, calc-granofels, quartzite and schist. The most important radioactive mineral is carnotite which is highly concentrated in places but absent in others.

Heavy mineral sands consisting of quartz, magnetite, biotite, monazite and other heavy minerals frequently show radiometric anomalies significantly higher than the readings over the Red Granite-Gneiss from which they are derived. The heavy minerals have been concentrated by water action along narrow stream courses and thus are partly alluvial. They are also partly of deflation origin, the sand having been winnowed by the action of the south-westerly winds in summer and the easterly or "Föhn" winds in winter.

7.2. Origin

Several hypotheses for the origin of the radioactive occurrences are presented below but need to be supported by more detailed mineralogical work.

The formation which is most highly radioactive on a regional scale is the Red Granite-Gneiss. This rock is regarded as being the protore of the uranium deposits in the Alaskitic Pegmatitic Granites. The *Red Granite-Gneiss* is interpreted as being partly of pre-Nosib age and partly the result of anatexis of Nosib Group metasediments; its origin has been discussed on page 150. One line of evidence for these rocks being partly of pre-Nosib age is their radioactivity. This is generally higher than that of the Etusis and Khan Formations, for the Rote Adlerkuppe dome, Vredelus anticline and Rooikuiseb anticlinorium structures, comprising Etusis Formation rocks, display low radioactivities.

Although it is uncertain whether the radioactivity in these rocks is an original or introduced feature, its regional distribution and consistent levels suggest that it is largely an original characteristic of the Red Granite-Gneiss. It is possible that uranium and thorium in the volcanics, conglomerates and sediments of the Nosib Group have also contributed to the level of radioactivity. Much of it, however, was probably derived from pre-Nosib rocks (equivalent to the Abbabis Formation(?)) which may have been composed largely of igneous rocks such as granites and volcanics, prior to their Damaran tectonism. Silicic igneous rocks generally carry greater amounts of uranium and thorium than others and according to Rogers and Adams

(1969a, p. 92-E-4; 1969b, 90-E-3) average abundances of uranium and thorium in silicic igneous rocks fall in the ranges 1-10 ppm U and 10-20 ppm Th with average Th/U ratios of about 3,5 - 4. The average uranium content of volcanic rocks appears to be about the same as that of the plutonic varieties (Coats, 1956; Heinrich, 1958; Rogers and Adams, 1969a). Larsen and Phair (1954) have suggested that silicic hypabyssal and volcanic rocks may contain slightly higher radioactivity than their plutonic equivalents and Stanton (1972) states that siliceous tuffs may contain larger amounts of uranium than associated intrusives but in general they can be expected to carry similar amounts.

The problem of correlation of the Red Granite-Gneiss with the rocks of the Abbabis Formation near Usakos remains unsolved at present but it may be noted that the airborne radiometric survey maps show that the Abbabis rocks are not as radioactive as the Red Granite-Gneiss. Whether the cause of this may lie in the masking effect of the sand in that area is not known.

The *Salem Granite Suite* represents a differentiation sequence (Miller, 1972) and the fact that its latest phase, the leucogranite, is most highly radioactive is in accordance with what has been reported elsewhere (Rogers and Adams, 1969a; Heinrich, 1958; Larsen et al., 1956). The leucogranite crystallised as a fairly coarse-grained granitic rock with disseminated mineralisation and the uranium, derived through anatexis of the Witpoort Formation, has been concentrated, through fractional crystallisation processes, into this final stage.

Uranium and thorium tend to remain in melts until the final stages of crystallisation and, therefore, are normally found in pegmatites. Because of the generally low concentration of uranium this element often does not crystallise as discrete mineral species and a large proportion of it in many igneous rocks is easily leached (Larsen et al., 1956). It occurs in the following ways (Rogers and Adams, 1969a):

as isomorphous substitutions,
in defect structures in minerals,
adsorbed along crystal imperfections and grain boundaries,
as inclusions of microcrystals of uranium minerals.

Where biotite is present most of the uranium may occur in it (Larsen et al., 1956).

It is proposed that uranium was concentrated in the *Alaskitic Pegmatitic Granites* by incorporation into early melts and solutions during progressive anatexis. A moderately enriched protore is a pre-requisite for the formation of the mineralised G_4 bodies and this appears to exist in the form of the Red Granite-Gneiss and perhaps the Nosib Group metamorphites.

Uranium may be rather sensitive to changes of metamorphic grade and, although insufficient data are available, suggestions have been made that uranium tends to become depleted in metamorphic rocks at higher grades of metamorphism (Heier, 1962). Although Heier and Adams (1965) have demonstrated this for an area in Norway, Rogers and Adams (1969a) and Fairbridge (1972) have pointed out that far too little is yet known about this aspect for generalisations to be made with certainty.

During progressive metamorphism uranium can be released from host minerals in several ways (Yermolayev, 1971):

(i) through recrystallisation of minerals causing them to rid themselves of uranium in lattice sites and defects,

(ii) through desorption of uranium adsorbed onto grain surfaces and along interfaces,

(iii) through breakdown of uranium-carrying minerals such as biotite and sphene,

(iv) through anatexis of pre-existing rocks.

According to McKelvey et al. (1955), the uranous ion, U^{4+}, is the most abundant cation in nature and is stable under reducing conditions, more or less the same as those under which H_2S, HS^- and S^{2-} exist. In the uranous form uranium is relatively immobile; however, in aqueous solution it can be oxidised to the uranyl form, U^{6+}, which combines with oxygen:

$$U^{4+} + 2\ H_2O = (U^{6+}O_2)^{2+} + 4H^+ + 2e.$$

This ion is stable and can be considered a complex ion like $(NH_4)^+$ and in this form uranium is soluble in solutions and highly mobile.

During metamorphism fO_2 was rather high in rocks of the Nosib Group (see section on metamorphism) and probably also high in the Red Granite-Gneiss where uranium was present either in the uranyl form or was converted to it during metamorphism. With increasing intensity of metamorphism uranium was taken into solutions and anatectic melts. The melts must have been water-saturated because the alaskites, as now observed, are relatively coarse grained and contain irregular segregations of pegmatitic material. It is unlikely that such melts would have risen for any great distance in the rock pile because a drop in pressure would result in crystallisation (Cann, 1970) and this provides an explanation why the G_4 bodies are never found far from outcrop areas of the Red Granite-Gneiss and Nosib Group.

Uraniferous anatectic melts were thus produced, their uranium content having been derived through "leaching" of the moderately enriched protore, the Red Granite-Gneiss. Final crystallisation of the melts and deposition of uranium were probably controlled by both structural and chemical factors.

Structural traps existed in the form of the marbles of the Rössing and Husab Formations since there is a clear association of significantly mineralised alaskites and overlying carbonates. It is apparent in the field that the marbles have exerted a "damming up" effect on G_4 bodies and pegmatites and many uraniferous alaskite melts rose to the level of the marbles and were trapped there, to crystallise with eventual drop in temperature and pressure.

Chemical controls which were probably operative include:

(i) Release of pressure through uprise of the melts, resulting in crystallisation of many bodies within the Red Granite-Gneiss itself or within the metamorphosed Nosib rocks.

(ii) Several G_4 bodies in the Khan Formation show patchy mineralisation

University of Cape Town

and there is an association of uranium with opaque oxides like magnetite and haematite, especially the latter. The inter-relationship of uraninite and haematite has been ascribed to oxidation of Fe^{2+} to Fe^{3+}, resulting in reduction of the uranyl ion to the uranous form and precipitation of both haematite and uraninite (McKelvey et al., 1955):

$$3\ H_2O + 2\ Fe^{2+} + (U^{6+}O_2)^{2+} = Fe_2O_3 + U^{4+}O_2 + 6\ H^+.$$

The association of these two minerals provides an explanation for the observation that the reddish-to brownish-coloured alaskites tend to be more heavily mineralised.

(iii) The existence of reducing conditions in the Damara rocks overlying the Nosib Group is shown by graphitic schists and marbles and some of the latter are fetid (Smith, 1965, p. 29). The Rössing Formation is characterised by disseminated sulphide mineralisation, mainly pyrite and pyrrhotite, the weathering of which has produced the brown-and red-stained surfaces that distinguish this group of rocks from other strata. In addition, widespread disseminated copper sulphide mineralisation characterises the Khan Formation (e.g. Ida Mine) in western Damaraland. Smith (1965) and Toens (unpubl. lecture, 1973) have suggested that the mineralisation is syngenetic in origin. Be that as it may, the important point is that sulphides were present in the uppermost parts of the Khan Formation and in the Rössing Formation in the general area around the Khan and Swakop Rivers at the time of metamorphism. During progressive metamorphism sulphides undergo certain mineralogical changes, for example, pyrite breaks down to pyrrhotite, and sulphur is released (McDonald, 1967; Vokes, 1969). It is very likely that this occurred in the Rössing Formation and that, when the intruding alaskite melts entered this reducing environment, the complex uranyl ion was reduced to U^{4+} and precipitation occurred, mainly in the form of uraninite.

(iv) Other chemical factors having an influence on precipitation of uranium include the changes produced in composition of late-stage fluids, escaping from the final melt, through metasomatic reaction with country rocks to produce the skarn bodies, and the precipitating action of biotite-rich margins and xenoliths.

The structural and chemical controls exerted by the rocks of the Rössing Formation may help to explain why uranium occurrences are localised, in several places, at this stratigraphic level but it is emphasised that any other horizon with similar chemical properties during metamorphism, e.g. reducing conditions, should be as effective.

The processes postulated above for the mobilisation of uranium as the uranyl ion should result in a geochemical separation of uranium and thorium because the oxidation of U^{4+} to U^{6+} is not accompanied by a similar change in the oxidation state of Th^{4+} (McKelvey et al., 1955; Heier, 1962; Heier and Adams, 1965). It can therefore be expected that the Th/U ratio should be lower in the alaskites than in the Red Granite-Gneiss protore if uranium has been preferentially mobilised. This appears to be the case because the Th/U ratio in the Red Granite-Gneiss (varying between 1 and 10, and averaging 5) is significantly higher than that in the Alaskitic Pegmatitic Granites

(0,01 - 0,5) (pers. communs. Dr. P.D. Toens and Anglo American Corporation).

In pegmatites, uranium derived from the same source as the pegmatite-forming fluids remained in solution until late in the crystallisation history before finally being incorporated into complex minerals or crystallising as uraninite. The distribution of radioactive minerals in the pegmatites is erratic but is normally confined to the outer, or wall zones, of such bodies. Where mineralisers like fluorine were present the uranium was probably held in solution as fluoride complexes (Robinson, 1960) until a very late stage when it was finally precipitated during hydrothermal and greisening processes.

The formation of uranium-bearing minerals in the Cenozoic calcretes still needs investigation. The occurrences in calcrete in the general area of the Langer Heinrich-Schieferberge-Bloedkoppie have three possible sources:

a) Conglomerates in the Etusis Formation
b) Layered pegmatites in the vicinity
c) Bloedkoppie granite and associated pegmatites.

The first alternative can be eliminated on the grounds that the radioactivity in the conglomerates is caused by thorium; the geomorphology and the drainage pattern also militate against such a source. The layered pegmatites of Donkerhoek age are not mineralised and thus cannot constitute source rocks.

The radioactivity of the Bloedkoppie Granite and associated internal pegmatites is considerably higher than that of the surrounding metasediments and layered pegmatites and it is considered that this body has provided the uranium which is now found in the calcretes.

Leaching by meteoric groundwaters has probably extracted uranium from the Bloedkoppie Granite in the mobile U^{6+} form. The groundwater solutions moved through the adjacent and overlying calcrete formations partly through the influence of gravity and partly through capillary action. The uranium was likely to have been transported as the uranyl dicarbonate or uranyl tricarbonate ion, both of which are stable and soluble over a wide range of Eh and pH conditions (Hostetler and Garrels, 1962). The most common uranium mineral in the calcretes under discussion is carnotite, which is stable over a wide range of Eh and pH and is a common constituent of "oxidised ores" of Colorado Plateau type (Heinrich, 1958; Fischer, 1968). However, its stability is very sensitive to changes in ionic activity and its precipitation is critically controlled by the amounts of uranium, vanadium and CO_2 in solution (Hostetler and Garrels, 1962). Vanadium and potassium also derived from the Bloedkoppie Granite, were carried in the groundwaters and under oxidising conditions the uranyl ions were fixed by combination with K^+ and V^{5+} ions to form the mineral carnotite (KUO_2VO_4). The arid climate in the region has helped to prevent the carnotite on surface from being subsequently removed in solution.

University of Cape Town

MAP 2

Simplified geological map showing major structural features, positions of subareas and grid for sample localities

Scale – 1 : 250 000

5 km 10

15°15'

22° 30'

15°00'

15°30'

22°45'

Welwitsch Hills syncline

Gürtel Hills syncline

Ida dome

Zebra-berge

Husabberg

Rote Adlerkuppe dome

Vredelus anticline

Arysap Hills syncline

Rooikuiseb anticlinorium

SWAKOP RIVER

Langer Heinrich dome

Rabenklucken anticline

5 6 7 8 9a,b,c 9d 10 11a 11b 12 13a,b 13c 14 15a 15b,c 17 18a 18b 18c 18d 18e,f

OTHER GRANITES

SALEM GRANITE SUITE

RED GRANITE-GNEISS

POST-DAMARA

DAMARA GROUP

NOSIB GROUP

Anticline

Syncline

(7) Subarea ; number refers to text figure

REFERENCES

COATS, R.R. (1956) Uranium and certain other trace elements in felsic volcanic rocks of Cenozoic age in western United States. *U.S. Geol. Surv., Prof. Paper* 300, 75–78.

FAIRBRIDGE, R.W. (Ed.) (1972) *Encyclopedia of geochemistry and environmental sciences,* IV A. Van Norstrand Reinhold, New York, 1215–1228.

FISCHER, R.P. (1968) The uranium and vanadium deposits of the Colorado Plateau region. In: Ridge, J.D. (Ed.), *Ore Deposits of the United States,* 1. Amer. Inst. Min. Metall. Petrol. Eng., New York, 735–746.

HEIER, K.S. (1962) Spectometric uranium and thorium determinations on some high-grade metamorphic rocks on Langöy, northern Norway. *Norsk Geol. Tidsskr.,* 42, 143–156.

——— & ADAMS, J.A.S. (1965) Concentration of radioactive elements in deep crustal material. *Geochim. Cosmochim. Acta,* 29, 53–61.

HEINRICH, E.W. (1958) *Mineralogy and geology of radioactive raw materials.* McGraw-Hill Book Co., New York, 654p.

HOSTETLER, P.B. & GARRELS, R.M. (1962) Transportation and precipitation of uranium and vanadium at low temperatures, with special reference to sandstone-type uranium deposits. *Econ. Geol.,* 57, 137–167.

LARSEN, E.S., GOTTFRIED, D. & SMITH, W.L. (1956) Uranium in magmatic differentiation. *U.S. Geol. Surv., Prof. Paper* 300, 65–74.

——— & PHAIR, G. (1954) The distribution of uranium and thorium in igneous rocks. In: Faul, H. (Ed.), *Nuclear Geology.* John Wiley & Sons, New York, 75–89.

MARTIN, H. (1949) Unpubl. Rep., Geol. Surv. South Africa.

McDONALD, J.A. (1967) Metamorphism and its effects on sulphide assemblages. *Mineral. Dep.,* 2, 200–220.

McKELVEY, V.E., EVERHART, D.L. & GARRELS, R.M. (1955) Origin of uranium deposits. *Econ. Geol. 50th Anniv. vol.,* 464–533.

ROBINSON, S.C. (1960) Economic uranium deposits in granitic dykes, Bancroft District, Ontario. *Canad. Mineral.,* 6, 513–521.

ROGERS, J.J.W. & ADAMS, J.A.S. (1969a) Uranium. In: Wedepohl, K.H. (Ed.), *Handbook of Geochemistry,* 2, pt. 1, Springer-Verlag, Berlin.

——— ——— (1969b) Thorium. In: Wedepohl, K.H. (Ed.), *Handbook of Geochemistry,* 2, pt. 1, Springer-Verlag, Berlin.

SATTERLY, J. (1957) Radioactive mineral occurrences in the Bancroft area. *Ann. Report, Ontario Dept. Mines,* 65, 6 (for 1956), 179p.

SCHWELLNUS, C.M. (1941) Radioactive mineral deposits in the Swakopmund district, South West Africa. *Unpubl. Final Rep., Geol. Surv. South Africa.*

——— & KUSCHKE, G.S.J. (1940) Radioactive mineral deposits in the Swakopmund district, South West Africa. *Unpubl. Prelim. Rep., Geol. Surv. South Africa.*

VOKES, F.M. (1969) A review of the metamorphism of sulphide deposits. *Ear. Sci. Rev.*, 5, 99-143.

VON BACKSTRÖM, J.W. (1967) Radioactive ore at the Ida Mine, Swakopmund district, South West Africa. *Confidential Rep., Atomic Energy Board.*

——— (1970) The Rössing uranium deposit near Swakopmund, South West Africa. In: *Uranium Exploration Geology*, I.A.E.A., Vienna, 143-148.

YERMOLAYEV, N.P. (1971) Processes of redistribution and extraction of uranium in progressive metamorphism. *Geochem. Intern.*, 8, 599-609.

MAP 1

GEOLOGICAL MAP OF AN AREA EAST OF THE KHAN-SWAKOP CONFLUENCE, SOUTH WEST AFRICA

0 1 2 4 6 8 10 KILOMETRES

0 1 2 3 4 5 6 7 MILES

SCALE 1:100,000

SECTIONS

VERTICAL SCALE = HORIZONTAL SCALE

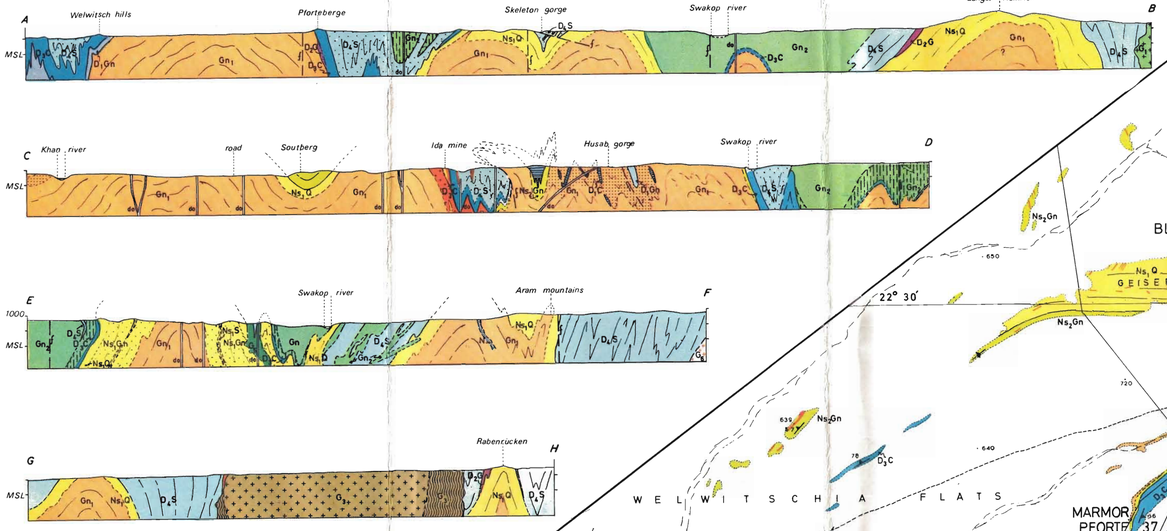

LEGEND

- Alluvium, calcrete, sand, scree, gravel
- Dolerite — KARROO
- Pegmatite; aplite(ap); quartz vein (qv)
- G_4 Donkerhoek granite
- G_3 Horebis granite; anastomosing in country rock
- G_4 Alaskitic, pegmatitic granite
- Schematic trend of G_4 in Gn_1
- G_3 Gawib granite, in places porphyritic; where foliated — POST DAMARA
- G_2 Achas granite
- G_1 Bloedkoppie granite
- N Basic intrusives

D_4S	Biotite schist, paragneiss	WITPOORT FORMATION	KHOMAS SUBGROUP — DAMARA GROUP
D_3C	Biotite schist, calc-silicate rock, quartzite, marble	TINKAS FORMATION	
D_2C	Marble with biotite schist, calc-silicate rock	HUSAB FORMATION	
D_2O	Meta-tilloid	CHUOS FORMATION	
D_1Gn D_1C	Quartzite, paragneiss, conglomerate, biotite schist; marble, calc-silicate rock	ROSSING FORMATION	
Ns_2Gn	Biotite-amphibole schist, amphibole-pyroxene gneiss	KHAN FORMATION	NOSIB GROUP
Ns_1S	Biotite schist, quartzite	ETUSIS FORMATION	
Ns_1Q	Quartzite, conglomerate, quartzo-feldspathic paragneiss		
Ns_1Gn	Quartzo-feldspathic paragneiss, amphibole-pyroxene gneiss, quartzite		
Ns_1S	Biotite schist, marble		

METAMORPHIC EQUIVALENTS

- Gn_2 Porphyritic, in places gneissic Salem granite
- Gn_2 Non-porphyritic Salem gneiss
- Gn_1 Metasedimentary skialiths in Gn_1
- Gn_1 Red granite-gneiss

SYMBOLS

- Horizontal, inclined, vertical, inverted and contorted bedding
- Horizontal, inclined and vertical foliation
- 20 Direction and plunge of lineation
- Fault
- Thrust
- Lithologic boundary
- Lithologic boundary, approximate
- Structural form lines
- A — B Trace of geological profile
- Homestead
- River and watercourse
- Road
- 712 Trigonometrical beacon with height in metres
- ·340 Spot heights in metres
- Old narrow-gauge railway

LOCALITY MAP

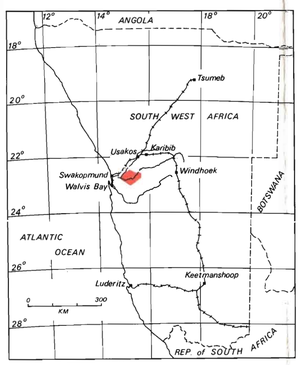

Mapped and drawn by R. Jacob, 1969-71, for the Precambrian Research Unit, University of Cape Town.

Printed by National Lithoprint (Pty) Ltd